AD-A117 918 BOEING AEROSPACE CO SEATTLE WA ENGINEERING TECHNOLOGY DIV F/G 20/6
DEVELOPMENT AND TEST OF A DIGITAL/OPTICAL LINEAR POSITION TRANS--ETC(U)
JUN 82 G E MILLER, T A LINDSAY, B E JOHNSON DAAK51-80-C-0028
UNCLASSIFIED USAAVRADCOM-TR-82-D-6 NL

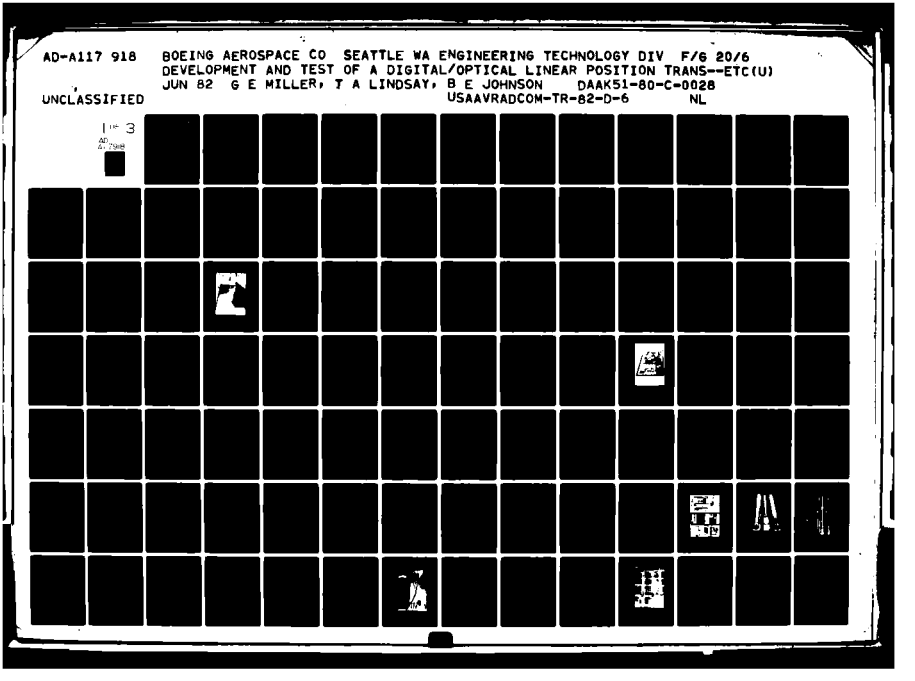

USAAVRADCOM-TR-82-D-6

(12)

DEVELOPMENT AND TEST OF A DIGITAL/OPTICAL LINEAR POSITION TRANSDUCER

G. E. Miller, T. A. Lindsay, B. E. Johnson, J. M. Ewing
BOEING AEROSPACE COMPANY
Engineering Technology
P. O. Box 3999
Seattle, Wash. 98124

June 1982

Final Report for Period August 1980 - February 1982

Prepared for

APPLIED TECHNOLOGY LABORATORY
U. S. ARMY RESEARCH AND TECHNOLOGY LABORATORIES (AVRADCOM)
Fort Eustis, Va. 23604

APPLIED TECHNOLOGY LABORATORY POSITION STATEMENT

This report is considered to provide reasonable insight into the design and development of an optical linear position transducer. It was not intended that the hardware resulting from this effort be of flight quality, and this needs to be considered when reviewing the test results. The problems which occurred during the life cycle and environmental tests require solution prior to making firm conclusions about the flight quality of such a transducer. This effort was one of six efforts to develop digital/optical transducers and all six efforts should be examined to gain the most insight into such transducers.

This developmental work has provided technology for the digital/optical transducers which will be used on the Advanced Digital/Optical Control System (ADOCS) Flight Demonstrator Program (FDP).

Mr. Russell O. Stanton of the Aeronautical Systems Division served as project engineer for this effort.

UNCLASSIFIED

SECURITY CLASSIFICATION OF THIS PAGE *(When Data Entered)*

REPORT DOCUMENTATION PAGE	READ INSTRUCTIONS BEFORE COMPLETING FORM
1. REPORT NUMBER: USAAVRADCOM TR 82-D-6 — 2. GOVT ACCESSION NO: AD-A117918	3. RECIPIENT'S CATALOG NUMBER:
4. TITLE *(and Subtitle)*: DEVELOPMENT AND TEST OF A DIGITAL/OPTICAL LINEAR POSITION TRANSDUCER	5. TYPE OF REPORT & PERIOD COVERED: FINAL Aug 1980 through Feb 1982
	6. PERFORMING ORG. REPORT NUMBER:
7. AUTHOR(s): G.E. Miller - B.E. Johnson; T.A. Lindsay - J.M. Ewing	8. CONTRACT OR GRANT NUMBER(s): DAAK51-80-C-0028
9. PERFORMING ORGANIZATION NAME AND ADDRESS: Boeing Aerospace Company, Engineering Technology, P.O. Box 3999 Seattle, Washington 98124	10. PROGRAM ELEMENT, PROJECT, TASK AREA & WORK UNIT NUMBERS: 1L263211D315
11. CONTROLLING OFFICE NAME AND ADDRESS: Applied Technology Laboratory, US Army Research and Technology Laboratories (AVRADCOM), Fort Eustis, Virginia 23604	12. REPORT DATE: June 1982
	13. NUMBER OF PAGES: 198
14. MONITORING AGENCY NAME & ADDRESS *(if different from Controlling Office)*	15. SECURITY CLASS. *(of this report)*: Unclassified
	15a. DECLASSIFICATION/DOWNGRADING SCHEDULE

16. DISTRIBUTION STATEMENT *(of this Report)*

Approved for public release; distribution unlimited.

1
F

17. DISTRIBUTION STATEMENT *(of the abstract entered in Block 20, if different from Report)*

18. SUPPLEMENTARY NOTES

19. KEY WORDS *(Continue on reverse side if necessary and identify by block number)*

Fiber Optics
Digital Status Monitor
Measurement
Transducer
Sensor
Linear Position
Linear Displacement

20. ABSTRACT *(Continue on reverse side if necessary and identify by block number)*

This report covers the design, development, fabrication, and testing of an optically analog linear position transducer with a full-scale displacement of 6 inches and an equivalent resolution of twelve bits. The transducer is electrically passive and interfaces with the associated Electronic Interface Unit through fiber optics only. The EIU provides the necessary analog-to-digital conversion. The transducer was tested both functionally and environmentally.

DD FORM 1 JAN 73 1473 EDITION OF 1 NOV 65 IS OBSOLETE

UNCLASSIFIED

SECURITY CLASSIFICATION OF THIS PAGE *(When Data Entered)*

TABLE OF CONTENTS

TABLE OF CONTENTS (Continued)

TABLE OF CONTENTS (Continued)

TABLE OF CONTENTS (Continued)

Page

APPENDIXES (continued)

LIST OF ILLUSTRATIONS

LIST OF ILLUSTRATIONS (Continued)

LIST OF ILLUSTRATIONS (Continued)

LIST OF ILLUSTRATIONS (Continued)

2
B

LIST OF TABLES

1.0 INTRODUCTION AND SUMMARY

Fiber optics technology is noted for its immunity to electrical interference, light weight and small size; therefore, it is an obvious candidate for use in various aircraft data or control systems. The Army plans to exploit the features of fiber optics by building and demonstrating an optical flight control system.

This contract was performed to support those plans by developing and testing a digital/optical system for measuring linear position over a 6-inch range with 12-bit resolution. The system comprised a transducer, an Electronic Interface Unit (EIU), and a fiber optic link to interconnect the transducer with the EIU. Most conventional transducers are electrically excited and respond with an encoded electrical output signal. The transducer developed under this contract is considered electrically passive, in that both the input excitation and the encoded output signal was optical, and the only interconnections were by means of fiber optics. The transducer used analog encoding, and the conversion to a 12-bit electrical gray-coded digital was accomplished electronically within the EIU.

The objectives of this contract were:

1. To select, from alternative designs, a transducer approach which best meets the performance and configuration goals set forth in the contract.

2. To carry out the detailed design and fabrication of six feasibility models based on the selected approach.

3. To perform extensive testing of the units to evaluate their performance and compliance with the goals set forth in the contract.

4. To analyze the test data to develop recommendations relating to production configurations of the transducer system. Budgetary estimates for production configuration units were also to be developed.

The contract was performed in two phases. Phase I consisted of item 1 above.

Four distinct transducer approaches were studied by Boeing during Phase I. Three of the approaches involved use of Gray-coded digital encoding patterns and were distinguished by the number of cables and optical emitters and detectors in the electronic interface unit (EIU). The fourth approach used an analog encoding scheme wherein variable-width slits were translated past a pair of viewing apertures to form a position-dependent differential signal. This signal was then converted to digital signals by an A/D converter in the EIU.

Based on several comparative criteria and a numerical scoring system, the analog approach was selected for development in Phase II. The analog approach was selected mostly on the basis of simplicity, producibility, maintainability, reliability, cost, and weight savings.

The feasibility model fiber optic analog transducers produced under this contract have linearities ranging from ± 0.53% to ± 2.00% full scale range (FSR) with a 12-bit digital resolution of ±1.466 mils (infinite analog resolution). In comparison, conventional electrical analog linear variable differential transformer (LVDT) transducers have standard linearities ranging from ± .25% to ± 1.00% FSR (± .05% on special order) with nearly infinite resolution. The digital resolution of the fiber optic analog transducer is determined by the number of bits in the EIU A/D converter. The LVDT is subject to the same restrictions in terms of digital resolution.

LVDTs have been in use for over three decades in both commercial and military applications. During this long time period there has been considerable work involved with improving the linearity of the LVDT, the results being the linearity figures shown in the above paragraph.

In contrast, the fiber optic analog transducer work has only begun with this contract. The transducers produced under this contract were not corrected for linear operation. It is believed that the linearity performance of the fiber optic transducers is excellent given the development nature of this contract and could be improved to meet or exceed LVDT linearity performance by programming the correction needed into the computer-generated encoding plate artwork.

2.0 THE FOUR BOEING DESIGN APPROACHES

2.1 MULTIPLE-EMITTER/SINGLE-DETECTOR DIGITAL CONFIGURATION

The multiple-emitter/single-detector configuration shown in Figure 1 encodes mechanical displacement by means of a digital encoding element with twelve parallel tracks, each track corresponding to a specific bit of a Gray-coded binary word and consisting of alternating reflective and absorbing areas. A reflective area represents, for example, a binary "1", and an absorbing area represents a binary "0". Each of the twelve tracks is illuminated and sensed by a pair of fibers, each with viewing apertures equal in width to the desired resolution. The fibers are oriented at 20° conjugate angles with respect to the surface normal. The fibers are glass-clad with a 100-micron core diameter and a 140-micron cladding diameter. The encoding element consists of 1/8-inch-thick IR-absorbing glass plate with an antireflective coating and a thin-film chromium encoding pattern.

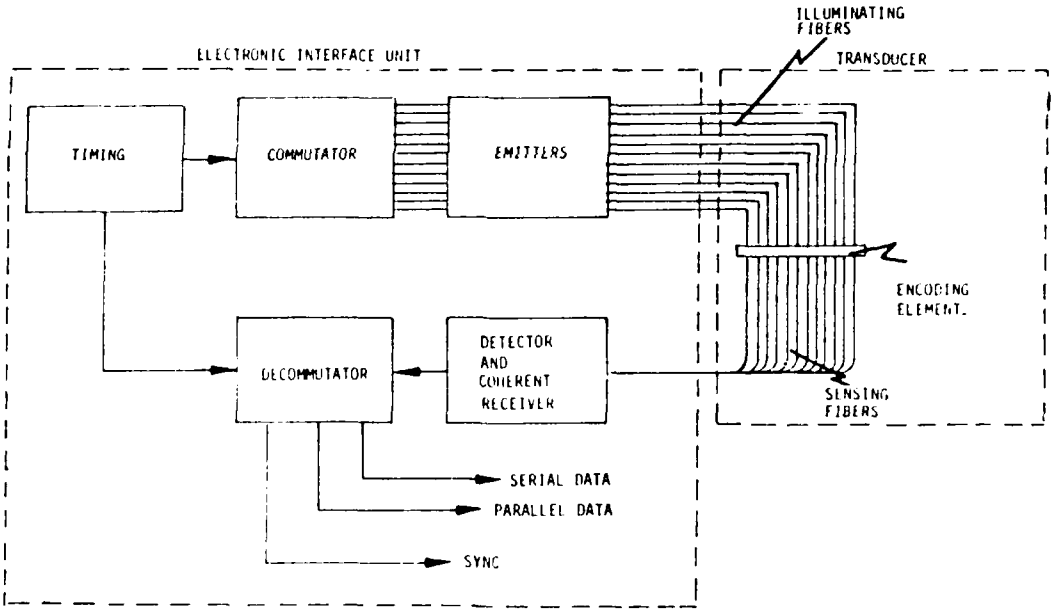

Figure 1. Multiple-emitter, single-detector concept - block diagram.

The twelve illuminating fibers are returned individually to the EIU, where each is illuminated by a separate Light-Emitting Diode (LED). The response fibers are optically combined inside the transducer with a ¼ pitch Selfoc lens and returned collectively to the EIU by a single 200-micron core fiber, where the transmitted light is detected by a single PIN photodiode. The array of emitters is scanned sequentially by an electronic commutator so that the encoding element tracks are illuminated in decreasing order of significance.

The electrical output from the detector is a serial 12-bit Gray-coded word which uniquely defines the position of the encoding element relative to the sensing fibers. The serial word is subsequently processed within the EIU into a 12-line parallel output. The LED's are pulsed "on" for 75 microseconds at a 10 kHz system repetition rate. The low data rate permits the use of complementary metal oxide semiconductor (CMOS) logic, with resulting low power consumption and no special layout problems.

2.2 MULTIPLE-EMITTER/MULTIPLE-DETECTOR DIGITAL CONFIGURATION

The multiple-emitter, multiple-detector approach shown in Figure 2 is identical to the multiple-emitter, single-detector approach with the exception of the number of fiber paths and some differences in the EIU. This approach requires only seven fiber optic paths between the transducer and the EIU instead of thirteen. This is accomplished by commutating the inputs to four LED emitters and decommutating the outputs from three receivers. The optical output from each of the four emitters is split three ways within the transducer by a Selfoc lens to illuminate three tracks of the encoding element. The optical outputs of the sensing fibers are combined by a Selfoc lens within the transducer, in groups of four, into three single paths, the outputs from which are detected by three separate PIN detectors. In effect, each of the twelve bits can be identified by a unique position within a matrix of four interrogation paths and three response paths.

Where p represents the number of emitters, and q represents the number of detectors, an encoding element with (p x q) tracks can be read with (p + q) fiber paths with the proper coding of the emitters and detectors. It is apparent that the previously described multiple-emitter, single-detector configuration is simply a special case of this more general configuration.

As before, a 10-kHz system clock rate is used allowing LED's, PIN detectors, and CMOS logic. The fibers between the transducer and EIU are 200-micron core glass-clad, whereas the internal fibers are again 100-micron core.

With the exception of the different number of Selfoc lenses and cables used, the mechanical designs of the two approaches are identical.

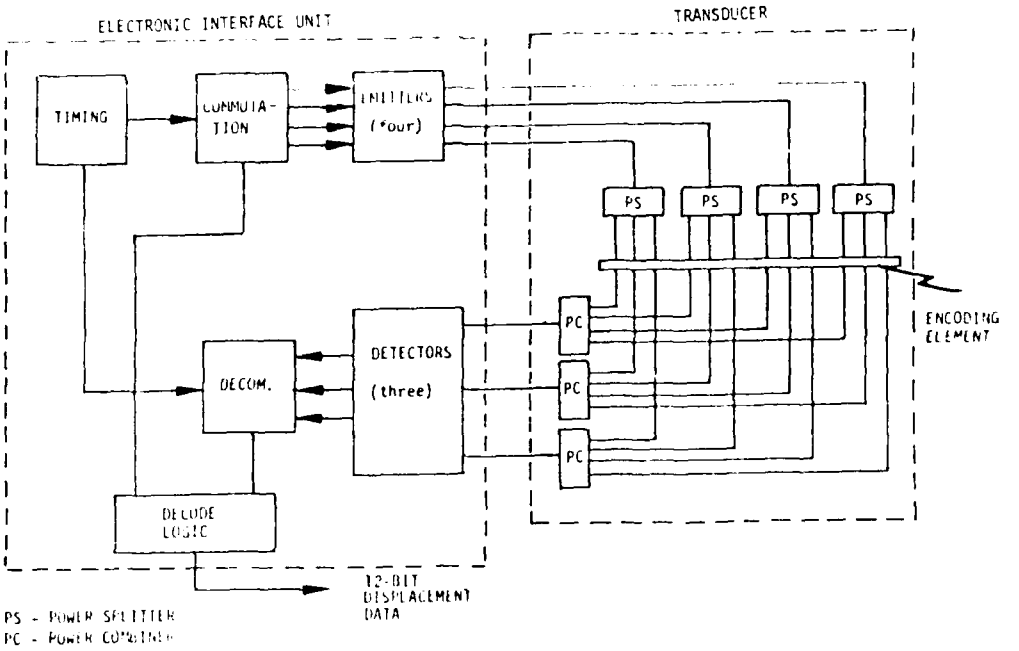

Figure 2. Multiple-emitter, multiple-detector concept - block diagram.

2.3 TIME-DOMAIN DIGITAL CONFIGURATION

The time-domain configuration shown in Figure 3 uses a 12-track encoding element which is identical to those previously described except for the addition of one continuously reflective track which generates a word sychronization pulse and provides a means for automatic compensations; optical fiber pairs are used

to illuminate and to sense the code through a pair of slits. Regardless of the number of tracks, the number of fiber paths to and from the transducer can be reduced to as few as one by making use of the delay properties of optical fibers.

The time-domain configuration was conceived and developed at the Boeing Aerospace Company, and a U.S. Patent was applied for. At the time of this writing, the patent is pending in the U.S. Patent and Trademark Office, and has progressed to the prosecution stage.

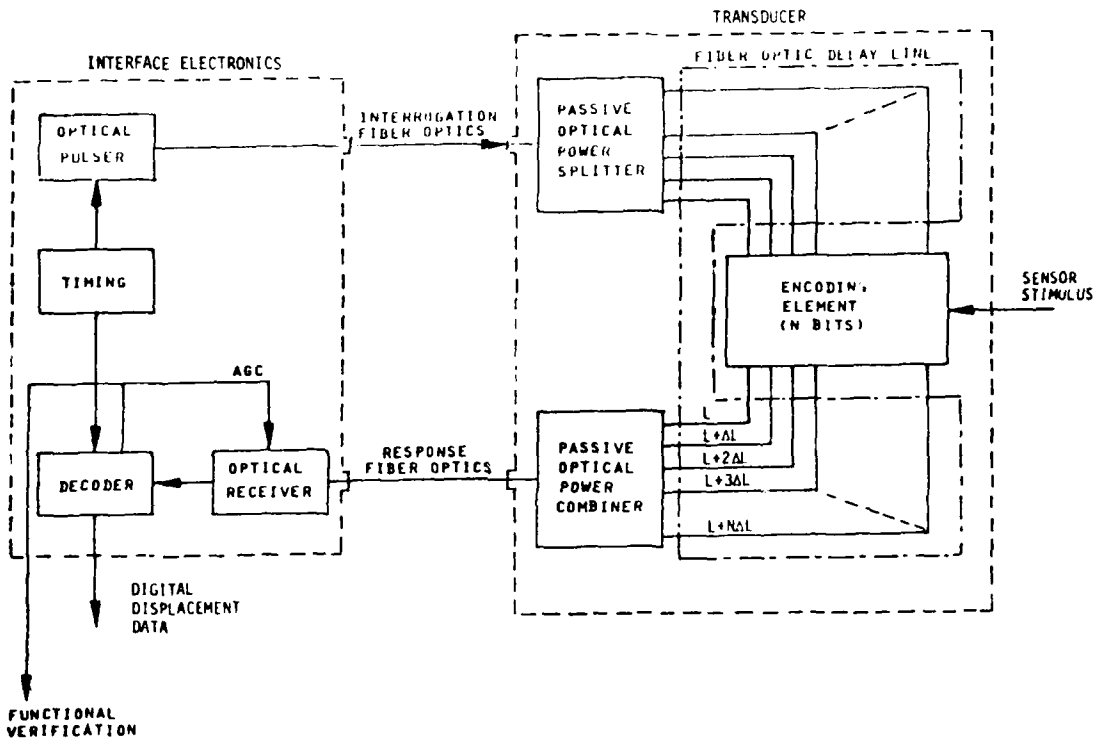

Figure 3. Time-domain concept - block diagram.

These properties make it possible to divide a single short-duration optical pulse among several optical fibers of differing lengths and produce, at the far ends of the fibers, a like number of short-duration optical pulses essentially identical in shape and amplitude but spaced in time. If each of these fibers is used to illuminate a different track of a multi-track optical encoder, then those tracks become sequentially interrogated by the time-spaced pulses. If the time-spaced responses are sensed and recombined, they form a serial binary word. In effect, a form of time-division multiplexing is achieved.

The time-domain transducer consists of the encoding element, the read head, the fiber optic delay-line assembly, one each passive optical splitter and combiner, and fiber optic connectors. The read head assembly is identical to those of the

previous two configurations plus the addition of the extra pair of fibers. The delay-line fibers are again 100-micron core glass-clad, and the two fibers connecting the EIU to the transducer are again 200-micron core glass-clad. Selfoc lenses are used to perform the optical combining and splitting functions.

The interface electronics contains an optical pulser which uses a pulsed injection laser diode as a source, and which emits a repetitive high-energy train of optical interrogation pulses. The interrogation pulses are transmitted by the 200-micron fiber to the transducer where the Selfoc power splitter divides the pulse energy uniformly between the input 100-micron fiber optic delay lines. After being encoded by the encoding element, the time-displaced optical pulses are collected by the output fiber optic delay lines and are recombined by the Selfoc power combiner. The resultant serial data train is returned through the response 200-micron fiber to a single wideband gain-controlled amplifier. The serial output of the receiver is decoded and processed as necessary. The first bit of each response word is a reference bit which is always present regardless of the actual data bits. The automatic gain control maintains the reference bit at a constant amplitude, and thereby allows the system to self-compensate for varying path losses and component degradation. Emitter-coupled logic is used to perform the high-speed digital functions.

The mechanical design is similar to that of the other two digital approaches. However, a small bobbin was added externally to house the delay-line fibers.

2.4 ANALOG CONFIGURATION

The analog transducer shown in Figure 4 consists of a moving element carrying two mirrored plane surfaces which are mutually perpendicular and which intersect in a line which is parallel to the reference plane but skew to the direction of motion. Three stationary rectangular optical waveguides lie in a plane which is normal to the line of intersection of the two mirrored surfaces, and hence also between the two outputs. All three waveguides lie in a plane which is normal to the line of intersection of the two mirrored surfaces. The input waveguide is perpendicular to both output waveguides, and all three waveguides form 45-degree angles with the two mirrored surfaces. Light entering the input waveguide reflects from the two mirrored surfaces into the two output waveguides. The division of optical power between the two mirrored surfaces, and hence also between the two output waveguides, is determined by the longitudinal position of the moving element relative to the plane of the waveguides. In either end position, the power is coupled entirely into one output waveguide or the other.

The transducer is coupled by three fiber optic paths into the EIU. A single emitter illuminates the transducer input, and the two differential outputs from the transducer are coupled into separate detectors followed by separate

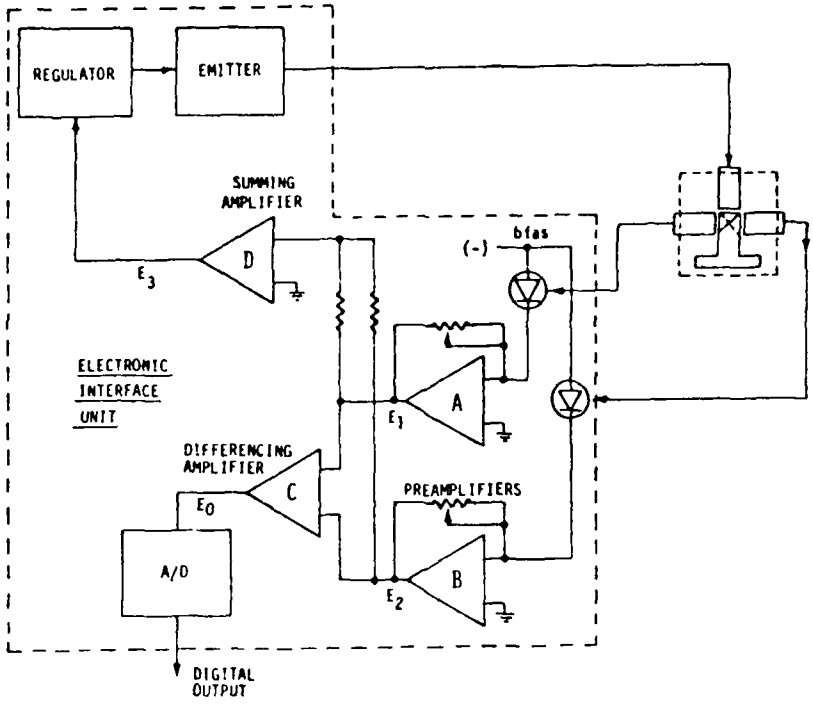

Figure 4. Analog concept - block diagram.

preamplifiers A and B to produce differential voltages E_1 and E_2 which are linearly related to the transducer displacement. The sum of the two detected signals is constant and is used in an AGC fashion to control the drive level to the LED and to form the reference voltage for the 12-bit A/D converter. The difference between the two detected signals is fed to the A/D converter as the input signal. After conversion, the digital signals are displayed.

The LED signal is chopped at a 10-kHz rate and is synchronously demodulated before being applied to the A/D converter. This allows AC coupling within the two receiver channels and eliminates thermal drift concerns.

The physical package of the analog transducer is identical to the digital approaches except that the multiple-fiber-pairs read head, combiners, and splitters are removed and replaced by the three mixing rods.

2.5 APPROACH SELECTION AND RATIONALE

The four transducer approaches were numerically scored in terms of both Army and Boeing criteria. These criteria are listed in Table 1 with their corresponding weighting or "importance" factors. Each transducer approach was given a raw score criterion on a scale from 0 to 10. The final score was determined by dividing each of the raw scores by the sum (of the four raw scores) and multiplying that value by the weighting factor for that criterion.

TABLE 1. WEIGHTED AVERAGE NUMERICAL SCORES

	Multiple Emitter Single Detector		Multiple Emitter Multiple Detector		Time Domain		Analog		Weighting Factors
	Raw Score	Final Score	Raw Score	Final Score	Raw Score	Final Score	Raw Score	Final Score	
a. Accuracy	7	1.62	7	1.62	7	1.62	5	1.15	6
b. Linearity	7	1.62	7	1.62	7	1.62	5	1.15	6
c. Resolution	5	1.75	5	1.75	5	1.75	5	1.75	7
d. System Power Margin	8	2.80	3	1.05	4	1.40	5	1.75	7
e. Flight Safety/Reliability	5	2.39	5	2.39	5	2.39	6	2.86	10
f. Weight Inc. EIU	7	1.40	6	1.20	5	1.00	7	1.40	5
g. Cost	4	0.87	5	1.09	6	1.30	8	1.74	5
h. Maintainability	5	1.50	5	1.50	4	1.20	6	1.80	6
i. Simplicity of Manufacture	5	0.50	3	0.30	5	0.50	7	0.70	2
j. Number of Signal Paths	3	0.68	4	0.91	8	1.81	7	1.59	5
k. Installation Ease	5	0.75	5	0.75	5	0.75	5	0.75	3
l. Electronic Complexity	4	0.63	4	0.63	3	0.41	8	1.26	3
m. Mechanical Complexity	6	1.00	3	0.50	7	1.17	8	1.33	4
n. Possible Incorporation into Actuator	2	0.83	2	0.83	2	0.83	6	2.50	5
o. Self Check Capability	3	1.00	3	1.00	8	2.67	7	2.33	7
p. Probability of Gross Error	3	0.71	3	0.71	8	1.90	7	1.67	5
q. Tolerance to Component Degradation	6	1.43	5	1.19	4	0.95	6	1.43	5
r. Ease of Multiplexing	5	0.43	6	0.52	7	0.61	5	0.43	2
s. Tolerance to Mechanical Wear	5	1.25	5	1.25	5	1.25	5	1.25	5
t. Susceptibility to Contamination	4	0.42	4	0.42	4	0.42	7	0.74	5
u. Developmental Risk	5	1.32	4	1.05	3	0.79	7	1.84	5
CUMULATIVE SCORES		24.90		22.28		26.34		31.42	

As can be seen from the table, the first choice for optimum design is the analog concept followed by the time-domain, multiple-emitter/single-detector, and finally the multiple-emitter/multiple-detector concept. With only a few exceptions, the analog circuit was the leader in all categories. The major reason the analog circuit was optimum was the simplicity of the design -- optically, mechanically and electrically. The total reduction in parts counts will provide

lower cost, improved reliability, lower weight, and lower power requirements. The analog head will be immune to bit dropping/adding problems and should provide the resolution, accuracy, and linearity required for the application. The final output will, of course, still be digital, as performed by the A/D converter.

Discussions of the detailed design, fabrication, testing, and test analyses of the Boeing analog transducers are presented in the following sections.

3.0 BREADBOARD DEVELOPMENT PROGRAM

The intent of the breadboard development program was to explore and evaluate the analog transducer concept. Several optical variations were studied, and a transmissive approach was chosen and fabricated. An EIU was breadboarded and integrated with the optical parts, and the assembly was subjected to several tests for evaluation. The studies, the fabrication processes, the testing methods, and the analyses are described in this section.

3.1 SELECTION OF OPTICAL DESIGN APPROACH

The analog baseline design approach during Phase I of the contract involved a reflective encoding element. Toward the end of Phase I, a transmissive approach was considered and appeared to have potentially improved characteristics. The first task to be performed during Phase II was to evaluate the two concepts and choose between them. It appeared that choosing a transmissive approach would have negligible effect on the outcome of the Phase I approach selection scoring.

3.1.1 THE TRANSMISSIVE ANALOG TRANSDUCER CONCEPT

A fundamental transmissive analog design was accomplished. This design consisted of a moving transparent encoding plate with a pair of thin-film tapered slits deposited along the plate's length. The two slits were deposited side by side and were tapered in opposite directions. An LED in the EIU coupled light through a fiber bundle to the transducer where the bundle was split into two equal smaller bundles. The smaller bundles were coupled to separate mixing rods which served to convert the discrete outputs of the individual fibers into a uniform optical field across the full width of the respective slits. The quantity of optical power passing through the slits was a function of their width which was a function of the longitudinal position of the encoding plate. After passing through the plate, the light was collected by a pair of response mix rods and focused into a pair of separate response fiber bundles. The pair of bundles was returned to a pair of matching detectors in the EIU in the same fashion as for the reflective analog concept. Similar to the reflective approach, the sum of the two detected signals was constant and was used to control the drive level to the LED and to form the reference voltage for the 12-bit A/D converter. The difference between the two detected signals varied with the position of the encoding plate and was fed to the A/D converter as the input signal for decoding and display. In essence, the EIU was identical for the reflective and the transmissive analog approaches. The physical packages would also be similar, the major difference being that the mixing rods would appear on both sides of the element for the transmissive concept.

3.1.2 THE REFLECTIVE ANALOG TRANSDUCER CONCEPT

Two basic reflective analog encoding schemes were considered in the trade study. The original concept used a machined encoder consisting of two

mutually perpendicular mirrored plane surfaces and which intersected in a line parallel to the reference plane but skew to the direction of motion. This scheme is discussed in more detail in Section 2.4. A second scheme under consideration used an encoder consisting of two tapered reflecting patterns deposited on an absorbing substrate. This encoding pattern was essentially identical to that used in the transmissive concept, but with reflective areas substituted for the transmissive areas, and with absorptive areas substituted for the reflective areas.

3.1.3 TRANSMISSIVE VS. REFLECTIVE TRADE STUDY

The results of the transmissive vs. reflective approach trade study indicated that the transmissive approach was superior, and the decision was made to develop it in the breadboard program. The following parameters were included in the study:

1. Producibility
2. Reproducibility
3. Power margin
4. Mechanical guideway tolerance requirements
5. Differential channel crosstalk
6. Availability of materials
7. Packaging
8. Ruggedness
9. Thermal effects

Issues 6 through 9 had little effect on the choice of approach because they impact a reflective or transmissive approach to similar levels. Issues 1 through 5 did contribute to the choice, with all but issue 5 indicating that the transmissive approach is favorable.

The transmissive approach is more producible because a straightforward vacuum deposition process would be used to manufacture the encoding element. Flat glass makes an excellent substrate. Also, the accuracy of the element should be superior because of the benefit of enlarged artwork and optical reduction. A reflective approach would have to be manufactured actual size and the accuracy requirements would be correspondingly more stringent.

The reproducibility of the transmissive approach should be superior because all encoding elements would be produced from a common mask, whereas each reflective element would be individually machined.

Power margin for the transmissive approach would be better for two reasons. First, because the whole encoding pattern is closer to the illumination rods, the rods may be made smaller than for the reflective case (for similarly sized elements). This fact allows for a greater power density to fall onto the element. Secondly, the higher refractive index of the glass substrate of the encoder element will reduce the divergence of the beams, which implies that a higher percentage of power can be coupled into similarly sized pickup mix rods.

Mechanical guideway tolerance can also be more relaxed for the transmissive approach because the spacing between the illumination and pickup mix rods is constant and does not vary with any motion of the encoding element. For the reflective approach, the image of the pickup rod, for example, would move twice the distance of any encoding element motion perpendicular to the intended direction. Due to light beam divergence, such motion would cause a change in the amount of coupled power and, therefore, a modulation of the true reading. A very careful mix rod design could alleviate this problem. However, the problem does not even exist in the transmissive approach.

There is some possibility of cross-channel interference in the transmissive approach due to reflections within the glass substrate. Antireflective coatings could eliminate the problem and, if necessary, a metallized barrier could be placed between the paths. The reflective sensor would be relatively immune to cross-channel interference.

The detailed transmissive breadboard design discussion follows.

3.2 ANALOG TRANSDUCER OPTICAL DESIGN AND FABRICATION

Figure 5 shows the preliminary optical design of the transmissive approach. It is clear how the illumination bundle from the EIU is split and coupled to the two illumination mixing rods, whereas the two response mixing rods are coupled to separate bundles which run individually to the EIU. The mixing rods are shown oriented at right angles to the encoding element.

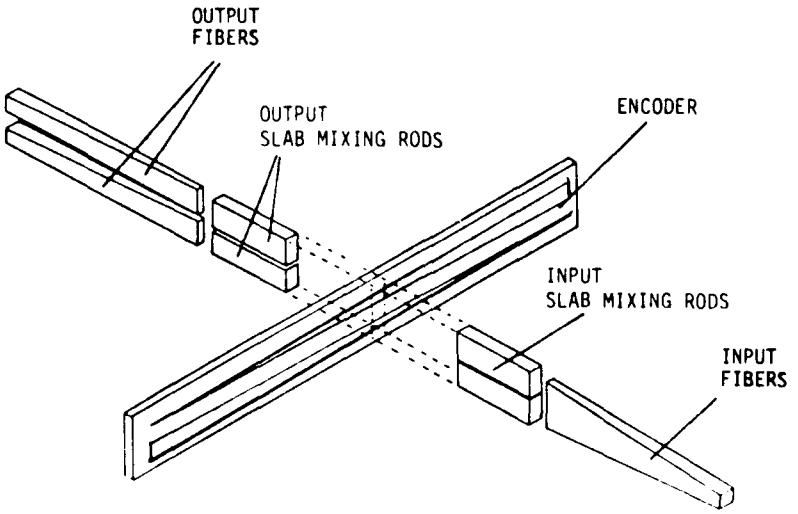

Figure 5. Preliminary optical design.

3.2.1 FIBER OPTIC CABLES

Bundle cables were chosen for all three fiber optic paths based on the need to have a large area and so that the fibers could be grouped into a shape compatible with thin glass mixing rods. Galite 2000 was selected because it met these requirements and had a large core to cladding ratio for efficient coupling with an LED. Its attenuation was greater than other available bundle types, but due to the short cable lengths (5 meters) between EIU and transducer, the loss was not an issue.

3.2.2 LIGHT-EMITTING DIODE

A Spectronics SE 3353-002 was chosen for the LED. Extrapolated from data sheets, the SE 3353-002 can couple approximately 4 mwatt peak (@ 200 ma) into a 1.14 mm bundle, such as Galite 2000. This was verified in the laboratory.

3.2.3 PIN PHOTODIODE

The photodiodes selected were Texas Instruments TIED 80's because of their low capacitance and large active diameter (2.54 mm). Responsivity of these detectors at 820 nm, the LED center wavelength, is 0.5 amps per watt.

3.2.4 FIBER OPTIC CONNECTORS

For the breadboard, connectors were not used between the cables and the transducer mixing rods. Connectors were used, however, between the cables and the EIU. Amphenol 905-series connectors were selected because of Boeing's success with them in previous applications and because of availability. The LED and the two detectors were mounted in Amphenol receptacles which were mounted in the EIU. EPO-TEK 353ND epoxy was used to cement the bundles into the connectors.

3.2.5 TRANSMISSIVE ENCODING ELEMENT

The encoding plate is shown in Figure 5. The glass substrate was cut from 0.063-inch photographic plate chosen for its uniformity. The thin-film metallization was chromium. The transparent slits were 6.50 inches long, 0.30 inch longer than necessary for the 6.00-inch travel plus 0.20-inch overtravel. The 0.30 inch was added so that the very ends of the tapers were not used and as such, concerns about slit diffraction and pattern irregularity could be ignored. Therefore, the portion of the pattern actually used was between 0.15 and 6.35 inches. At either of these end points, the width of the narrower slit was 0.236 mils and the width of the wider slit was 0.100 inch. The spacing between the outer edge of the two slits was 0.48 inch. The slit widths and spacing were chosen as trade-offs with the width and spacing of the mixing rods discussed in Section 3.2.6.

The thin-film analog pattern was generated on a Haag-Streit Coordinatograph used normally to cut patterns for hybrid microcircuits. The pattern was cut into Ruby Studnite and was oversized by a factor of 5.5. Each cut was made along the same axis of the machine and in the same direction, thereby reducing (if not cancelling) any fixed tracking errors the machine may have. The artwork was then photoreduced on a Borrowsdale Microminiaturization camera onto photographic glass to actual size. The glass plate was then used as a mask for thin-film deposition of the pattern onto the final 0.063-inch substrate. After deposition, the substrate was scribed and broken to size.

3.2.6 MIXING ROD DESIGN

Since each slit can be thought of as a linearly varying shutter, the optical power through the slit will be linear if and only if the optical power density across the slit is constant. This requirement places restrictions on the geometry of the illumination rods:

a. The mixing rod must have a sufficient length-to-fiber-diameter ratio so that the multiple fields from the individual bundle fibers at the input end of the rod are fused into a uniform single field at the illuminating end. This assumes equal power coupled from each individual fiber.

b. Since the power coupled from the individual fibers may vary slightly due to imbalances in coupling or fiber attenuation, the mixing rod ideally should have sufficient length-to-width ratio such that any individual fiber at any point along the input to the mixing rod will produce a uniform field at the rod's illuminating end. The total field strength would then be the sum of the field strengths of the individual fibers.

c. The width of the rods (in the direction perpendicular to slit travel) must be sufficient to ensure that the slit remains in the rod's near field region of maximum power density.

Figure 6 illustrates the power density regions that would appear across the end of a rectangular mixing rod. Region 3 is characterized by constant power density (in the dimension shown), and this is the region in which the slit must remain. Region 2 is characterized by a decreasing power density out to Region 1, where no light would be measured. The angle θ, the maximum angle which a ray can emerge from the rod, is determined by the NA of the optical system which, in this case, is determined by the NA of the bundle fibers (0.66 for Galite 2000).

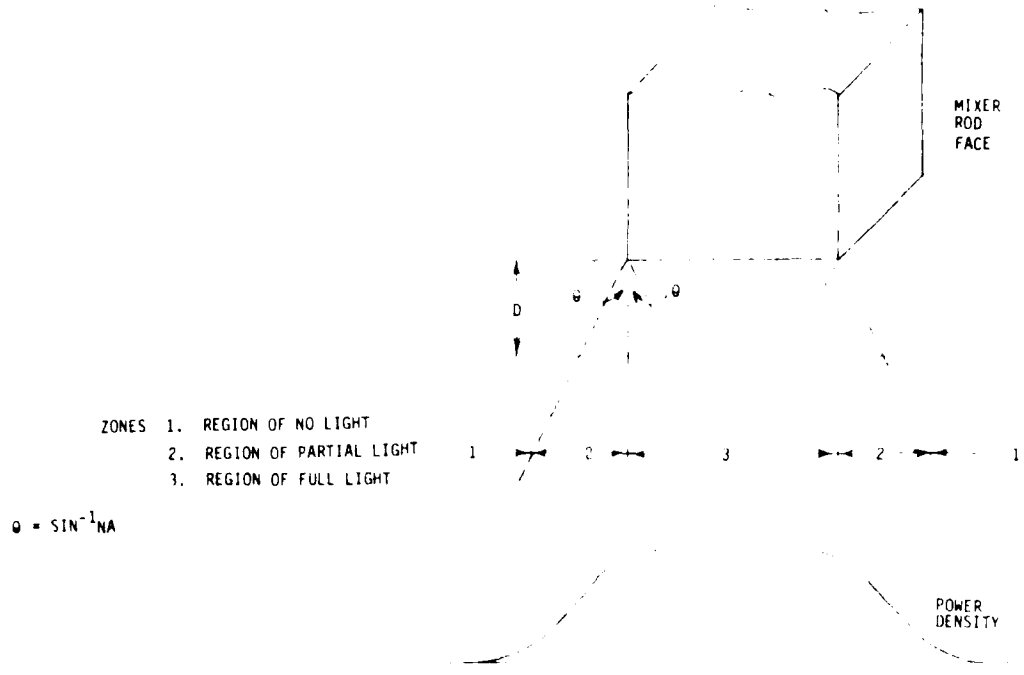

Figure 6. Power density zones.

Similar requirements are imposed upon the geometry of the response mixing rods. Since their function is, in essence, the converse of the function of the illumination rods, all items above are applicable. Item (a) applies because of the need to eliminate the discreteness due to the presence of individual fibers. Item (b) applies because the coupling from the mixing rods to the detectors may vary for the individual fibers. Item (c) applies because it is essential that all light passing through the slit (in the direction perpendicular to travel) be gathered by the response rods.

Galite 2000 contains approximately 210 fibers per bundle, and each fiber diameter is 2.68 mils. For optimum coupling from the response mixing rods into the return bundles, the butting area of the rods should not exceed the area of the respective bundles. The following design was established:

1. Each return bundle was reshaped into two rows stacked one upon the other of 105 fibers each. Two rows were chosen because that was a best compromise between maximum rod width and minimum rod thickness, the latter being no less than 5 mils.

2. The width of the rods was to be no greater than 105 x 2.68 mils or 0.281 inch. The width chosen for the response rods was 0.27 inch.

3. The length of the rods was a compromise between items (a) and (b) of the mixing rod requirements. A length of 0.70 inch represents a

length-to-fiber-diameter ratio of 260 and a length-to-width ratio of 2.6.

4. By angular analysis of light rays through the encoding plate (allowing for mechanical tolerance on the encoding plate travel and assuming a plate to mixing rod gap of 0.02 inch), the maximum slit width of 0.10 inch was chosen.

5. By similar angular analysis, and with a gap of 0.02 inch, an illumination mixing rod width of 0.16 inch was chosen. This width is compatible with two rows of fibers of 52 or 53 fibers each at the input end. (Recall that the illumination bundle is split into halves, with 105 fibers coupled to each illumination rod). These mixing rods' dimensions satisfy item (c) of the mixing rod requirements.

The response mixing rods were placed 0.10 inch apart. This was determined to be sufficient to prevent cross-talk between the two response channels caused by reflections internal to the encoding plate substrate. As a result, the two pattern slits were spaced 0.48 inch outside edge to outside edge.

Microscope slide covers were used for the mixing rods. Their thickness was approximately 5 mils, the thinnest readily available glass. The loss was measured through a 0.70-inch sample and was found to be roughly 1 dB.

An investigation was conducted wherein small cylindrical lenses were placed along the edges of the mixing rods in an attempt to focus the light in the direction parallel to encoding plate travel. The lenses would have no effect on the light pattern perpendicular to encoding plate travel. The investigation did not show any noticeable improvement in coupling efficiency, and thus the idea was rejected due to added construction complexity. The lens approach should prove beneficial if extra care is taken to ensure proper shape and size. However, it was determined that their use was not necessary anyway, as power margin was later measured and found to be ample.

The mixing rods were made by first scribing and breaking them to slightly above their final dimensions. A sandwich of three like-sized rods was cemented together and to a lapping fixture. The center rod of the three was used in the breadboard model, since it was always the one with the fewest chips along the edges. Four sandwiches were lapped, since four mixing rods were required.

3.2.7 FIBER AND MIXING ROD ASSEMBLY

The bundle fibers and the mixing rods were integrated into illumination and response heads. These two heads were very similar, the only exceptions being that the illumination head contained a single split bundle whereas the response head had two separate bundles, and the mixing rod widths were different. Due to the similarity, only one head manufacture is discussed below.

The head was built as two parts: the fibers' mount and the mixing rods' mount. The two parts were machined as a single piece and then cut to ensure that alignment was good when later remated. Alignment rods were added to ensure that such was the case.

The fibers were laid into 6-mil-deep channels. Another piece was laid over the top to confine them into the channels. A section of 5-mil slide cover glass was then gently pushed in from the outsides of the channels to force the fibers into the desired two stacked rows mentioned earlier. The fibers were cemented in place and the ends lapped flush with the end of their mounting surface.

The mixing rods were laid into the mating channels of the second part and again forced gently in from the sides. The mixing rods were clamped in silicon RTV to provide a low-index (1.40) cladding. As with the fibers, the mixing rods were also lapped flush with their mounting surface.

The two portions of each head were then remated, butting the fiber rows together with their respective rods. They were secured into place on an aluminum jig containing a slot through which the encoding plate could travel. The jig with the heads and the encoding plate was fixed to a precision milling machine to form the breadboard test bed. Figure 7 is a photograph of the test bed.

3.3 ELECTRONIC INTERFACE UNIT DESIGN AND FABRICATION

The design of the electronic interface unit (EIU) was divided into three parts: receiver design, transmitter design, and display circuitry design. A preliminary trade study indicated that virtually drift-free operation could be anticipated if an LED transmitter was driven by a square wave carrier current source. On the basis of this plan, the receiver portion of the EIU was designed with two AC amplifier paths, demodulator and filter circuits, and a quality A/D converter.

3.3.1 RECEIVER DESIGN

There are two separate optical inputs to the EIU receiver, "A" and "B". Texas Instruments TIED80 photodiodes were selected as the optical detectors because their large active area is compatible with the bundle fibers being used. To determine the best method of converting the AC carrier signals to DC, precision full-wave detectors were compared with synchronous demodulators. It was found that a synchronous demodulator rejects quadrature signals and also rejects low frequency noise, while the precision full-wave rectifier does neither. The synchronous demodulator was therefore selected.

The analog EIU was specified to have a difference amplifier which determined the relative power in channels A and B, and a summing amplifier which determined total optical power for a reference signal and also served as a

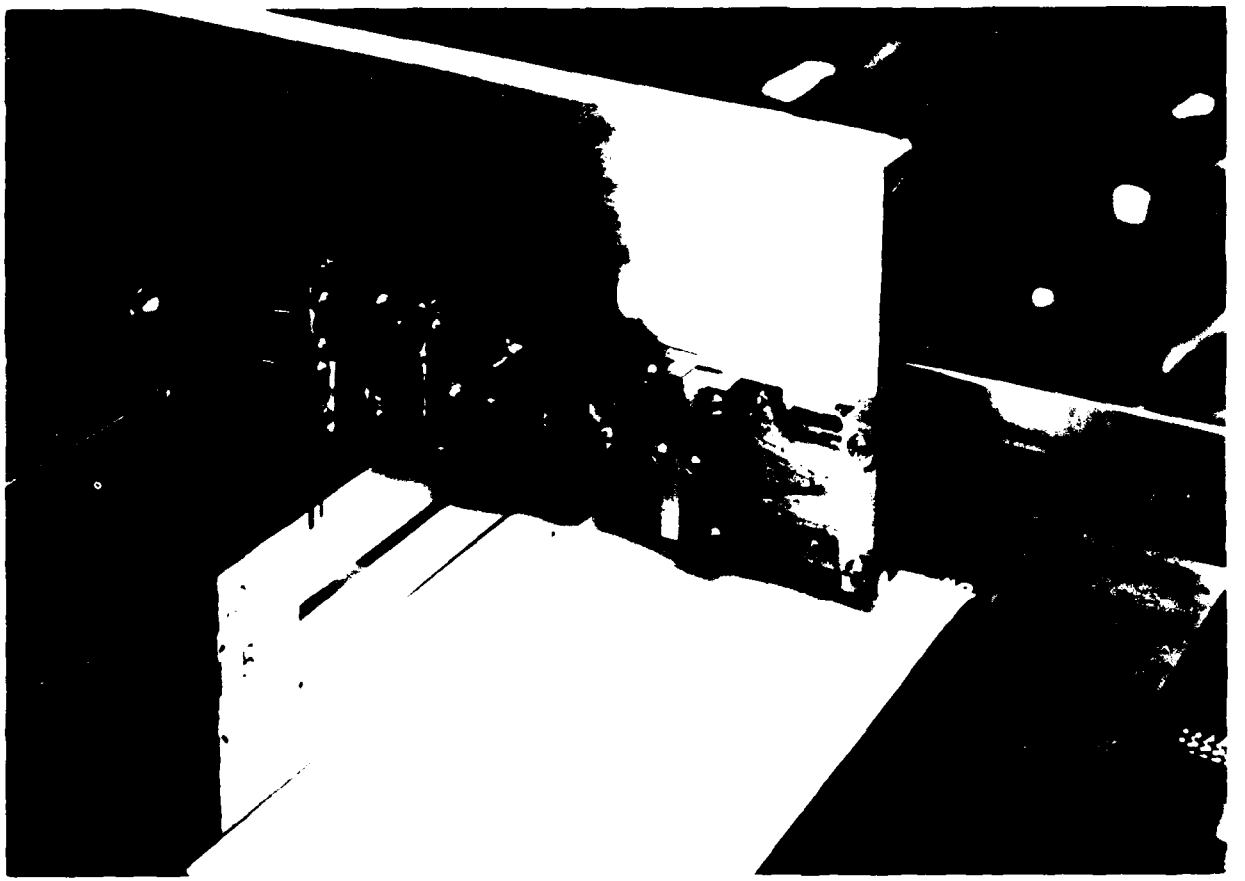

Figure 7. Breadboard test setup.

reference for the A/D converter. Whether these amplifiers should operate on the AC signals before demodulation or on the filtered DC signals after demodulation was decided after evaluating the relative stability of circuits based on the two approaches. Experience has shown that summing and difference amplifiers are much easier to stabilize than are filters and demodulators. For a circuit which takes the sum and difference of AC signals and then demodulates the sum and difference separately, it was calculated that a 5% relative gain change in the two demodulator-filter paths would cause a worst-case error of 2.5% in the A/D output. For the circuit which first demodulates and filters the A and B receiver inputs and then derives the sum and difference voltages, a 5% relative change in the two demodulator-filter paths would cause a worst-case error of only 1.22%. The second approach offers overall stability roughly twice that of the first approach and was therefore chosen in the design.

The AC amplifier stages of the EIU included a transimpedance preamplifier and a postamplifier. A National Semiconductor LF356AH BI-FET operational amplifier was selected for the preamplifier because of its high input impedance, low drift and low noise characteristics. For the postamplifier and following analog circuits, a Texas Instruments TL084 was selected because it provides four high quality op amps in a single package. This type of package facilitates efficient analog parts layout and provides flexibility for design changes. A Siliconix DG189 analog switch was selected for the synchronous demodulator because of its extremely low ON resistance.

An important requirement for the position transducer is that a slew rate of 6 inches per second not cause an error in the EIU output greater than 0.015 inch. Analysis of the circuit conditions required to meet this specification led to the decision to use a 10 kHz square wave carrier frequency and a three-section Butterworth low-pass filter following the synchronous demodulator. This carrier frequency and filter combination also made twelve-bit resolution possible, as required, by providing adequate carrier rejection.

The analog-to-digital (A/D) converter used in the EIU receiver had to meet several strict requirements. The conversion time had to be fast enough to meet the transducer slew rate vs. accuracy specification. The converter had to provide a serial data output to meet contract requirements, and a parallel data output to provide twelve bits for the dual EIU display. The micro network MN5204 A/D converter was chosen because it fulfilled all requirements and is available in a military version, the MN5204H.

A block diagram of the final EIU circuit is shown in Figure 8. The difference amplifier provides the A/D converter with an analog signal that ranges from +5 volts for a 0-inch transducer position to -5 volts for a 6-inch position. The reference signal from the summing amplifier is nominally -10.0 volts, and this same signal is used to control the LED current in the transmitter.

3.3.2 TRANSMITTER DESIGN

A Spectronics (Honeywell) SE3353-002 LED was chosen as the emitter for the EIU transmitter because of its high power output and its compatibility with a fiber optic bundle cable. To provide the 200 mA maximum peak LED current, a Siliconix VMOS power FET (2N6659) was selected.

As shown in Figure 8, a clock circuit drives both the transmitter and the synchronous demodulator. The clock is based on a 1 MHz crystal oscillator divided down to 10 kHz, and a delay circuit synchronizes the clock to the delayed receiver signals for the synchronous demodulator. A test circuit was included in the transmitter design so that the EIU receiver section could be tested without any optical apparatus.

The power regulator circuit uses the -10.0V reference voltage from the summing amplifier to control the transmitter power so that total optical input power to the receiver is held within ± 1% of a nominal value, until the LED emitter approaches the maximum rated current of 200 mA due to excessive loss in the

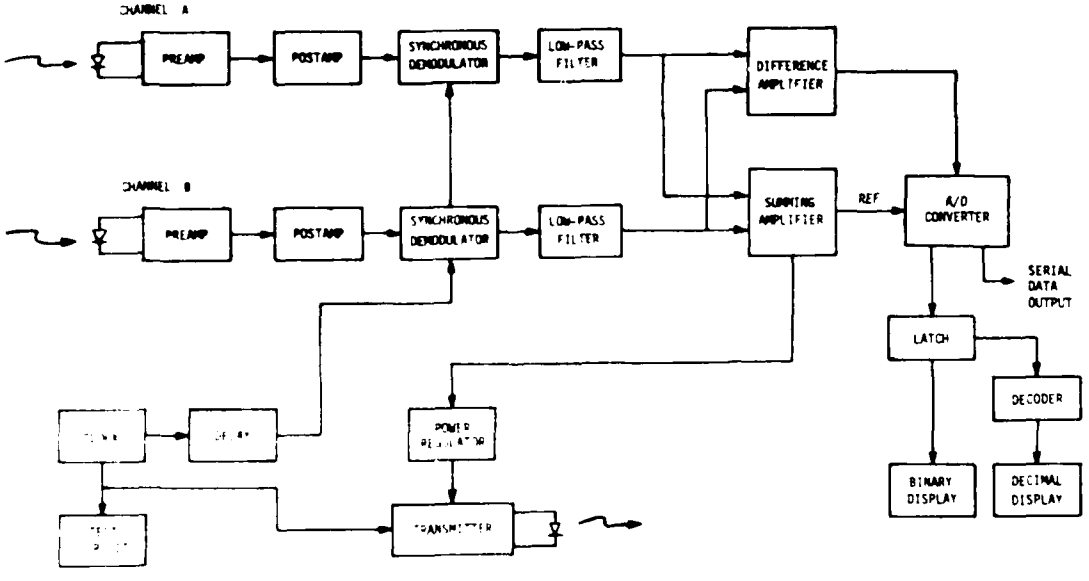

Figure 8. EIU block diagram.

system. A monitor circuit was planned but not implemented that will output a failure warning signal when the LED current approaches the 200 mA limit. This would indicate degradation of either the LED or some other link in the optical system.

3.3.3 DISPLAY CIRCUITRY DESIGN

The MN5204 updates its 12-bit output over 15,000 times each second. To avoid blurring the display, this rate was divided down and a latch was designed to be updated at a rate slightly below 4 Hz. The latch outputs drive twelve point-source displays to indicate the 12-bit position word, and gates derive the overtravel displays for transducer positions outside the nominal 6-inch travel.

Various methods for deriving a decimal display from the binary A/D output were considered and an erasable-programmable read only memory (EPROM) look-up table was selected because of its accuracy and simplicity. The midpoint of travel, 3 inches, was defined as binary 100 000 000 000. From this definition, and from the requirement for overtravel indication, a conversion table was developed and the table was programmed into two 2732 EPROMs. The BCD outputs of the EPROMs drive four LED displays to provide the required decimal information in inches.

3.3.4 EIU FABRICATION

The breadboard EIU was assembled on two separate pieces of perforated Vector breadboard material so that the EIU digital circuit noise would not interfere with analog circuit operation. The analog components were soldered onto pushpins to facilitate design changes, and the entire analog breadboard was shielded in an aluminum chassis. A ribbon cable connected the analog circuit to the digital breadboard, and a 14-pin connector was used to attach external power supplies adjusted to +15V and +5V.

3.4 BREADBOARD TEST PROGRAM

The purpose of the breadboard tests was to either demonstrate or provide insight into the following areas:

a. Optical power margin
b. Linearity and accuracy
c. Positional tolerance for the encoding element
d. Mixing rod uniformity
e. Materials selection for mixing rods, epoxies, pattern substrate, and pattern thin-film
f. Component selection or design including emitter, detectors, cables, connectors, and EIU electronics

The following tests were performed to accomplish the test goals set forth above:

a. Optical power vs. displacement (each channel)
b. Optical power margin
c. EIU readout vs. displacement
d. Encoding plate positional tolerance (perpendicular to travel)
   (1) Horizontal
   (2) Vertical
e. Mixing rod optical density scans

3.4.1 OPTICAL POWER VS. DISPLACEMENT

Figure 9 shows the quantity of optical power coupled from a test LED through each channel of the optical portions of the breadboard. The LED was a unit identical to that used in the breadboard EIU. The power was measured with a UDT-11A power meter.

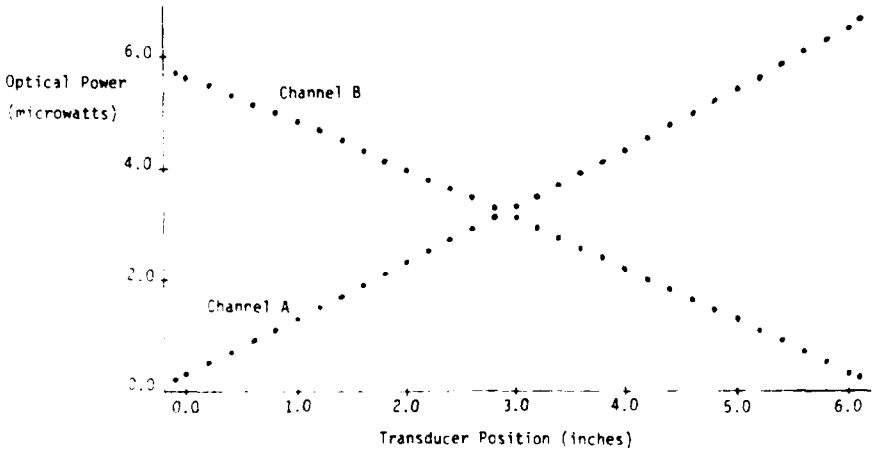

Figure 9. Optical power profile of the breadboard transducer.

To be completely linear, each of the individual channel curves must be linear. Some curvature is evident, and this results in some nonlinearity for the whole system. The difference in slopes between the two plots indicates a small imbalance in attenuation between the two channels. However, this is easily compensated by the EIU adjustments.

3.4.2 OPTICAL POWER MARGIN

To accomplish this test, the optics were connected to the EIU and the system was aligned. The encoding plate was set at the midpoint (3.000 inches) and a precision voltage source was connected to the cathode of CR18 to control the drive level to the LED and hence, the optical power output.

Two types of optical power margin tests could be performed. The first type would add attenuation into the optical paths until the EIU readout began to falter. In this case, due to the feedback action within the EIU, the drive level applied to the LED would increase further, the SUM voltage applied as the reference to the A/D converter would increase from approximately -10.0 volts to approximately -9 volts at which point the A/D converter would become inoperative, and the display would be in error. This is the type of optical power margin test run according to the Test Plan (Appendix A) for the production transducer systems.

The second type of optical power margin test, and the type performed on the breadboard, involves adding attenuation to the optical path but also increasing the gains in the EIU channels to maintain the A/D reference voltage near -10.0. By this type of test, the ultimate attenuation limit is determined. The EIU display would indicate the correct position until the input optical signals became so weak that noise in the preamplifier stages became significant and masked the true signals from the detectors. Two things may be learned: the sensitivity limit of the EIU and the maximum allowable loss through the optical portion of the transducer. In the actual breadboard test, the attenuation was added artificially by reducing the drive to the LED.

From the tests, the sensitivity limit for the EIU is 0.1 microwatt total optical power. Since the average power coupled into the input cable from the LED is 900 microwatts, the maximum allowable optical loss is 39.5 dB.

3.4.3 EIU READOUT VS. DISPLACEMENT

The EIU alignment procedure includes adjustments that compensate for differences in optical attenuation for the two optical channels and for a constant offset between the channels. Because of this, the EIU readout at 0, 3 and 6 inches will correspond to transducer displacement once the EIU is aligned. To determine the accuracy and linearity of the transducer, data on EIU readout versus displacement was taken at 0.1-inch increments for the entire 6 inches of transducer travel, and the deviation of the EIU readout from actual position was then tabulated. Figure 10 shows a plot of deviation versus displacement for the breadboard system.

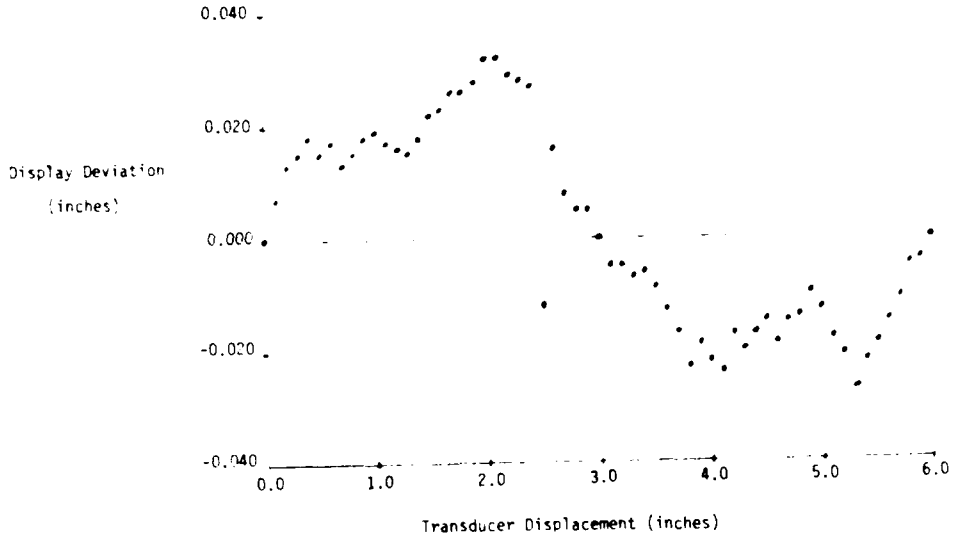

Figure 10. Deviation of EIU readout from transducer diaplacement.

Since a definite nonlinear pattern was observed in the deviation plot, tests were conducted to determine if this nonlinearity was caused by the EIU electronics or by the optics in the transducer. The tests showed that the EIU display closely tracked the outputs of the EIU preamplifiers, and that the outputs of the preamplifiers closely tracked the optical input power. Therefore, almost all of the nonlinearity in the deviation plot was shown to be caused by the transducer optics.

3.4.4 ENCODING PLATE POSITIONAL TOLERANCE

The transmissive encoding plate concept was selected for the optical transducer in order to minimize the effects of lateral and vertical motion of the encoding plate needed for mechanical tolerances and wear. Ideally, all the variation in optical output power between the two fiber optic channels should be caused by longitudinal motion of the encoding plate, and the field of light across the two patterns on the encoding plate should be uniform for system linearity. The following tests were conducted to check the effects of lateral and vertical encoding plate motion on the EIU readout.

3.4.4.1 LATERAL TOLERANCE

There was a gap of about 4 mils (0.004 in.) between each side of the encoding plate and the ends of the mixing rods. To determine the effect on EIU readout of changing these gaps, the encoding plate was moved laterally in each direction about 3 mils. This test was performed with the transducer set at three different positions: 0.100 inch, 3.000 inches, and 5.900 inches. The normal readings and variations obtained were as follows:

Mechanical Position (in.)	Normal Reading (in.)	Minimum Reading (in.)	Maximum Reading (in.)
0.100	0.106	0.104	0.106
3.000	2.999	2.996	3.003
5.900	5.894	5.894	5.894

Small variations were observed, especially at the midpoint.

3.4.4.2 VERTICAL TOLERANCE

If variation in the EIU readout were observed due to small vertical motion of the encoding plate, the optical field from the mixing rods would not be uniform and nonlinear transducer operation would result. Also, the readout would be sensitive to vibration and plate wear. To determine the effect of vertical motion, the encoding plate was lowered and raised ±.004 inch vertically between the mixing rods. This was performed with the transducer set at 0.100 inch, 3.000 inches, and 5.900 inches. The results were as follows:

Mechanical Position (in.)	Normal Reading (in.)	Minimum Reading (at -0.004 in.)	Maximum Reading (at +0.004 in.)
0.100	0.107	0.100	0.113
3.000	3.000	3.000	3.001
5.900	5.897	5.893	5.890

Again, small variations were observed. However, the variations were greater near the end points than at the midpoint. This situation was opposite that observed during the horizontal tolerance test.

3.4.5 MIXING ROD OPTICAL DENSITY SCANS

For linear operation, a uniform field must be incident onto the encoding plate. Also, all differential areas across the pattern width must equally couple their optical power into the receiving mixing rods. To assess the ability of the optical elements (mixing rods) to achieve these goals, scan tests were run to measure the uniformity. For each channel, the encoding plate was translated toward the appropriate end point where the width of the encoding slit for that channel was

very narrow. These points were each 0.1 inch past the normal 6-inch stroke range or at the overtravel limits. At these points, the respective pattern widths were 0.0025 inch. To test channel A, the transducer was set at -0.100 inch whereas, to test channel B, the transducer was set to 6.100 inches.

The optical cable to the transducer was excited by the LED in the EIU and was held at its maximum output power. The response cables were coupled (one at a time) to a UDT-11A optical power meter while the respective 0.0025-inch slit was translated vertically past the mixing rods. The scan results are plotted in Figures 11 and 12. The plots show a reasonably flat response pattern for channel A and a sloping response pattern for channel B.

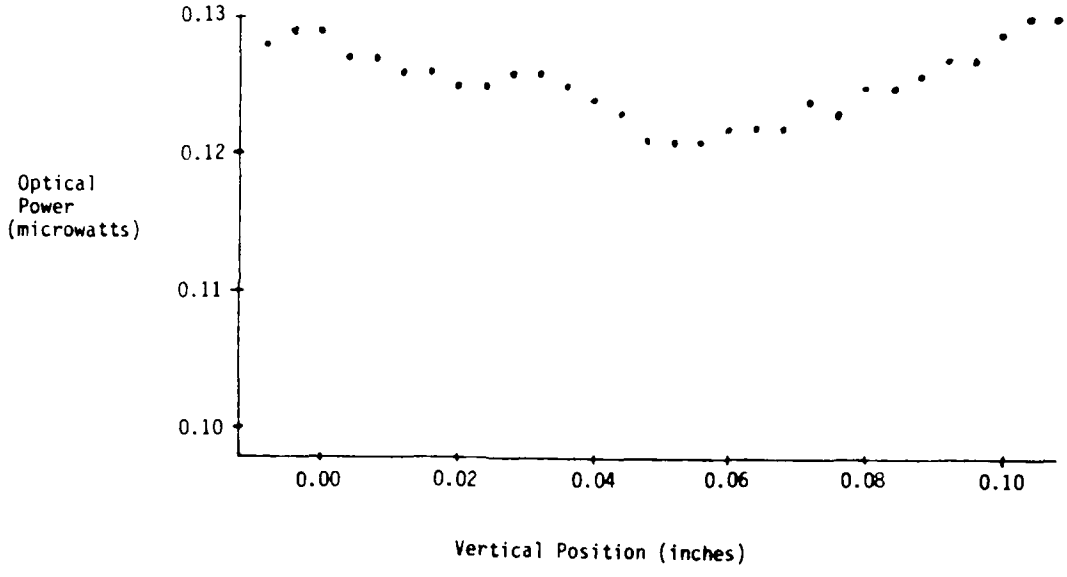

Figure 11. Channel A optical power density.

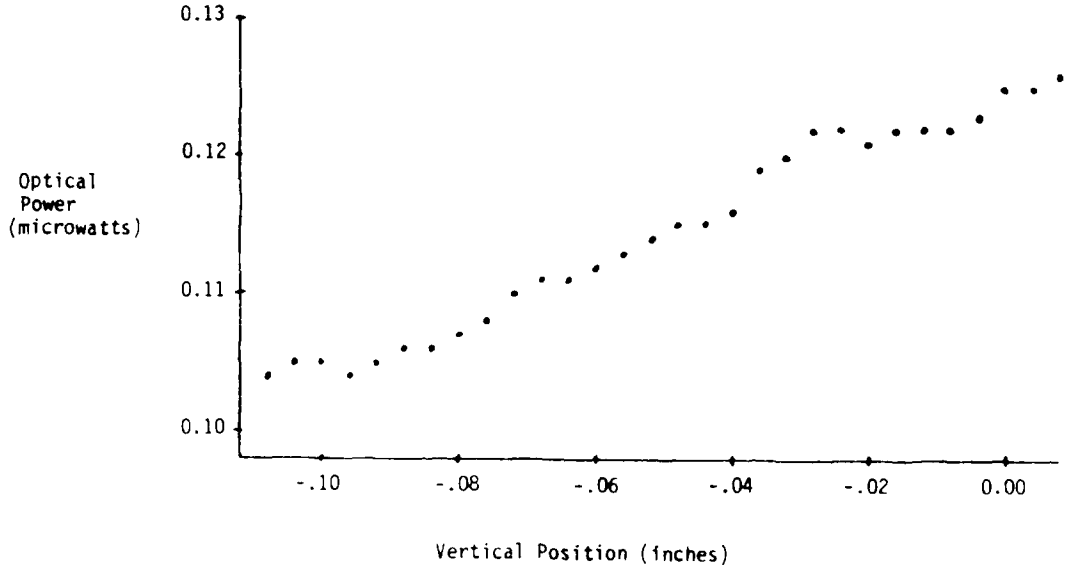

Figure 12. Channel B optical power density.

3.4.6 BREADBOARD TEST ANALYSIS

The test results were analyzed and conclusions were drawn in three categories: optical power margin, positional tolerance, and linearity. The conclusions are presented below.

3.4.6.1 OPTICAL POWER MARGIN

The optical power margin test showed that the maximum allowable optical loss for the transducer and cables was 39.5 dB. Measured optical power loss through the system was 23 dB, giving an optical power margin of 16.5 dB. This is considered adequate to allow for device degradation and tolerances.

3.4.6.2 ENCODING PLATE POSITIONAL TOLERANCE

The horizontal and vertical positional tolerance tests had some small effects on the readout. Ideally, only longitudinal movement would affect the readout. The effects due to the vertical movement were caused by nonuniformity in the optical fields across the mixing rods. As the pattern was lowered or raised, it entered regions of greater or lesser intensity, thereby altering the throughput powers and the readings. The nonuniformities were verified by the optical scan tests described in Section 3.4.5. The effects observed during the horizontal tests can be explained by similar reasoning.

3.4.6.3 LINEARITY

The causes for nonlinear operation of the breadboard optics (nonlinear optical power versus distance, sloped light distributions on the encoding plate, etc.) were not clearly understood. A simple 2-D computer ray trace program was developed to analyze and/or isolate causes of optical nonlinearity. The issues studied included:

a) Length of mix rods
b) NA of fibers
c) Angular offset of fibers
d) Positional offset of fibers
e) Both c) and d)

Optical rays were traced from the input fibers through the illumination mix rods and onto the encoding plate. Ray density techniques were used to compute the light distribution on the encoding plate tracks, with the total number of optical rays traced being 50,000 (50 fibers with 1000 rays/fiber). A listing of the FORTRAN computer ray trace program is provided in Appendix D. For linear operation of the transducer, the light distribution must be constant across the encoding plate tracks as discussed in Section 3.2.6.

3.4.6.3.1 LENGTH OF MIX RODS

Figure 13 shows the calculated effect of illumination mix rod length (inches) on optical power density at the encoding plate. The uniformity of optical power across the encoding plate slit is expressed in terms of standard deviation. The mix rod width was 0.16 inch and the length was 0.78 inch, which is seen to be in a region of highly uniform light distribution (low standard deviation); therefore, the mix rod length of 0.78 inch should not affect the linearity significantly.

3.4.6.3.2 FIBER NA

The calculated optical power density at the encoding plate is dependent on the input fiber numerical aperture (NA) as shown in Figure 14. In these calculations, the NA of each source fiber was assumed to be filled; the mix rod length was the same as in the breadboard transducer (0.78 inch). The optical fiber cables

(Galite 2000) used in the breadboard program had an NA of 0.66 which results in a highly uniform optical field (standard deviation 1.2) and therefore should not affect the linearity significantly.

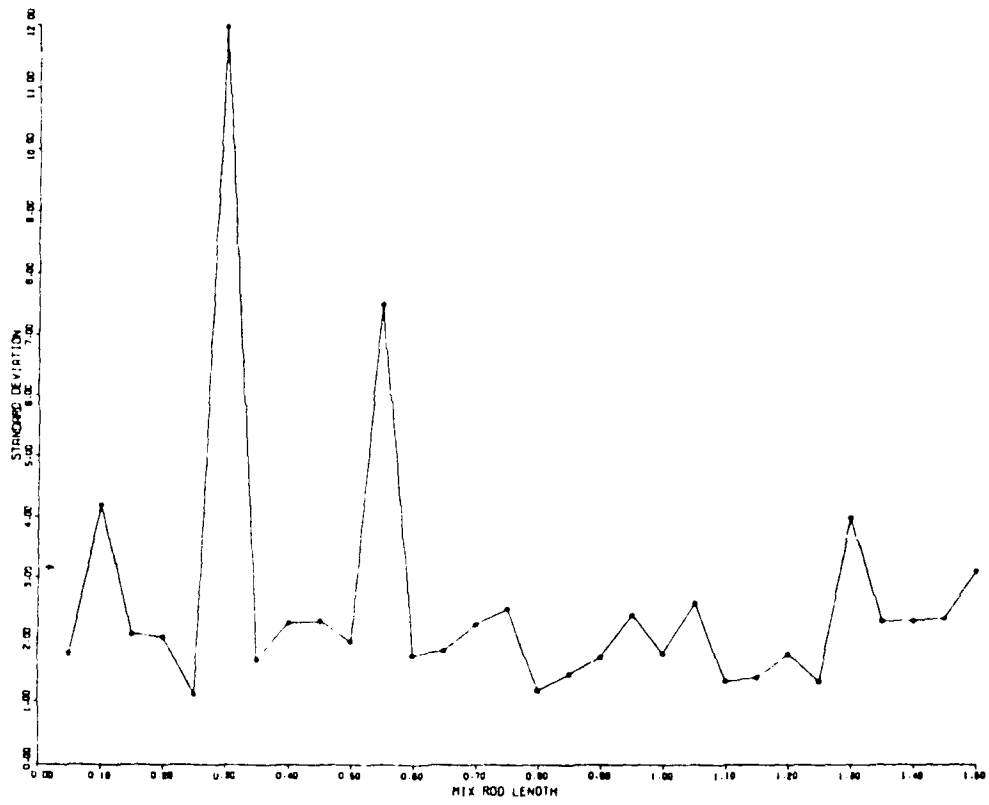

Figure 13. Calculated effect of mixing rod length changes for the breadboard transducer.

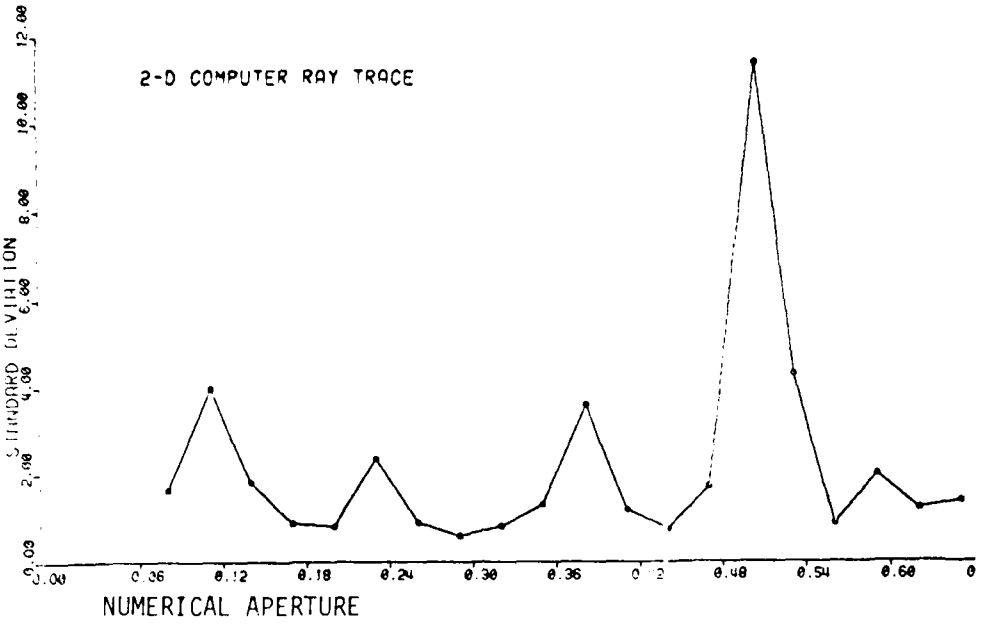

Figure 14. Calculated effect of changing input NA to the breadboard mix rods.

3.4.6.3.3 ANGULAR OFFSET OF INPUT FIBERS

Computer ray trace results show that an angular offset of the input fibers generally produces a sloping optical density profile at the encoding plate. This will result in nonlinear operation of the transducer, since the optical power is not a linear function of displacement. Measurements using a HeNe laser on the breadboard transducer revealed that the channel A input fibers were tilted at -1.6 degrees with respect to normal incidence and that the channel B input fibers were tilted at 3.6 degrees. For the case of the input fibers tilted at 3.6 degrees, the computer ray trace showed that a sloping optical power density profile with a standard deviation of 2.4 resulted. The decrease in optical uniformity from angle input fibers should produce nonlinear transducer operation.

3.4.6.3.4 POSITIONAL OFFSET OF INPUT FIBERS

Theoretically, a positional offset of the input fibers decreases the optical density uniformity (for short mix rods). Computer ray trace results show that this condition arises when the end of the mix rod is not fully illuminated by the input

fibers, as was found to be the case in the breadboard transducer where, of the total 0.16 inch of rod width, only 0.135 inch was illuminated. Computer ray trace results show that, for 0.135 inch of rod illumination, the standard deviation of optical power density increased to 2.2. A pure positional offset of 0.135 inch should decrease the linearity of the transducer slightly.

Computer results show that, if both angular and positional offsets occur simultaneously, significant degradation in optical uniformity may result as shown in Figure 15. Figure 15 illustrates the computed optical power density for channel B in the breadboard transducer. The standard deviation is 11.5 (15.8% variation between maximum and minimum).

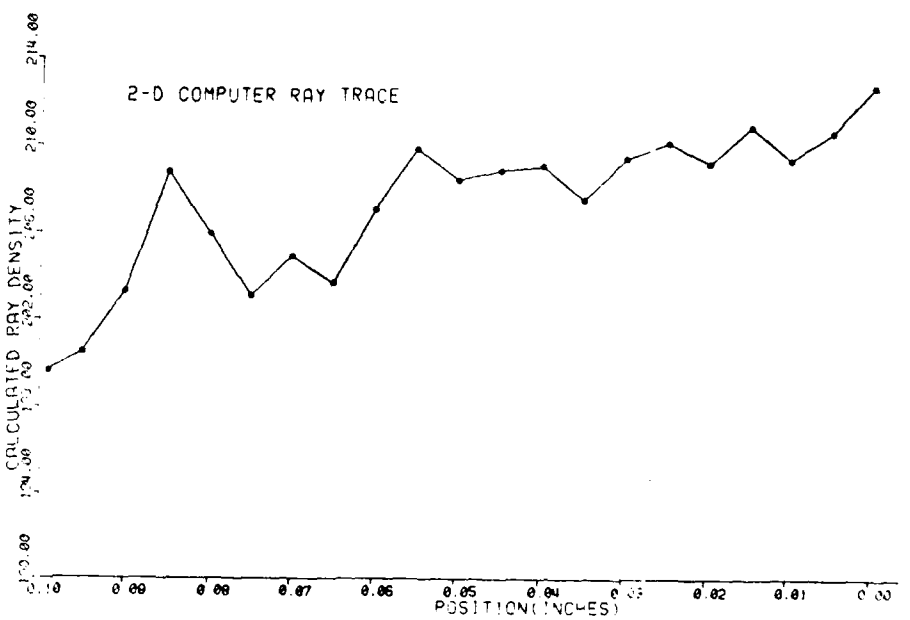

Figure 15. Calculated optical power density profile for an angular offset of 3.6 degrees and .135 inch of the mix rod illuminated.

3.4.6.3.5 OPTICAL LINEARITY ANALYSIS

A comparison of Figures 12 and 15 shows that the predicted channel B optical power density profile from ray tracing across the encoding plate slit is in reasonable agreement with the measured optical power density. The peak variation in Figure 12 is (.126/.104) -1 = 21.1%. The peak variation in Figure 15

is 15.8%, corresponding to an error of -5.3% in the computer ray trace model. It is believed that the difference between the computed and measured optical power densities is due mainly to the input fibers having unequal source powers.

Analysis has shown that the major contributors to breadboard transducer nonlinearity were positional and angular offset of the input fibers.

3.4.7 RECOMMENDATIONS

In general, testing of the breadboard transducer accomplished the goals set forth. However, the tests showed areas where further improvement was needed. This section summarizes areas where deficiencies might be best corrected in the prototype program.

Linearity and accuracy testing showed that the breadboard transducer exhibited some degree of nonlinearity under static test conditions. The origins of nonlinearity were identified as being primarily in the transducer optics and not the electronics. Testing and computer ray trace analysis asserted that the major sources of nonlinearity were angular and positional offset of input fibers. This should be corrected in the prototype with careful alignment of the optical components. In particular, the illumination fibers should uniformly cover the entire end of the mixing rod and also be coupled truly parallel to the mixing rods.

If the illumination fibers and illumination mixing rods are correctly aligned, the problems noticed during the vertical and horizontal positional tests should also be eliminated due to improved uniformity of the optical fields.

It is recommended that the mixing rods be thicker to minimize corner chipping noticed during the lapping process. In addition, making the mixing rods longer should help the optical uniformity by more thorough mixing. The breadboard transducer mix rods were made from a low quality Corning cover plate glass. The prototype mix rods should be of high optical quality glass such as fused silica or Vycor 7913 glass (96% silica). These materials are not as lossy and are of better uniformity.

It is also recommended that the encoding plate substrate be made of a similar material. The material used for the pattern thin-film (chrome) is adequate, but should be overcoated with silicon dioxide to protect the surface from environmental effects. Epoxies such as the Bi Pax 2143 used in the breadboard optical components should be adequate since it will operate over the full temperature range (-50°C to +135°C).

The breadboard EIU analog electronics were mounted on perforated vector board. It is recommended that the analog circuitry be mounted on printed circuit board which would include an optional second postamplifier stage. Due to the sensitivity to connector rotation, the prototype EIU should incorporate a mixing rod at the emitter to distribute the power equally to all the fibers.

The fiber optic cables used in the breadboard were stiff and unwieldy. The selection of more flexible fiber optic cables should be investigated for the prototype transducer. The optical properties of the breadboard cables were satisfactory.

Except for the silicon dioxide overcoat on the encoder plate, all of the above recommended changes were incorporated into the prototype model.

4.0 PROTOTYPE PROGRAM

During the prototype program, the optical design was refined considerably. Having established the optical design, it was then possible to complete the mechanical design.

4.1. MODIFICATION OF THE OPTICAL DESIGN

Although laboratory evaluation of the breadboard transducer proved the soundness of the transmissive encoding technique, it was readily apparent that the straight-line optical path used in the breadboard did not lend itself well to a compact transducer design. It was also felt that the large number of comparatively difficult grinding, polishing, and alignment operations required for fabrication would be quite costly and would probably result in a product with poor uniformity or low yield. Figure 16 shows schematically the straight-line optical path of the breadboard transducer. Although the square mixing rods shown at each of the optical ports were not employed in the breadboard, they would probably be required if a final design were equipped with detachable fiber optic cables. The slab mixing rods, shown on either side of the encoder, projected perpendicularly from the encoder and thereby established the minimum width of the transducer package. If the slab mixing rods were made long enough to perform effective mixing, then the transducer width would be excessive. It was concluded that this problem could be best solved by laying the slab mixing rods parallel to the encoder and using prisms to bend the transmission path normal to the encoder.

Figure 17 shows schematically the folded optical path design used in the prototype transducer. At each of the three optical ports, this design uses only a single element to perform the functions of a mixing rod, a transition section, and two prisms to fold the optical path. These special mixing rod/prisms minimize the number of optical components and the number of optical interfaces. They also eliminate the tedious task of positioning several hundred individual fibers to form the transitions used in the breadboard.

4.2 PROTOTYPE MECHANICAL DESIGN

Figure 18 is a semi-exploded view of the transducer showing the three major subassemblies: (1) the motion assembly, (2) the lower body assembly, and (3) the upper body assembly. The two body halves are fastened together with sixteen stainless machine screws, and the bearing/seal housing is fastened to both body halves with four lock-wired stainless machine screws. The bearing/seal housing fits closely into a cylindrical bore shared by the lower and upper body sections, thereby precisely aligning all three subassemblies. The other ends of the two body halves are aligned by a close-fitting bushing which also serves as the mounting bearing for that end. The body joints are sealed by an O-ring between

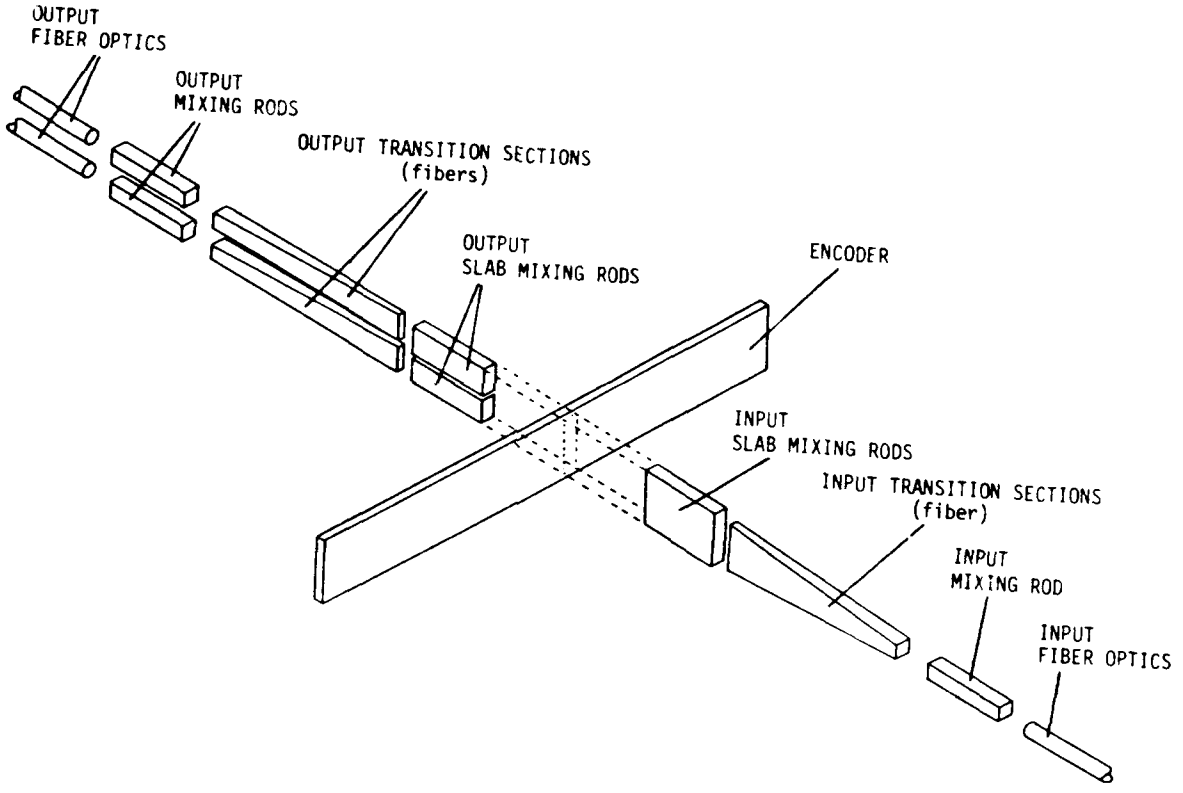

Figure 16. Breadboard optics.

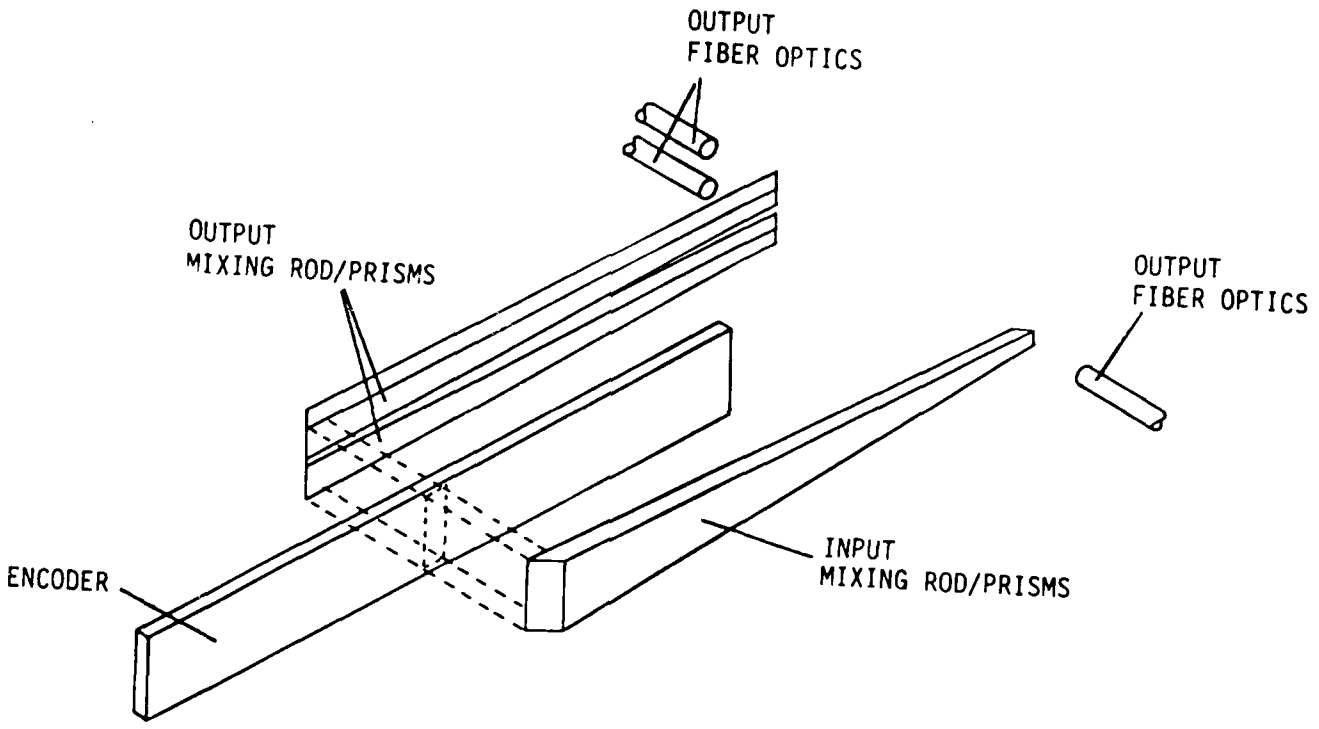

Figure 17. Prototype folded optics.

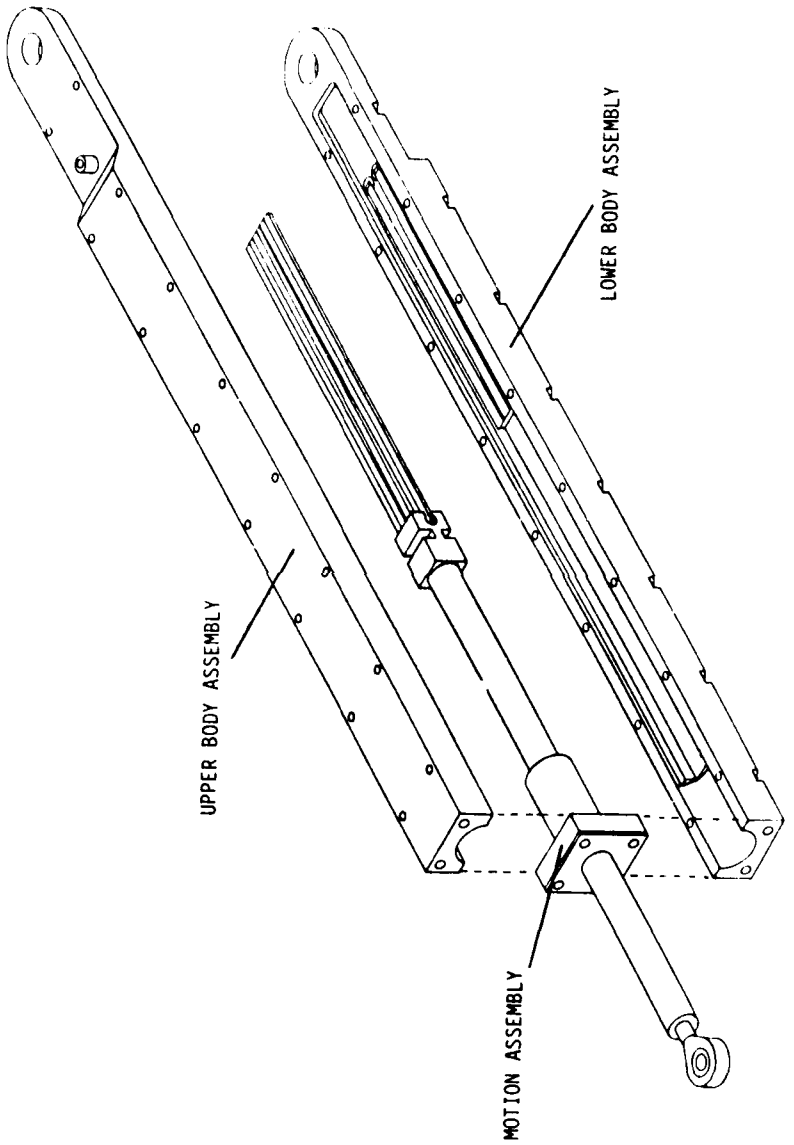

Figure 18. Transducer subassemblies.

the bearing/seal housing and the two body halves, and by an overall high-temperature urethane conformal coating which also seals and locks all of the assembly screws.

Further details of the mechanical design will be found in Appendix F.

4.3 PROTOTYPE EIU DESIGN

Two major tasks were accomplished as the EIU moved from the breadboard phase to the prototype phase. The breadboard analog circuit was laid out on a printed circuit board, and a DC/DC converter was obtained to meet contract power supply specifications. The digital and display functions of the EIU were retained from the breadboard with only minor changes.

The EIU analog breadboard had been configured so that conversion to a printed circuit board would involve minimum engineering effort. Because of this, it was decided that a manual PCB layout would be more cost effective than a computer-aided design. The postamplifier section of the board was arranged so that an additional stage could be added to the postamplifier by means of short jumpers. When actual prototype evaluation took place, it was found that this additional stage of amplification in the postamplifier was indeed required since less optical power was available from the transducer than had been hoped for.

The EIU is specified to perform all required functions, except displays, with an operating voltage (DC input) from 22.0 to 31.5. Since the EIU circuits require +15, -15 and +5 supply voltages, a DC/DC converter system was needed that would use the nominal +28 VDC input to provide the three required circuit power supply voltages. Of the very few DC/DC converters available which met all specifications, the Stevens-Arnold supply was selected because it was the least expensive. The power supply was enclosed underneath the EIU electronics to minimize noise interference in the sensitive analog circuitry.

The prototype EIU is shown in Figure 19.

4.4 PROTOTYPE TESTS AND TEST RESULTS

The microprocessor-based test system was checked out using the prototype transducer, cables and EIU. Figures 20 through 23 show static test data produced by the microprocessor test system with the prototype transducer as the test article. Figures 20 and 21 show plots of EIU position versus actual mechanical position. The data of Figure 20 was taken while scanning in the upward direction (from 0-inch mechanical to 6-inches mechanical), and the data of Figure 21 was taken while scanning in the downward direction. Figures 22 and

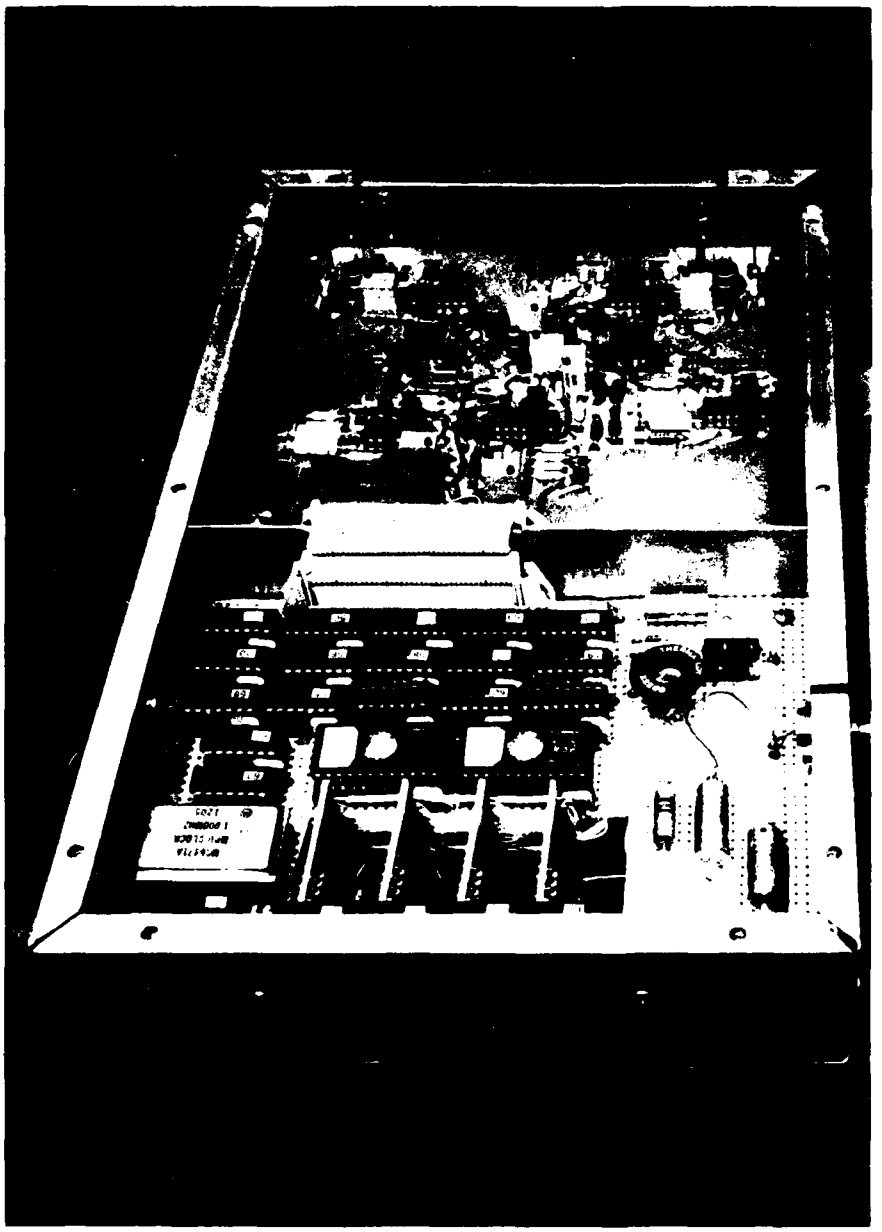

Figure 19. Prototype EIU.

23 show the indicated position error versus actual mechanical position for the upward and downward scans respectively. The plots of Figures 20 to 23 each contain 961 points (every fifth point out of 4801). Figure 24 shows a tabulation of error at 13 points during the upward and downward scans. Note that there is from 1 to 3 bits of hysteresis between upward and downward scans. Figure 25 shows that one monotonicity error occurred during the upward scan and no error occurred during the downward scan.

4.4.1 LINEARITY AND ACCURACY

The test data generated by the microprocessor-based test system was used to evaluate linearity and accuracy of the prototype transducer. The prototype transducer exhibited response as shown in Figures 20 to 24. The error curve is approximately sinusoidal with a maximum deviation of +0.040 inch, -0.027 inch (+0.667%FSR, -0.45%FSR) or 1.1% FSR.

An optical power vs. displacement scan was measured with a UDT 11A optical power meter and is presented in Figure 26. Some curvature is evident which will result in some nonlinearity for the whole system. This shows that the nonlinear response noted in Figures 20 to 24 was due primarily to the optics in the transducer.

4.4.2 OPTICAL POWER MARGIN

The optical power loss through the transducer optical system was measured to be 23.5 dB. Based on the system margin of 39.5, the optical power margin was 16 dB.

4.4.3 TEST ANALYSES

As the data of Figures 20 through 25 shows, the microprocessor-based test system worked properly and therefore was used to evaluate the production transducers. The source of the prototype nonlinearity was believed to be the result of mechanical misalignment of the optics due to loose mechanical tolerances. It was felt that nonlinearity whould be reduced in the production transducers maintaining tighter tolerances. Due to the beveled and tapered shape of the mix rods (prisms) used in the prototype transducer, a 2-D computer ray trace analysis could not be performed with confidence due to the large number of skew rays propagated by such devices. Therefore, it was not known how uniform the optical power density was at the surface of the encoding plate. The measured optical power margin of 16 dB is considered adequate to allow for device degradation.

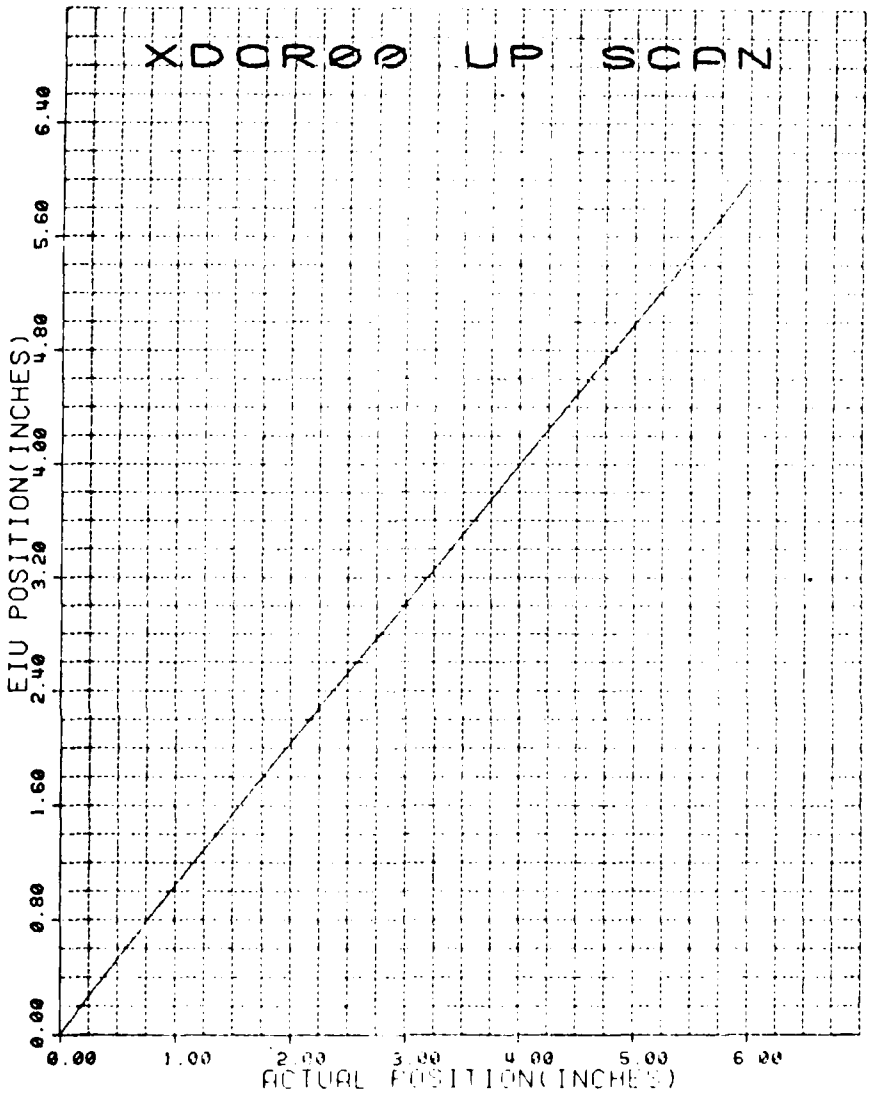

Figure 20. Up-scan prototype transducer performance.

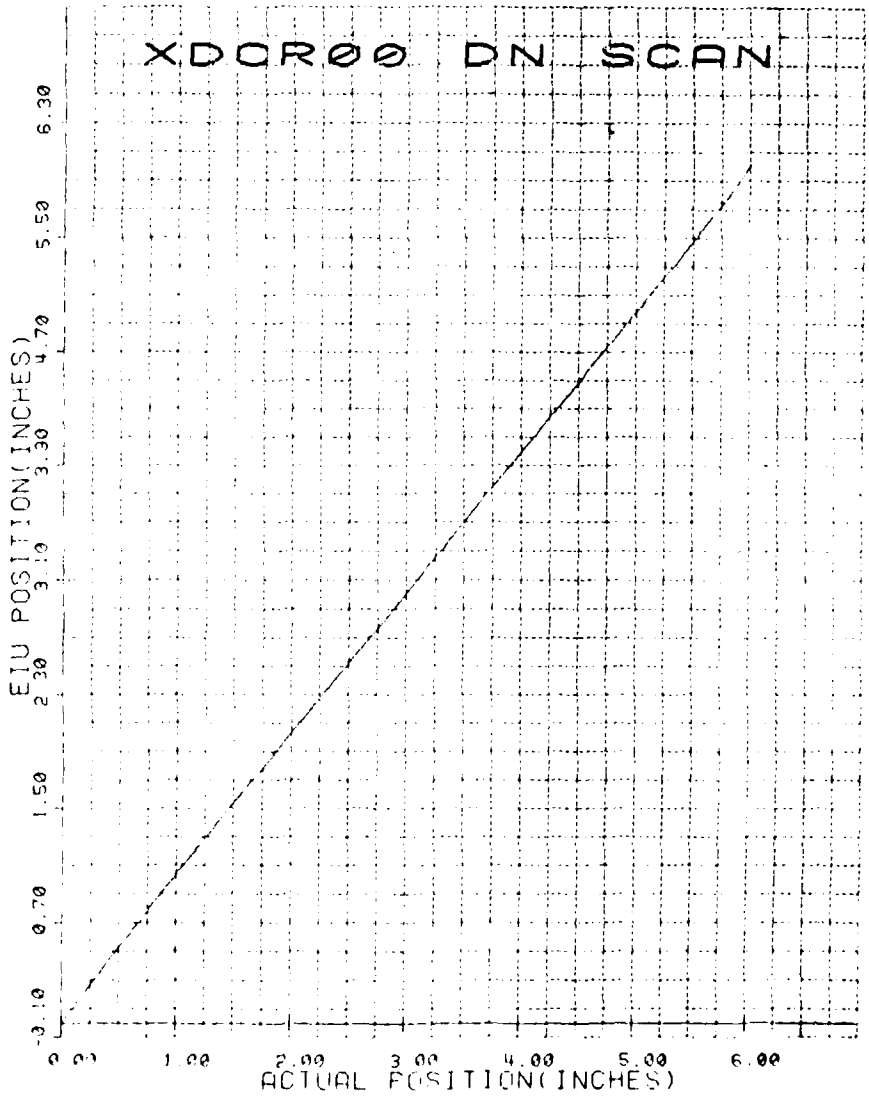

Figure 21. Down-scan prototype transducer performance.

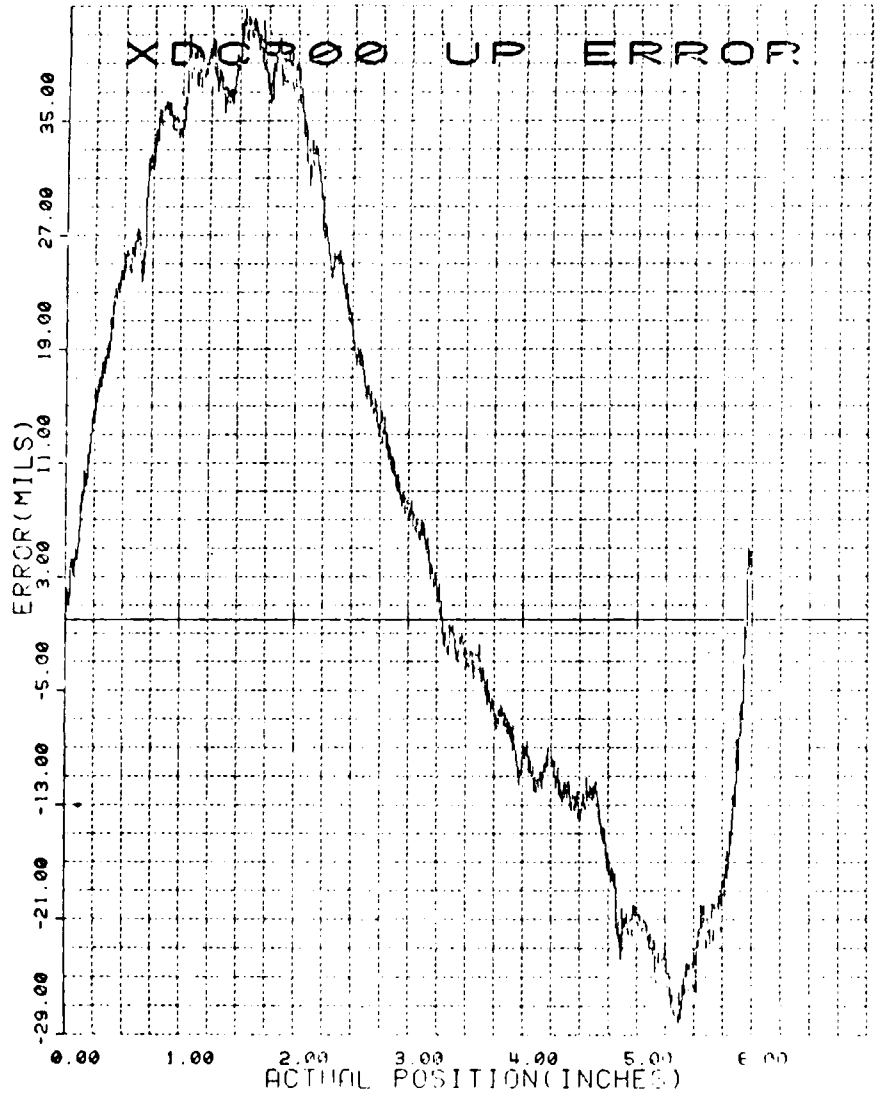

Figure 22. Up-scan prototype transducer error curve.

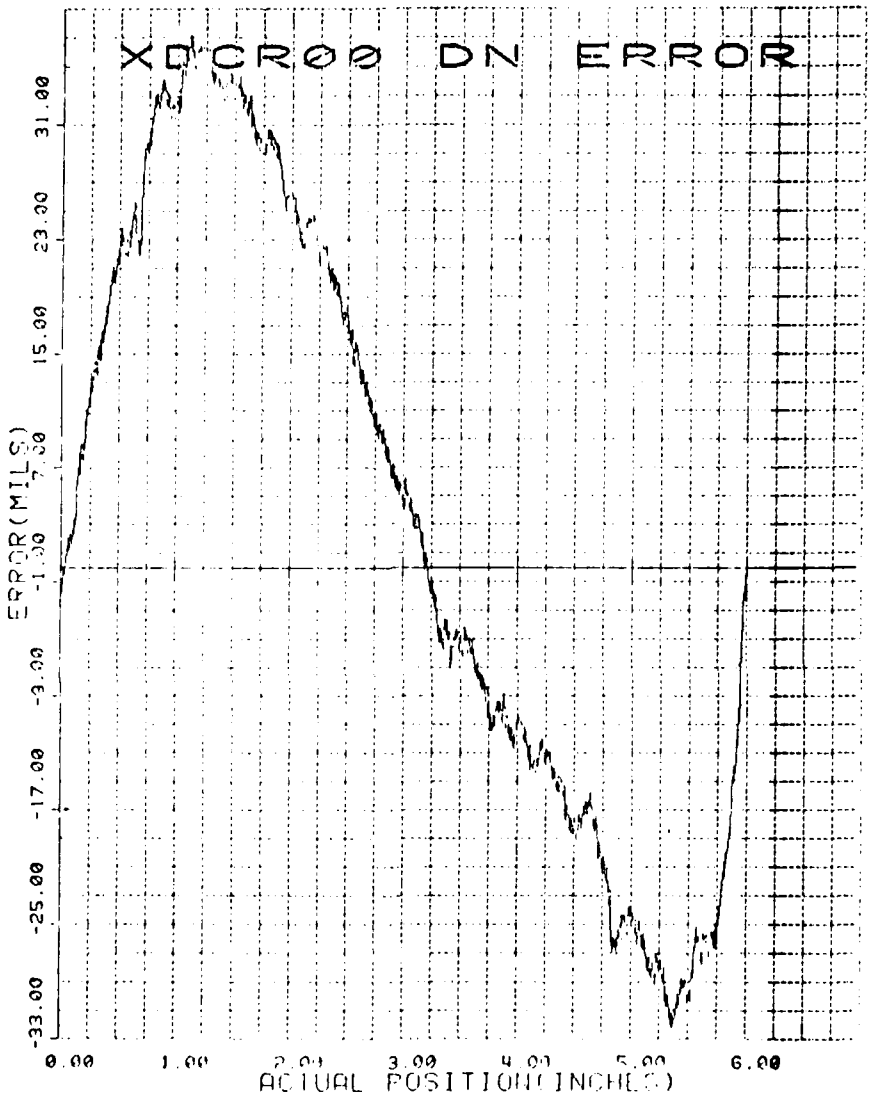

Figure 23. Down-scan prototype transducer error curve.

ATL DIGITAL/OPTICAL LINEAR POSITION TRANSDUCER

STATIC ACCURACY DATA AND ANALYSIS

TRANSDUCER: 0 09/09/81

POINT	INCHES	EIU SCALE	STEPPER SCALE	ERROR IN BITS	ERROR IN INCHES
1	0.00	2	0	0	0.000000
2	0.50	359	400	16	0.023460
3	1.00	706	800	22	0.032258
4	1.50	1048	1200	23	0.033724
5	2.00	1385	1600	19	0.027859
6	2.50	1719	2000	12	0.017595
7	3.00	2051	2400	3	0.004399
8	3.50	2386	2800	-3	-0.004399
9	4.00	2722	3200	-8	-0.011730
10	4.50	3061	3600	-10	-0.014663
11	5.00	3398	4000	-14	-0.020528
12	5.50	3736	4400	-17	-0.024927
13	6.00	4095	4800	1	0.001466
13	6.00	4094	4800	0	0.000000
12	5.50	3732	4400	-21	-0.030792
11	5.00	3395	4000	-17	-0.024927
10	4.50	3058	3600	-13	-0.019062
9	4.00	2721	3200	-9	-0.013196
8	3.50	2383	2800	-6	-0.008798
7	3.00	2050	2400	2	0.002933
6	2.50	1717	2000	10	0.014663
5	2.00	1382	1600	16	0.023460
4	1.50	1046	1200	21	0.030792
3	1.00	705	800	21	0.030792
2	0.50	357	400	14	0.020528
1	0.00	1	0	-1	-0.001466

Figure 24. Prototype transducer static accuracy printout.

RESOLUTION AND MONOTONICITY TESTS

UP SCAN

POSITION (INCHES)	ERROR (BITS)
2.006250	-1

DOWN SCAN

Figure 25. Prototype transducer resolution/monotonicity printout.

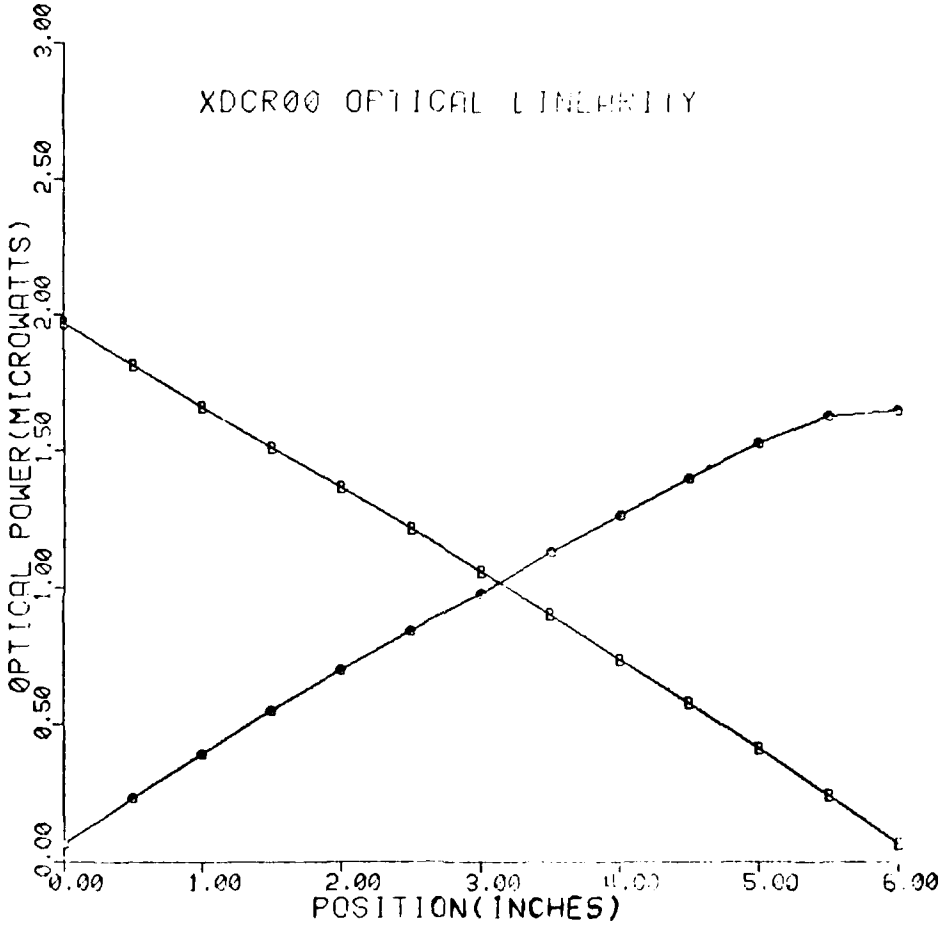

Figure 26. Optical power versus position for prototype transducer (S/N 00).

5.0 PRODUCTION PROGRAM AND TESTS

Under the production program, six transducers, four EIUs, and six sets of fiber optics were produced. Except for very minor differences, their design was the same as for the prototype. Of the six units, all were functionally tested, one was life-cycle tested, and three were environmentally tested.

5.1 PRODUCTION AND TEST OF TRANSDUCERS S/N 01, 02 AND 03

Because of manufacturing problems with encoders and prisms, transducers S/N 01, 02 and 03 were fabricated and functionally tested first. It is probably fortunate that all six were not assembled at the same time, because performance anomalies were discovered which led to minor design changes in transducers S/N 04, 05 and 06.

The production transducer static accuracy/linearity tests were performed using the microprocessor-based system described in Section 4.4 and Appendix G. The results of the static accuracy/linearity tests on transducers S/N 01, 02 and 03 are shown in Figures 27, 28 and 29 respectively. If the error plots of the three figures are compared, it will be noted that the peak-to-peak amplitudes are comparable (approximately ± 0.6%), but the shapes of the plots are sufficiently dissimilar that no single correction could be applied to linearize all three transducers. Since eventual linearity correction was one of the contractor-imposed design objectives, an effort was made to determine the cause of the nonlinearity and the reason for the dissimilarities. Possible reasons included the following:

1. Encoder error --- This would be very difficult to verify. Also,since all encoders were photographically produced from a single master, it is very unlikely that the encoders could be that dissimilar.

2. EIU electronic nonlinearity --- The optical power output from a transducer was measured by an independent means and was found to exhibit a similar nonlinearity as a function of displacement.

3. Prism mechanical imperfections --- The prism facet angles were measured with an optical comparator and were found to be accurate within 2 minutes of arc. The prisms were also examined with HeNe laser light and were found to be free of significant chips, cracks and scratches. It was found, however, that the prism facets had been felt polished rather than pitch polished, and were not optically flat. This appeared to be one likely cause of error, and plans were made to produce new prisms with optically flat facets.

4. Prism optical imperfections --- The HeNe examination did not reveal significant bubbles or inclusions in the Vycor prism material. It did, however, disclose imperfections in the metalization of the prism facets. It was decided that metalization of the new prisms would be done by a different process under more careful control,

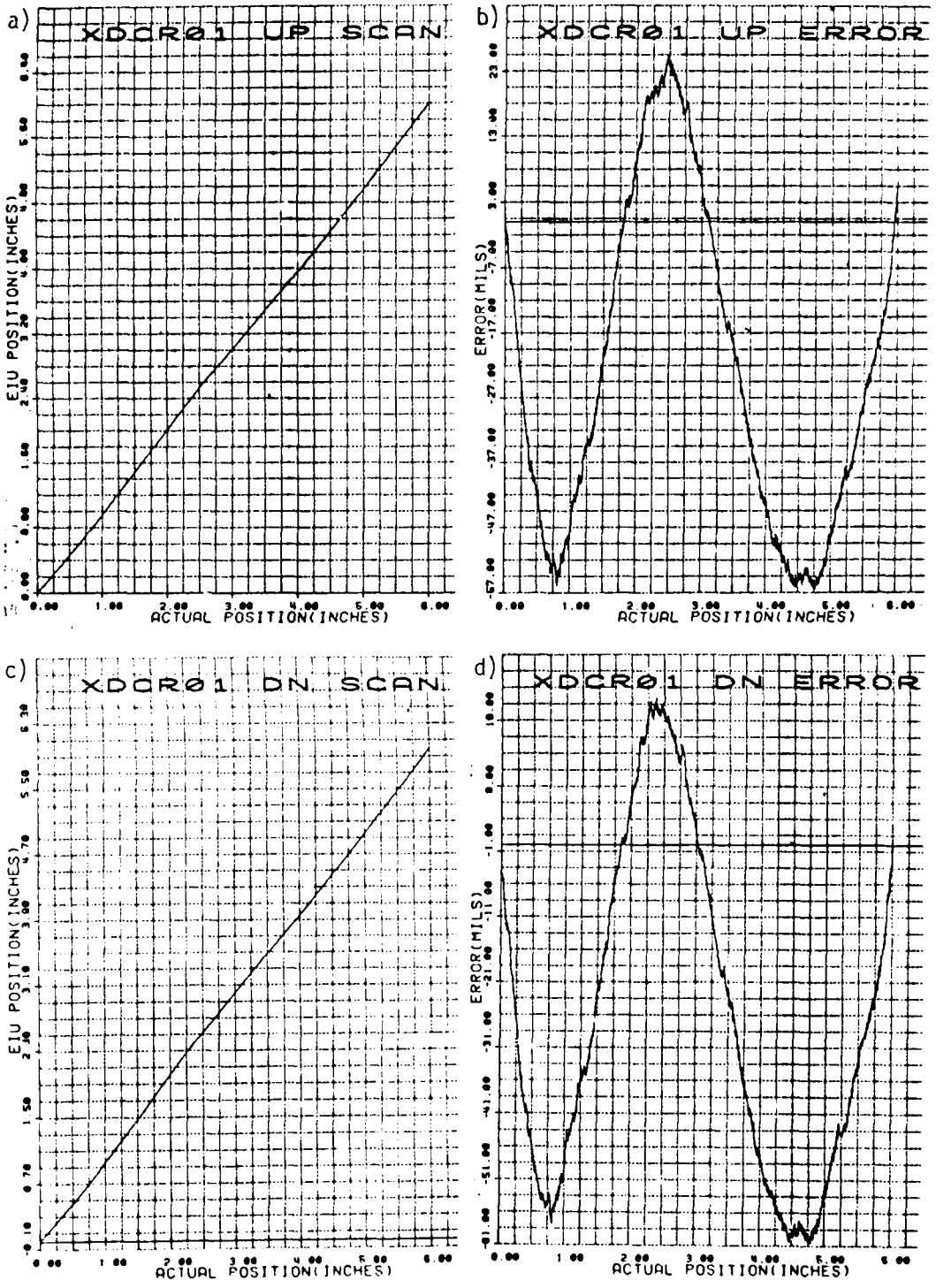

Figure 27. Transducer S/N 01 static accuracy/linearity.

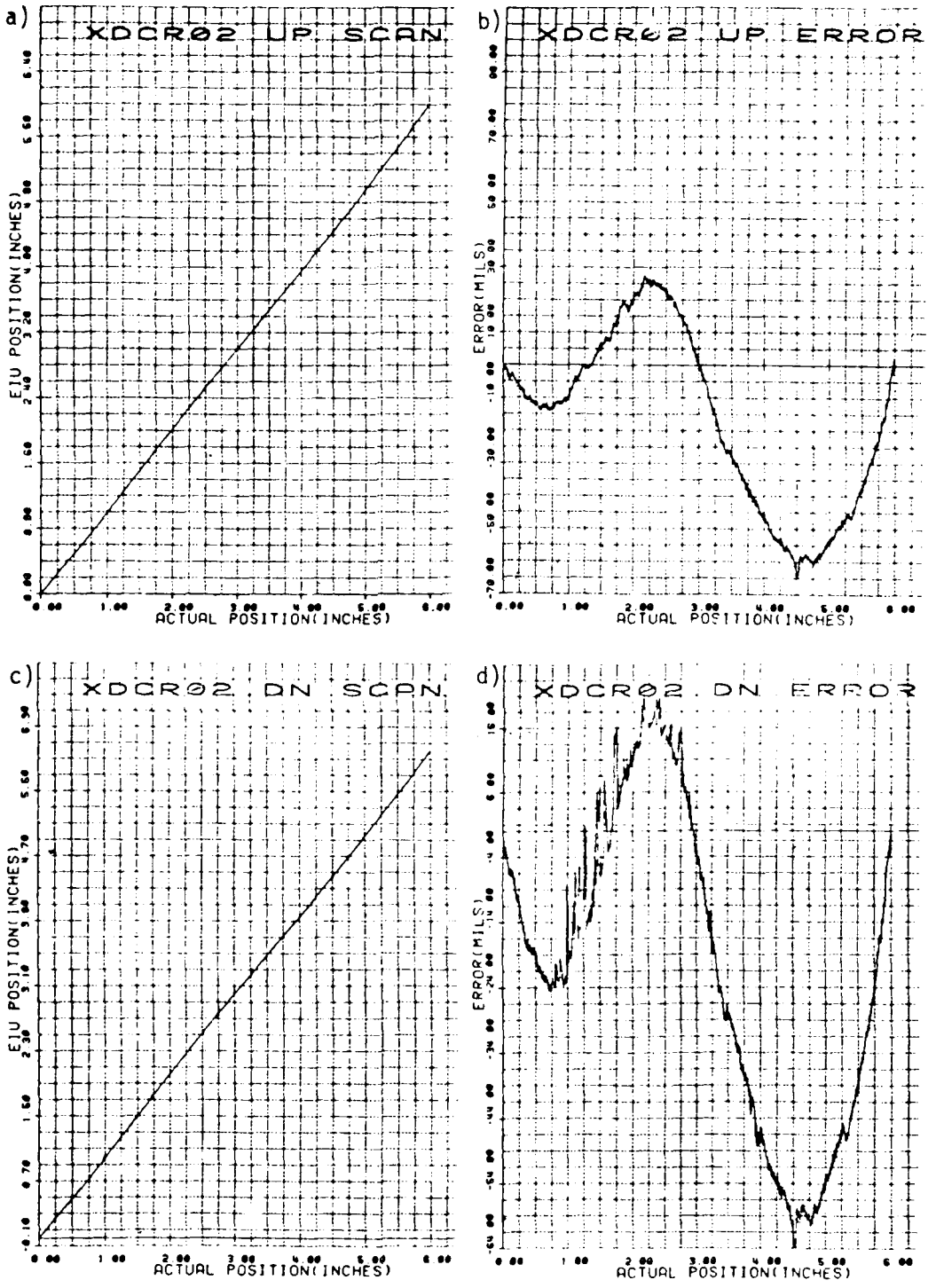

Figure 28. Transducer S/N 02 static accuracy/linearity.

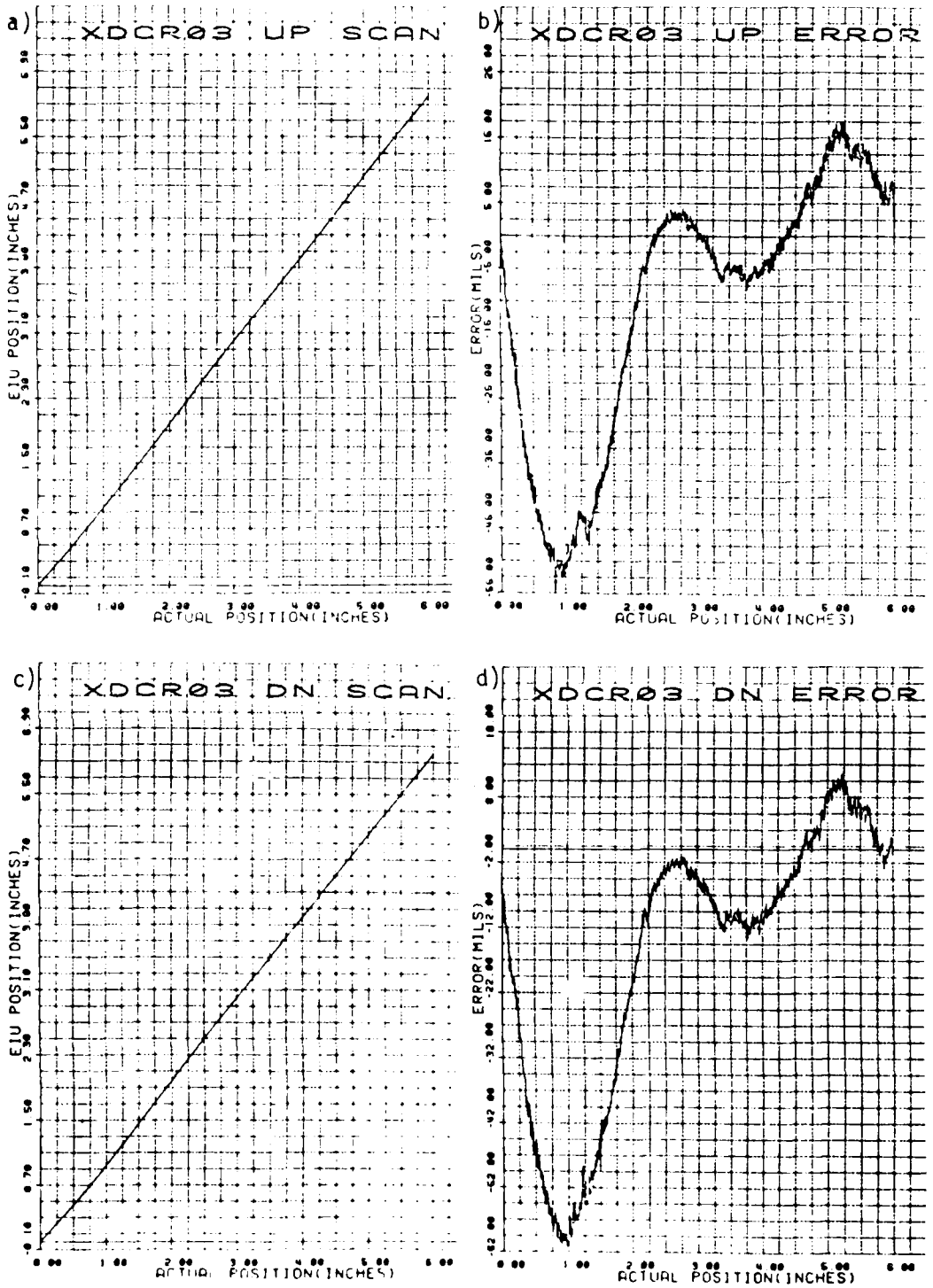

Figure 29. Transducer S/N 03 static accuracy/linearity.

and that the metalization would be given a protective coating of silicon dioxide.

5. Prism geometry and tolerances --- Transducer linearity requires that the full width of the encoder tracks be uniformly illuminated. To insure illumination uniformity, the prisms were designed to be wide enough for all mechanical tolerance extremes. A scan of a prism showed, however, that the illumination near the prism edges was not as uniform as thought. This edge effect, combined with the discovery that the encoder patterns were not all centered on the substrates within the specified tolerances, led to this being singled out as the most likely cause of the inconsistency between transducers. This theory was further substantiated when it was found that the transducers were slightly sensitive to gravitational orientation, due to the encoding plate moving sideways.

5.2 PRODUCTION AND TEST OF TRANSDUCERS S/N 04, 05 AND 06

In the attempt to resolve the nonlinearity problem, new prisms were designed with 20% greater width, optically flat pitch-polished facets were specified, and the bodies of transducers S/N 04, 05 and 06 were remachined to accommodate the larger prisms. This action was taken even though it was realized that the modification would increase the insertion loss approximately 0.8 dB.

The results of the static accuracy/linearity tests on transducers S/N 04, 05 and 06 after the prism modification are shown in Figures 30, 31 and 32 respectively. The error plots for these transducers show that their shapes are much more consistent than were the shapes of the unmodified transducers; however, the peak-to-peak errors are greater and less consistent.

The prism modification corrected the error curve shape problem as intended, but increased the magnitude of the error. It is believed that the error increased because changing the prism width without also changing the length effectively made the prisms shorter and hence less effective as mixing rods.

The prism modification did effectively eliminate the sensitivity to gravitational orientation.

5.3 PERFORMANCE TEST PROCEDURES AND RESULTS

Group 1 and Group 2 tests were used to characterize the performance of the six transducer systems before and after any other tests (e.g., environmental and life-cycle). The group 1 and group 2 tests are described in the Hardware Test Plan (Appendix A). Group 1 tests include:

1. EIU warm-up drift
2. Sensitivity to power supply variations
3. Fiber optic connector repeatability
4. Weight of transducer system
5. Transducer actuating force

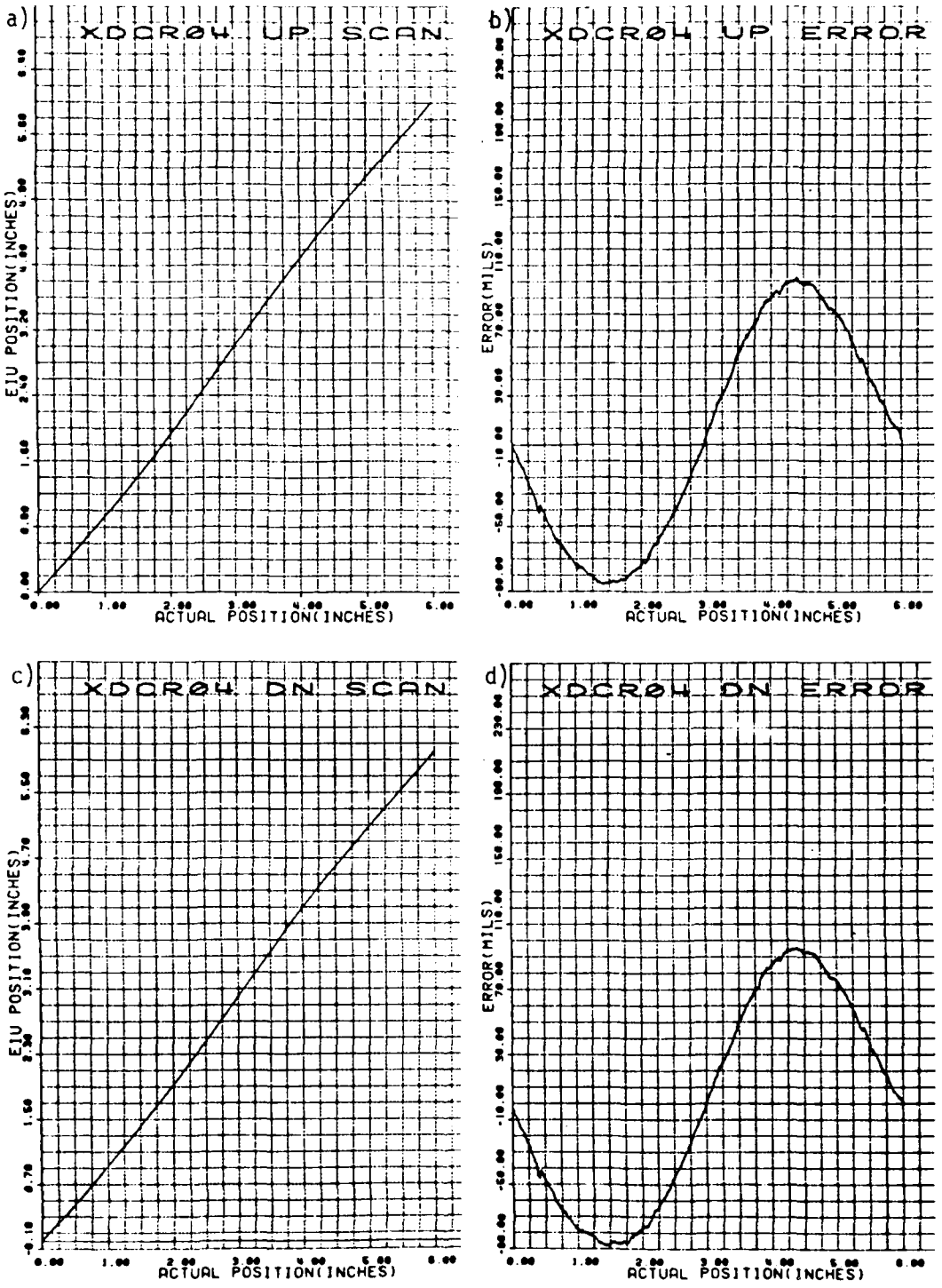

Figure 30. Transducer S/N 04 static accuracy/linearity.

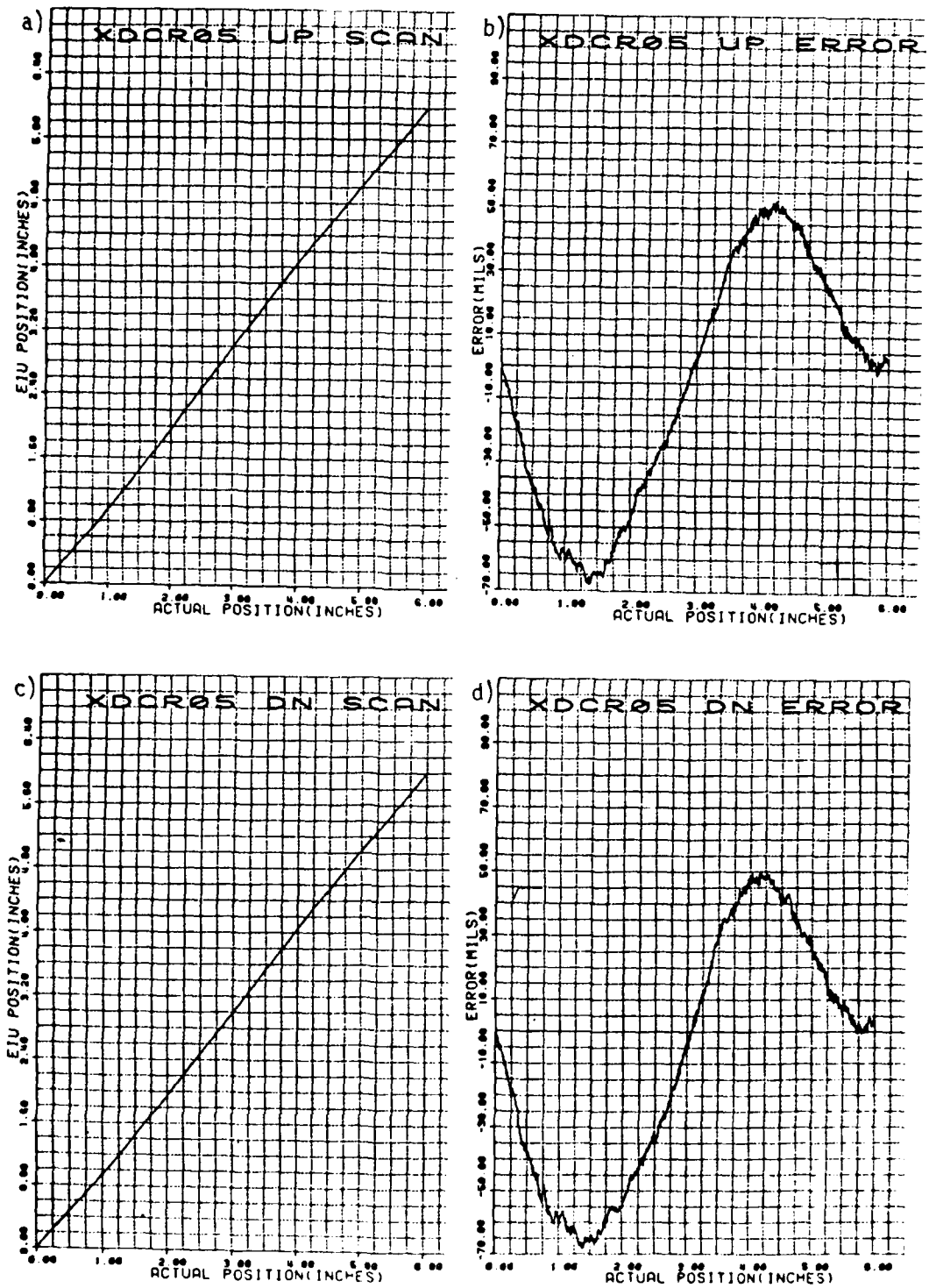

Figure 31. Transducer S/N 05 static accuracy/linearity.

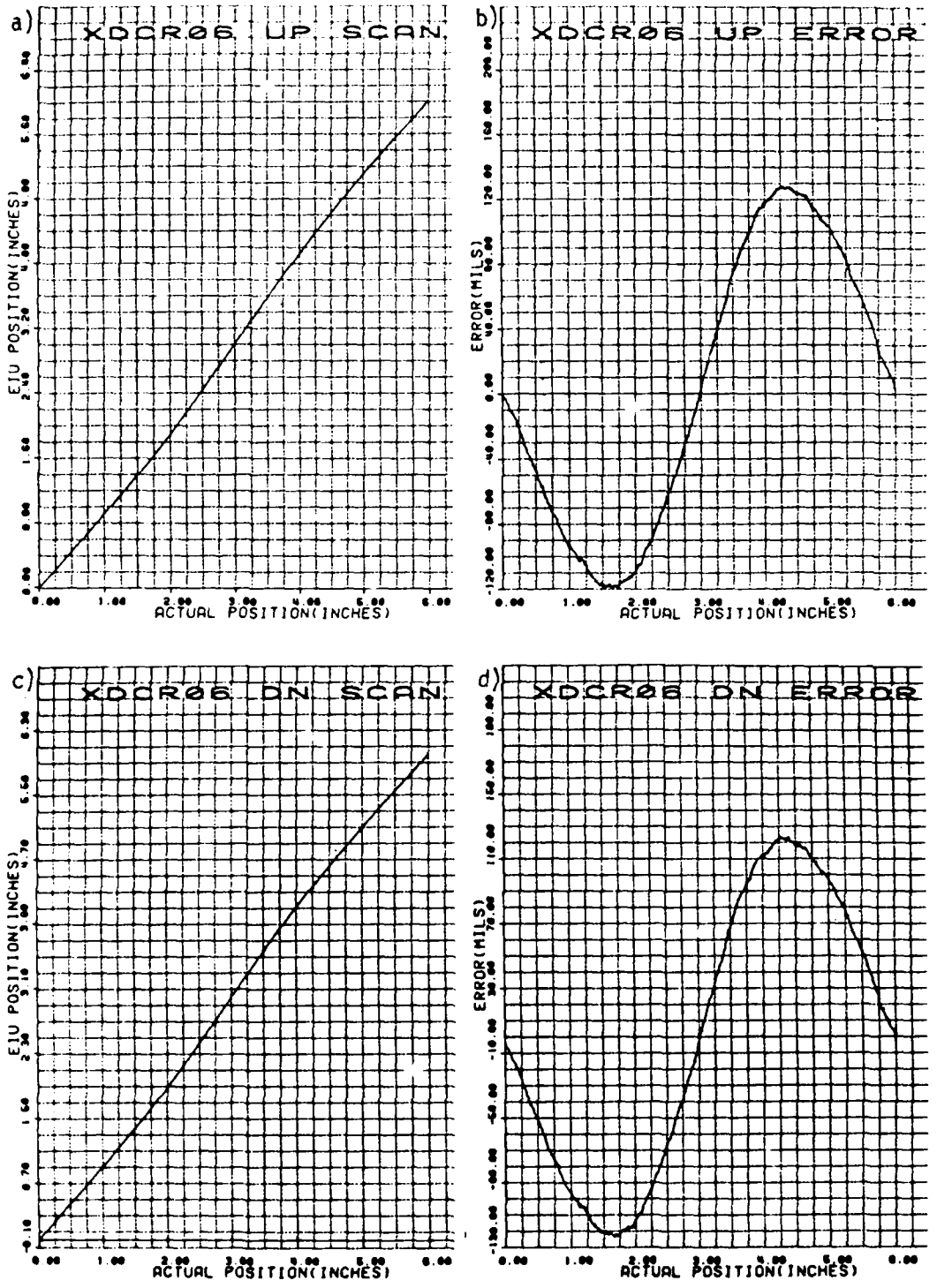

Figure 32. Transducer S/N 06 static accuracy/linearity.

Group 2 tests include:

1. Static accuracy, linearity, resolution, and monotonicity
2. Dynamic accuracy
3. Optical power margin

Transducer system 1 consisted of transducer S/N 05, fiber optic cables S/N 05, and EIU S/N 04. This transducer system was group 1 and group 2 tested, followed by the life-cycle and post-group 2 tests.

Transducer systems 2, 3 and 4 consisted of transducers S/N 01, S/N 02, and S/N 03; cable assemblies S/N 01, S/N 02, and S/N 03; and EIUs S/N 01, S/N 02, and S/N 03 respectively. These systems were group 2 tested, followed by MIL-STD-810C environmental tests and finally by post-group 2 test.

Transducer systems 5 and included transducers S/N 04 and S/N 06, cable assemblies S/N 04 and S/N 06, and EIUs S/N 04 and S/N 04 respectively. These transducer systems were group 2 tested only.

5.3.1 GROUP 1 PERFORMANCE TESTS

All group 1 tests involved transducer S/N 05, cable assembly S/N 05, and EIU S/N 04.

5.3.1.1 WARM-UP DRIFT

The transducer was mounted in the calibration fixture at mechanical position 3.000 inches and 28 VDC was applied to the EIU. EIU readings were recorded as a function of time. Drift over a 1-hour warm-up period was approximately 0.003 in. (0.05% full-scale error) and is summarized in Table 2.

TABLE 2. WARM-UP DRIFT

Time from startup (min)	EIU reading (in.)
0	3.000
1	3.001
2	2.999
5	2.999
10	3.000
20	2.999
60	2.997

5.3.1.2 SENSITIVITY TO POWER SUPPLY VARIATIONS

With the transducer mounted on the calibration fixture at mechanical position 3.000 inches (power on for 2 hours), the input power was varied in 1-volt increments from 22 VDC to 32 VDC. The EIU showed excellent stability over this input voltage range,as shown in Table 3.

TABLE 3. SENSITIVITY TO POWER SUPPLY VARIATIONS

DC input voltage	EIU reading (in.)
22	2.997
23	2.997
24	2.997
25	2.997
26	2.997
27	2.997
28	2.997
29	2.997
30	2.997
31	2.997
32	2.997

5.3.1.3 FIBER OPTIC CONNECTOR REPEATABILITY

Fiber optic connector repeatability was checked at three transducer mechanical positions: 3.000, 5.900, and 0.100 inches. Each of the six fiber optic Amphenol 905 connectors was disconnected and immediately reconnected. The EIU display readout was recorded before and after each operation. Rotation marks were used on the connectors so they could be returned to the same orientation and all connectors were finger tight (~2 in.-lb of torque).

No changes in EIU readings were noted for the mechanical positions 0.100 and 5.900 inches for any of the six connectors. At 3.000 inches mechanical, the variation was 0.007 inch (0.12% full-scale error), as shown in Table 4.

TABLE 4. FIBER OPTIC CONNECTOR REPEATABILITY (3-IN. MECHANICAL)

Connector	EIU Reading (in.)	
	Before	After
Emitter/EIU	3.000	3.000
Channel A/EIU	3.000	3.000
Channel B/EIU	3.000	2.999
Emitter/Transducer	2.999	2.997
Channel B/Transducer	2.997	2.996
Channel A/Transducer	2.996	2.993

Other tests indicated that fiber optic connector repeatability can be improved by using a torque wrench in combination with rotation marks and torquing all connectors to the same value (~7 in.-lb). Fiber optic connector repeatability can also be enhanced by using a keyed multi-pin connector.

The EIU was recalibrated after the fiber optic connector repeatability test.

5.3.1.4 WEIGHT

The transducer system consists of the EIU, the fiber optic cable assembly, and the transducer. The total weight of a transducer system (to the nearest ounce)

was 7 lb, 4 oz and is broken down as follows:

EIU	= 4 lb, 2 oz
Transducer	= 2 lb, 12 oz
Cables	= 6 oz (2 oz each)

5.3.1.5 TRANSDUCER ACTUATING FORCE

The transducer actuating force was measured near the mid point with a Chatillon force gauge (5 lbs full scale, ± 2% full scale) and was found to be 2 lb, 5 oz. (both directions).

5.3.2 GROUP 2 PERFORMANCE TESTS

All transducer systems were group 2 performance tested prior to any life cycle or environmental tests. Transducer system 1 underwent the group 1 performance test prior to group 2 tests.

5.3.2.1 STATIC ACCURACY, LINEARITY, RESOLUTION, AND MONOTONICITY

The static accuracy, linearity, resolution, and monotonicity tests were performed using the microprocessor-based test system described in Appendix G. All EIU's were calibrated with their corresponding transducers prior to these tests using the calibration fixture. The scan rate during testing was approximately 0.016 inch/second for the entire 6-inch transducer stroke.

The static accuracy and linearity tests show that all of the transducers exhibited small nonlinearities and errors over the 6-inch stroke range, as shown in Figures 7 through 32. In each of the figures, four plots are shown. Plot (a) shows EIU display position (inches) plotted against the actual transducer position (inches) while scanning in the upward direction (0 inches to 6 inches). Plot (b) is the corresponding up-scan error (mils) as a function of actual position (inches). Plots (c) and (d) correspond to plots (a) and (b), but represent down-scans of the transducer (6 inches to 0 inches). All error plots were automatically scaled in the plotting software.

Peak error tabulations are summarized in Table 5. All error tabulations are from up-scan information.

TABLE 5. PEAK TRANSDUCER ERRORS

Transducer Serial Number	Peak Positive Error (mils)	Peak Negative Error (mils)	Peak to Peak Error (mils)	Average Full-Scale Error (%)
01	25	57	82	0.68
02	25	65	90	0.75
03	17	55	72	0.6
04	100	85	185	1.54
05	50	68	118	0.98
06	120	120	240	2.00

The average full-scale errors exceeded the error desired (± 0.25%) for static ambient conditions by a factor of three to eight times.

Figures 27 to 29 show static accuracy data for the first three transducers which had the small input prisms. In this case the error curve appears to be 1½ cycles of a sinusoid. The cause of the "noise" in the down scan of transducer S/N 02 is not known. Transducer S/N 03 exhibited the smallest peak-to-peak error of any of the transducers (except the prototype, S/N 00, which had a peak-to-peak error of ± 0.53%).

Static accuracy data for transducers S/N 04 to S/N 06 is shown in Figures 30 to 32. These transducers had the new larger input prisms (20% wider). The error curve now appears to be a near-perfect sinusoid which should be very repeatable and easy to correct for in the encoding pattern. The peak-to-peak errors were greater than those of the first three transducers, indicating that mixing action had been reduced by widening the prisms.

The plots of Figures 27 to 32 will be used to see if any change occurs in the transducers from environmental or life-cycle tests. For these plots, the LED current in each EIU was set to 60-70ma peak. All static accuracy printouts are contained in Appendix C. Resolution and monotonicity information was also obtained from data stored during the scan. Since the EIU data was recorded for each 0.00125 inch of travel (eight steps of the stepper motor), and the average resolution width of the transducer is 0.00146 inch, most words should differ from the previous word by one bit reading. However, due to the slight mismatch, and allowing for lead screw errors, a change of 0, 1, or 2 bits was allowed. If successive stored words differed by more than these allowable limits, the quantity and sign of the deviation was printed and identified by its position along the 6.000 inches of travel.

A sample monotonicity and resolution scan is shown in Figure 33 for transducer S/N 02. This monotonicity and resolution data corresponds to the static accuracy and linearity plot of Figure 28. Transducer system S/N 01, S/N 06, and S/N 05 were perfectly monotonic. The other transducers were not perfectly monotonic. All resolution and monotonicity data is contained in Appendix C for the initial group 2 tests. Tests indicate that most nonmonotonic regions in the

RESOLUTION AND MONOTONICITY TESTS

UP SCAN

POSITION (INCHES)	ERROR (BITS)
3.003750	-1
2.881250	3
2.762500	0
4.757500	-1
4.573750	-1
1.917500	-1
1.903750	3
1.781250	3
1.775000	-1
1.773750	-1
1.705000	3
1.611250	-1
1.601250	3
1.573750	3
1.570000	-1
1.556250	3
1.555000	3
1.508750	-1
1.501250	-1
1.492500	-1
1.491250	-1
1.480000	3
1.470000	3
1.466250	-1
1.462500	3
1.457500	-3
1.456250	-4
1.447500	0
1.446250	0
1.443750	-2
1.442500	-2
1.435000	3
1.423750	-1
1.421250	3
1.417500	-2
1.411250	-2
1.408750	3
1.395000	3
1.381250	-1
1.373750	3
1.362500	-1
1.361250	-2
1.350000	0
1.288750	-1
1.287500	-2
1.286250	-1
1.285000	-1
1.278750	-1
1.271250	3
1.265000	3
1.262500	3
1.256250	-2
1.255000	-1
1.251250	3
1.213750	-1
1.211250	0
1.192500	-1
1.190000	-1
1.186750	-1
1.151250	-1
1.133750	-1
1.125000	0
1.102500	-1
1.085000	3
1.013750	-1
1.005000	-1
0.990000	0
0.986750	0
0.903750	-1
0.897500	-1
0.891250	-1
0.880750	3
0.820000	3

DOWN SCAN

Figure 33. Sample resolution/monotonicity printout.

transducer scans stemmed from contamination of the encoding plate or from prism (mix rod) defects.

5.3.2.2 DYNAMIC ACCURACY

For the dynamic accuracy test, the transducer was mounted on the life-cycle test fixture. A computer-controlled hydraulic actuator (MTS model 204.62, 15K capacity, 6-inch stroke) was used to provide the stroke and sweep rate for the test. The low speed sweep rate was 0.06 inch/second (.0064Hz, ± 1.5 inch stroke). The control waveform to the actuator was sinusoidal in all cases. Dynamic accuracy was tested in both scan directions. These tests were performed at standard ambient conditions per paragraph 3.1 of MIL-STD-810C.

An LED/PIN detector pair was clamped to the transducer housing near the midpoint of the transducer stroke. An opaque rod (Delrin) with the end sharpened to a knife edge was connected to the transducer shaft near the rod end bearing and was channeled such that it would pass between the LED/PIN detector pair (see Figure 34). The passing edge of the Delrin rod caused a rising TTL pulse to be generated which was used to interrogate the EIU and lock in the EIU display.

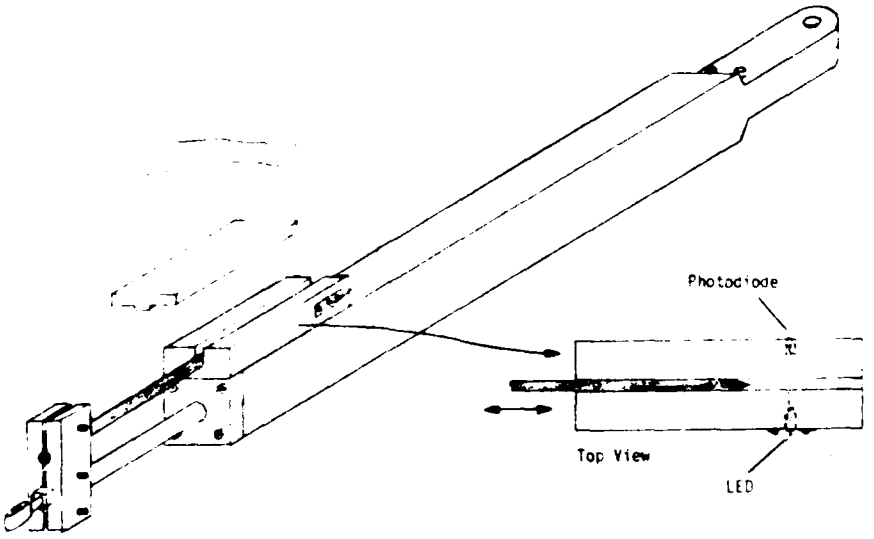

Figure 34. Dynamic accuracy test fixtures.

A block diagram of the dynamic accuracy electronics is shown in Figure 35. An infrared LED was used as a light source and a PIN diode with a small active area (Texas Instruments TIED 56) as a detector. A transimpedance amplifier with a 116 millivolts/microwatt optical response was used as an amplifier followed by a comparator with hystersis for logic signals. Two buffers were used following the comparator for pulse selection. The up-scan EIU A/D start-of-convert (SOC) signal was provided by the first buffer and the down-scan EIU A/D SOC was derived from the second buffer. This assures that initially the EIU A/D SOC will be low (A/D reset) and go high (A/D convert followed by hold) when the edge of the Delrin rod passes between the LED/PIN detector pair. Several wire wrap changes were necessary on the EIU to facilitate running of the dynamic accuracy tests.

The bandwidth and delay through the dynamic accuracy electronics was chosen such that the delay at 6 inches/second transducer slew rate would be less than ½ of a bit time. At 6 inches/second, one bit time is 6 inches/4093 bits or 1 bit = 244 microseconds. The observed delay was ~0.85 microseconds or 0.35 of a bit time. This bandwidth and delay was sufficient to guarantee that the mechanical trip position at 6 inches/second slew was within ± 0.513 mils (less than ½ of a bit).

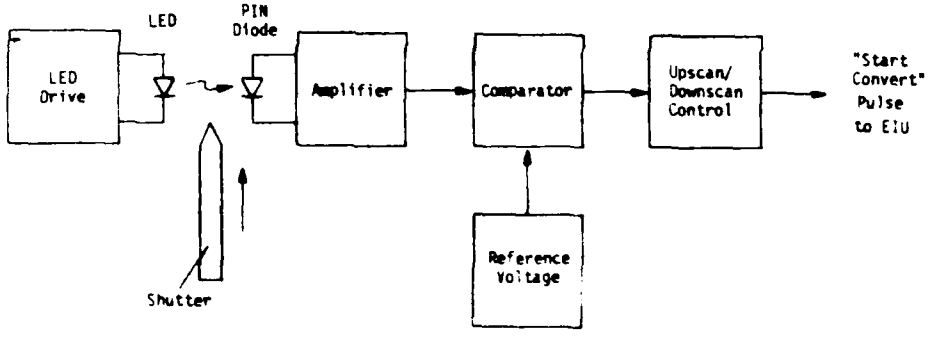

Figure 35. Dynamic accuracy electronics block diagram.

Transducers S/N's 01 through 06 were tested for dynamic accuracy in accordance with paragraph 5.2 of the Hardware Test Plan (Appendix A). The transducers were individually set up in the hydraulic exerciser which was later used for the life-cycle test. Each transducer was swept at a very low rate of 0.06 inches/second, and then again at a rate of 6 inches/second. The difference between the EIU readings is the dynamic error at 6 inches/second. The optical strobe generator was adjusted to approximately 3 inches mechanical. The transducers were tested in both transducer movement directions (up-scan and down-scan). The data for the six transducers is as follows:

TABLE 6. DYNAMIC ACCURACY TEST RESULTS

Up-scan (0 to 6 inches) Dynamic Accuracy

Serial Number	EIU Reading At Low Rate (in.)	EIU Reading At High Rate (in.)	Dynamic Error (in.)	EIU S/N
01	3.001	2.996	-0.005	01
02	3.029	3.025	-0.004	02
03	2.996	2.991	-0.005	03
04	3.009	3.003	-0.006	04
05	3.004	3.001	-0.003	04
06	2.972	2.966	-0.006	04

Down-scan (6 to 0 inches) Dynamic Accuracy

Serial Number	EIU Reading At Low Rate (in.)	EIU Reading At High Rate (in.)	Dynamic Error (in.)	EIU S/N
01	2.996	3.001	+.005	01
02	3.025	3.029	+.004	02
03	2.991	2.996	+.005	03
04	3.003	3.008	+.005	04
05	3.000	3.003	+.003	04
06	2.979	2.985	+.006	04

The above dynamic errors were well within the contract design goal of ± 0.015 inch. Transducer S/N 03 was also swept at additional rates to determine dynamic error versus sweep rate. This data is presented in Figure 36.

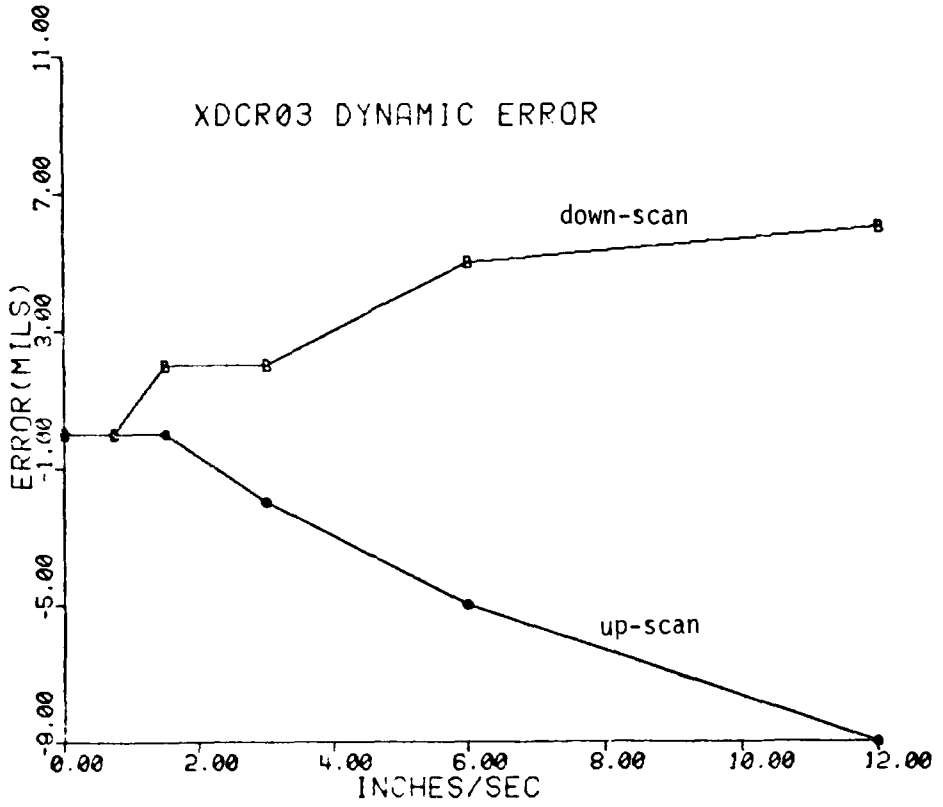

Figure 36. Transducer S/N 03 dynamic error versus sweep rate.

5.3.2.3 OPTICAL POWER MARGIN TESTS

Optical power margin tests were performed per paragraph 5.3 of the Hardware Test Plan (Appendix A) at ambient conditions per paragraph 3.1 of MIL-STD-810C. Due to the design approach taken for the EIU, it was anticipated that the errors versus optical power curve would exhibit a sharp threshold effect. The EIU output was expected to vary from a very low bit error rate to a very high bit rate within less than 1 dB of the optical power change near threshold. Therefore the following test for optical power margin was performed (see Figure 37):

1. With the transducer connected in its normal fashion and locked at 3.000 inches mechanical on the calibration fixture, the input fiber to the transducer was disconnected and the optical power from the input fiber was measured.

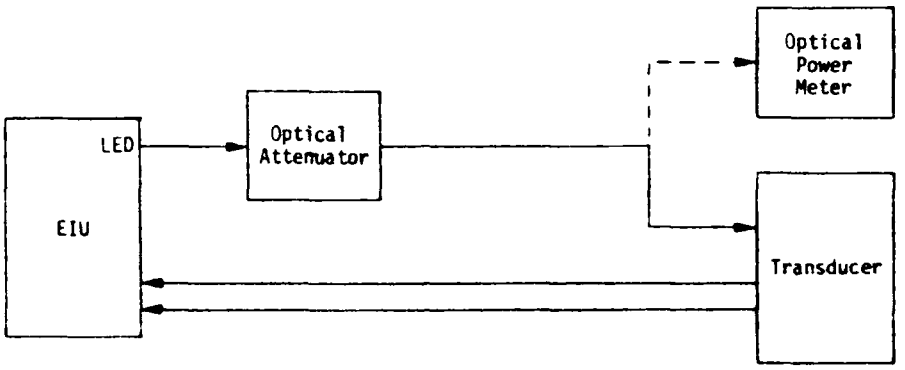

Figure 37. Optical power margin test.

2. The input fiber was then reconnected and a variable optical attenuator was inserted into the path between the EIU emitter port and fiber optic path by backing out the connector at the EIU emitter port.

3. The optical attenuation was increased until the display varied at a rapid rate between more than two readout values.

4. The optical power was then measured as in step 1) above. The difference between the two optical powers, expressed in dB, is the optical power margin.

The power meter utilized was a United Detector Technology Model 11A.

Results from this test show that the optical power margin was about 5 dB, as shown in Table 7. The optical power margin in these cases was approximately given by the ratio of the EIU AGC current turned all the way on to the AGC current when the EIU was in normal operation at the mechanical midpoint. Since the EIU's are normally calibrated to an AGC current of approximately 65 ma, and the AGC current at maximum on is 200 ma, the optical power margin would be 10 log (200 ma/65 ma) = 4.9 dB.

Since the optical power margin was restrained by the level at which the AGC was set, an additional power margin test was performed on transducer S/N 00, EIU S/N 04, and cable assembly S/N 00. EIU S/N 04 had 500K gain pots on R46 and R53.

TABLE 7. OPTICAL POWER MARGIN TEST RESULTS

Transducer Serial Number	Initial Power (microwatts)	Final Power (microwatts)	Optical Power Margin (dB)
01	720	189	5.8
02	575	180	5.0
03	600	190	5.0
04	610	185	5.2
05	600	180	5.2
06	560	175	5.1

The AGC current was set to 27 ma with R46 and R53 gain pots set to 480K and 504K respectively when the EIU was calibrated. The optical power margin was measured to be 8.7 dB and a scan of the transducer was made with the microprocessor-based test system. This scan was compared to the original scan made with the AGC set at 70 ma, and the data is presented in Figures 38 and 39. Figure 38 shows a scan of transducer S/N 00 with the AGC set at 70 ma (EIU S/N 00), and Figure 39 shows the same transducer with the AGC set at 27 ma (EIU 04). Note the vertical scale change between Figures 38 and 39. It is evident that the peak-to-peak error has increased and the signal-to-noise ratio diminished by increasing the optical power margin.

5.3.3 INTERCHANGEABILITY

An interchangeability test was conducted using the transducers available at that time. Transducers S/N 01, 02, and 03 were in environmental test and S/N 05 was in life-cycle test. That left only S/N 04 and 06 which, fortunately, have similar optics. Because the optics in S/N 01, 02, and 03 have optics of one type and S/N 04, 05, and 06 have optics (prisms) of another type, one would not expect, for example, to find S/N 01 interchangeable with S/N 04.

An EIU was aligned with transducer S/N 04. Without realignment, S/N 04 was replaced by S/N 06. Rotation marks were used to preserve fiber orientation. The errors noted were 0.003 inch at zero displacement, 0.030 inch at mid scale, and 0.006 inch at full scale. Units turned out on a manufacturing scale would probably be more interchangeable than these either because of tighter manufacturing control or because adjustments would be provided to standardize all units.

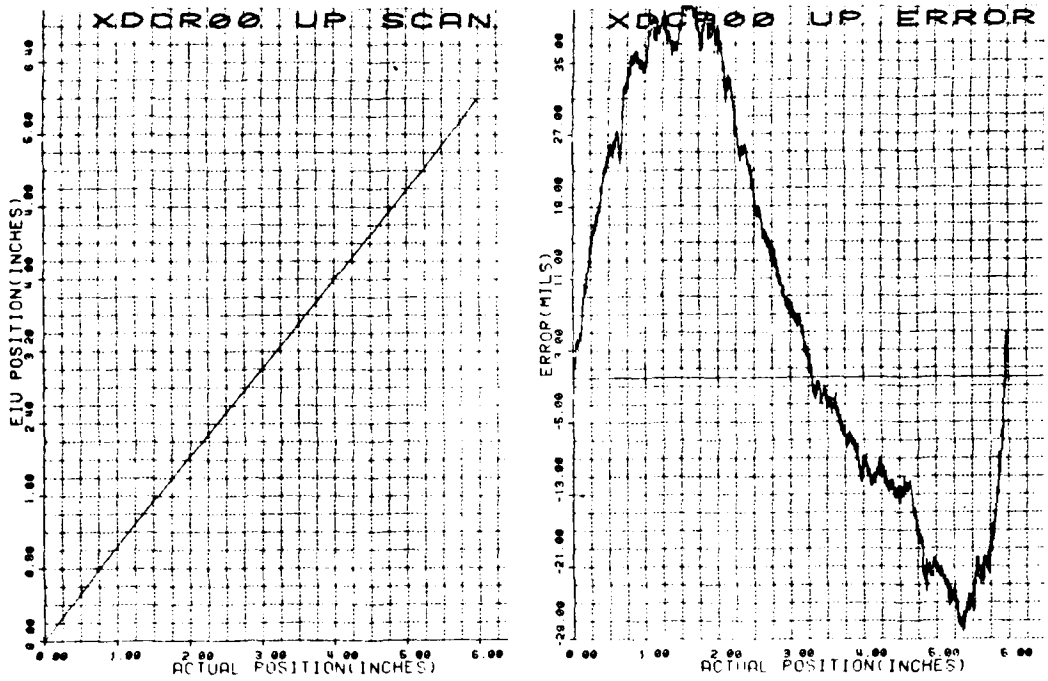

Figure 38. Transducer S/N 00 static accuracy/linearity with AGC set at 70 ma.

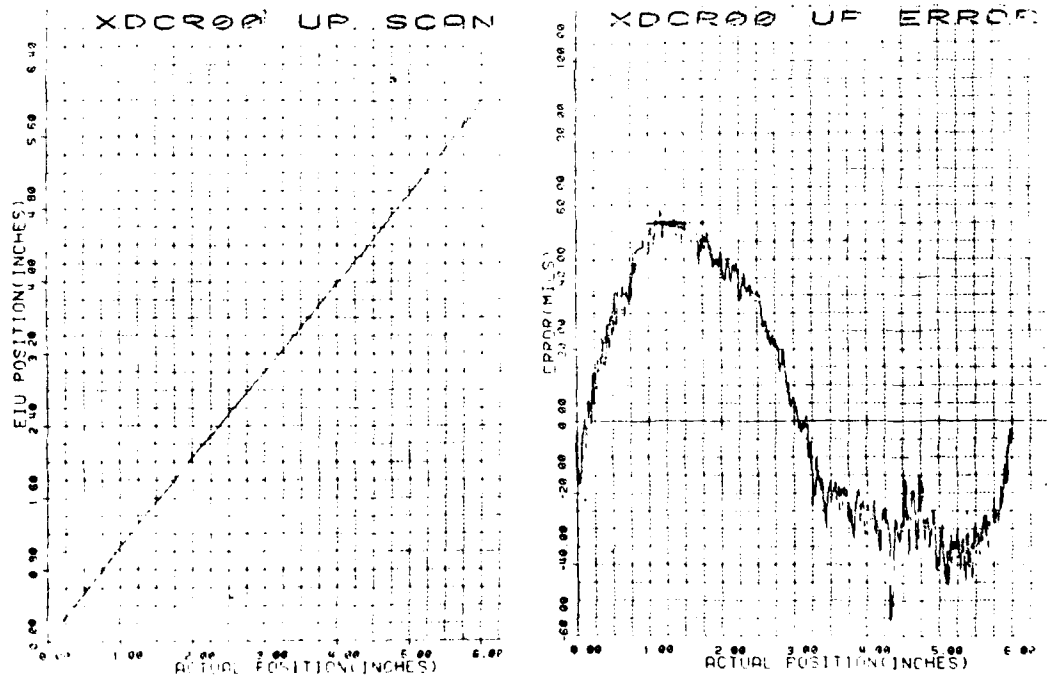

Figure 39. Transducer S/N 00 static accuracy/linearity with AGC set at 27 ma.

5.4 LIFE-CYCLE TEST PROCEDURES AND RESULTS

Life-cycle testing was performed based on a procedure described by paragraph 4.7.8.2.1 of MIL-C-5503C and at ambient conditions per paragraph 3.1 of MIL-STD-810C. The test also conformed to paragraph 6.0 of the Hardware Test Plan (Appendix A).

The life-cycle test configuration is shown in Figure 40. A computer- controlled hydraulic actuator (MTS model 204.62, 15K capacity, 6-inch stroke) with internal LVDT was used to provide the required transducer motion. The transducer was attached with clevices. An LVDT external to the actuator was used to monitor the strokes. Two microswitches 6.2 inches apart were used to prevent mechanical overtravel of the actuator. When one of these microswitches was activated, a hydraulic dump valve was triggered, which disabled the actuator hydraulics. The computer program controlled stroke length, number of cycles and test frequency. The transducer was initially calibrated on the calibration fixture. The transducer was initially set to mechanical position 3.000 inches as indicated by the EIU display, and all cycling was about this point according to the schedule presented in Table 8.

TABLE 8. LIFE-CYCLE TEST SCHEDULE

Test	Stroke Length (±3%)	No. of cycles	Frequency(Hz)
1	± 3 inches	45,000	0.32
		5,000	0.16
2	± 1.5 inches	225,000	0.64
		25,000	0.32
3	± 0.3 inch	630,000	3.2
		70,000	1.6
4	± 0.06 inch	900,000	16
		100,000	8.0
	Totals:	2,000,000: cycles in approx. 244 hours	

After test 2 (300,000 cycles of operation), it was noted that the calibration had changed +0.264 inch at the midpoint (mechanical 3.000 inches) and there was an accumulation of black powder around the shaft seal. With customer approval, the test was interrupted and the transducer was disassembled to determine the cause.

The interior of the transducer was found to be covered with the same black powder that had been noted earlier on the exterior. Further investigation showed that the powder was from a badly worn shaft seal, a Fluorocarbon Co. Type AR 10400-206GC, self-lubricated seal composed of 85% tetrafluoroethylene and 15% graphite. Figures 41 and 42 show the interior of the disassembled transducer. Note that the black powder generally distributed over the prisms and encoder and piled up in the corners of the guideways.

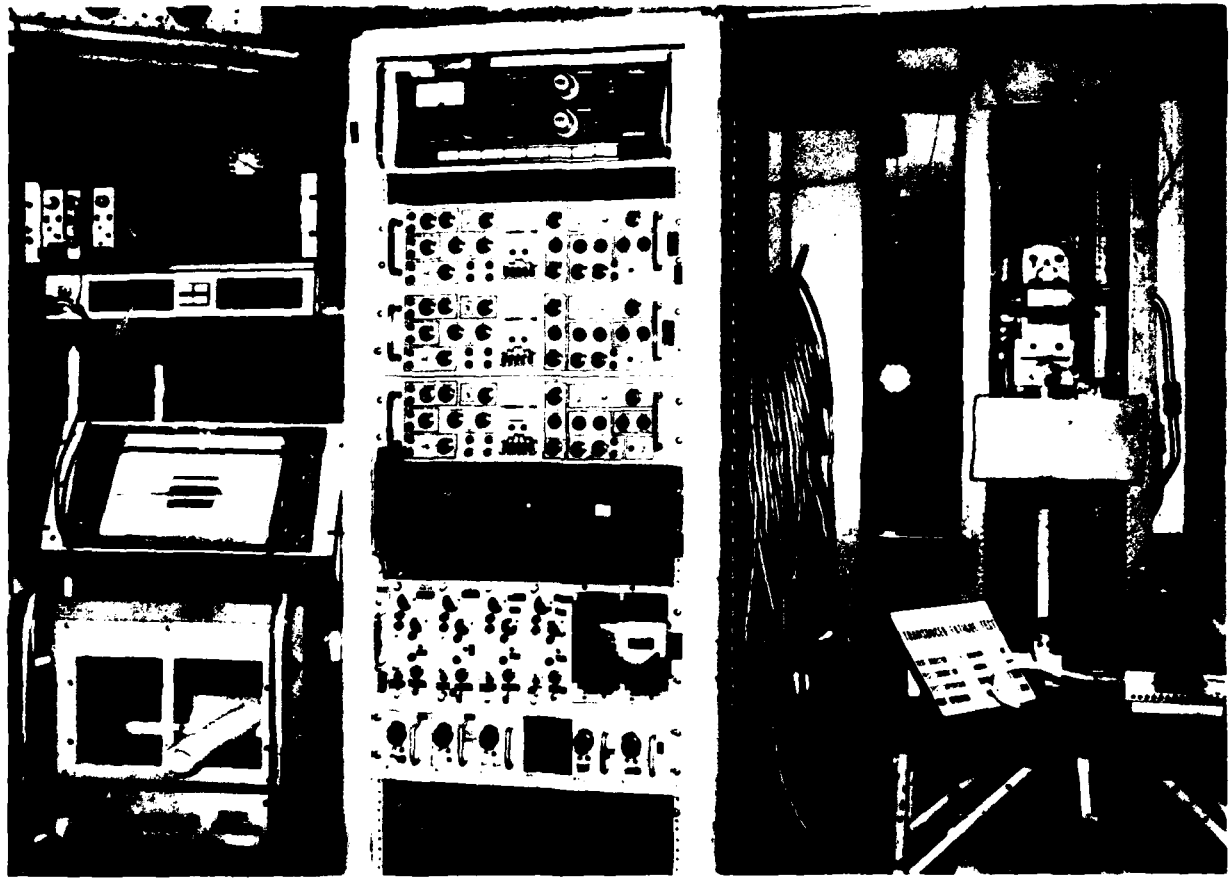

Figure 40. Life-cycle test configuration.

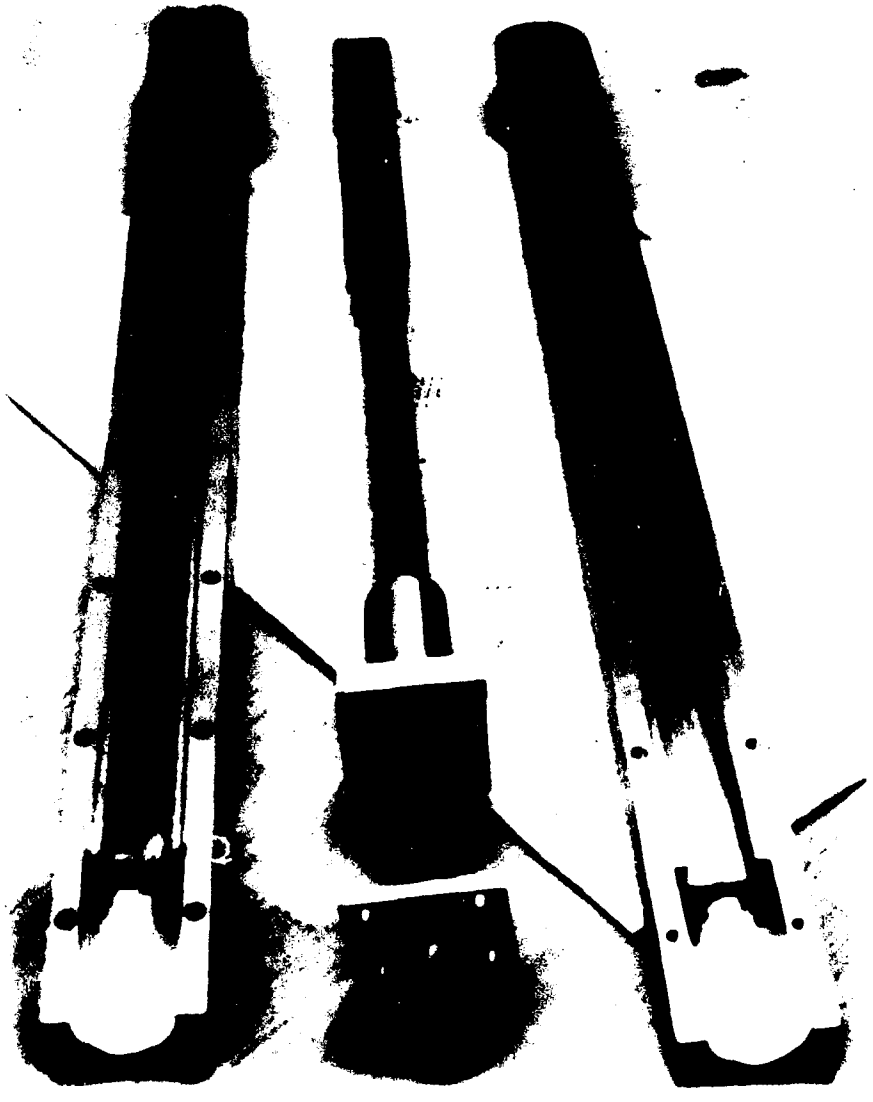

Figure 41. Transducer S/N 05 interior showing seal wear products.

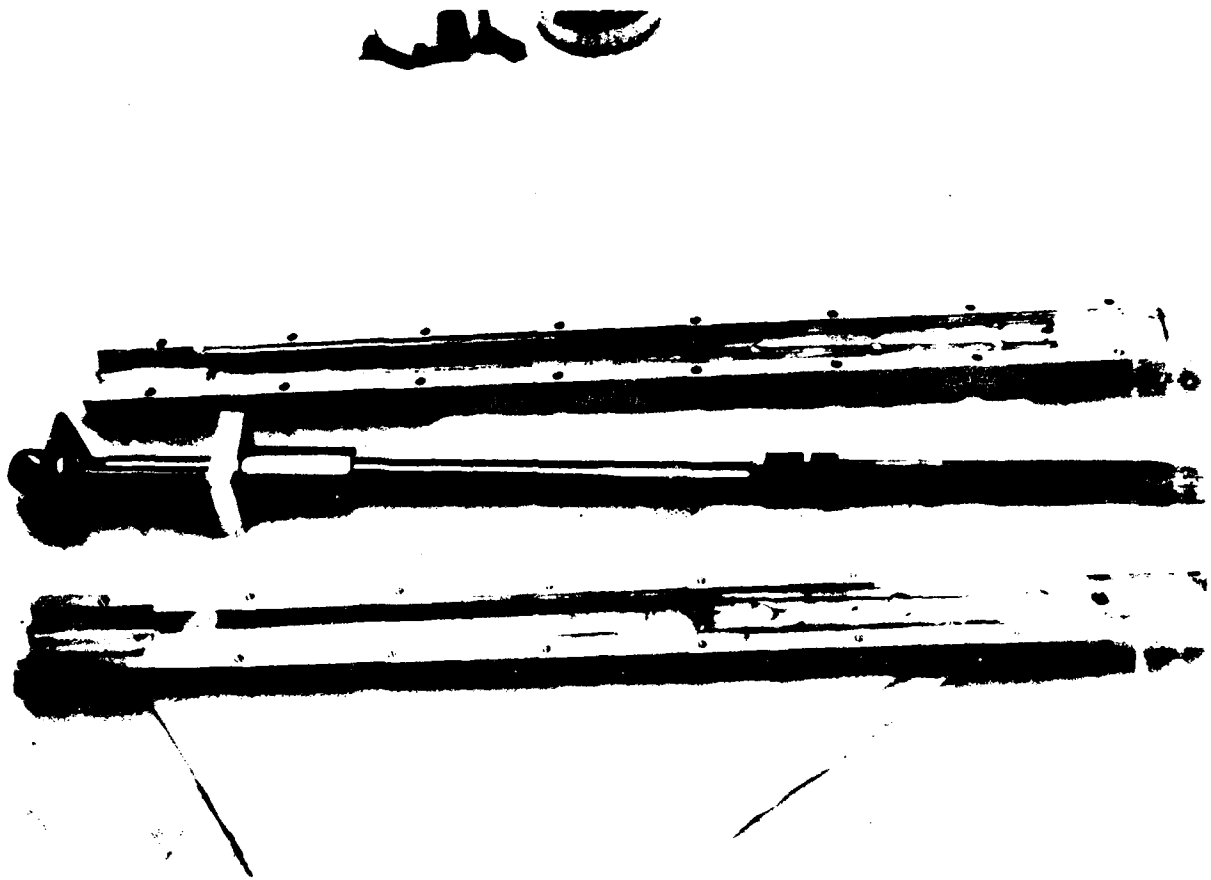

Figure 42. Transducer S/N 05 Rulon isolater/shaft separation.

A large part of the calibration error was due to an actual change in the position of the encoder relative to the actuating shaft. Apparently, enough of the seal wear products got into the guideway to cause the isolator to jam and cause the actuating rod to be pulled approximately 0.2 inch out of the isolator. It was calculated from shear strength and shear area that to do so required a force of at least 200 pounds. This force was easily provided by the hydraulic actuator used for the life-cycle test. Figure 42 shows clearly the separation between the Rulon isolator and the stainless steel actuating shaft. The isolator actuating shaft, bearings and guideway were all checked and were found well within tolerance and without visible evidence of wear. Only the seal appeared to have failed.

The transducer interior was cleaned as well as possible, and again with customer approval, was reassembled without a seal and the life-cycle test was resumed. Because the isolator was still firmly attached to the actuating shaft, no attempt was made to restore it to its original position.

The remainder of the life-cycle test was performed without incident.

5.4.1 POST LIFE-CYCLE GROUP 2 TESTS

Following the life-cycle tests, group 2 performance tests were run to determine the amount of degradation that had occurred. The results of the static accuracy tests are shown in Figures 31, 43, 44, and 45.

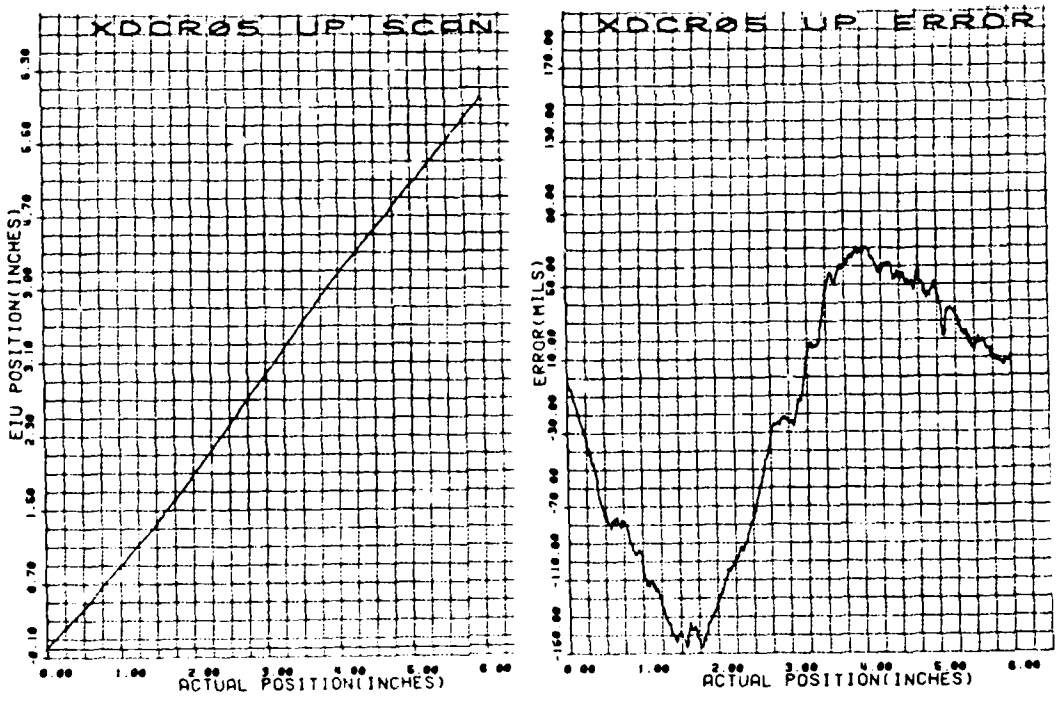

Figure 43. Transducer S/N 05 post-life-cycle static accuracy/linearity.

Figure 43 shows that transducer error relative to the pretest scan had increased due to life-cycle testing. The degradation is believed to be from seal wear products that worked loose during the last 1,700,000 cycles of the test.

A comparison of Figures 31, 44, and 45 shows that there was some permanent degradation caused by the life-cycle test. This degradation is believed to be due to seal wear products which could not be readily removed. For example, a considerable amount of the black powder worked its way under the prisms and could not be removed without risking breakage of the prisms. This problem could be eliminated in production units by making the prisms from three-layer clad material so that surface contaminants could not affect the optical properties of the prisms.

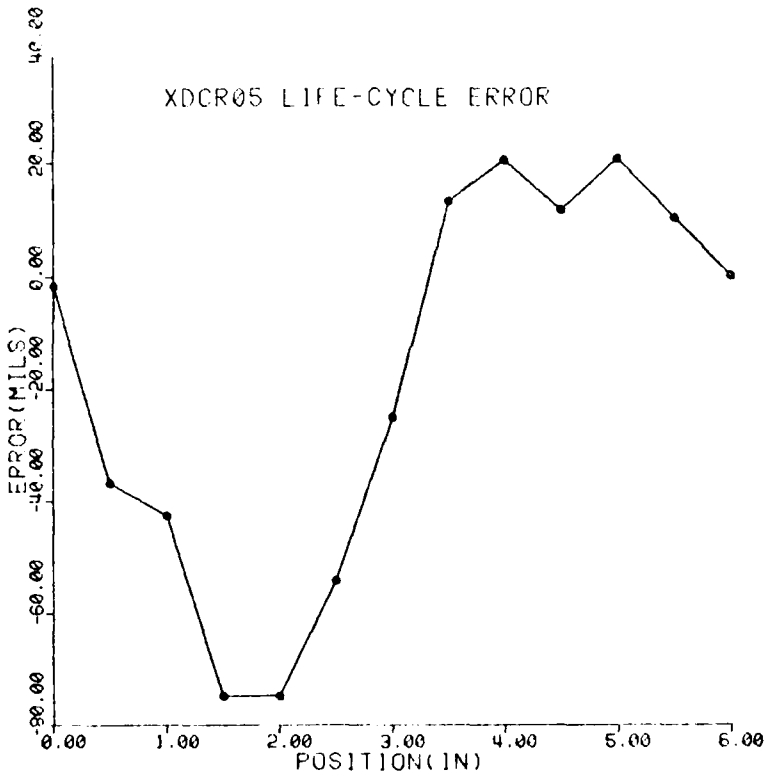

Figure 44. Transducer S/N 05 error due to life-cycle test.

Additional testing revealed that life-cycle tests did not affect dynamic accuracy significantly. A summary of pre- and post-life-cycle dynamic accuracy tests is provided. A small difference in dynamic accuracy readings is believed to be from transducer anomalies.

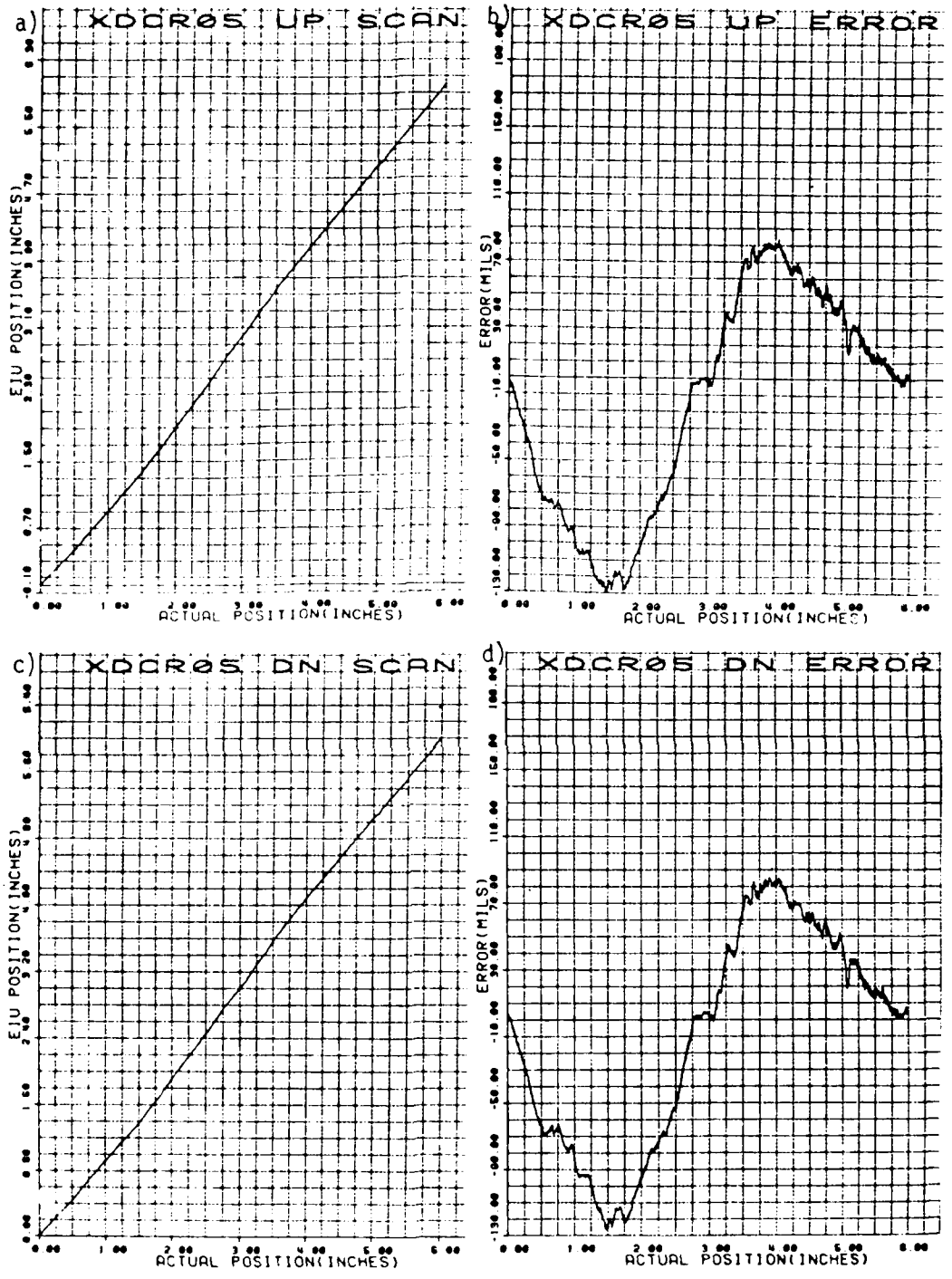

Figure 45. Post-life-cycle static accuracy/linearity for transducer S/N 05 (EIU calibrated).

Pre-life-cycle dynamic accuracy

Up-scan = -.003 inch
Down-scan = +.003 inch

Post-life-cycle dynamic accuracy

Up-scan EIU reading at low rate = 3.023 inches
Up-scan EIU reading at high rate = 3.021 inches
Down-scan EIU reading at low rate = 3.029 inches
Down-scan EIU reading at high rate = 3.034 inches

Up-scan = -.002 inch
Down-scan = +.005 inch

The change in dynamic accuracy from life-cycle testing

Up-scan = -.001 inch
Down-scan = +.002 inch

Optical power margin decreased slightly due to the life-cycle test. The reason for the decrease is believed to be the collection of seal wear products around the prisms which could not be removed for fear of breaking the prisms.

The power margin data is as follows:

Pre-Life-Cycle Optical Power Margin

Initial Power	Final Power	Optical Power Margin
600 milliwatts	180 milliwatts	5.2 dB

Post-Life-Cycle Optical Power Margin

Initial Power	Final Power	Optical Power Margin
600 milliwatts	254 milliwatts	3.7 dB

The change in Optical Power Margin = 1.5 dB

5.5 ENVIRONMENTAL TEST PROCEDURES AND RESULTS

Several environmental tests were performed on transducer systems S/N 01, 02, and 03. The tests were from MIL-STD-810C and were included in the following order:

1. Low temperature (Method 502.1)
2. High temperature (Method 501.1, Procedure II)
3. Low pressure (altitude)(Method 500.1)

4. Salt fog (Method 509.1)

5. Humidity (Method 507.1, Procedure I)

6. Dust (Method 510.1, Procedure I)

7. Vibration (Method 514.2, Procedure I, Part I, Category "C")

8. Shock (Method 516.2, Procedure I)

Performance (group 2) tests were conducted before and after the environmental tests. The order of environmental testing is different from that shown in paragraph 7.0 of the Hardware Test Plan (Appendix A) due to the difficulty of scheduling tests in the environmental chambers.

All parts of paragraph 3.0 of 810C, "General Requirements", apply to the environmental tests except for item a.(1) of Section 3.2.6, "Failure Criteria". No performance limits were established for failure determination due to the R&D level of this work. Performance data was monitored and recorded at environmental extremes, however. All of the environmental tests took place at the Boeing Earth Environment Labs, 18.24 Bldg., Kent Space Center, except for the dust test, which took place at the Naval Undersea Warfare Engineering Station, Keyport, Washington.

In all cases, only the transducers and those portions of the fiber optic cables necessary to penetrate the test chambers were required to be subjected to the environmental tests. The EIU's (laboratory type electronics) were located outside of the test chambers and operated at ambient conditions per paragraph 3.1 of MIL-STD-810C and powered "on" for not less than 1 hour.

All three transducer systems were tested simultaneously for all environmental tests.

Prior to any environmental tests, transducer S/N 01, S/N 02, and S/N 03 bodies were sealed with two coats of the conformal coating Uralane 5750, manufactured by M and T Chemical Co. This material has good bond strength, resists salt, dust, hydraulic fluid, and tolerates the required temperature range (-50°C to +135°C).

The conformal coating is clear after mixing and turns color to a golden-brown only after prolonged exposure to temperatures above 120°C. The tail bearings of the transducers were sealed with 3M aluminum foil tape #425. On the connector sleeves, locknuts were epoxied in place to allow high torque values on the fiber optic connectors (5-7 inch-pounds).

The transducer seal was tested with a low pressure de-ionized filtered air-source (3-4 psi) entering at one of the fiber-optic connector sleeves. The other connectors were capped. Air leaks were detected with soap film.

5.5.1 LOW TEMPERATURE TEST

The low temperature tests was conducted in accordance with paragraph 7.3 of the Hardware Test Plan (Appendix A). All three transducers were tested simultaneously.

The first attempt at conducting this test was aborted after the first day due to a malfunctioning refrigeration compressor. The test was started over as soon as another suitable test chamber became available. The transducers were operated during the entire test.

The test chamber used for the low (and high) temperature tests is shown in Figure 46. Three thermocouples were used to monitor temperature: two in the air in the chamber and one on the part. The part thermocouple is visible taped near the tail bushing on the center transducer.

The test article was first soaked at -70°F for 24 hours. At the end of this period, EIU readings were recorded. The test article temperature was then stabilized at -58°F (-50°C) in accordance with Step 4 of Method 502.1 and the EIU readings were recorded again. Since the EIU readings were in error and/or unstable at this temperature, EIU readings vs. part temperature readings were made when the test articles returned to ambient temperature.

A graph of the change in EIU readings vs. temperature for all three transducers is shown in Figure 47. All three transducers returned to their pretest values at ambient conditions, indicating that none of the test specimens were damaged by low temperature operation. From Figure 47, it is evident that transducer S/N 01 was the least affected by cold temperature. The error in this case was +0.011 inch at -55°F, which corresponds to 0.18% full-scale error. The readings on transducers S/N 02 and S/N 03 were unstable until about -45°F where they stabilized. At -35°F, the full-scale errors on transducers S/N 01, 02, and 03 were 0.18%, 0.87%, and 0.82% respectively.

The low temperature behavior of the transducers is not completely understood. Measurements of the LED emitter current at -70°F and -58°F showed that the AGC in the EIU was turned on all the way, indicating that a low-temperature loss mechanism was present in the transducers. The fact that transducer S/N 01 performed much better than either S/N 02 or S/N 03 indicates that considerable improvement could be made in the low-temperature performance if the degradation mechanisms were adequately understood. The cold-induced attenuation is believed to be from a combination of:

1. Change of NA and attenuation of fiber cables with temperature (not likely)
2. Possible water vapor in transducer
3. Collapse of NA of mix rods due to silicone cladding (most likely)

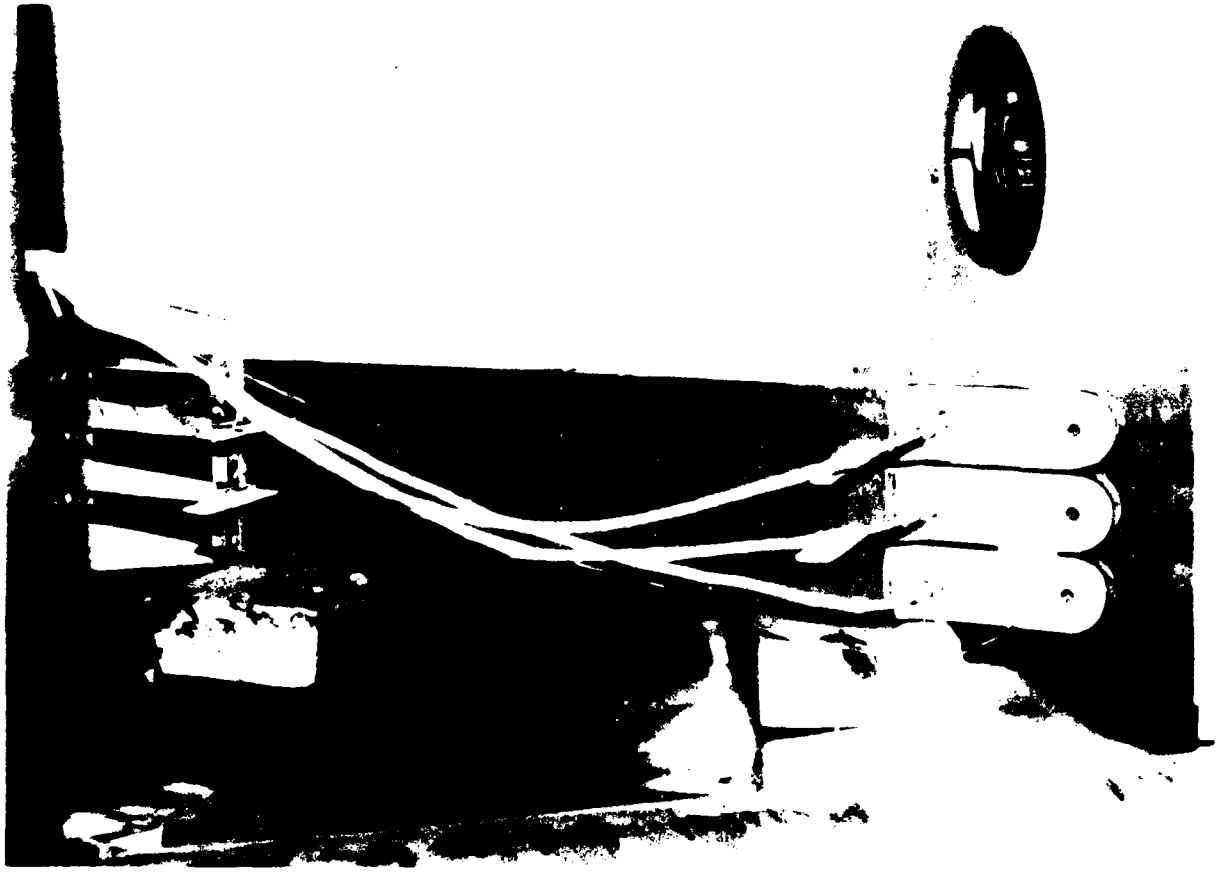

Figure 46. Transducers S/N 01, 02, 03 in low (high) temperature test chamber.

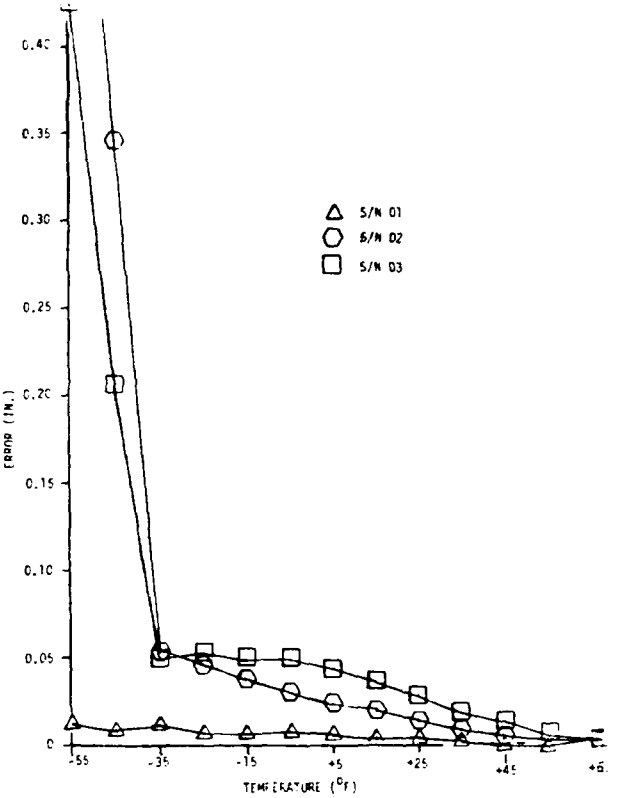

Figure 47. Low-temperature test results.

Mechanism 3 (cold temperature NA collapse of mix rods) is the most likely candidate for the sharp cutoff of transducer low-temperature performance. This can be shown by a simple calculation using the optical material properties for the mix rod material (Corning 7913 glass) and the cladding material (General Electric RTV 602). The mix rod NA decrease due to low temperature operation is given by

$$\text{NA decrease} = (n_1^2 - n_2^2)^{1/2} - \left((n_1 + \Delta T \frac{dn_1}{n_1 dT})^2 - (n_2 + \Delta T \frac{dn_2}{n_2 dT})^2\right)^{1/2}$$

$$= .366 - .161$$

$$= .205$$

where λ_o = .82 microns

n_1 = mix rod refractive index (23°C) = 1.452

n_2 = cladding refractive index (23°C) = 1.405

ΔT = 23°C - (-50°C) = 73°C

$$\frac{dn_1}{n_1 dT} \cong 9 \times 10^{-6}/^{o}C$$

$$\frac{dn_2}{n_2 dT} \cong 5.3 \times 10^{-4}/^{o}C$$

The NA decrease of .366 (23°C) to .161 (-50°C) represents an optical power loss of $(.161)^2/(.366)^2$ = 7.13 dB. An optical power loss of 5 dB would occur at a temperature of -39°C (-38.2°F) from NA effects. The EIU AGC circuitry can only compensate for ~5dB of optical attenuation, as was shown in Section 5.3.2.3. The calculated -38.2°F temperature for EIU unstable operation correlates closely with the data presented in Figure 47 for transducers S/N 02 and S/N 03.

5.5.2 HIGH TEMPERATURE TEST

The high temperature test was conducted in accordance with paragraph 7.1 of the Hardware Test Plan (Appendix A). All three transducers were tested simultaneously. The test chamber is illustrated in Figure 46.

The test articles were cycled between +120°F and +160°F for 36 hours prior to stabilizing at the highest temperature at which the test article is designed to operate (+275°F). Temperature cycling results for the three transducers showed that the maximum deviations for transducers S/N 01, 02 and 03 were -0.33%, -0.25%, and -0.88%, respectively, relative to ambient conditions.

After the transducers had stabilized at +275°F, they were returned to ambient conditions. A plot of EIU deviation vs. temperature is shown in Figure 48 for all three transducers for a temperature range of +275°F to 75°F. Transducer S/N 01 has the best performance with a peak deviation of about 0.5% of full scale over this temperature range. The causes of the thermal drift have not yet been fully analyzed. All three transducers returned to their pretest values at ambient conditions, indicating that none of the test specimens were damaged by high temperature operation.

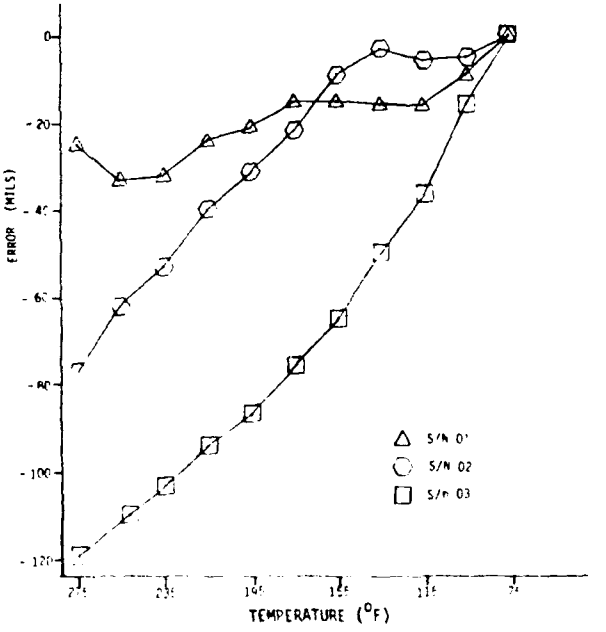

Figure 48. High-temperature test results.

5.5.3 ALTITUDE TEST

The low-pressure (altitude) test was performed in accordance with paragraph 7.2 of the Hardware Test Plan (Appendix A). All three transducers were tested simultaneously and operated during the entire test.

The test chamber pressure was decreased to 429.1 mm of Hg (15,000 ft. above sea level) at a rate not to exceed 2,000 fpm and held for at least 1 hour. The chamber pressure was then returned to sea level (at 2,000 fpm). Tabulated below are the EIU readings (inches) for the transducers taken at sea level before and after the test and at 15,000 feet altitude.

	S/N 01	S/N 02	S/N 03
Initial sea level	3.004	3.012	2.997
Initial at 15,000 ft.	3.006	3.015	3.000
After 1 hr. at 15,000 ft.	3.006	3.013	2.999
Final sea level	3.004	3.012	2.997

The errors produced by altitude change are very small and at this time, unexplained. The transducers returned to their pretest values, indicating that they were not damaged by 15,000 feet above sea level operation.

5.5.4 SALT FOG TEST

During the salt fog test, the transducers were tested simultaneously and operated continuously during the test duration.

The test articles received 48 hours of exposure to salt fog at a temperature of 35°C (95°F). After the 48-hour exposure period, the test item was allowed to corrode in an ambient atmosphere for 48 hours. The test item was subjected to a gentle wash in running water prior to the corrosion period. The transducers in the salt fog chamber immediately after the 48-hour exposure period are shown in Figure 49. Note the corrosion on the shaft locks.

The transducers were initially set to their 3-inch mechanical midpoint using the standard calibration fixture. They were then locked in those positions for the 48-hour exposure period and the EIU readout was monitored for changes. After the 48-hour exposure period, the transducers were cycled thirty times (per paragraph 7.5 of Hardware Test Plan) prior to a gentle wash in fresh water. They were then reset to their mechanical midpoints and another set of EIU readings was taken.

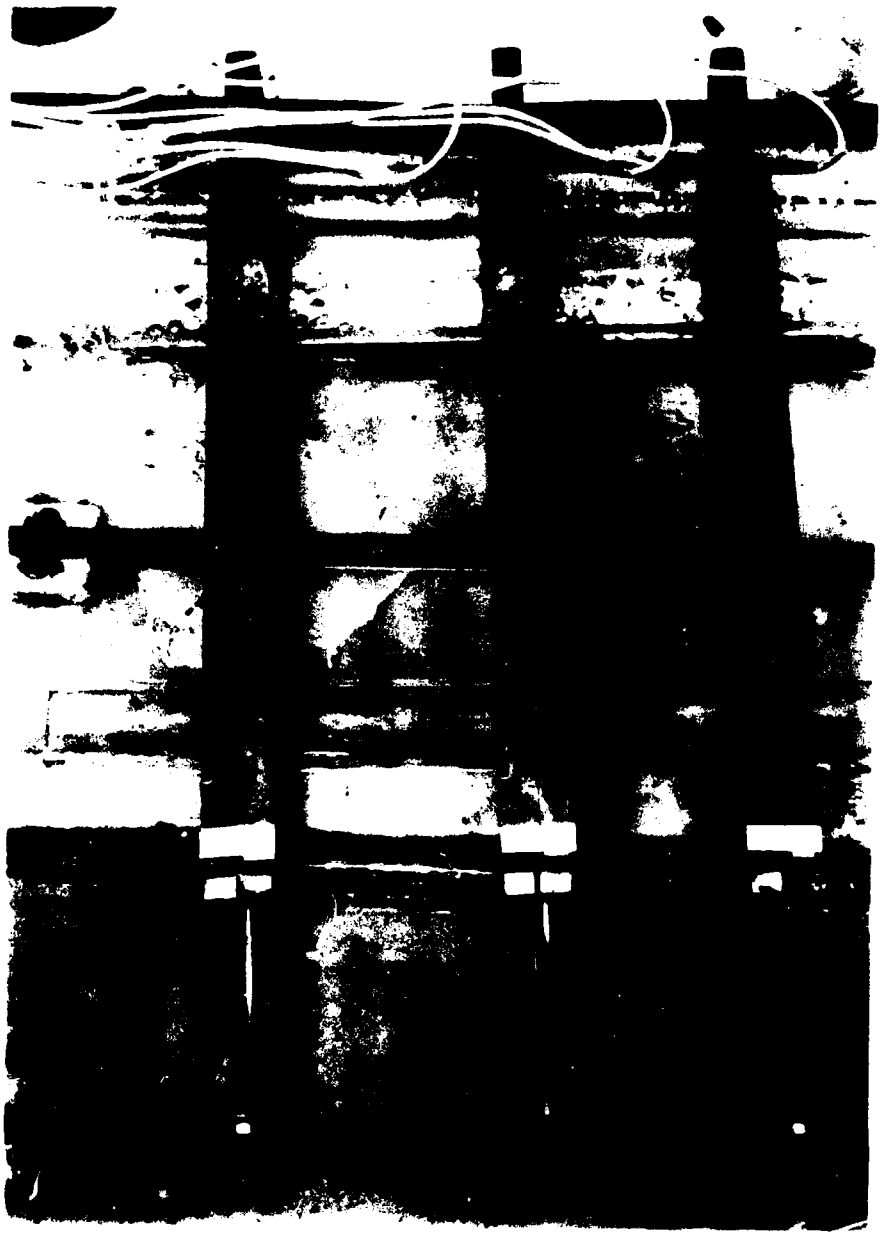

Figure 49. Transducer in salt fog chamber immediately after 48-hour exposure period.

After the 48-hour corrosion period, another set of EIU readings was taken. The four sets of EIU readings (inches) were as follows:

	S/N 01	S/N 02	S/N 03
Pretest	3.182	3.080	2.846
After 48-hour exposure	2.906	2.990	2.872
After cycling	2.955	2.930	2.774
After 48-hour corrosion	1.978	3.526	2.437

Or, in terms of percent error:

	S/N 01	S/N 02	S/N 03
Pretest	0%	0%	0%
After 48-hour exposure	- 9.5	- 3.3	+ 0.9
After cycling	- 7.7	- 5.4	- 2.6
After 48-hour corrosion	-60.8	+14.1	-16.8

Note that most of the degradation occurred during the 48-hour corrosion period. These transducers were not disassembled to determine the cause of degradation because they were scheduled for other environmental tests. However, the optical connectors were removed and a cursory examination was conducted. Moisture was found on the tips of the Amphenol 905 fiber optic plugs, indicating that the connector assemblies had not been sealed adequately even though they had been tightened with a torque wrench to 5 inch-pounds. During final assembly, the transducers were pressure tested to determine the integrity of the various joints and the conformal coating. In retrospect, there should have been a test fitting installed on the transducer specifically for pressure testing, and the pressure test should have been conducted with all fiber optic connections in place. Also, it appears that an O-ring seal in the connectors might have eliminated the problem.

The degradation which occurred during the 48-hour corrosion period is believed to be primarily due to salt corrosion of the aluminized facets of the prisms. This suspicion is supported by the abnormal pattern seen when looking into the optical ports, by the 3-dB increase in transducer insertion loss, and by examining the prisms of transducer S/N 01 when it was disassembled after all environmental tests were complete.

The aluminized facets of the prisms in transducers S/N 01, S/N 02, and S/N 03 were unprotected and quite vulnerable to salt corrosion. Had the salt fog test been conducted on transducers S/N 04, S/N 05, and S/N 06, it is unlikely that the facets would be damaged. The facets in those transducers had been given an overcoating of silicon dioxide, mostly to protect them from possible abrasion during the assembly process.

5.5.5 HUMIDITY TEST

The humidity test was conducted in accordance with paragraph 7.4 of the Hardware Test Plan. All three transducers were tested simultaneously and operated during the test duration.

The test articles received ten 24-hour cycles of temperature/humidity cycling. EIU readings were taken at three times with the tranducers locked at their mechanical midpoints. First, EIU readings were taken at ambient conditions prior to the start of the test. Next, per Step 6 of MIL-STD-810C, Method 507.1, Procedure 1, EIU readings were taken at the conclusion of the tenth cycle, while still at 30°C (86°F) and 85% relative humidity. Lastly, EIU readings (inches) were taken after return to ambient conditions. Tabulated below are the results of the humidity test:

	S/N 01	S/N 02	S/N 03
Pre-Test (Ambient)	1.947	3.443	2.327
After Tenth Cycle	2.516*	3.348	2.204
Post-Test (Ambient)	2.437*	3.356	2.214

Or in terms of percent error
* = unstable

Pre-Test (Ambient)	0%	0%	0%
After Tenth Cycle	+22.5	-2.8	-5.6
Post-Test (Ambient)	+20.1	-2.6	-5.1

Transducer S/N 01 EIU display became unstable after the eighth day of humidity testing. Measurements of LED emitter current revealed that the AGC in the EIU emitter was turned on all the way, indicating that a humidity-related loss mechanism was present in the transducer. Additional AGC measurements on S/N 02 and S/N 03 showed that these EIUs were on the verge of instability, indicating that humidity-dependent loss mechanisms were present in these transducers as well.

The degradation caused by hur ity was investigated. These transducers were not disassembled to determine the cause of degradation, since they were scheduled for other environmental tests. However, a cursory examination was conducted which revealed the presence of moisture on the fiber optic plugs and inside the transducer bodies. A static accuracy scan of transducer S/N 02 was made using EIU S/N 00 (prototype) and cable assembly S/N 04. This scan appears in Figure 50. EIU S/N 00 was calibrated to transducer S/N 02 with the AGC set to 60 ma prior to the scan. Note that this scan shows possible evidence of encoding plate contamination from water droplets in the transducer.

In order to remove the water from transducers S/N 01, 02, and 03, they were placed in an oven and dried for a period of 7 hours at a temperature of 110°C (230°F). The fiber optic connectors were loosened to allow steam to escape.

A post drying cycle static accuracy scan (Figure 51) was made with transducer S/N 02, EIU S/N 00, and cables S/N 04 which showed that the bulk of the optical contaminants had been removed by drying. However, not all of the contamination was removed. The rest of the contamination is believed to be left over from salt and corrosion deposits from the salt fog test.

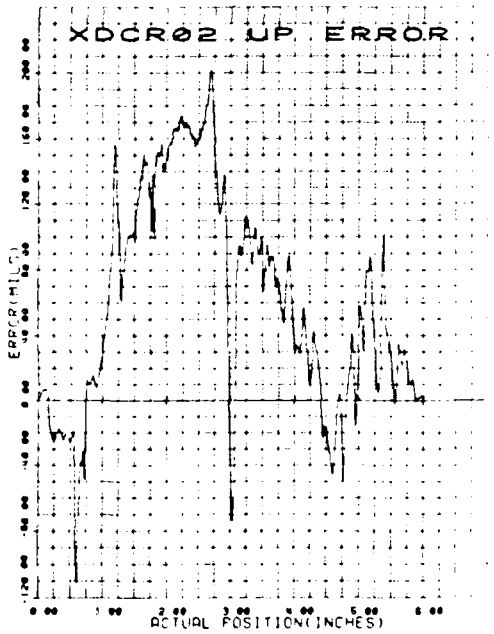

Figure 50. Post-humidity error curve for Transducer S/N 02.

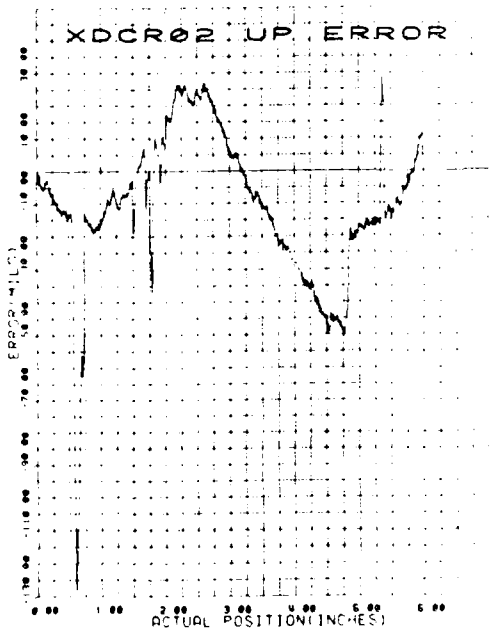

Figure 51. Post-humidity error curve for Transducer S/N 02 after drying.

AD-A117 918 BOEING AEROSPACE CO SEATTLE WA ENGINEERING TECHNOLOGY DIV F/G 20/6
DEVELOPMENT AND TEST OF A DIGITAL/OPTICAL LINEAR POSITION TRANS--ETC(U)
JUN 82 G E MILLER, T A LINDSAY, B E JOHNSON DAAK51-80-C-0028
UNCLASSIFIED USAAVRADCOM-TR-82-D-6 NL

2 OF 3
AD A117918

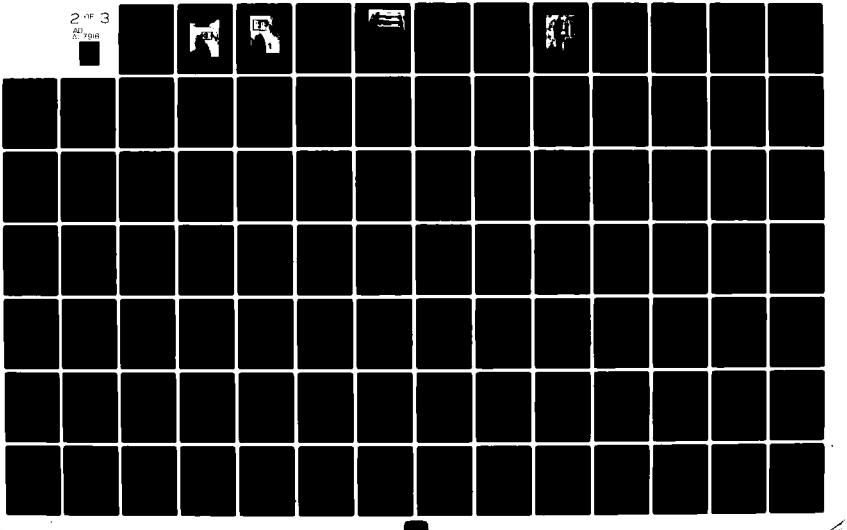

5.5.6 DUST TEST (fine sand)

The dust test was conducted in accordance with paragraph 7.6 of the Hardware Test Plan (Appendix A). All three transducers were tested simultaneously in the dust test facility at the Naval Undersea Warfare Engineering Station, Keyport, Washington. Figure 52 illustrates the transducers in the dust chamber before testing.

The test articles were first subjected to 6 hours of high-velocity (~1850 ft/min) dust at ambient conditions. EIU readings were recorded before and after this period. Even though transducers S/N 01 and S/N 03 were badly out of calibration due largely to bad fiber optic cables, the cables were not replaced prior to the dust test because the supply of spares was nearly exhausted. It was felt that gross changes in the transducers could be detected during the test even with the bad cables. With the transducers locked at 3 inches mechanically, the initial EIU readings (inches) were:

S/N 01	0.642
S/N 02	3.180
S/N 03	0.995

EIU readings (inches) after 6 hours of ambient high-velocity dust were:

			Error
S/N 01	0.626	=	-0.016
S/N 02	3.148	=	-0.032
S/N 03	0.949	=	-0.006

Next, the test articles were subjected to 16 hours of low-velocity air (300 ft/min) at elevated temperature (145°F) and EIU readings were recorded.

EIU readings (inches) after 16 hours of low-velocity/high-temperature air were:

			Error
S/N 01	0.679	=	+0.037
S/N 02	3.188	=	+0.008
S/N 03	0.941	=	-0.014

Finally, after the transducers underwent 6 hours of high-velocity (1850 ft/min), high-temperature (145°F) dust, the EIU readings (inches) were:.

			Error
S/N 01	0.647	=	+0.005
S/N 02	3.015	=	-0.165
S/N 03	0.730	=	-0.255

The transducers in the dust chamber after testing are shown in Figure 53.

Figure 52. Transducers in sand and dust chamber before testing.

Figure 53. Transducers in sand and dust chamber after testing.

The transducer systems were then transported back to the Kent Space Center for post-test cycling and measurements. When the transducers were connected to their respective EIU's, it was evident that some cable fatigue fractures had occurred. The cables were checked and the ones that had failed were replaced with new cables. EIU readings were recorded before and after 30 full stroke cycles. The results are summarized below. The EIU's were not recalibrated.

EIU readings (inches) prior to cycling (at 3 inch mechanical) were:

S/N 01	2.516
S/N 02	2.941
S/N 03	3.982

EIU readings (inches) after thirty cycles (3 inch mechanical) were:

			Error
S/N 01	2.472	=	-0.044
S/N 02	2.941	=	0.000
S/N 03	3.953	=	-0.029

The transducers survived the dust test with minimal damage except that a fraction of the fibers in each of several fiber optic cables was fractured, apparently due to fatigue from the wind in the dust chamber. Prior to the dust test, some of the fiber optic cables had already suffered considerable damage. During the humidity test and the drying cycle which followed, many fibers were fractured and it is likely that others became much more susceptible to fatigue failure.

The changes in the EIU readings at the end of the dust test were permanent and are believed to be from three sources: 1) cable fatigue fracture caused by high winds in the dust chamber, 2) bad fiber optic connector seal, and 3) bad transducer shaft seal.

5.5.7 VIBRATION TEST

Vibration tests were conducted in accordance with paragraph 7.8 of the Hardware Test Plan (Appendix A). All three transducers were tested simultaneously and operated throughout the test. The transducers were locked in the test fixture at approximately the midpoint as shown in Figure 54. The definition of axes for vibration (and shock) is shown in Figure 55. A computer-controlled Ling 249 vibrator was used.

Prior to the vibration and shock tests, the screws and connectors of the transducers which were not covered by conformal coating were locked down to prevent movement during testing. The four screws that secure the shaft/seal housing to the main body of the transducer were lock-wired together. Also, the fiber optic connectors were tightened to 5 inch-pounds of torque and locked in place with the epoxy Metric-grip 303.

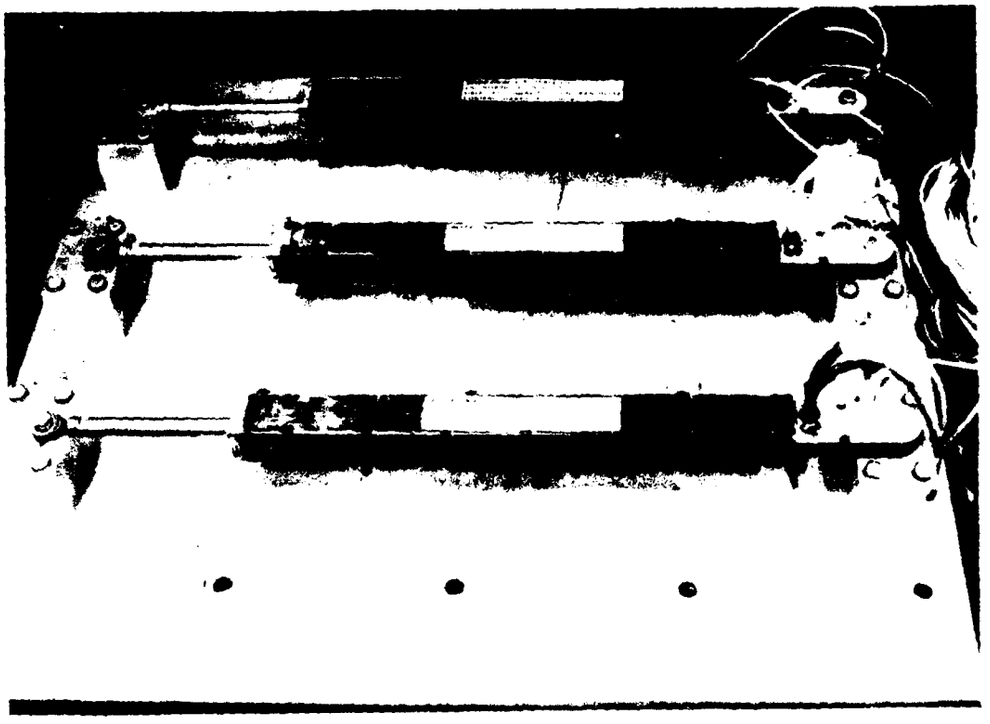

Figure 54. Vibration/shock test fixture.

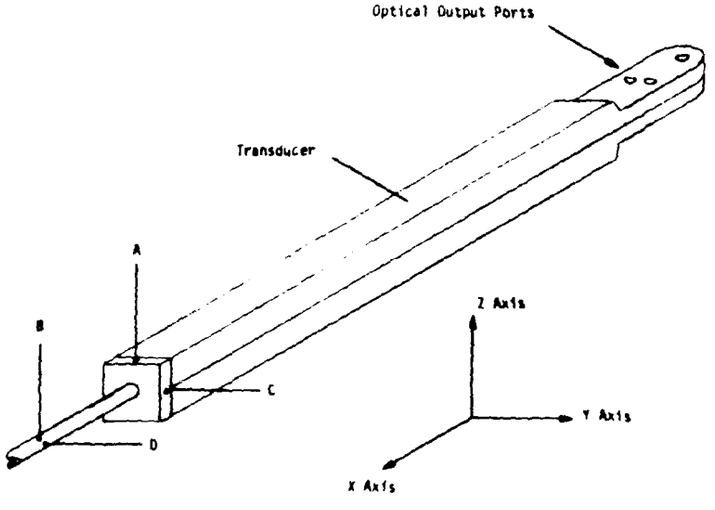

Figure 55. Definition of transducer axes for shock/vibration.

The Z-axis vibration was run first because it was expected to be the worst axis in terms of potential glass breakage. The parts experienced five cycles of sinusoidal frequency sweep from 5 Hz to 2000 Hz to 5 Hz. At frequencies below 33 Hz, the input to the vibration table was ±2g and above 52 Hz the input was ±5g. During the Z and Y axes of vibration, two instrumentation accelerometers were utilized at points A, B and C, D respectively on transducer S/N 03 to monitor resonances. The prototype EIU was calibrated to transducer S/N 03 to act as a control during the tests, since the EIU readings were unstable. A typical vibration curve of peak acceleration versus frequency is shown in Figure 56 (X-axis). The other vibration curves are contained in Appendix E.

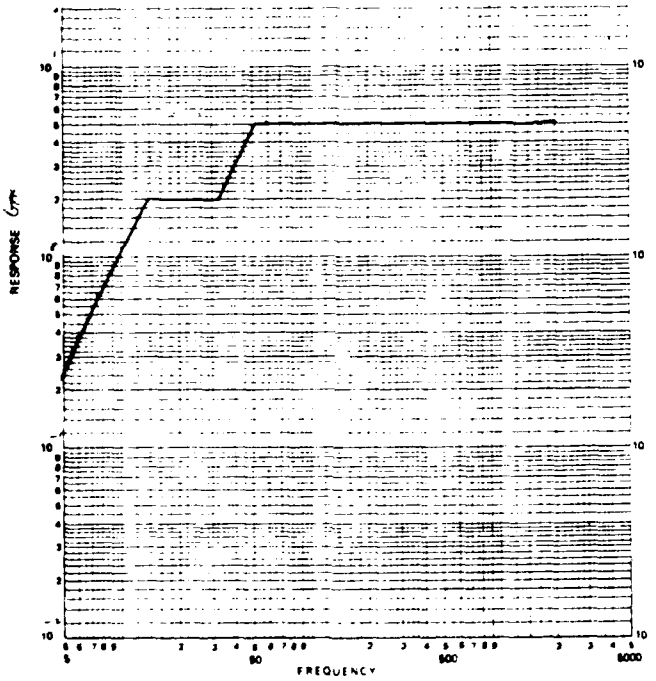

Figure 56. Typical MIL-STD-810C vibration curve.

Z-axis Test

A low-level (± ½g) sinusoidal sweep was run on transducer S/N 03 and revealed two major resonances at approximately 114 Hz and 568 Hz. The Q factors were 40 and 16 respectively, measured on the shaft accelerometer (B in Figure 55). These would correspond to peak-to-peak g levels of 400 (at 114 Hz) and 160 (at 568 Hz) at the full MIL-STD-810C ± 5g input levels. Since it was only 400 g's on the shaft, it was decided to run a full-level sweep with transducer S/N 03 to test its response. No noticeable change occurred in transducer S/N 03 for the test sweep. The other two transducers were then mounted on the test fixture and the Z-axis vibration test was run. EIU readings were recorded before and after vibration.

Pre-test EIU readings (in.)

S/N 01	1.660
S/N 02	3.174
S/N 03	2.968

Post-test EIU readings (in.)

			Error
S/N 01	1.708	=	+.048
S/N 02	3.164	=	-.010
S/N 03	2.968	=	0.000

Two rod end bearings were broken off during the course of the test after passing through the 114 Hz resonance. A rod end bearing was broken on transducer S/N 01 1 hour 47 minutes into test and is shown in Figure 57. Another rod end bearing was lost on transducer S/N 02 2 hours 40 minutes into test. In both cases the vibration table was stopped, the broken rod end bearing was replaced, and the test was continued. The failed rod end bearings were made of a mild steel. The failure could have been prevented by replacing them with bearings made of higher strength steel.

At the conclusion of the Z-axis vibration test, the transducers were examined for evidence of glass breakage. No evidence of glass breakage was observed when the transducers were translated over their 6-inch stroke range.

Y-axis Test

A low-level (± ½g) sinusoidal sweep was run on transducer S/N 03 which revealed two major resonances at 118 Hz (Q = 16) and at 570 Hz (Q = 11). The instrumentation accelerometers were placed at locations C and D in Figure 57. EIU readings were recorded before and after vibration.

pre-test EIU readings (in.)

S/N 01	1.809
S/N 02	3.147
S/N 03	2.940

post-test EIU readings (in.)

		Error
S/N 01	1.808	-0.001
S/N 02	3.144	-0.003
S/N 03	2.972	+0.032

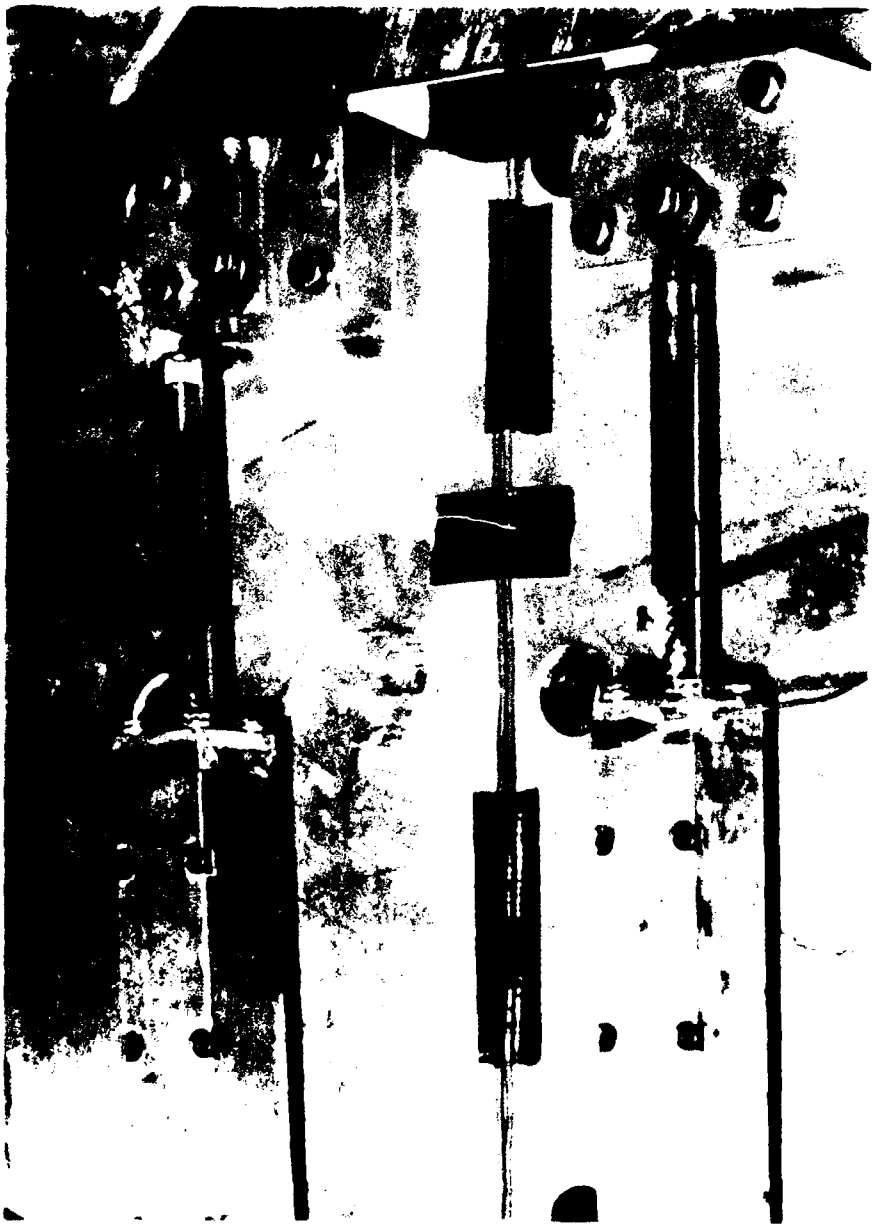

Figure 57. Broken rod end bearing during Z-axis vibration.

The rod end bearing on transducer S/N 02 failed 1 hour 55 minutes into the test. It was replaced and the test was resumed. No evidence of glass breakage was observed in any of the transducers.

X-axis Test

No instrumentation accelerometers were utilized for the X-axis vibration test. The EIU readings before and after vibration are summarized below.

Pre-test EIU readings (in.)

S/N 01	1.802
S/N 02	3.130
S/N 03	2.978

Post-test EIU readings (in.)

			Error
S/N 01	1.780	=	-0.022
S/N 02	3.130	=	0.000
S/N 03	2.979	=	+0.001

Transducer S/N 03 survived Z, Y, X axis vibration intact (no broken rod end bearings). Some fatigue fracture of fibers evidently occurred from vibration.

5.5.8 SHOCK TEST

The shock test was conducted in accordance with paragraph 7.7 of the Hardware Test Plan (Appendix A). All three transducers were tested simultaneously and operated during the test duration. The definition of axes for shock is shown in Figure 55. Shock pulses were provided by the same computer-controlled Ling 249 vibrator used for vibration test. Shock tests for the axes Z, Y, X took place immediately after vibration tests for axes Z, Y, X.

MIL-STD-810C, Method 516.2, Procedure I (flight vehicle equipment) requires that each axis receive six sawtooth shock pulses (20 g peak, 11 millisecond duration). Three of the six shock pulses for each axis are positive (+g's) and the other three pulses are negative (-g's). Typical shock pulses are shown in Figures 58 and 59. These shock pulses were from the X-axis.

Z-axis Test

EIU readings were taken before and after each shock pulse. Z axis shock did not have any measurable effect on transducer operation. The pre-shock EIU readings (in.) were:

S/N 01	1.708
S/N 02	3.161
S/N 03	2.962

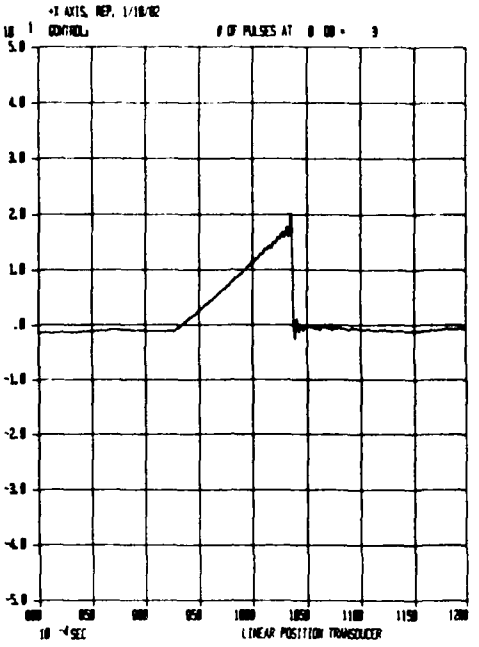

Figure 58. Typical sawtooth shock pulse (positive).

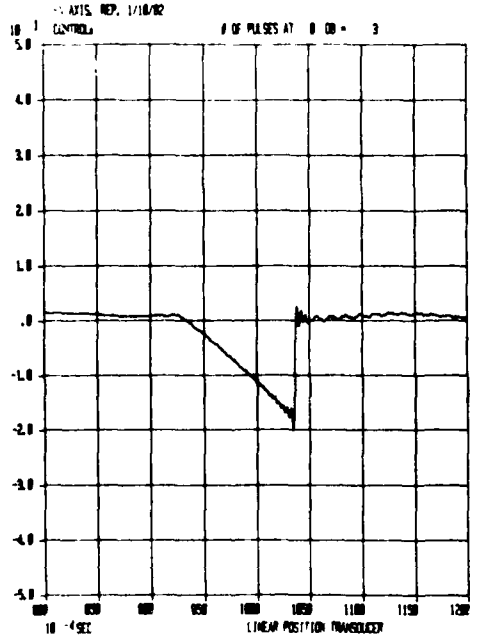

Figure 59. Typical sawtooth shock pulse (negative).

The EIU readings did not change before/after any of the six shock pulses.

Y-axis Test

The pre-shock EIU readings (in.) were:

			Error
S/N 01	1.809	=	0.000
S/N 02	3.144	=	0.000
S/N 03	2.972	=	0.000

The post-shock EIU readings (in.) were:

			Error
S/N 01	1.809	=	0.000
S/N 02	3.144	=	0.000
S/N 03	2.975	=	+0.003

The EIU reading for S/N 03 changed to 2.975 inches after the first shock pu (positive). It did not change for any of the other five pulses.

X-axis Test

The pre-shock EIU readings (in.) were:

S/N 01	1.780
S/N 02	3.130
S/N 03	2.979

The EIU readings did not change before or after any of the six shock pulses.

5.5.9 POST-ENVIRONMENTAL PERFORMANCE TEST RESULTS

Following the MIL-STD-810C environmental tests, Group 2 performance tests (described in Section 5.3) were performed in accordance with the Hardware Test Plan (Appendix A), except that calibration procedures were done prior to these tests.

It had been shown that most of the degradation suffered during environmental testing was due to fracture of the fiber optic cables. Post-environmental checkout of the fiber optic cable assemblies S/N 01, 02, 03 revealed that of the nine total cables, five had failed catastrophically (greater than 15 dB attenuation increase), three had degraded significantly (greater than 3 dB attenuation increase), and one had degraded slightly (1.5 dB). These tests, therefore, were performed with good cables (S/N 04), which meant that the EIU had to be recalibrated. EIU S/N 04 was used for these tests.

5.5.9.1 STATIC ACCURACY, LINEARITY, RESOLUTION, AND MONOTONICITY

The static accuracy/linearity tests showed that transducers S/N 01, S/N 02 and S/N 03 suffered permanent degradation as a result of environmental testing (Figures 60 to 63). The results of the static accuracy test are shown in Figures 27, 60, 28, 61, 29, 62, and 63. Figures 27, 28, and 29 show pre-environmental static accuracy/linearity test data for comparison.

The degradation in transducer static accuracy/linearity from environmental testing is characterized by an increase in peak-to-peak error and an increase in RMS "noise" (decrease in monotonicity). A tabulation of pre- and post-environmental peak-to-peak errors is presented below.

TABLE 9. PRE-ENVIRONMENTAL AND POST-ENVIRONMENTAL PEAK TRANSDUCER ERRORS

Transducer	Pre-environmental Peak-to-Peak Error (in.)	Post-environmental Peak-to-Peak Error (in.)	Peak-to-Peak Error Difference (in.)
S/N 01	0.082(±.68%FSR)	0.118(±.98%FSR)	+0.036(±.3%FSR)
S/N 02	0.090(±.75%FSR)	0.165(±1.37%FSR)	+0.075(±.63%FSR)
S/N 03	0.072(±.60%FSR)	0.120(±1.00%FSR)	+0.048(±.4%FSR)

From environmental testing, the average peak-to-peak error difference was only ±0.45% full scale, there were no catastrophic failures, and all the transducers still performed as transducers when the defective cables were replaced. The monotonicity of the transducers decreased, as evidenced by the lack of smoothness in the error curves.

Figure 63 shows static accuracy/linearity information from transducer S/N 03 without EIU calibration. EIU S/N 03 was used and the fiber optic cables were replaced with cable set S/N 06. Note that the transducer S/N 03 is still a transducer, but the peak error has increased without calibration.

The permanent degradation observed in static accuracy/linearity of transducers S/N 01, S/N 02, and S/N 03 as a result of environmental testing is believed to be primarily from two sources:

1. Contamination of the encoding plate and prisms from salt fog and humidity

2. Increased transducer attenuation caused by salt fog corrosion of mirrored prism facets.

These two sources of degradation were verified when transducer S/N 01 was opened after all post-environmental testing was complete.

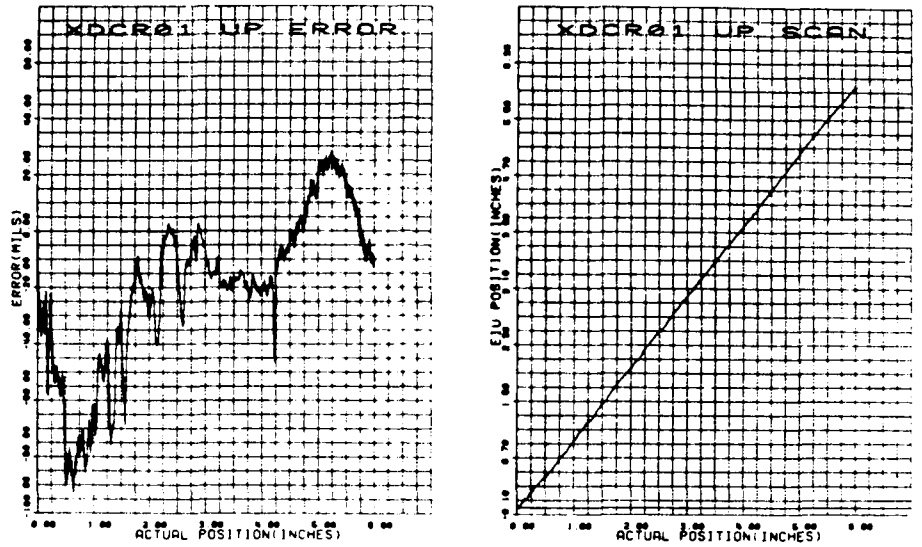

Figure 60. Transducer S/N 01 static accuracy/linearity after environmental testing.

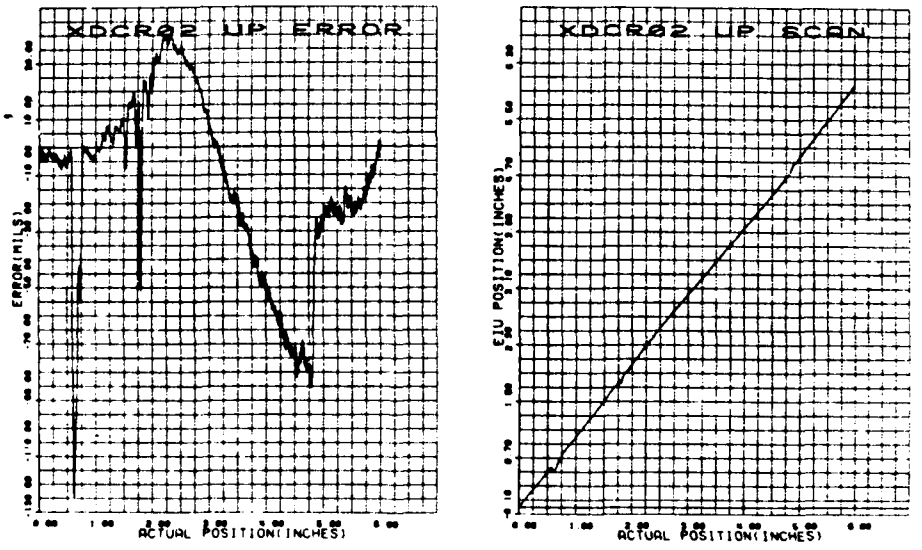

Figure 61. Transducer S/N 02 static accuracy/linearity after environmental testing.

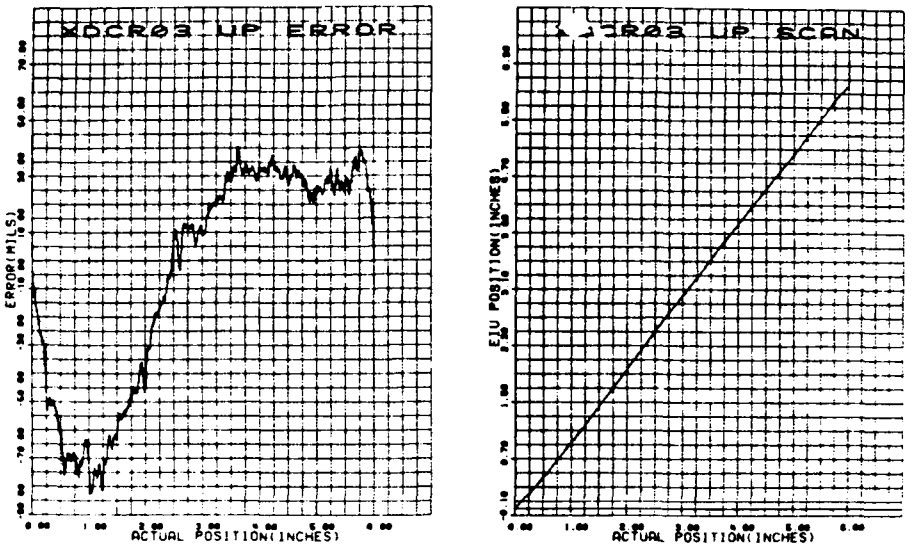

Figure 62. Transducer S/N 03 static accuracy/linearity after environmental testing.

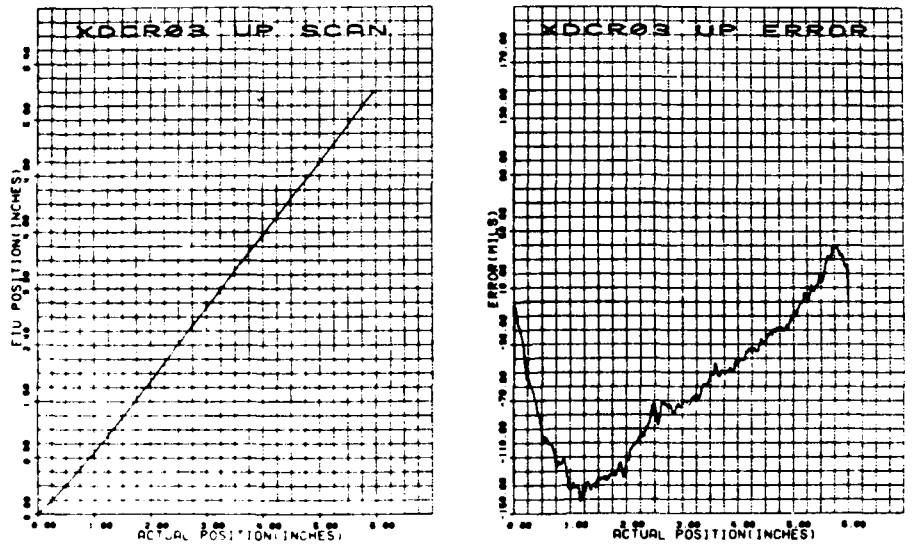

Figure 63. Transducer S/N 03 static accuracy/linearity after environmental testing (no calibration).

5.5.9.2 DYNAMIC ACCURACY

Following environmental testing, transducers S/N 01, S/N 02, and S/N 03 were tested for dynamic accuracy in accordance with paragraph 5.2 of the Hardware Test Plan (Appendix A). The results of these tests were compared to the dynamic accuracy before environmental testing and are presented below.

Pre-Environmental Dynamic Accuracy (in.)

S/N 01	Up-Scan	-0.005
S/N 01	Down-Scan	+0.005
S/N 02	Up-Scan	-0.004
S/N 02	Down-Scan	+0.004
S/N 03	Up-Scan	-0.005
S/N 03	Down-Scan	+0.005

Post-Environmental Dynamic Accuracy (in.)

				Change
S/N 01	Up-Scan	-0.005	=	0.000
S/N 01	Down-Scan	+0.005	=	0.000
S/N 02	Up-Scan	+0.002	=	+0.006
S/N 02	Down-Scan	+0.005	=	+0.001
S/N 03	Up-Scan	-0.006	=	-0.001
S/N 03	Down-Scan	+0.005	=	0.000

Note that with the exception of transducer S/N 02, there is insignificant variation in dynamic accuracy before and after environmental testing. The change in transducer S/N 02 (Up-Scan) dynamic accuracy is believed to be from encoding plate contamination in the salt fog test.

5.5.9.3 OPTICAL POWER MARGIN

Optical power margin decreased due to environmental testing, as shown in the following data. The post-environmental test was performed in the same manner as in Section 5.3.2.3. The changes in optical power margin are as follows:

Pre-Environmental Optical Power Margin

Transducer	Initial Power (microwatts)	Final Power (microwatts)	Optical Power Margin (dB)
S/N 01	720	189	5.8
S/N 02	575	180	5.0
S/N 03	600	190	5.0

Post-Environmental Optical Power Margin

Transducer	Initial Power (microwatts)	Final Power (microwatts)	Optical Power Margin (dB)
S/N 01	702	290	3.8
S/N 02	670	249	4.3
S/N 03	670	360	2.7

Margins for transducers S/N 01, S/N 02, and S/N 03 were -2.0 dB, -0.7 dB, and -2.3 dB, respectively.

The degradation of optical power margin is attributed to destruction of the mirrored prism facets and salt/corrosion deposits on the encoding plate from the salt fog test (see next section).

5.5.9.4 TRANSDUCER S/N 01 DISASSEMBLY

After all post-environmental performance tests were complete, transducer S/N 01 was opened to determine the extent of damage caused by the environmental tests. It was confirmed that salt fog had entered the transducer, apparently through the connectors, had left deposits on the prisms (and encoding plate), and had almost completely destroyed the mirrored surfaces on the prisms. As mentioned previously, the mirrored surfaces in transducers S/N 01, S/N 02 and S/N 03 were unprotected and susceptible to salt corrosion. A large concentration of salt crystals in the fiber optic connectors was noted, along with salt corosion (white) around the shaft bearing housing. Also, some black colored corrosion products were found in the transducer body apparently from seal corrosion and dust particles from the dust test. There was no evidence of any glass damage to either the encoding plate or the mixing rods.

5.6 TEST ANALYSES

In general, the feasibility model transducers S/N 01 through 06 successfully completed performance, life-cycle, and environmental testing. However, testing revealed areas in which improvement is needed before a production program should be considered. This section of the final report analyzes and summarizes test data to determine areas where deficiencies exist in transducer performance, probable causes for the deficiencies, and how the deficiencies might be best corrected.

5.6.1 PEFORMANCE TESTS

All of the feasibility model transducers exhibited some degree of nonlinearity under static accuracy testing, as was shown in Section 5.3.1. The major sources of nonlinear operation were identified as being optical in nature. Installation of wider input prisms in transducers S/N 04, 05 and 06 was successful in generating a consistent nonlinearity which was sinusoidal in shape. This nonlinearity can be corrected by programming the correction needed in the computer-generated encoding plate artwork or by careful mix rod design.

A cursory computer ray trace analysis was performed in order to isolate and/or analyze possible optical origins of nonlinearity. The tapered beveled prisms meant that a 2-D ray trace analysis was insufficient in view of the large number of skew rays propagated by such waveguides. Therefore, a 3-D computer ray trace program was written which could accommodate waveguides with arbitrary tapers and bevels. A listing of the FORTRAN 3-D computer ray trace program is contained in Appendix D.

Approximately 20,000 rays were traced from the input fibers through the input prism (mix rod) and onto the plane of the encoding plate. Ray tracing was performed without the 45-degree prisms on the input and output ends of the input mix rod. The ray density incident on the encoding plate was computed to determine the uniformity of the optical density profile and plotted in 3-D perspective. The ray trace analysis was performed using the same prism dimensions used in fabrication of the production transducers.

Results of the ray trace analysis are shown graphically in Figures 64 to 66 for the input prisms of transducers S/N 04, 05 and 06. Figure 64 shows the calculated optical power density profile viewed in graphical 3-D perspective. The z-axis values represent the ray density, and the x and y axis values represent the position in inches at the plane of the encoding plate. Figures 65 and 66 show the computed ray density viewed under different rotation angles to show the top and side details.

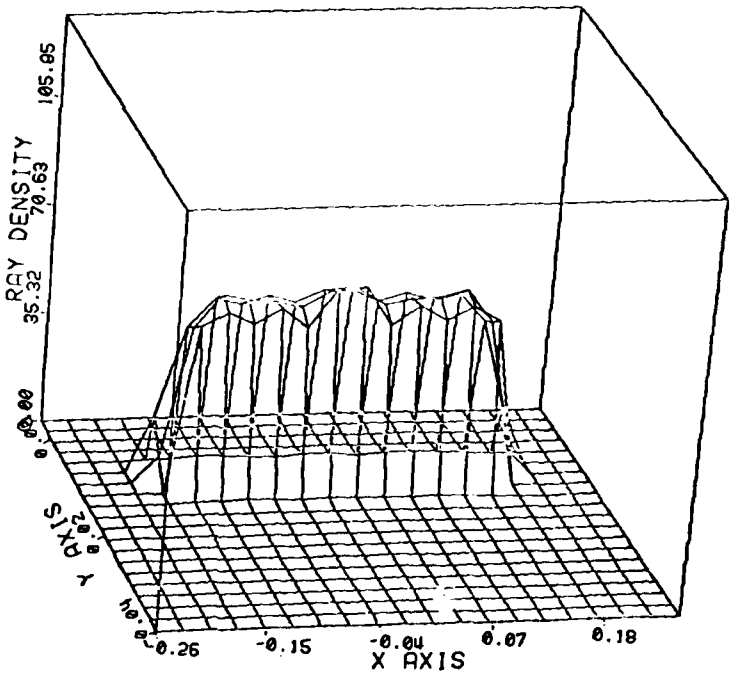

Figure 64. Calculated optical power density profile at the encoding plate for Transducers S/N 04, 05, 06 - viewed in 3-D perspective.

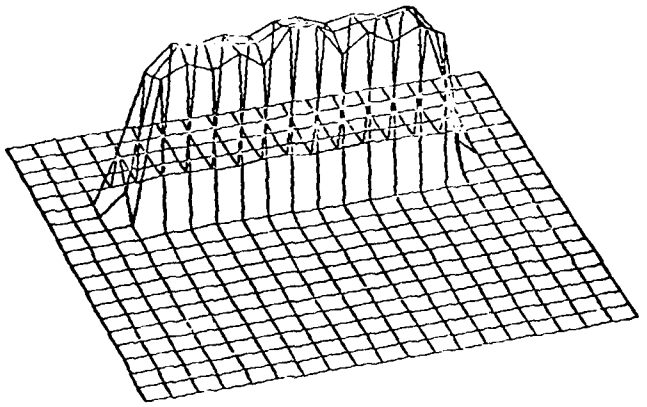

Figure 65. Calculated optical power density profile rotated to show top detail.

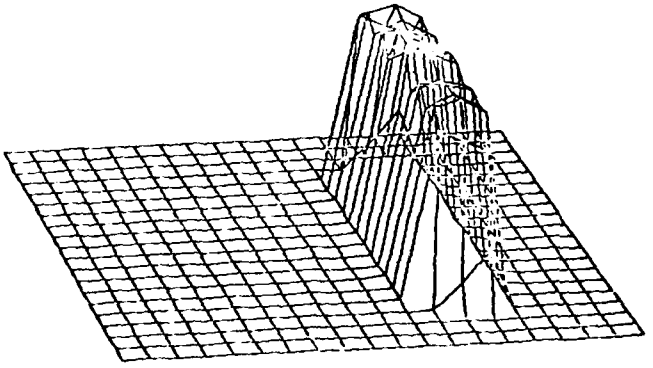

Figure 66. Calculated optical power density profile rotated to show side detail.

Measurements taken on transducer S/N 05 showed that the actual optical power distribution at the encoding plate (Figure 67) was in close agreement with the calculated optical power distribution of Figure 64. The data plotted in Figure 67 was from a single optical power scan taken across the center in the wide dimension of the input prism at the surface of the encoding plate. These results show that, although the optical power is more uniform than observed in the breadboard transducer (6.5% vs 9.21% max deviation on the encoding plate tracks), the nonlinearity was greater in transducer S/N 05 than the breadboard. The nonuniform optical power density found in the production transducers at the encoding plate should cause nonlinear operation but not of the magnitude found in the production units.

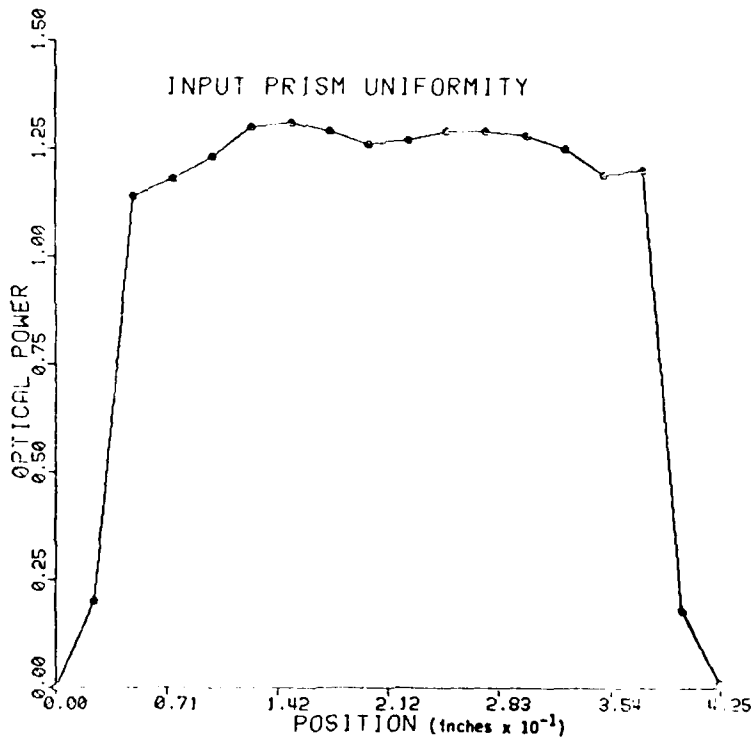

Figure 67. Measured optical power density for Transducer S/N 05 at the encoding plate.

It is believed likely that a part of the nonlinearity is due to the small 1.24-degree angular displacement between the input and output prisms used to space the output prism ports far enough apart for connector access. Time did not permit experimental (or computer ray trace) investigation of the true effect of prism angular misalignment.

Dynamic accuracy testing showed that all of the transducers were well within the 0.015-inch dynamic error design goal at 6 inches/second slew rate and could probably meet this design goal at slew rates as high as 12 inches/second.

Tests revealed that the optical power margin of the production transducers was approximately 5 dB due to the calibration of the EIU's with an AGC current of 65 ma. Breadboard EIU optical power margin tests showed that the optical system margin was 39.5 dB. Using the measured loss through the production transducers of 25 dB (transducer S/N 05), this should give an excess optical power margin of 14.5 dB with the proper DC and AC gain settings in the EIU receiver circuitry. This should be adequate for degradation and device tolerances. An approximate 1 dB of additional power margin could be obtained by antireflection coating the six glass-air interfaces in the optics.

5.6.2 LIFE-CYCLE TEST

Potential seal problems were identified from life-cycle testing due to seal wear products contaminating the optics and jamming the mechanical motion assemblies. Despite contamination from seal wear products, the life-cycle transducer still functioned as a transducer when it was examined at the end of 300,000 cycles of operation prior to cleaning. The wide apertures of the transmit, receive prisms and the encoding plate will tolerate a much higher degree of contamination than in a digital transducer of comparable resolution before catastrophic transducer failure occurs. With the exception of the seal, the rest of the life-cycle transducer mechanical parts showed very little wear after the full 2,000,000 cycles of operation. The choice of a seal for production units should be further investigated.

5.6.3 ENVIRONMENTAL TESTS

The accuracy of the feasibility model transducers S/N 01, 02 and 03 was a function of temperature in the low and high temperature MIL-STD-810C tests. Transducers S/N 02 and S/N 03 exhibited an approximate 0.100-inch error over 200°F (0.0002777 inch error/°C). Using linear expansion coefficients for the materials in the transducers and the fact that the transducers were clamped at the midpoint, the approximate position error due to expansion/contraction of materials should be the sum of the contributions from the materials:

5 in. 302 stainless rod at 12 ppm/°C	=	0.0006 in./°C
4.75 in. TJ 6061 Alumimum at 23.9 ppm/°C	=	0.0001135 in./°C
5.5 in. 7900 Vycor glass at .7 ppm/°C	=	0.00000385 in./°C
.75 in. Rulon J at 36.1 ppm/°C	=	0.0000271 in./°C
TOTAL		0.000204 in./°C

The calculated error from expansion/contraction of materials is 0.000204in./°C. The magnitude of the measured expansion/contraction is ~ 35% greater. The reason for this is not known at this time, but is believed to be the choice of resins for cladding material on the prisms. The failure in transducer operation at temperatures below -35°F is believed to be due to N.A collapse of the prisms (Section 5.5.1). Choosing of a wide temperature resin or using glass claddings on the prisms should improve temperature performance.

The rest of environmental testing showed that most of the degradation in transducer performance was from fiber optic cable fracture, indicating that further work is needed in this area. The fiber optic connectors should be sealed with O-rings to prevent entry of salt fog, dust, and humidity. Also, a rod end bearing with greater strength is indicated, since the ones on the transducers were made from mild steel.

6.0 PRODUCTION COST ESTIMATE

The cost estimate for the "Digital/Optical Linear Position Transducer" was based on the basic feasibility model units with some modifications. The cost estimates were made for production quantities of 1,000 and 10,000 units. Each unit consists of a transducer, an electronics interface module, and the fiber optic cabling for interfacing.

The feasibility model electronics module had a display section which was deleted for the production units. The transducer and fiber optic cabling was estimated "as is". It is believed that the costs could be reduced substantially by redesigning certain parts for high volume production and possibly by hybridizing the electronics. It was assumed that fabrication, assembly and test were all done by contractors familiar with the techniques and equipped to handle the specified quantities.

The EIU electronics were estimated for a multilayer printed wiring board fabricated to MIL-P-55110C with discrete components and IC's and assembled per MIL-P-28809. The transducer mechanical assemblies were estimated using appropriate mil-specs for materials, mechanical tolerances and surface finishes and treatments. In addition, the estimates were based on the transducer system satisfying the MIL-STD-810C requirements presented in Section 5.5 with the upper operating temperature for the electronics at +71°C.

The following cost estimates for the units include material, fabrication, test and checkout, and final marking for deliverable hardware suitable for shipping.

Unit Cost

	QTY 1,000	QTY 10,000
Electronics	$1200.00 - $1850.00	$ 700.00 - $1400.00
Transducer and Fiber Optic Cables	$ 700.00 - $1000.00	$ 350.00 - $ 750.00
TOTAL	$1900.00 - $2850.00	$1050.00 - $2150.00

7.0 CONCLUSIONS AND RECOMMENDATIONS

In conclusion, it is believed that the feasibility of a fiber optic analog displacement transducer with 12-bit A/D conversion has been successfully demonstrated. However, improvements are needed before a production program should be considered. This section of this final report contains conclusions from the program, and offers recommendations as to how some necessary refinements might be best realized.

7.1 OPTICAL

All of the feasibility-model transducers were found to have some degree of nonlinearity and, although several plausible origins were postulated, the true origin of the nonlinearity was not conclusively determined during the course of the contract. Throughout the program, one objective was to produce a group of transducers with a nonlinearity which was as small as possible but, even more important, which was consistent from transducer to transducer. The original encoder pattern having been computer-generated, it would be a relatively simple matter to program the correction needed to linearize the characteristic.

It is likely that a part of the nonlinearity is due to the small (1.24^{o}) angular displacement between the input prism and the output prisms, this being the result of placing the output connectors far enough apart to permit easy connection and disconnection. Either wider track spacing or the use of connectors which would permit closer spacing would allow the prisms to be parallel and thereby improve the coupling efficiency and possibly eliminate some of the nonlinearity. The true effect of the prism angular misalignment is difficult to determine with confidence analytically, but could be accurately evaluated with a fairly simple laboratory experiment. It is recommended that such an experiment be performed.

Field application of these transducers would likely require that they be completely interchangeable to a specified tolerance without realignment. Although it might be possible in production to control all of the variables sufficiently well, it might be more practical to provide the transducers with fine adjustments which would permit all of them to be standardized within the specified tolerance during manufacture and during subsequent depot-level maintenance.

In the feasibility-model transducers, it was expedient to use three standard off-the-shelf single fiber optic connectors. In production, it would be preferable to use a single connector containing three termination pins. This would permit the use of a single fiber optic cable, would make incorrect connections impossible, would insure that individual terminations could not be rotated, and would simplify installation because access would be required to only one side of the transducer. Figure 68 shows how the three prisms in the feasibility model transducers interface with their respective fiber optic connectors. Note that the use of a single connector is not possible because the input and output ports are on opposite sides of the transducer body.

Figure 69 shows one method for locating all three ports on the same surface so that a single connector with three termination pins can be used. The input facet of the input prism is slanted in the opposite direction from that in Figure 68 and a short length of light pipe is included to extend the input port and put all three ports in the same plane. This arrangement also requires that the prisms be somewhat longer than the stroke, whereas, in the feasibility models, the prisms were 5 inches long for a 6-inch stroke.

The prisms in the feasibility model were fabricated from Vycor 96% silica glass and were cemented into place with RTV-602, a silicone elastomer. The cladding was largely air, except for those relatively small areas coated with the silicone resin. This design approach is deficient in two respects: (1) the areas which are effectively air-clad are susceptible to contamination by dust particles and condensed moisture, and (2) those areas which are clad with silicone resin suffer from increased loss and shrinkage of numerical aperture at low temperature. It is recommended that glass sheet with glass cladding be considered for the fabrication of future prisms. Alternatively, allover cladding of the prisms with one of the newer low-temperature, low-refractive-index resins should be considered.

The aluminized mirror surfaces of the prisms should be given an overcoating of silicon dioxide to protect them from mechanical damage and corrosion. This was done on transducers S/N 04, 05 and 06.

Between the transducer input and output ports, there are six refractive index discontinuities, each of which reflects approximately 4 percent of the incident power. Giving all of these surfaces an antireflective coating could reduce the transducer insertion loss by as much as 1 dB.

7.2 MECHANICAL

The mechanical design of the feasibility-model transducers assumed there would be a need to open them up for inspection and/or repair following the environmental and life-cycle testing. For that reason, they were designed with three major subassemblies which could be easily taken apart. If ease of disassembly were not a consideration, then weight and cross-sectional area could be reduced and the package could be more easily sealed if the body halves were pressed into a round tube. Also, if the body could be supported at both ends instead of only one, the whole package size could be reduced considerably.

The combinations of bearing materials selected for the feasibility models were quite successful for the specified life-cycle test. However, it is inevitable that the optics would eventually become contaminated with wear particles. One way to minimize sliding friction as well as minimize wear particles would be to use linear ball bearings instead of sleeve bearings; however, this would somewhat increase the diameter of the body.

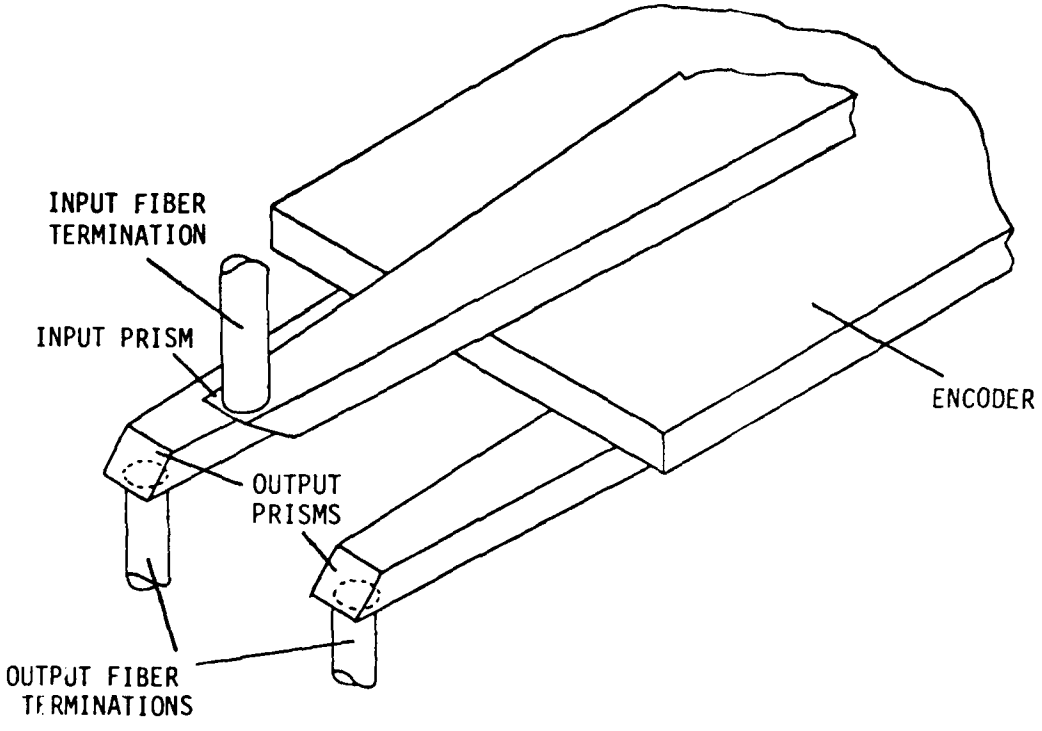

Figure 68. Prototype terminal interfaces.

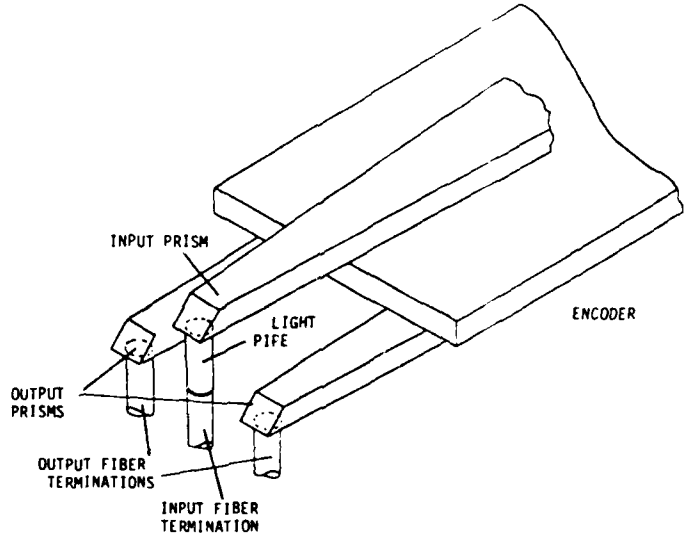

Figure 69. In-line terminal interfaces.

Because no seal is perfect, there will always be some risk of contamination in optical transducers -- particularly if the design involves a shaft seal. One approach which would be helpful would be to pressurize the interior of the transducers with dry nitrogen fed through a tubing from a regulated pressure source. All transducers in a system could be pressurized from a common source and it would add very little to the weight or complexity of the system.

Even if the transducers are not pressurized, they should be equipped with a pressure fitting to permit testing of the seal integrity under pressure.

9
F

APPENDIX A
DIGITAL/OPTICAL LINEAR POSITION TRANSDUCERS
TEST PLAN

1.0 Purpose

The purpose of this test plan is to define the procedures necessary for evaluation of the Optical Linear Position Transducer Systems developed under contract to ATL. The tests will evaluate the transducer units, the fiber optic cables, and the electronic interface units (EIU's) for several performance, environmental, and life-cycle tests.

2.0 General Instructions and Scope

Six transducer units, six fiber optic cable sets, and four EIU's will be available for testing. The following statements define the hardware configuration and the scope of testing for each of the hardware pieces.

Configuration Definitions

9
B

A. System 1 will include transducer 1, fiber optic cable set 1, and EIU 1; System 2 consists of transducer 2, fiber optic cable set 2, and EIU 2; and likewise up through system 4.

B. Transducer units 5 and 6 and fiber optic cable sets 5 and 6 will be respectively coupled and tested only with EIU 4. These will be known as systems 5 and 6, respectively.

Scope of Test Definitions

A. System 1 shall undergo Group 1 Performance Tests as defined in Section 4.0, followed by Group 2 Performance Tests as defined by Section 5.0, Life Cycle Tests as described by Section 6.0, and a final Group 2 Performance Test per Section 5.0

B. System 2, 3 and 4 shall each undergo Group 2 Performance Tests as defined in Section 5.0, followed by Environmental Tests per Section 7.0, and a final repeat of the Section 5.0 Group 2 Performance Tests.

C. System 5 and 6 shall be performance tested per the Group 2 Performance Tests as defined in Section 5.0.

Figure A-1 summarizes the hardware configurations. Figure A-2 summarizes the scope of testing.

The order of the testing shall be as follows:

1. Group 1 performance testing for System 1.

2. Group 2 performance testing for all systems.

3. Life-cycle testing and environmental testing. These tests may be run concurrently or at separate times since they involve different transducer systems.

4. A repeat of group 2 performance testing for systems 1-4.

The order of testing within each test program (performance, environmental, life-cycle) shall be the same as the order in which the individual tests are presented.

3.0 Preparation

Prior to any of the testing discussed, each piece of hardware shall undergo a series of simple visual and/or operative inspection steps. Each transducer unit shall be manually tested for freedom of movement and absence of backlash over the full measurement and overtravel range. Each

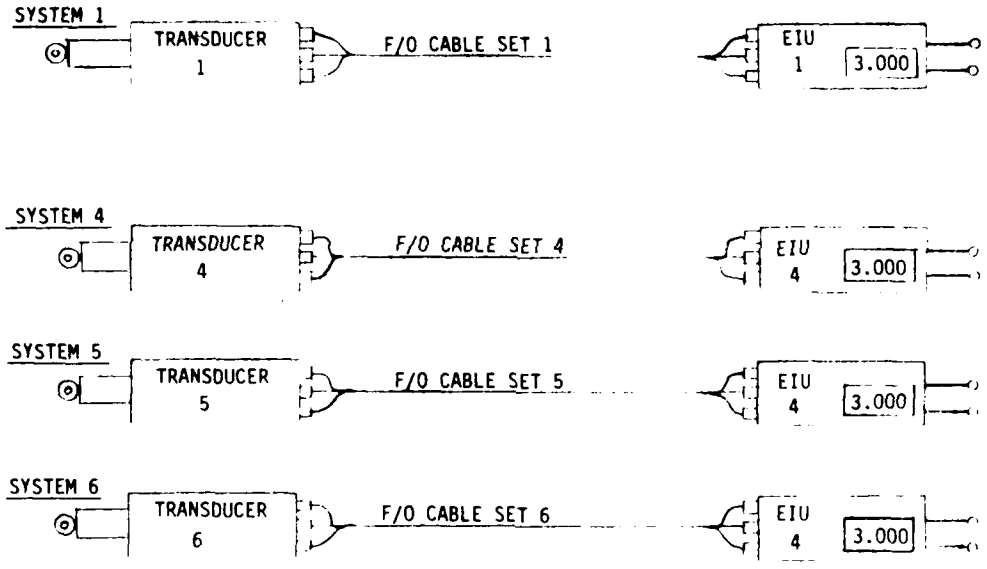

Figure A-1. Transducer system definition.

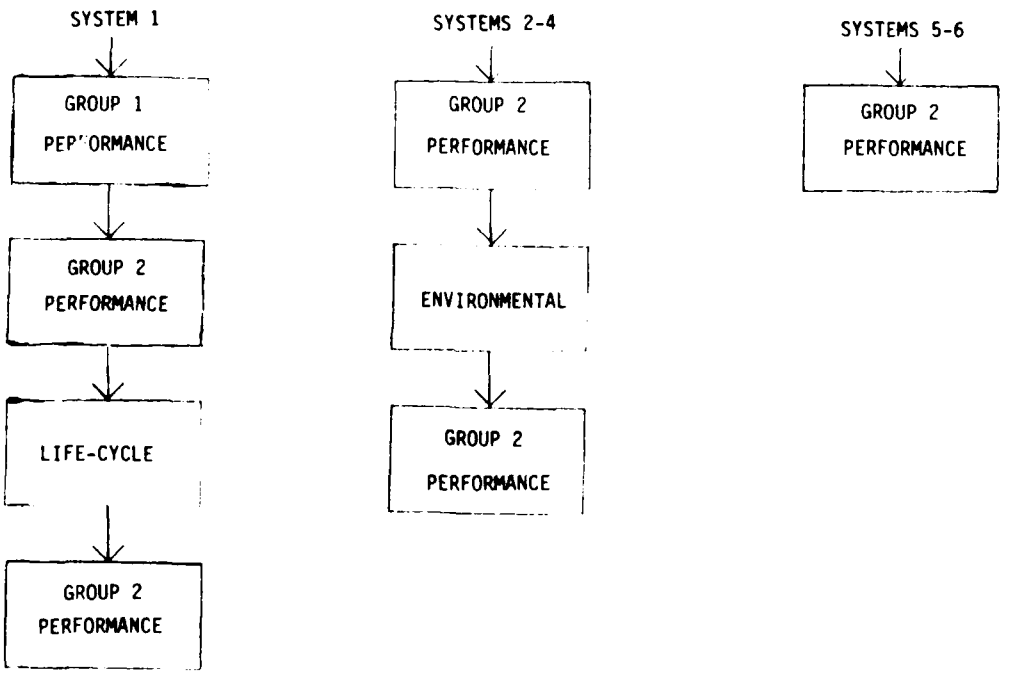

Figure A-2. Test sequence for transducer systems.

transducer unit shall be tested optically by illuminating the input port and visually examining the two output ports for uniform brightness and depth of modulation as the encoding element is exercized over its full travel range. A visual inspection to search for loose components, bad seals, or any other deviation shall also be conducted.

Each fiber optic cable within each set (three cables per each of the six sets) shall be visually inspected for jacket flaws and proper terminations. Each termination shall be inspected under a 30X stereo microscope for fiber end scratches, chips, stirations, hackles or pitted areas, and a proper polished finish. Each cable shall then be tested with a standard emitter (Spectronics SE 3353 @ 100 ma DC bias current) and an optical power meter to measure transmitted power.

Each EIU shall be individually inspected for loose wiring, solder bridges, loose components, or any anomalies which may affect acceptable operation. If everything appears satisfactory, 28 ± 1 VDC shall be applied to the power input terminals to enact a "smoke" test. The display should light and read near zero inches (fibers not connected).

All of the above inspections are to be performed in a normal laboratory environment. If all inspection tests are passed, the equipment is then ready for calibration as described by the "Calibration Procedure" document. Calibration must be performed on each system prior to its detailed test sequence.

4.0 Group 1 Performance Tests - The following tests are to be conducted with System I only and are for characterization purposes . The tests shall be conducted with the equipment at standard ambient conditions per MIL-STD-810C, paragraph 3.1. Tests described in paragraphs 4.2 and 4.3 below shall be performed on a fully stabilized system (calibrated and powered "on" for not less than one hour).

4.1 Warm-up Drift - The transducer shall be mounted to the Calibration Test fixture. After the 28 VDC power has been removed from the EIU for a period of not less than one hour, the transducer shall be set to mechanical position 3.000 inches and power reapplied to the EIU. Display readout shall be recorded at turn-on (t = 0), t = 1 minute, t = 2 minutes, t = 5 minutes, t = 10 minutes, t = 20 minutes, and t = 60 minutes.

4.2 Sensitivity to Power Supply Variations - The transducer shall be mounted to the Calibration Test fixture. With the transducer set to mechanical position 3.000 inches, the input power shall be varied in 1 volt increments from 22 VDC to 32 VDC. The display readout shall be recorded for each data point.

4.3 Fiber Optic Connector Repeatability - The transducer shall be mounted to the Calibration Test fixture. With the transducer set to mechanical position 3.000 inches, all of the six fiber optic connectors (one at a time) shall be disconnected and immediately reconnected. The display readout shall be recorded before and after each operation. This test set shall then be fully repeated twice, once with the transducer set to mechanical position 0.100 inch, and again with the transducer set to mechanical position 5.900 inches. Upon completion of all of these tests, the EIU shall be recalibrated, if necessary, and so indicated.

4.4 Weight - The weight of the transducer system shall be determined on a set of scales or a balance. The system consists of the EIU, the fiber optic cable assembly, and the transducer. Each of these three items shall be weighed separately to the nearest ounce, and the data recorded.

4.5 Transducer Actuating Force - Attach a spring scale to the rod end bearing of the transducer. With the transducer set near its midpoint, secure the transducer housing and gradually increase tension

on the spring scale until transducer deflection begins to occur. The scale reading is the actuating force, and will be recorded.

5.0 Group 2 Performance Tests

These tests shall be conducted with the equipment at standard ambient conditions per MIL-STD-810C, paragraph 3.1. All tests decribed below shall be performed on a fully stabilized system (powered "on" for not less than one hour). The transducer systems must undergo calibration procedures prior to these tests except when they are to occur following the life-cycle or the environmental tests.

5.1 Static Accuracy, Linearity, Resolution, and Monotonicity - Figure A-3 shows the configuration for this set of tests. The following is a description of its operation.

The transducer to be tested shall be mounted in the test fixture. Following the proper input command, the transducer will be translated towards 0.000 inches by the stepper motor. The microcomputer will monitor the EIU output and when the 0.000 inch point is reached, the stepping will cease.

After reaching the endpoint, the microcomputer will instruct the stepper motor to translate the transducer towards the 6.000 inch endpoint. The microcomputer will interrogate and store the EIU data for each 0.00125 inch of transducer travel (8 steps of the motor) over the full 6.000 inch stroke.

The data will be stored on floppy disc and operated on by either the microcomputer system or transferred to a Harris/6 minicomputer for

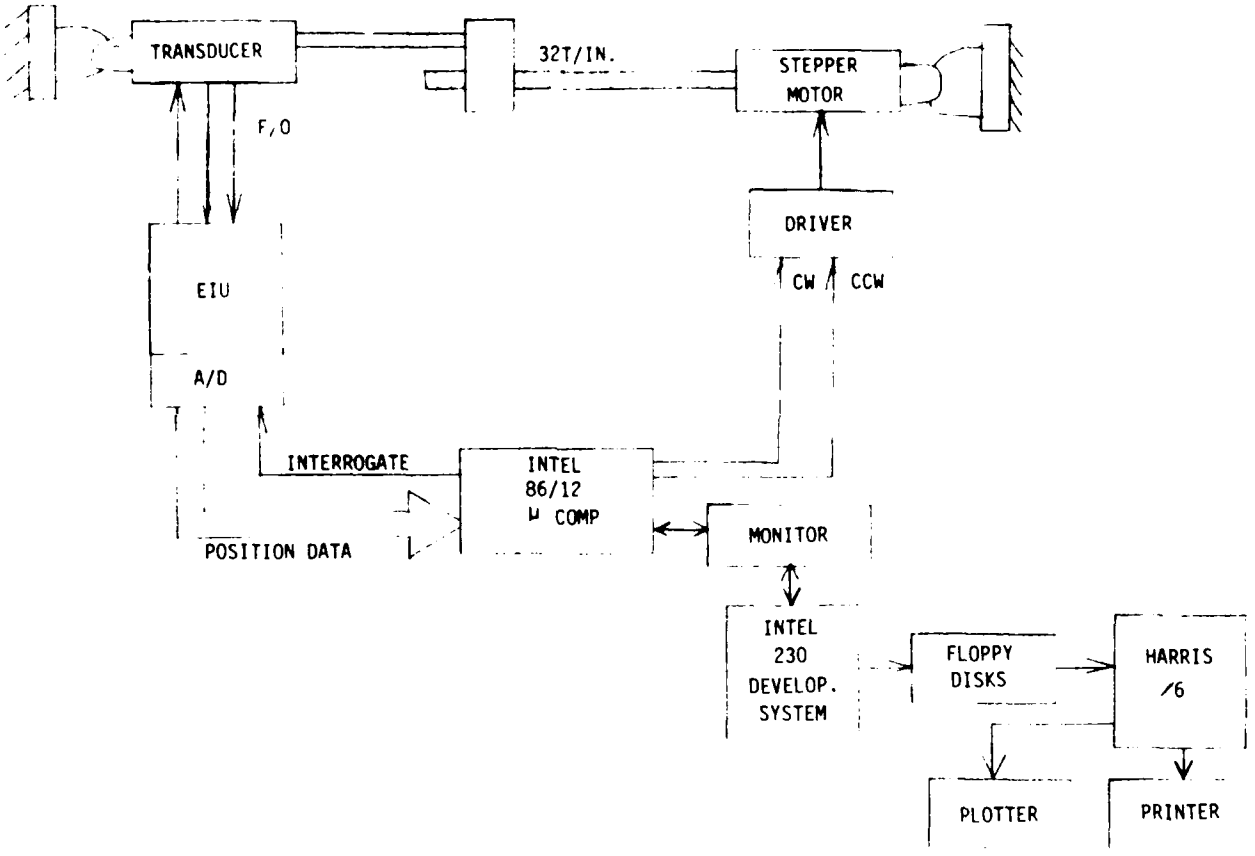

Figure A-3. Static accuracy, linearity and resolution test setup.

detailed analysis, printing and plotting. Accuracy will be determined by comparing the EIU words with the mechanical position (determined by knowledge of the number of motor steps and the leadscrew properties). Both absolute data and error data will be printed and plotted. Linearity will be determined by analyzing the accuracy data.

Resolution (and monotonicity) information will also be obtained from the data stored during the scan. Since the EIU data is recorded for each 0.00125 inch of travel, and the average resolution width of the transducer is 0.00146 inch, most words should differ from the previous word by one bit reading. However, due to the slight mismatch, and allowing for leadscrew errors, a tolerance of $\pm$ one bit will be allowed for any reading. If successive stored words differ by more than the allowable limits, the quantity and the sign of the deviation will be printed and identified by its position along the 6.000 inches of travel.

The scan direction shall also be reversed to run the transducer from 6.000 inches to 0.000 inches. Similar outputs will be given and the two directions will be compared. Scan rates shall not exceed 0.1 inch per second for these tests.

5.2 Dynamic Accuracy - The transducer shall be mounted into the life-cycle test fixture (Figure A-5). A small metal (opaque) tab will be attached to the transducer/actuator joint and an LED/PIN detector pair will be mounted to the test fixture stand. The test will be configured such that the tab will pass between the LED and detector near the midpoint of a transducer stroke. The passing tab will cause a pulse to be generated (from an amplifier) which will interrogate the EIU and lock in the EIU display reading at that instant.

The tab will first be passed through the LED/detector pair very slowly to determine its exact (static) position. It will then be passed through at the maximum slew rate (6 inches per second) to determine the dynamic reading. The difference between the slow and the fast readings is the dynamic accuracy.

This test will be performed with the transducer being slewed in both directions.

5.3 Optical Power Margin - Due to the design approach taken for the EIU, it is anticipated that the errors vs. optical power curve will exhibit a sharp threshold effect. The EIU output is expected to vary from a very low bit error rate to a very high bit error rate within less than 1 db of optical power change near the threshold. Therefore, the following test for optical power margin will be performed. See Figure A-4.

a) With the transducer connected in its normal fashion, and set to read 3.000 inches, the optical fiber shall be disconnected from the input port to the transducer and the optical power shall be measured from the fiber with an optical power meter.

b) The fiber shall be reconnected to the transducer and a variable optical attenuator shall be inserted into the path between the EIU emitter port and the fiber optic path.

c) The optical attenuation shall be increased until the EIU display either varies by more than $\pm$ 0.003 inch from 3.000 inches or the display varies at a rapid rate between more than two readout values.

d) The optical power shall be measured from the cable as in step (a) above. The difference betwen the two optical powers, expressed in db, is the optical power margin.

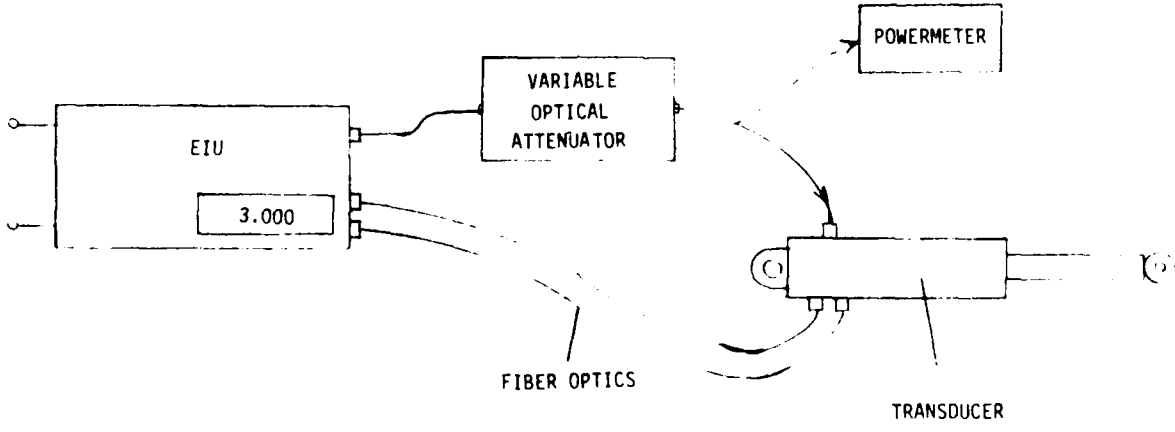

Figure A-4. Optical power margin test.

6.0 Life-Cycle Testing

Life-cycle testing shall be performed based on a procedure described by paragraph 4.7.8.2.1 of MIL-C-5503C. These tests are to be performed at standard ambient conditions per paragraph 3.1 of MIL-STD-810C. Throughout the tests, the system shall be connected and fully stabilized (powered "on" for not less than one hour).

The test configuation is depicted by Figure A-5. A computer controlled hydraulic actuator shall be secured in a vertical stand with the piston connected to the transducer rod end bearing. The clevis end of the transducer housing shall also be secured to the vertical stand. Mechanical stops shall be included to prevent overtravel damage to the transducer in the event of actuator failure. The computer program controls stroke length, number of cycles, and test frequency.

The transducer shall be set to mechanical position 3.000 (as indicated by the EIU display) and all mechanical cycling shall be centered about this value. The transducer shall be cycled as follows:

Test#	Stroke Length(±3%)	No. of cycles	Frequency (Hz)
1	± 3 inches	45,000	0.32
		5,000	0.16
2	± 1.5 inches	225,000	0.64
		25,000	0.32
3	± 0.3 inch	630,000	3.2
		70,000	1.6
4	± 0.06 inch	900,000	16
		100,000	8.0
	Totals:	2,000,000; to take approx. 254 hours	

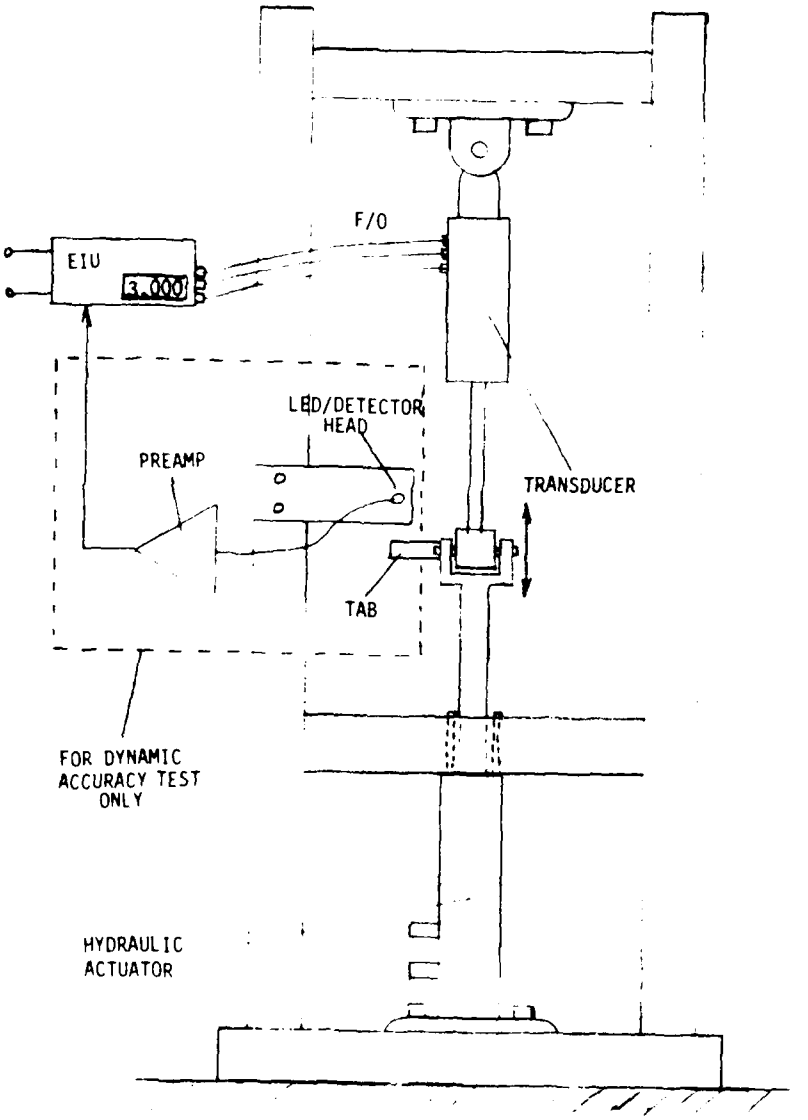

Figure A-5. Life-cycle test.

All of the cycling shall be sinusoidal. The first entry for each of the four tests has been determined such that the transducer shall travel through the midpoint (3.000 inches) at a rate of 6 inches per second. The second entry dictates that the transducer shall travel through the midpoint at 3 inches per second.

The transducer system shall be investigated before and after each individual test to verify proper operation or determine failure. Brief monitoring shall occur during each test also. Items such as catastrophic or structural failure, mechanical binding, loose parts, or improper EIS readings that indicate component failure or a hazard to personnel safety, or any other deviation from normal operation shall be determined (if it occurs) during the tests and reported.

7.0 Environmental Tests

Several environmental tests shall be performed on three transducer systems. The tests include (to be performed in the order given):

a. high temperature
b. low pressure (altitude)
c. low temperature
d. humidity
e. salt fog
f. dust
g. shock
h. vibration

As was discussed in the General Instructions and Scope section of this document, performance testing (Section 5.0) shall occur both before and after the above group of environmental tests.

Each of the environmental tests shall be based on the methods described by MIL-STD-810C, unless stated otherwise herein. All parts of paragraph

3.0 of 810C, "General Requirements", shall apply except for item a.(1) of Section 3.2.6, "Failure Criteria". No performance limits shall be established for failure determination due to the R & D level of this work. Performance data will be monitored and recorded at environmental extremes, however.

Prior to each environmental test, each transducer system will be tested on the Calibration Test fixture to determine its reading at the fixture midpoint. Each transducer will then be retested on the fixture after each environmental test for comparison. During the environmental tests, the transducers will be mounted into special test fixtures which will hold them at their mechanical mid-points. At the beginning, ending, and the extremes of each environmental test, the EIU display shall be monitored and recorded. The transducers will not be mechanically cycled during the tests.

Only the transducers and those portions of the fiber optic cables necessary to penetrate the test chambers shall be subject to the environmental tests. The EIU's shall be located outside of the test chambers and operated in a standard laboratory environment per paragraph 3.1 of MIL-STD-810C. All environmental tests are to be performed with the transducer systems fully stablized (powered "on" for not less than one hour).

All three transducer systems shall be tested simultaneously for all environmental tests except for shock and vibration. The systems shall be tested independently for shock and vibration.

The following sections identify the particular test procedures from MIL-STD-810C to be used for the environmental tests.

7.1 High Temperature - Based on Method 501.1, Procedure II. The maximum temperature required in step 7 of paragraph 3.2 of Method 501.1 shall be +135°C.

7.2 Low Pressure (Altitude) - Based on Method 500.1.

7.3 Low Temperature - Based on Method 502.1. The minimum temperature required in step 4 of paragraph 3.1 of Method 502.1 shall be -50°C.

7.4 Humidity - Based on Method 507.1, Procedure I.

7.5 Salt Fog - Based on Method 509.1.

"After the completion of the exposure to the salt fog, the tansducer shall be cycled thirty times prior to a gentle wash and prior to taking the post test mid-point reading." R

7.6 Dust - Based on Method 510.1

10 "After the completion of the exposure to the dust, the transducer shall be cycled thirty times prior to taking the post test mid-point reading." R

7.7 Shock - Based on Method 516.2, Procedure I. The saw-tooth shock pulse shall be used, and the transducer shall be considered as flight-vehicle equipment.

"The EIU readings will be monitored and recorded after each individual shock." R

7.8 Vibration - Based on Method 514.2, Procedure I, part I, category "C".

APPENDIX B

EIU CALIBRATION PROCEDURE

The EIU contains an internal signal source which is useful for verifying proper performance of the EIU without need for optical signals. In the following procedure, the EIU is first adjusted using the internal signal source to verify that the EIU is functioning properly, after which final adjustments are made using the optical input signals.

To eliminate possible errors due to stray pickup from the internal signal source, the signal source should be disabled by wire wrapping U60-6 (on the EIU digital board) to ground when the source is not in use.

All calibration measurements and adjustments must be made after the EIU has had a minimum 1 minute warm-up period. Unless otherwise specified, all measurements and adjustments are made on the EIU analog board. Drawings of the EIU analog and digital boards are attached.

10 B

1.0 Apply 28 volts DC (± 2 volts) to the DC INPUT jacks on the EIU break-out box. Verify that the voltages on C34, C35 and C36 are within ± 2% of +5V, +15V and -15V respectively.

2.0 With no signal inputs, verify that the DC offset levels at U8-8 and U10-14 are zero volts ±1 volt DC. If necessary, replace U8 and/or U10 to achieve the required level.

3.0 With no signal inputs, adjust R36 for zero volts ± 1 mV DC output from the summing amplifier at U3-1. Adjust R37 for zero volts ±1 mV DC output from the difference amplifier at U3-8.

4.0 Insert jumpers between TP1 and TP3 and between TP2 and TP4.

4.1 Adjust R96 so that the voltage at U3-1 is between -10.0 and -10.1 volts DC.

4.2 Adjust R43 and/or R50 for equal channel gains as indicated by a display of 3.000.

4.3 Repeat 4.1 and 4.2 once.

5.0 Remove the jumper between TP2 and TP4. Insert this jumper between TP1 and TP2.

5.1 Adjust R96 so that the voltage at U3-1 is between -10.0 and -10.1.

5.2 Adjust R26 if necessary to obtain a display of 6.000 with >6 inch overflow.

5.3 If it was necessary to adjust R26, repeat 5.1 and 5.2 once.

6.0 Remove the jumper between TP1 and TP3. Insert this jumper between TP2 and TP4.

6.1 Adjust R96 so that the voltage at U3-1 is between -10.0 and -10.1.

6.2 Adjust R20 if necessary to obtain a display of 0.000 with <0 inch overflow.

6.3 If it was necessary to adjust R20, repeat 6.1 and 6.2 once.

6.4 Remove both jumpers and disable the signal source by wirewrapping U60-6 (on the digital board) to ground.

7.0 Repeat 3.0.

8.0 Select R62 (near CR17 on the digital board) so that the peak current through CR17 is between 200 and 210 mA as measured with a current probe.

The following adjustments are for normal operation with optical signal inputs from the transducer.

9.0 Mechanically position the transducer to the midpoint. Select R46 and R53 to set channel gains so that the current through CR17 on the digital board is between 60 and 70 mA peak.

9.1 Select R44, R46, R51 and R53 so that the display can be adjusted to 3.000 by using pots R43 and R50.

9.2 Adjust R43 and R50 to achieve a display of 3.000 and verify that the peak current through CR17 is between 60 and 70 mA. Verify that U3-1 is between -9.9 and -10.3 volts DC.

10.0 Set the transducer to mechanical position 6.000 inches. Adjust R26 to set gain of summing amplifier for 6.000 displayed with no >6 inch overflow. Change R25 if necessary to obtain the correct display.

11.0 Set the transducer to mechanical position 0.000 inch. Adjust R20 for 0.000 displayed with no <0 inch overflow.

12.0 Reposition the transducer to the midpoint.

12.1 Repeat 9.2, 10.0 and 11.0 once.

13.0 Insert an optical attenuator in the optical path from the emitter (J6) to the transducer. Set the transducer to the mechanical midpoint.

13.1 Attenuate the optical signal until the peak current through CR17 is between 180 mA and 190 mA.

13.2 Verify that the voltage at U3-1 is between -9.7 and -10.3 volts DC. Verify that the display reads between 2.990 and 3.010 inclusive.

This completes the calibration procedure for the EIU.

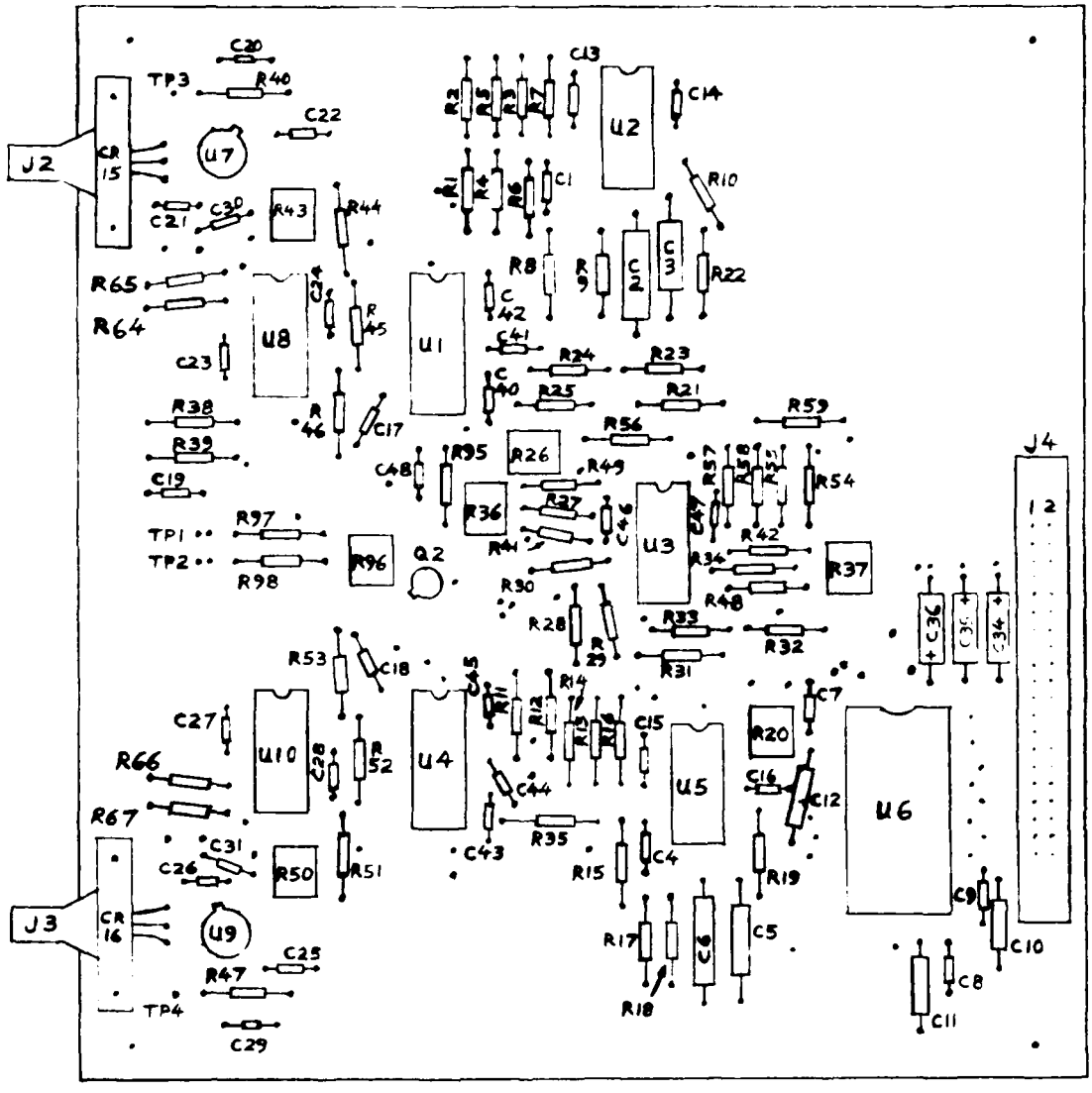

EIU ANALOG BOARD

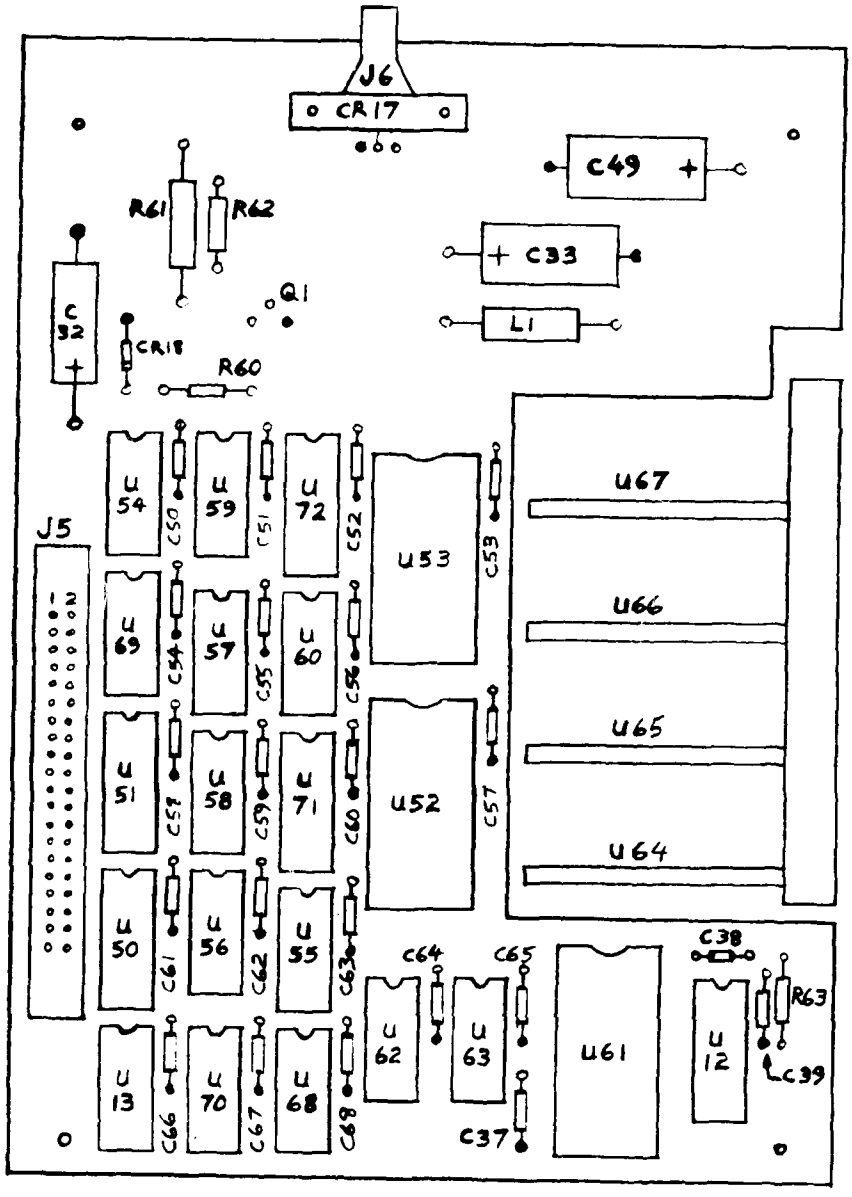

EIU DIGITAL BOARD

NOTE:
• INDICATES GROUND CONNECTION.

APPENDIX C

INITIAL STATIC ACCURACY, LINEARITY, RESOLUTION, AND MONOTONICITY PRINTOUTS FOR PRODUCTION TRANSDUCERS S/N 01, 02, 03, 04, 05, AND 06

AIL DIGITAL/OPTICAL LINEAR POSITION TRANSDUCER

STATIC ACCURACY DATA AND ANALYSIS

TRANSDUCER: 1 10/16/81

POINT	INCHES	EIU SCALE	STEPPER SCALE	ERROR IN BITS	ERROR IN INCHES
1	0.00	2	0	0	0.000000
2	0.50	314	400	-29	-0.042522
3	1.00	651	800	-33	-0.048387
4	1.50	1011	1200	-14	-0.020528
5	2.00	1372	1600	6	0.008798
6	2.50	1723	2000	16	0.023460
7	3.00	2051	2400	3	0.004399
8	3.50	2376	2800	-13	-0.019062
9	4.00	2700	3200	-30	-0.043988
10	4.50	3033	3600	-38	-0.055718
11	5.00	3379	4000	-33	-0.048387
12	5.50	3734	4400	-19	-0.027859
13	6.00	4095	4800	1	0.001466
13	6.00	4094	4800	0	0.000000
12	5.50	3730	4400	-23	-0.033724
11	5.00	3376	4000	-36	-0.052786
10	4.50	3031	3600	-40	-0.058651
9	4.00	2698	3200	-32	-0.046921
8	3.50	2374	2800	-15	-0.021994
7	3.00	2049	2400	1	0.001466
6	2.50	1721	2000	14	0.020528
5	2.00	1371	1600	5	0.007331
4	1.50	1010	1200	-15	-0.021994
3	1.00	650	800	-34	-0.049853
2	0.50	312	400	-31	-0.045454
1	0.00	0	0	-2	-0.002933

RESOLUTION AND MONOTONICITY TESTS

UP SCAN

POSITION (INCHES)	ERROR (BITS)

DOWN SCAN

ATL DIGITAL/OPTICAL LINEAR POSITION TRANSDUCER

STATIC ACCURACY DATA AND ANALYSIS

TRANSDUCER: 2 10/16/81

POINT	INCHES	EIU SCALE	STEPPER SCALE	ERROR IN BITS	ERROR IN INCHES
1	0.00	2	0	0	0.000000
2	0.50	335	400	-8	-0.011730
3	1.00	678	800	-6	-0.008798
4	1.50	1028	1200	3	0.004399
5	2.00	1380	1600	14	0.020528
6	2.50	1722	2000	15	0.021994
7	3.00	2048	2400	0	0.000000
8	3.50	2370	2800	-19	-0.027859
9	4.00	2699	3200	-31	-0.045454
10	4.50	3028	3600	-43	-0.063050
11	5.00	3375	4000	-37	-0.054252
12	5.50	3727	4400	-26	-0.038123
13	6.00	4095	4800	1	0.001466
13	6.00	4094	4800	0	0.000000
12	5.50	3726	4400	-27	-0.039589
11	5.00	3376	4000	-36	-0.052786
10	4.50	3028	3600	-43	-0.063050
9	4.00	2699	3200	-31	-0.045454
8	3.50	2370	2800	-19	-0.027859
7	3.00	2046	2400	-2	-0.002933
6	2.50	1717	2000	10	0.014663
5	2.00	1374	1600	8	0.011730
4	1.50	1025	1200	0	0.000000
3	1.00	677	800	-7	-0.010264
2	0.50	330	400	-13	-0.019062
1	0.00	1	0	-1	-0.001466

RESOLUTION AND MONOTONICITY TESTS

UP SCAN

POSITION (INCHES)	ERROR (BITS)

DOWN SCAN

3.003750	-1
2.881250	3
2.762500	4
2.757500	-1
2.573750	-1
1.917500	-1
1.903750	3
1.781250	3
1.775000	-1
1.773750	-1
1.705000	3
1.611250	-1
1.601250	3
1.573750	3
1.570000	-1
1.556250	3
1.555000	3
1.506750	-1
1.501250	-1
1.492500	-1
1.491250	-1
1.480000	3
1.470000	3
1.466250	-1
1.462500	3
1.457500	-3
1.456250	-4
1.447500	6
1.446250	4
1.443750	-2
1.442500	-2
1.432500	3
1.423750	-1
1.421250	3
1.417500	4
1.411250	-2
1.408750	3
1.392500	3
1.381250	-1
1.373750	3
1.362500	-1
1.361250	-2
1.360000	6
1.286750	-1
1.287500	-2

1.246250	-1
1.258000	-1
1.278750	-1
1.271250	-3
1.265000	-3
1.262500	-2
1.256250	-1
1.253000	-3
1.251250	-1
1.213750	-1
1.211250	-1
1.192500	-1
1.190000	-1
1.186750	-1
1.151250	-1
1.133750	-1
1.125000	-3
1.102500	-3
1.085000	-1
1.013750	-1
1.005000	-1
0.990000	-1
0.986750	-1
0.903750	-1
0.897500	-1
0.891250	-3
0.888750	-3
0.820000	

AIL DIGITAL/OPTICAL LINEAR POSITION TRANSDUCER

STATIC ACCURACY DATA AND ANALYSIS

TRANSDUCER: 3 10/16/81

POINT	INCHES	EIU SCALE	STEPPER SCALE	ERROR IN BITS	ERROR IN INCHES
1	0.00	0	0	-2	-0.002933
2	0.50	316	400	-27	-0.039589
3	1.00	649	800	-35	-0.051319
4	1.50	948	1200	-27	-0.039589
5	2.00	1356	1600	-10	-0.014663
6	2.50	1708	2000	1	0.001466
7	3.00	2049	2400	1	0.001466
8	3.50	2386	2800	-3	-0.004399
9	4.00	2727	3200	-3	-0.004399
10	4.50	3072	3600	1	0.001466
11	5.00	3421	4000	9	0.013196
12	5.50	3761	4400	8	0.011730
13	6.00	4095	4800	1	0.001466
13	6.00	4094	4800	0	0.000000
12	5.50	3757	4400	4	0.005865
11	5.00	3417	4000	5	0.007331
10	4.50	3069	3600	-2	-0.002933
9	4.00	2723	3200	-7	-0.010264
8	3.50	2382	2800	-7	-0.010264
7	3.00	2045	2400	-3	-0.004399
6	2.50	1705	2000	-2	-0.002933
5	2.00	1352	1600	-14	-0.020528
4	1.50	994	1200	-31	-0.045454
3	1.00	643	800	-41	-0.060117
2	0.50	312	400	-31	-0.045454
1	0.00	0	0	-2	-0.002933

RESOLUTION AND MONOTONICITY TESTS

UP;SCAN

POSITION (INCHES)	ERROR (BITS)
0.007500	-1
0.011250	3
0.015000	-2
0.023750	-1
0.031250	-1
0.036250	3
0.045000	3
0.048750	-1
0.053750	3
0.057500	-1
0.070000	3
0.107500	-1
0.116250	-1
0.125000	-1
0.131250	-1
0.138750	-1
0.156250	-1
0.182500	-1
0.191250	-1
0.198750	-1
0.207500	-1
0.220000	3
0.232500	-1
0.241250	-1
0.246250	3
0.256250	-1
0.263750	-1
0.272500	-1
0.297500	-1
0.330000	-1
0.386250	-1
0.411250	-1
0.420000	-1
0.426750	-1
0.461250	-1
0.477500	-1
0.508750	-1
0.533750	-1
0.576250	-1
0.730000	-1
0.827500	-1
0.993750	-1
1.363750	-1
1.541250	-1
4.551250	-1
4.742500	3
5.243750	3
5.267500	3

5.361250	3
5.505000	3
5.621250	-1
5.636250	-1
5.645000	-1
5.666250	3
5.670000	-1
5.736750	-1
5.827500	3
5.862500	3
5.906250	3

DOWN SCAN

5.792500	-1
5.732500	-1
5.707500	3
5.683750	-1
5.676250	-1
5.647500	-1
5.622500	-1
5.528750	3
5.432500	3
5.346250	-1
5.317500	-1
5.303750	-1
5.282500	-1
5.261250	-1
5.245750	-1
4.942500	-1
4.925000	3
4.886250	-1
4.882500	3
4.878750	-1
4.712500	-1
4.698750	-1
4.691250	-1
4.507500	-1
1.488750	3
1.482500	-1
1.097500	-1
1.078750	-1
1.042500	-1
1.022500	-1
0.885000	-1
0.878750	-1
0.846250	-1
0.831250	-1
0.825000	-1
0.710000	3
0.663750	-1
0.642500	-1
0.623750	-1
0.537500	-1
0.516250	-1

AIL DIGITAL/OPTICAL LINEAR POSITION TRANSDUCER

STATIC ACCURACY DATA AND ANALYSIS

TRANSDUCER: 4 12/02/81

POINT	INCHES	EIU SCALE	STEPPER SCALE	ERROR IN BITS	ERROR IN INCHES
1	0.00	2	0	0	0.000000
2	0.50	314	400	-29	-0.042522
3	1.00	634	800	-50	-0.073314
4	1.50	967	1200	-58	-0.085044
5	2.00	1316	1600	-50	-0.073314
6	2.50	1679	2000	-28	-0.041056
7	3.00	2051	2400	3	0.004399
8	3.50	2427	2800	38	0.055718
9	4.00	2791	3200	61	0.089442
10	4.50	3138	3600	67	0.098240
11	5.00	3467	4000	55	0.080645
12	5.50	3782	4400	29	0.042522
13	6.00	4095	4800	1	0.001466
13	6.00	4094	4800	0	0.000000
12	5.50	3778	4400	25	0.036657
11	5.00	3463	4000	51	0.074780
10	4.50	3134	3600	63	0.092375
9	4.00	2788	3200	58	0.085044
8	3.50	2423	2800	34	0.049853
7	3.00	2048	2400	0	0.000000
6	2.50	1676	2000	-31	-0.045454
5	2.00	1313	1600	-53	-0.077712
4	1.50	966	1200	-59	-0.086510
3	1.00	631	800	-53	-0.077712
2	0.50	311	400	-32	-0.046921
1	0.00	0	0	-2	-0.002933

150

RESOLUTION AND MONOTONICITY TESTS

UP SCAN

POSITION (INCHES)	ERROR (BITS)
1.535000	3

DOWN SCAN

ATL DIGITAL/OPTICAL LINEAR POSITION TRANSDUCER

STATIC ACCURACY DATA AND ANALYSIS

TRANSDUCER: 5 11/16/81

POINT	INCHES	EIU SCALE	STEPPER SCALE	ERROR IN BITS	ERROR IN INCHES
1	0.00	2	0	0	0.000000
2	0.50	318	400	-25	-0.036657
3	1.00	644	800	-40	-0.058651
4	1.50	981	1200	-44	-0.064516
5	2.00	1333	1600	-33	-0.048387
6	2.50	1691	2000	-16	-0.023460
7	3.00	2049	2400	1	0.001466
8	3.50	2411	2800	22	0.032258
9	4.00	2764	3200	34	0.049853
10	4.50	3101	3600	30	0.043988
11	5.00	3430	4000	18	0.026393
12	5.50	3758	4400	5	0.007331
13	6.00	4095	4800	1	0.001466
13	6.00	4095	4800	1	0.001466
12	5.50	3759	4400	6	0.008798
11	5.00	3430	4000	18	0.026393
10	4.50	3099	3600	28	0.041056
9	4.00	2763	3200	33	0.048387
8	3.50	2410	2800	21	0.030792
7	3.00	2045	2400	-3	-0.004399
6	2.50	1685	2000	-22	-0.032258
5	2.00	1329	1600	-37	-0.054252
4	1.50	981	1200	-44	-0.064516
3	1.00	644	800	-40	-0.058651
2	0.50	317	400	-26	-0.038123
1	0.00	2	0	0	0.000000

RESOLUTION AND MONOTONICITY TESTS

UP SCAN

POSITION (INCHES)	ERROR (BITS)

DOWN SCAN

ATL DIGITAL/OPTICAL LINEAR POSITION TRANSDUCER

STATIC ACCURACY DATA AND ANALYSIS

TRANSDUCER: 6 12/1/81

POINT	INCHES	EIU SCALE	STEPPER SCALE	ERROR IN BITS	ERROR IN INCHES
1	0.00	2	0	0	0.000000
2	0.50	310	400	-33	-0.048387
3	1.00	621	800	-63	-0.092375
4	1.50	945	1200	-80	-0.117302
5	2.00	1292	1600	-74	-0.108504
6	2.50	1665	2000	-42	-0.061583
7	3.00	2050	2400	2	0.002933
8	3.50	2439	2800	50	0.073313
9	4.00	2811	3200	81	0.118768
10	4.50	3156	3600	85	0.124633
11	5.00	3482	4000	70	0.102639
12	5.50	3792	4400	39	0.057185
13	6.00	4095	4800	1	0.001466
13	6.00	4094	4800	0	0.000000
12	5.50	3789	4400	36	0.052786
11	5.00	3478	4000	66	0.096774
10	4.50	3152	3600	81	0.118768
9	4.00	2807	3200	77	0.112903
8	3.50	2435	2800	46	0.067448
7	3.00	2046	2400	-2	-0.002933
6	2.50	1662	2000	-45	-0.065982
5	2.00	1289	1600	-77	-0.112903
4	1.50	943	1200	-82	-0.120234
3	1.00	619	800	-65	-0.095308
2	0.50	308	400	-35	-0.051319
1	0.00	0	0	-2	-0.002933

RESOLUTION AND MONOTONICITY TESTS

UP SCAN

POSITION (INCHES)	ERROR (BITS)

DOWN SCAN

APPENDIX D

COMPUTER SOFTWARE

This appendix contains the following computer software:

2-D Computer Ray Trace (FORTRAN)

Microprocessor Translation Fixture Controller (PLM 86)

Intel MDS Static Test Data Upload (PLM 80)

Static Test Data Download (FORTRAN)

Static Test Data Analysis (FORTRAN)

Static Test Data Graphics (FORTRAN)

3-D Computer Ray Trace (FORTRAN)

11
F

```
C         MIX ROD RAY TRACE PROGRAM
C         BRUCE E. JOHNSON  2-3751 / 3-8877
C    ****************************************
C         SET PARAMETERS FOR MIX ROD
C         THIS PROGRAM IS FOR TAPERED MIX RODS
      COMMON/SUB1/HT
      COMMON/SUB2/NY(500),YIN(100)
      COMMON/SUB21/SA1,DELTAY
      COMMON/SUB4/NY1(500),NS1,YN2(500),AM
      COMMON/SUB41/SA2
      COMMON/SUB3/DPLATE,WPAT,NMXR
      COMMON/SUB5/AN(500),NAFIB
      COMMON/SUB6/NS3
      DIMENSION FLUX1(30),FLUX2(30)
      DIMENSION WPTN(30)
C        THIS PROGRAM USES WEIGHTED RAYS TO SIMULATE DISTRIBUTION
C        DISTRIBUTION IS COSINE(N*THETA)
      REAL NAFIB,NAMXR,NMXR,MF,M(1500)
C      ********************************************************
C             PARAMETERS
      NS3=20
       DO 327 JJ=1,NS3
C      ********************************************************
      NFIB=40
      YMAX=.05
      XMAX=4.5
      NRAYS=1000
      NS=100
      HT=.02777777
C       OFFSET PARAMETER REFERS TO TAN(OFFSET ANGLE OF FIBERS)
      OFFSET=.087489
      NMXR=1.46
      NAFIB=.4
      DPLATE=.0625                                              11
      DW=.1/FLOAT(NS3)                                          B
      WPAT=DW*FLOAT(JJ)
      WPTN(JJ)=WPAT
      NS1=100
      ACIL=YMAX-.00001
C       ************************************************************
C
C       ************************************************************
      WRITE(6,221) ACIL
221   FORMAT(/,10X,21HACTUAL ILLUMINATION= ,F8.4,/)
      WRITE(6,223) HT
      WRITE(6,224)NFIB
224   FORMAT(10X,29HTHE NUMBER OF SOURCE FIBERS= ,I6,/)
223   FORMAT(/,10X,18HTAPER HALF-ANGLE= ,F8.4,09H(RADIANS),/)
C       THE PARAMETER HA REFERS TO THE TAPER HALF-ANGLE OF MIX ROD
C       THE PARAMETER ACIL(ACTUAL ILLUMINATION) REFERS TO HOW MUCH OF
C       MIX ROD IS ACTUALLY ILLUMINATED(SAME UNITS AS YMAX)
4     FORMAT(10X,25HMIX ROD REFRACTIVE INDEX=,F7.4,5X,6HSFCOS=,F8.4,/)
      NAMXR=NAFIB/NMXR
      SFCOS=ACOS(.1)/NAMXR
      WRITE(6,4)NMXR,SFCOS
      WRITE(6,5) NAFIB,NAMXR,XMAX,YMAX
      WRITE(6,6) DPLATE,WPAT,NRAYS,NS1
6     FORMAT(5X,6HDPLAT/,F5.3,10X,5HWPAT/,F5.2,10X,5HNRAYS,I5,9X,I5)
5     FORMAT(5X,6HNAFIB/,F5.2,10X,5HNAMXR,F5.2,10X,5HXMAX/,F5.2,9X,F5.2)
      DY=ACIL/FLOAT(NFIB+1)
C     FORM FIBER INPUT POSITION ARRAY
      DO 10 J=1,NFIB
      YIN(J)=DY*FLOAT(J)
```

```
10    CONTINUE
      WRITE(6,12)DY
12    FORMAT(10X,3HDY=,F6.3,/)
C         FORM RAY DISTRIBUTION FOR FIBER
C         USE ISOTROPIC SOURCE FILLED TO NA
      THETA=ASIN(NAMXR)
      SMAX=TAN(THETA)
      STOT=2.0*SMAX
      DM=STOT/FLOAT(NRAYS+1)
C     ECHO MAX RAY SLOPE
      WRITE(6,15)SMAX
15    FORMAT(10X,5HSMAX=,F6.3)
      WRITE(6,17)DM
17    FORMAT(10X,3HDM=,F6.3,/)
      WRITE(6,16)OFFSET
16    FORMAT(10X,21HANGULAR OFFSET=       ,F7.4,/)
      DO 20 J=1,NRAYS
      M(J)=SMAX-DM*FLOAT(J)
      M(J)=M(J)+OFFSET
20    CONTINUE
C     INTIALIZE COUNTERS FOR RAY DENSITY
      DO 30 J=1,NS
      NY(J)=0.0
30    CONTINUE
      DO 32 J=1,NS1
      NY1(J)=0.0
      YN2(J)=0.0
32    CONTINUE
C        **********************************
C        MAIN PROGRAM
C        **********************************
      DO 40 J=1,NFIB
      DO 50 K=1,NRAYS
C       COMPUTE RAY AMPLITUDE PARAMETER AM
      THETA3=ATAN(M(K))
      YYY=THETA3*SFCOS
      AM=COS(YYY)
      CALL RTRACE(YIN(J),M(K),YMAX,XMAX,YE,MF)
      CALL RTRAC1(YE,MF,YMAX,XMAX)
50    CONTINUE
40    CONTINUE
      TOT=0.0
      TOT1=0.0
      TOT2=0.0
      DO 60 J=1,NS
      XX=SA1-(FLOAT(J)*SA1/FLOAT(NS))
      TOT=TOT+FLOAT(NY(J))
60    CONTINUE
      DO 62 J=1,NS1
      XX=WPAT-(FLOAT(J)*WPAT/FLOAT(NS1))
      TOT1=TOT1+FLOAT(NY1(J))
      TOT2=TOT2+YN2(J)
      FLUX1(JJ)=TOT1
      FLUX2(JJ)=TOT2
62    CONTINUE
65    FORMAT(10X,I10,10X,I10,5X,F8.5,5X,F10.4)
      WRITE(6,67) TOT
      WRITE(6,67) TOT1
      WRITE(6,67) TOT2
67    FORMAT(10X,F10.3,/)
      AVE=TOT/FLOAT(NS)
      AVE1=TOT1/FLOAT(NS1)
```

```
      AVE2=TOT2/FLOAT(NS1)
      WRITE(6,70) AVE,AVE1,AVE2
70    FORMAT(10X,24HTHE AVERAGE # OF RAYS IS,F8.4,10X,F8.4,5X,F8.4)
C     COMPUTE STANDARD DEVIATION
      VAR=0.0
      VAR1=0.0
      VAR2=0.0
      DO 80 J=1,NS
      VAR=VAR+((FLOAT(NY(J))-AVE)**2)
      VAR1=VAR1+((FLOAT(NY1(J))-AVE1)**2)
      VAR2=VAR2+((YN2(J)-AVE2)**2)
80    CONTINUE
      VAR=VAR/FLOAT(NS)
      VAR1=VAR1/FLOAT(NS1)
      VAR2=VAR2/FLOAT(NS1)
      SDV1=SQRT(VAR1)
      SDV2=SQRT(VAR2)
      SDV=SQRT(VAR)
      WRITE(6,85)VAR,SDV
      WRITE(6,85)VAR1,SDV1
      WRITE(6,85)VAR2,SDV2
85    FORMAT(10X,4HVAR=,F8.4,10X,4HSDV=,F8.4,/)
      WRITE(6,86)
86    FORMAT(////////////////////////////////////////)
327   CONTINUE
      CALL PLOT(FLUX1,3,NAFIB,WPTN)
      WRITE(6,86)
      CALL PLOT(FLUX2,3,NAFIB,WPTN)
      STOP
      END
C       ***********************************************
C
C       ***********************************************
      SUBROUTINE RTRACE(YS,MS,YMAX,XMAX,YE,MF)
      COMMON/SUB1/HT
      REAL M,MS,MF,M11,M12,MO,MA
      Y0=YS
      B=YS
      X0=0.0
      X=X0
      M=MS
      NS=100
      YMIN=0.0
C       COMPUTE TAPER PARAMETERS
C       THIS SUBROUTINE IS FOR A TAPERED MIX ROD
C       HORN ANGLE IS HA(HALF-ANGLE)
      M11=TAN(HT)
      M12=-TAN(HT)
      B1=YMAX
      B2=YMIN
10    IF(M.GT.0.0)MA=M11
      IF(M.GT.0.0)BA=B1
      IF(M.LT.0.0)MA=M12
      IF(M.LT.0.0)BA=B2
      IF(M.EQ.0.0)YE=Y0
      IF(M.EQ.0.0)MF=M
      IF(M.EQ.0.0)GO TO 100
C        REFLECT RAY OFF OF BOUNDARY; CALCULATE INTERSECTION POINT
20    IF((M-MA).EQ.0.0)YE=M*XMAX+B
      IF((M-MA).EQ.0.0)MF=M
      IF((M-MA).EQ.0.0)GO TO 100
      X0=(BA-B)/(M-MA)
```

```
      IF(HT.LT.0.0)GO TO 25
      IF(ABS(M).LT.ABS(MA))YE=M*XMAX+B
      IF(ABS(M).LT.ABS(MA))MF=M
      IF(ABS(M).LT.ABS(MA)) GO TO 100
25    IF(X0.GE.XMAX)YE=M*XMAX+B
      IF(X0.GE.XMAX)MF=M
      IF(X0.GE.XMAX) GO TO 100
      Y0=MA*X0+BA
      XX1=2.0*ATAN(MA)-ATAN(M)
      M0=TAN(XX1)
      B=Y0-M0*X0
      M=M0
      X=X0
      GO TO 10
100   CALL RCOUNT(YE,NS,YMAX,YMIN,XMAX)
      RETURN
      END
C       ****************************************************
      SUBROUTINE RCOUNT(YE,NS,YMAX,YMIN,XMAX)
      COMMON/SUB1/HT
      COMMON/SUB2/NY(500),YIN(100)
      COMMON/SUB21/SA1,DELTAY
C     THIS SUBROUTINE COMPUTES THE RAY DENSITY/UNIT SAMPLE AREA
C     COUNTERS INTIALIZED TO 0 IN MAIN PROGRAM
      DELTAY=XMAX*TAN(HT)
      SA1=YMAX+2*DELTAY
      DYY=SA1/FLOAT(NS)
      DO 20 J=1,NS
      YMX1=(SA1-DELTAY)-DYY*FLOAT(J-1)
      YMX2=(SA1-DELTAY)-DYY*FLOAT(J)
      IF((YE.LT.YMX1).AND.(YE.GE.YMX2))NY(J)=NY(J)+1
      IF((YE.LT.YMX1).AND.(YE.GE.YMX2))GO TO 30
20    CONTINUE
30    YE=YE
      RETURN
      END
C     ****************************************************
      SUBROUTINE RTRAC1(YE,M,YMAX,XMAX)
      REAL M,M1,NMXR,MF1
      COMMON/SUB3/DPLATE,NPAT,NMXR
C       THIS SUBROUTINE TRACES RAYS FROM THE MIX ROD TO
C       THE ENCODING ELEMENT
C         DPLATE=SPACING BETWEEN MIX ROD AND ENCODING ELEMENT(MAIN)
      XMAX1=XMAX+DPLATE
C         MODIFY RAY SLOPE FOR GLASS/AIR INTERFACE
      IF(M.EQ.0.0) YE1=YE
      IF(M.EQ.0.0) MF1=M
      IF(M.EQ.0.0) BF1=YE
      IF(M.EQ.0.0) GO TO 20
      THETA0=ATAN(M)
      XXX=NMXR*SIN(THETA0)
      THETA1=ASIN(XXX)
      M1=TAN(THETA1)
      MF1=M1
C     CALCULATE POSITION ON ENCODING PLATE
      X0=XMAX
      Y0=YE
      B1=Y0-M1*X0
      BF1=B1
      YE1=M1*XMAX1+B1
20    YE=YE
```

```
      CALL RCOUN1(YE1,XMAX,YMAX)
      CALL ANGSP1(YE1,MF1,BF1)
      RETURN
      END
C     ***************************************************
      SUBROUTINE RCOUN1(YE1,XMAX,YMAX)
C        THIS SUBROUTINE COMPUTES RAY DENSITY ON ENCODING PLATE
C        COUNTERS INTIALIZED TO 0 IN MAIN PROGRAM
C        CALCULATE POSITION OF ENCODING PLATE SLIT
      COMMON/SUB4/NY1(500),NS1,YN2(500),AM
      COMMON/SUB41/SA2
      COMMON/SUB1/HT
      COMMON/SUB3/DPLATE,WPAT,NMXR
      DY1=WPAT/FLOAT(NS1)
      SA2=(2*YMAX+TAN(HT))/2.0+WPAT/2.0
      YMAX3=SA2
C        AM IS RAY AMPLITUDE PARAMETER
      DO 20 J=1,NS1
      YMX1=YMAX3-DY1*FLOAT(J-1)
      YMX2=YMAX3-DY1*FLOAT(J)
      IF((YE1.LT.YMX1).AND.(YE1.GE.YMX2))NY1(J)=NY1(J)+1
      IF((YE1.LT.YMX1).AND.(YE1.GE.YMX2))YN2(J)=YN2(J)+AM
      IF((YE1.LT.YMX1).AND.(YE1.GE.YMX2))GO TO 30
20    CONTINUE
30    RETURN
      END
C       *******************************************************
C       *******************************************************
C
C       SUBROUTINE PLOT; PRODUCES BAR GRAPH PLOTS
      SUBROUTINE PLOT(PLT,IFLAG1,WAFIB,WPAT)
      COMMON/SUB4/NY1(500),NS1,YN2(500),AM
      COMMON/SUB4A/DELTAA
      COMMON/SUB6/NS3
      DIMENSION WPAT(20)
      REAL WAFIB
C       PARAMETER IFLAG1 IS CONTROL FOR POSITION INFORMATION
C       IFLAG1=1; PLOTS ANGULAR SPECTRUM ON ENCODING PLATE
C       IFLAG1=0; PLOTS RAY DENSITY ON ENCODING PLATE
      DIMENSION M(120)
      DIMENSION PLT(500)
      DO 20 J=1,120
      M(J)=1H*
20    CONTINUE
C     COMPUTE SCALE FACTOR
      YMAX=0.0
      DO 25 J=1,NS1
      IF(PLT(J).GT.YMAX)YMAX=PLT(J)
25    CONTINUE
      SFAC=100.0/YMAX
      DO 30 K=1,NS3
      XY=SFAC*PLT(K)
      N=IFIX(XY)
      IF(IFLAG1.EQ.0)POS=WPAT-(FLOAT(K)*WPAT/FLOAT(NS1))
      IF(IFLAG1.EQ.1)POS=WAFIB-DELTAA*FLOAT(K)
      IF(IFLAG1.EQ.3)POS=WPAT(K)
      WRITE(6,3)POS,(M(J),J=1,N),PLT(K)
3     FORMAT(F10.4,100I1,F10.4)
30    CONTINUE
      WRITE(6,35)SFAC,YMAX
35    FORMAT(/,13HSCALE FACTOR=,F8.4,/,4HMAX=,F8.4,/)
      RETURN
      END
```

```
C       ***********************************************
C       ***********************************************
        SUBROUTINE ANGSP1(YS,MS,BS)
        REAL MS,NAFIB
        COMMON/SUB5/AN(500),NAFIB
        COMMON/SUB4/NY1(500),NS1,YN(500),AM
        COMMON/SUBA/DELTAA
C          SUBROUTINE ANGSP1(ANGULAR SPECTRUM CALCULATION)
C          COUNTERS INTIALIZED TO 0 IN MAIN PROGRAM
C          THIS PRUGRAM USES WEIGHTED RAYS
C          RAY AMPLITUDE PARAMETER IS AM
C
     DELTAA=2.0*NAFIB/FLOAT(NS1)
     DO 20 J=1,NS1
     YMX1=NAFIB-DELTAA*FLOAT(J-1)
     YMX2=NAFIB-DELTAA*FLOAT(J)
     IF((MS.LT.YMX1).AND.(MS.GE.YMX2))AN(J)=AN(J)+AM
     IF((MS.LT.YMX1).AND.(MS.GE.YMX2))GO TO 30
20   CONTINUE
```

CURRENT LISTING OF MODULES FOR ATL LINEAR SENSOR FOR USE ON INTEL SINGLE BOARD COMPUTER 86/12.

MODULE	PROCEDURE	DESCRIPTION
ATL1	SIX (MAIN)	USES POS6 AND SCAND TO START FROM SIX INCHES AND SCAN DOWN.
ATL2	ZERO (MAIN)	USES POS0 AND SCANU TO START FROM ZERO AND SCAN UP.
ATL3	FIND	FINDS CURRENT SCREW POSITION. USED BY MODULES 4 THROUGH 7.
ATL4	POS0	POSITIONS SCREW TO 0 INCHES.
ATL5	POS6	POSITIONS SCREW TO 6 INCHES.
ATL6	SCAND	STARTING FROM 6 INCHES, SCANS DOWN THROUGH 4801 POSITIONS AND STORES INDICATED POSITION.
ATL7	SCANU	STARTING FROM 0 INCHES, SCANS UP THROUGH 4801 POSITIONS AND STORES INDICATED POSITION.
PLOTUP	PLOTUP (MAIN)	IF USED AFTER ZERO, PLOTUP WILL PLOT EIU POSITION VS STEPPER POSITION
PLOTDN	PLOTDN (MAIN)	IF USED AFTER SIX, PLOTDN WILL PLOT EIU POSITION VS STEPPER POSITION

```
PL/M-86 COMPILER    ATL1


ISIS-II PL/M-86 V2.1 COMPILATION OF MODULE ATL1
OBJECT MODULE PLACED IN :F1:SIX.OBJ
COMPILER INVOKED BY:  PLM86 :F1:SIX.SRC DEBUG PRINT(:LP:)


   1          ATL1: DO;    /*SET ATL LINEAR SENSOR TO SIX INCHES AND SCAN DOWN*/

   2   1      POS6: PROCEDURE EXTERNAL; END POS6;
   4   1      SCAND: PROCEDURE EXTERNAL; END SCAND;

              /*SET 8255A PROGRAMMABLE PERIPHERAL INTERFACE CHIP*/
              /*ADDRESS 0CAH = PORTS PB7 - PB0,
                ADDRESS 0CCH = PORTS PC3 - PC0, INPUT LINES FOR A TO D*/
              /*ADDRESS 0C8H = PORT PA0, OUTPUT FOR A TO D CONTROL*/
              /*ADDRESS 0C8H = PORTS PA1, PA2 - STEP UP, STEP DOWN*/
              /*MODE 0 - BASIC I/O*/
   6   1      OUTPUT(0CEH)=8BH;    /*PA7-PA0, OUTPUTS, B,C, INPUTS*/

   7   1      CALL POS6;    /*POSITION SCREW TO 6 INCHES*/
   8   1      CALL SCAND;    /*SCAN DOWN AND STORE*/

   9   1      END ATL1;
```

```
PL/M-86 COMPILER    ATL2


ISIS-II PL/M-86 V2.1 COMPILATION OF MODULE ATL2
OBJECT MODULE PLACED IN :F1:ZERO.OBJ
COMPILER INVOKED BY:  PLM86 :F1:ZERO.SRC DEBUG PRINT(:LP:)


   1          ATL2: DO;    /*ZERO ATL LINEAR SENSOR AND SCAN UP*/

   2   1      POS0: PROCEDURE EXTERNAL; END POS0;
   4   1      SCANU: PROCEDURE EXTERNAL; END SCANU;

              /*SET 8255A PROGRAMMABLE PERIPHERAL INTERFACE CHIP*/
              /*ADDRESS 0CAH = PORTS PB7 - PB0,
                ADDRESS 0CCH = PORTS PC3 - PC0, INPUT LINES FOR A TO D*/
              /*ADDRESS 0C8H = PORT PA0, OUTPUT FOR A TO D CONTROL*/
              /*ADDRESS 0C8H = PORTS PA1, PA2 - STEP UP, STEP DOWN*/
              /*MODE 0 - BASIC I/O*/
   6   1      OUTPUT(0CEH)=8BH;    /*PA7-PA0, OUTPUTS, B,C, INPUTS*/

   7   1      CALL POS0;    /*POSITION SCREW TO 0 INCHES*/
   8   1      CALL SCANU;    /*SCAN UP AND STORE*/

   9   1      END ATL2;
```

```
 1          ATL3: DO;    /*FIND CURRENT SCREW POSITION*/
 2   1      FIND: PROCEDURE WORD PUBLIC;

 3   2      DECLARE(HIGH,LOW)BYTE;
 4   2      DECLARE PLACE WORD;

 5   2      OUTPUT(0C8H)=01H;    /*SET START CONVERT LOW*/
 6   2      CALL TIME(1);    /*100 MICROSECOND DELAY*/
 7   2      OUTPUT(0C8H)=00H;    /*SET START CONVERT HIGH TO START A TO D
 8   2      CALL TIME(1);    /*100 MICROSECOND DELAY*/
 9   2      LOW=INPUT(0CAH);
10   2      HIGH=INPUT(0CCH) AND 0FH;
11   2      PLACE=HIGH;
12   2      PLACE=SHL(PLACE,8);    /*SHIFT HIGH POSITIONS LEFT 8 BITS*/
13   2      PLACE=PLACE+LOW;    /*BIT POSITION OF SCREW*/

14   2      RETURN PLACE;
15   2      END FIND;
16   1      END ATL3;

PL/M-86 COMPILER    ATL4


ISIS-II PL/M-86 V2.1 COMPILATION OF MODULE ATL4
OBJECT MODULE PLACED IN :F1:POS0.OBJ
COMPILER INVOKED BY:  PLM86 :F1:POS0.SRC DEBUG PRINT(:LP:)


   1          ATL4  DO;    /*POSITION SCREW*/

   2   1      FIND: PROCEDURE WORD EXTERNAL;
   3   2         END FIND;

   4   1      POS0  PROCEDURE PUBLIC;    /*POSITION SCREW TO 0 INCHES*/

   5   2      DECLARE PLACE WORD;    /*POSITION OF SCREW*/
   6   2      DECLARE COUNT BYTE;

              /*STEP DOWN TO BIT POSITION 0*/
   7   2      PLACE=FIND;
   8   2      DO WHILE PLACE>0;
   9   3         OUTPUT(0C8H)=04H;    /*STEP DOWN*/
  10   3         CALL TIME(100);    /*10 MILLISECOND DELAY*/
  11   3         PLACE=FIND;
  12   3         END;

              /*STEP DOWN 12 MORE STEPS TO TAKE UP SLACK*/
  13   2      DO COUNT=1 TO 12;
  14   3         OUTPUT(0C8H)=04H;    /*STEP DOWN*/
  15   3         CALL TIME(50);    /*5 MILLISECOND DELAY*/
  16   3         OUTPUT(0C8H)=00H;    /*SET LEVEL HIGH*/
  17   3         CALL TIME(50);
  18   3         END;

              /*STEP UP TO BIT POSITION 2 (0 INCHES)*/
  19   2      PLACE=FIND;
  20   2      DO WHILE PLACE<2;
  21   3         OUTPUT(0C8H)=02H;    /*STEP UP*/
  22   3         CALL TIME(100);
  23   3         PLACE=FIND;
  24   3         END;
```

```
                /*STEP UP 4 MORE STEPS FOR CENTERING*/
  25    2       DO COUNT=1 TO 4;
  26    3          OUTPUT(0C8H)=02H;    /*STEP UP*/
  27    3          CALL TIME(50);
  28    3          OUTPUT(0C8H)=00H;    /*SET LEVEL HIGH*/
  29    3          CALL TIME(50);
  30    3          END;
  31    2       RETURN;
  32    2       END POS0;
  33    1       END ATL4;
PL/M-86 COMPILER    ATL5


ISIS-II PL/M-86 V2.1 COMPILATION OF MODULE ATL5
OBJECT MODULE PLACED IN :F1:POS6.OBJ
COMPILER INVOKED BY:  PLM86 :F1:POS6.SRC DEBUG PRINT(:LP:)


   1            ATL5: DO;    /*POSITION SCREW TO 6 INCHES*/

   2    1       FIND: PROCEDURE WORD EXTERNAL;
   3    2          END FIND;

   4    1       POS6:  PROCEDURE PUBLIC;

   5    2       DECLARE PLACE WORD;    /*POSITION OF SCREW*/
   6    2       DECLARE COUNT BYTE;

                /*STEP UP TO POSITION 4095*/
   7    2       PLACE=FIND;
   8    2       DO WHILE PLACE<4095;
   9    3          OUTPUT(0C8H)=02H;    /*STEP UP*/
  10    3          CALL TIME(100);    /*10 MILLISECOND DELAY*/
  11    3          PLACE=FIND;
  12    3          END;

                /*STEP UP 20 MORE STEPS*/
  13    2       DO COUNT=1 TO 20;
  14    3          OUTPUT(0C8H)=02H;    /*STEP UP*/
  15    3          CALL TIME(50);    /*5 MILLISECOND DELAY*/
  16    3          OUTPUT(0C8H)=00H;    /*SET LEVEL HIGH*/
  17    3          CALL TIME(50);
  18    3          END;

                /*STEP DOWN TO POSITION 4094 (6 INCHES)*/
  19    2       PLACE=FIND;
  20    2       DO WHILE PLACE>4094;
  21    3          OUTPUT(0C8H)=04H;    /*STEP DOWN*/
  22    3          CALL TIME(100);
  23    3          PLACE=FIND;
  24    3          END;

                /*STEP DOWN 4 MORE POSITIONS FOR CENTERING*/
  25    2       DO COUNT=1 TO 4;
  26    3          OUTPUT(0C8H)=04H;    /*STEP DOWN*/
  27    3          CALL TIME(50);    /*5 MILLISECOND DELAY*/
  28    3          OUTPUT(0C8H)=00H;    /*SET LEVEL HIGH*/
  29    3          CALL TIME(50);
  30    3          END;

  31    2       RETURN;
  32    2       END POS6;
  33    1       END ATL5;
```

```
PL/M-86 COMPILER    ATL6


ISIS-II PL/M-86 V2.1 COMPILATION OF MODULE ATL6
OBJECT MODULE PLACED IN :F1:SCAND.OBJ
COMPILER INVOKED BY:  PLM86 :F1:SCAND.SRC DEBUG PRINT(:LP:)


   1          ATL6: DO;    /*SCAN DOWN AND STORE*/

   2   1      DECLARE EIU(4801) WORD PUBLIC;    /*EIU POSITION*/

   3   1      FIND: PROCEDURE WORD EXTERNAL;
   4   2         END FIND;

   5   1      SCAND: PROCEDURE PUBLIC;    /*SCAN DOWN*/

   6   2      DECLARE (STEP, TEMP, LOOP) INTEGER;
   7   2      DECLARE COUNT BYTE;

              /*SCAN THROUGH 4801 POSITIONS*/
   8   2      DO LOOP=47 TO 0 BY -1;

   9   3       DO STEP=100 TO 1 BY -1;
  10   4          TEMP=STEP + LOOP * 100;
  11   4          EIU(TEMP)=FIND;

                  /*STEP DOWN 8 STEPS FOR 1 BIT*/
  12   4          DO COUNT=1 TO 8;
  13   5             OUTPUT(0C8H)=04H;    /*STEP DOWN*/
  14   5             CALL TIME(50);
  15   5             OUTPUT(0C8H)=00H;
  16   5             CALL TIME(50);
  17   5             END;

  18   4          END;

  19   3       END;

  20   2      EIU(0)=FIND;

  21   2      END SCAND;
  22   1      END ATL6;


MODULE INFORMATION

     CODE AREA SIZE     = 00A0H    160D
     CONSTANT AREA SIZE = 0000H      0D
     VARIABLE AREA SIZE = 2589H   9609D
     MAXIMUM STACK SIZE = 0004H      4D
     35 LINES READ
     0 PROGRAM ERROR(S)

END OF PL/M-86 COMPILATION
```

```
PL/M-86 COMPILER    ATL7


ISIS-II PL/M-86 V2.1 COMPILATION OF MODULE ATL7
OBJECT MODULE PLACED IN :F1:SCANU.OBJ
COMPILER INVOKED BY:  PLM86 :F1:SCANU.SRC DEBUG PRINT(:LP:)


   1          ATL7: DO;    /*SCAN UP AND STORE 4801D WORDS = 12C0H WORDS

   2   1      DECLARE EIU(4801) WORD PUBLIC;   /*EIU POSITION*/

   3   1      FIND: PROCEDURE WORD EXTERNAL;
   4   2         END FIND;

   5   1      SCANU: PROCEDURE PUBLIC;

   6   2      DECLARE LOOP BYTE;    /*BECAUSE OF INTEL SOFTWARE BUG*/
   7   2      DECLARE STEP BYTE;    /*STEPPER POSITION = STEP + LOOP * 100 */
   8   2      DECLARE COUNT BYTE;

              /*SCAN THROUGH 4801 POSITIONS*/
   9   2      DO LOOP=0 TO 47;

  10   3       DO STEP=0 TO 99;
  11   4         EIU(STEP+100*LOOP)=FIND;

                 /*STEP UP 8 STEPS FOR 1 BIT*/
  12   4         DO COUNT=1 TO 8;
  13   5            OUTPUT(0C8H)=02H;    /*STEP UP*/
  14   5            CALL TIME(50);    /*5 MILLISECOND DELAY*/
  15   5            OUTPUT(0C8H)=00H;    /*SET LEVEL HIGH*/
  16   5            CALL TIME(50);
  17   5            END;

  18   4         END;

  19   3        END;

  20   2      EIU(4800)=FIND;

  21   2      END SCANU;

  22   1      END ATL7;


MODULE INFORMATION:

     CODE AREA SIZE     = 0095H    149D
     CONSTANT AREA SIZE = 0000H      0D
     VARIABLE AREA SIZE = 2585H   9605D
     MAXIMUM STACK SIZE = 0004H      4D
     36 LINES READ
     0 PROGRAM ERROR(S)

END OF PL/M-86 COMPILATION
```

```
PL/M-86 COMPILER    PLOTDN


ISIS-II PL/M-86 V2.1 COMPILATION OF MODULE PLOTDN
OBJECT MODULE PLACED IN :F1:PLOTDN.OBJ
COMPILER INVOKED BY:  PLM86 :F1:PLOTDN.SRC LARGE DEBUG PRINT(.LP.)


   1          PLOTDN: DO;   /*PLOT EIU POSITION VS. STEPPER POSITION ON DOWN

   2   1      DECLARE XCHAN$PTR POINTER;    /*PLOTTER ADDRESS*/
   3   1      DECLARE YCHAN$PTR POINTER;
   4   1      DECLARE XCHAN BASED XCHAN$PTR WORD;    /*STEPPER POSITION*/
   5   1      DECLARE YCHAN BASED YCHAN$PTR WORD;    /*EIU POSITION*/
   6   1      DECLARE EIU$PTR POINTER;    /*LOCATION OF EIU POSITION IN MEMORY
   7   1      DECLARE EIU WORD AT(@EIU$PTR);  /*              "           */
   8   1      DECLARE EIUT$PTR POINTER;    /*              "           */
   9   1      DECLARE EIUT BASED EIUT$PTR WORD;    /*EIU POSITION IN MEMORY*/
  10   1      DECLARE (I,J) BYTE;     /*LOOP COUNTERS*/

  11   1      OUTPUT(0CEH)=8BH;    /*INITILIZE 8255A PPI*/

  12   1      XCHAN$PTR=8004H;    /*PLOTTER ADDRESS*/
  13   1      YCHAN$PTR=8002H;

  14   1      EIU$PTR=8EAH;    /*START OF EIU DATA*/
  15   1      EIUT$PTR=EIU$PTR;
  16   1      XCHAN=0;
  17   1      YCHAN=EIUT;
  18   1      DO I=1 TO 40;    /*1 SECOND DELAY*/
  19   2         CALL TIME(250);    /*25 MILLISECOND DELAY*/
  20   2         END;

               /*PLOT OUT 49 POINTS*/
  21   1      OUTPUT(0C8H)=08H;    /*DROP PEN*/
  22   1      DO J=0 TO 48;
  23   2         XCHAN=J*82;
  24   2         YCHAN=EIUT;
  25   2         DO I=1 TO 40;    /*1 SECOND DELAY*/
  26   3            CALL TIME(250);
  27   3            END;
  28   2         EIU=EIU+200;    /*SKIP 100 WORDS OR 200 BYTES*/
  29   2         EIUT$PTR=EIU$PTR;
  30   2         END;
  31   1      OUTPUT(0C8H)=00H;    /*LIFT PEN*/

  32   1      END PLOTDN;


MODULE INFORMATION:

     CODE AREA SIZE     = 0107H    263D
     CONSTANT AREA SIZE = 0000H      0D
     VARIABLE AREA SIZE = 0012H     18D
     MAXIMUM STACK SIZE = 0000H      0D
     39 LINES READ
     0 PROGRAM ERROR(S)
```

```
MEMORY: DO;   /*STORE 4001 WORDS OF DATA FROM DISK TO A MEMORY
                BUFFER AND OUT FROM INTELLEC*/

DECLARE BUFFER(10000) BYTE,   /*MEMORY BUFFER FOR FILE*/
DECLARE AFT$IN ADDRESS;
DECLARE STATUS ADDRESS;
DECLARE ACTUAL ADDRESS;
DECLARE I ADDRESS,   /*LOOP COUNTER*/
DECLARE OFFSET ADDRESS;
DECLARE A ADDRESS,   /*1KBYTE COUNTER*/
DECLARE IO(4) BYTE,
DECLARE J BYTE;   /*LOOP COUNTER*/
DECLARE (K,C) BYTE,

ERROR    /*OUTPUT ERROR MESSAGE ON SYSTEM CONSOLE*/
   PROCEDURE(ERRNUM) EXTERNAL,
   DECLARE ERRNUM ADDRESS,
   END ERROR,

OPEN    /*INTIIALIZE FILE FOR INPUT*/
   PROCEDURE(AFTNPTR,FILE,ACCESS,MODE,STATUS) EXTERNAL;
   DECLARE(AFTNPTR, FILE, ACCESS, MODE, STATUS) ADDRESS,
   END OPEN,

READ    /*TRANSFER DATA FROM FILE TO MEMORY*/
   PROCEDURE(AFTN, BUFFER, COUNT, ACTUAL, STATUS) EXTERNAL;
   DECLARE(AFTN, BUFFER, COUNT, ACTUAL, STATUS) ADDRESS,
   END READ,

CLOSE    /*TERMINATE INPUT OPERATION*/
   PROCEDURE(AFTN, STATUS) EXTERNAL;
   DECLARE(AFTN, STATUS) ADDRESS,
   END CLOSE,

/*TO2, SPORT ARE PROCEDURES IN DOES LIB USED FOR OUTPUTTING*/
TO2  PROCEDURE(CH) EXTERNAL,
   DECLARE CH BYTE,
   END,
SPORT  PROCEDURE (P,B) EXTERNAL;
   DECLARE (P,B) ADDRESS;
   END;

OUT    /*CONVERT A NIBLE TO A LEGAL ASCII CHARACTER AND OUTPUT
         FROM INTELLEC*/
   PROCEDURE(B),
   DECLARE (C,B) BYTE;
   C=B OR 30H,   /*CONVERT TO LEGAL ASCII*/
   CALL TO2(C),   /*OUTPUT CHARACTER*/
   END OUT,

TI2    /*PROCEDURE FOR INPUTTING*/
   PROCEDURE BYTE EXTERNAL;
   END;
    T2STS    /*SERIAL PORT 2 INPUT STATUS ROUTINE*/
      PROCEDURE BYTE EXTERNAL,
      END T2STS,

  CALL SPORT(2,300),   /*INITIALIZE OUTPUT PORT FOR 300 BAUD*/
  CALL OPEN( AFT$IN,  ('STORE 00 '), 1, 0,  STATUS),
  IF STATUS <> 0 THEN CALL ERROR(STATUS),
  CALL READ(AFT$IN,  BUFFER, 9774,  ACTUAL,  STATUS),
  IF STATUS <> 0 THEN CALL ERROR(STATUS),
  CALL CLOSE(AFT$IN,  STATUS),
  IF STATUS <> 0 THEN CALL ERROR(STATUS),
```

```
/*OUTPUT LOWER 3 NIBLES OF EACH OF 4801 WORDS*/
OFFSET=19;   /*ELIMINATE HEADER*/
I=1;
A=0;
DO WHILE I <= 9602;
   IF A=1024    /*DATA COMES IN 1KBYTE BLOCKS*/
      THEN DO; A=2; OFFSET=OFFSET + 09; END; /*ELIMINATE SPACER*/
      ELSE A=A + 2;

   /*ASSIGN A WORD TO 3 NIBLES*/
   IO(1)=(BUFFER(I+1+OFFSET) AND 0FH);
   IO(2)=(SHR(BUFFER(I+OFFSET), 4));
   IO(3)=(BUFFER(I+OFFSET) AND 0FH);

   DO J=1 TO 3;   /*OUTPUT WORD*/
      OUTPUT:  CALL OUT(IO(J));

      DO K=1 TO 250;  /*SEE IF CHARACTER RETURNS*/
         IF T2ST5   /*DATA READY FOR INPUT*/
            THEN IF (IO(J) OR 30H) = (TI2 AND 3FH)
               THEN GOTO LOOP1;   /*CORRECT CHARACTER*/
               ELSE DO;   /*WRONG CHARACTER*/
                  CALL TO2(42H);   /*ASCII B = 66 DECIMAL*/
                  DO C=1 TO 40;   /*DELAY*/
                     CALL TIME(250);
                     END;
                  GOTO OUTPUT;   /*TRY AGAIN*/
                  END;
         CALL TIME(25);
         END;

      GOTO OUTPUT;
      LOOP1:  C=0;
      END;

   I=I+2;
   END;

END MEMORY;
```

```
C ATL LINEAR SENSOR MICROPROCESSOR UPLOAD, CALCULATIONS, AND OUTPUT.
C READ IN ASCII CODED HEX NIBLES FROM INTELLEC AND FORM 4801 12-BIT WORDS
C
      INTEGER CHAR(14403),WORD(4801)
      INTEGER GETC
C
C INPUT DELAY PARAMETER FROM TERMINAL
      WRITE(3,2)
2     FORMAT(10X,19HDELAY FOR TERMINAL?,/)
      READ(3,4)ND
4     FORMAT(I4)
C
C DROP OFF FIRST 2 CHARACTERS
      OPEN 10
      DO 3 I=1,2
         CHAR(I)=GETC(10)
         WRITE(3,-) CHAR(I)
         CALL PUTC(CHAR(N),10)
    3    CONTINUE
C
C READ IN ASCII CHARACTERS USING EXTERNAL PROCEDURE GETC
      OPEN 10
      DO 10 N=1,14403
101      CHAR(N)=GETC(10)
CHECK FOR ERROR
         NTEMP=CHAR(N)
         IF (NTEMP .NE. 66) GOTO 12
C IF WRONG CHARACTER THEN SET UP TO REDO LAST VALUE
      WRITE(3,22)
22    FORMAT(10X,05HERROR)
            N=N-1
            GOTO 101
   12    WRITE(3,-) CHAR(N),N
C DELAY LOOP
         DO 15 J=1,ND
   15       CONTINUE
         CALL PUTC(CHAR(N),10)
   10    CONTINUE
C
C CONVERT ASCII CODED HEX TO 12 BIT WORDS    '017 = 0FH
      DO 5 I=1,4801
     -     WORD(I)=((CHAR(3*I-2).AND.'017)*256).OR.(((CHAR(3*I-1).AND.'017)
     *        *16).OR.(CHAR(3*I).AND.'017)
      WRITE(8,9) WORD(I)
9     FORMAT(I5)
    5    CONTINUE
C
C WRITE OUT NEW WORDS
      DO 20 J=0,199
         WRITE(6,25) (WORD(J*24+I),I=1,24)
   25    FORMAT( 24I5)
   20    CONTINUE
C
      WRITE(6,25) WORD(4801)
      WRITE(6,2)

      WRITE(6,4)ND
C
      STOP
      END
```

```
C PRINT OUT ATL LINEAR SENSOR DATA AND CALCULATIONS
C
      INTEGER WORD(4801), DWORD(4801)
      CHARACTER *8 MODAYR
C
C WHAT IS THE TRANSDUCER NUMBER AND DATE
      WRITE(3,45)
   45 FORMAT( 10X,'WHAT IS THE TRANSDUCER NUMBER? (TWO DIGITS)')
      READ(3,46) NUM
   46 FORMAT(I2)
      WRITE(3,47)
   47 FORMAT( 10X,'WHAT IS THE DATE? MM/DD/YY')
      READ(3,48) MODAYR
   48 FORMAT(A8)
C
C PRINT DESCRIPTION AND LABEL
      WRITE(6,50) NUM,MODAYR
   50 FORMAT( 40X,'ATL DIGITAL/OPTICAL LINEAR POSITION TRANSDUCER',//,
     140X,'STATIC ACCURACY DATA AND ANALYSIS',//,40X,'TRANSDUCER: ',I3,
     24X,A8)
      WRITE(6,55)
   55 FORMAT(///,10X,'POINT   INCHES   EIU SCALE   STEPPER SCALE   ERROR
     * IN BITS   ERROR IN INCHES',/,120('='),/)
C
C READ IN WORDS (EIU POSITIONS) OF UPSCAN
      DO 7 I=1,4801
12       READ (8,9) WORD(I)
F     9  FORMAT(I5)
      7  CONTINUE
C
C PRINT DATA OF UPSCAN
      DO 65 NPOINT=1,13
         NSTEP=(NPOINT-1)*400
         AINCH=(NPOINT-1)*0.5
         NRGDIF=-((341*NSTEP/400)+2-WORD(NSTEP+1))
         ERRIN=NRGDIF*1.46627E-3
         WRITE(6,60) NPOINT,AINCH,WORD(NSTEP+1),NSTEP,NRGDIF,ERRIN
   60    FORMAT( 10X,I3,4X,F6.2,5X,I5,9X,I5,12X,I5,9X,F10.6)
   65    CONTINUE
C
C READ IN WORDS OF DOWN SCAN
      DO 70 I=1,4801
         READ (7,75) DWORD(I)
   75    FORMAT(I5)
   70    CONTINUE
C
C PRINT DATA OF DOWN SCAN
      WRITE(6,80)
   80 FORMAT( //)
      DO 85 NPOINT=13,1,-1
         NSTEP=(NPOINT-1)*400
         AINCH=(NPOINT-1)*0.5
         NRGDIF=-((341*NSTEP/400)+2-DWORD(NSTEP+1))
         ERRIN=NRGDIF*1.46627E-3
         WRITE(6,60) NPOINT,AINCH,DWORD(NSTEP+1),NSTEP,NRGDIF,ERRIN
```

```
   85    CONTINUE
C
C RESOLUTION AND MONOTONICITY TESTS
      WRITE(6,90)
   90 FORMAT( ////////////////,40X,'RESOLUTION AND MONOTONICITY TESTS',//
     1,40X,'UP SCAN',//,30X,'POSITION (INCHES)     ERROR (BITS)',//,
     2120('-'),/)
C
C UPSCAN
      DO 95 I=1,4800
         IF((WORD(I).LE.WORD(I+1)).AND.(WORD(I)+2.GE.WORD(I+1)))
     *      GOTO 95
         POS=(I+1)*1.25E-3
         NER=WORD(I+1)-WORD(I)
         WRITE(6,100) POS,NER
  100    FORMAT( 33X,F10.6,13X,I3)
   95    CONTINUE
C
C DOWN SCAN
      WRITE(6,105)
  105 FORMAT( /,40X,'DOWN SCAN',/)
      DO 110 I=4800,1,-1
         IF((DWORD(I+1).GE.DWORD(I)).AND.(DWORD(I+1)-2.LE.DWORD(I)))
     *      GO TO 110
         POS=I*1.25E-3
         NER=DWORD(I+1)-DWORD(I)
         WRITE(6,100) POS,NER
  110    CONTINUE
C
      STOP
      END
```

12
B

```
C OUTPUT TRANSDUCER DATA TO BE PLOTTED TO MAGNETIC TAPE
C THIS PROGRAM IS FOR 961 POINTS
      REAL  ARRAY(50)
C
      OPEN 4
C
C ASSIGN A POINT TO THE ARRAY
      DO 15 K=1,961
        ARRAY(1)=FLOAT((K-1)*005)
        READ(8,5) NUP
        READ(7,5) NDOWN
5     FORMAT(I5)
        ARRAY(2)=FLOAT(NUP)-2.0
        ARRAY(3)=FLOAT(NDOWN)-2.0
        ARRAY(4)=ARRAY(2)-(341.0/400.0)*ARRAY(1)
        ARRAY(5)=ARRAY(3)-(341.0/400.0)*ARRAY(1)
        WRITE(3,-)K
          DO 10 J=1,4
            READ(8,5)NULL
            READ(7,5)NULL
10        CONTINUE
C USE BUFFER OUT TO WRITE TO TAPE
C
C INSERT SCALING VALUES ON FIRST POINT OF EACH ARRAY
        BUFFER OUT(4,ARRAY,B,100,1)
        CALL STATUS(4)
15    CONTINUE
      ENDFILE 4
      CLOSE 4
      STOP
      END
```

```
      DIMENSION X(1000),Y(1000),RPLOT(50)
      DIMENSION ISTRX(30),ISTRY(30)
C
      DATA IDIM /1000/
      DATA IPLOT /5/
      DATA IPHASE /1/
      DATA ITERM /1/
      DATA ITOUT /2/
      DATA IPLNUM /1/
      DATA IMAXN /50/
C
      OPEN IPLOT
C
C GET INDICIES FOR PLOT
C
      CALL MODE(0,1100,0,0)
500   CONTINUE
      REWIND IPLOT
      IND=0
      IPHASE = 1
      WRITE(ITOUT,530)IPLNUM
530   FORMAT("   ENTER INDICIES FOR PLOT #",I2)
      READ(ITERM,-)IND1,IND2
      IF(IND1.LE.0.OR.IND2.LE.0)GO TO 1000
      IF(IND1.GT.IMAXN)GO TO 1000
      IF(IND2.GT.IMAXN)GO TO 1000
C
C GET SCALE FACTORS
C
      WRITE(ITOUT,540)
540   FORMAT(" ENTER X,Y CONVERSION FACTORS---")
      READ(ITERM,-)XCONV,YCONV
      IF(XCONV.EQ.0.0)XCONV=1.0
      IF(YCONV.EQ.0.0)YCONV=1.0
C
C
1     CONTINUE
      BUFFER IN(IPLOT,RPLOT,0,100,ISTAT,NDUM)
      CALL STATUS(IPLOT)
      IF(ISTAT.NE.2)GO TO 900
      IF(IND.GE.IDIM)GO TO 900
      IND=IND+1
10    CONTINUE
      X(IND)=RPLOT(IND1)*XCONV
      Y(IND)=RPLOT(IND2)*YCONV
      GO TO 1
C
900   CONTINUE
      IF(IPHASE.EQ.1)CALL SCAN(X,Y,IND,440)
      IF(IPHASE.EQ.2)CALL DRAW(X,Y,IND,441)

      IND=1
      IF(ISTAT.EQ.2)GO TO 10
      IF(IPHASE.EQ.2)GO TO 999
      IPHASE=2
      CALL SCAN(X,Y,0,440)
      REWIND IPLOT
      IND=0
      GO TO 1
999   CONTINUE
C
C DRAW AXES
C
```

```
C
      WRITE(ITOUT,500)
      CALL GETSTR(ISTRX,LENX,ITERM)
      CALL GETSTR(ISTRY,LENY,ITERM)
      XV=FLOAT(LENX)+.2
      YV=FLOAT(LENY)+.2
      CALL AXES(XV,ISTRX,YV,ISTRY)
500   FORMAT("      ENTER X AXIS LABEL, 12 CHARACTERS THEN Y")
      WRITE(ITOUT,550)
550   FORMAT("   ENTER GRAPH TITLE---")
      CALL GETSTR(ISTRX,LENX,ITERM)
      IF(LENX.LE.0)GO TO 9876
      STRT=3.5 - (FLOAT(LENX)/5.0)
      CALL MODE(4,.166..25,9999.)
      CALL MODE(6,3..9999.,9999.)
      CALL NOTE(STRT,8.5,ISTRX,LENX)
C
C
C DRAW GRID
C
9876  CONTINUE
      CALL MODE(6,1.,9999.,9999.)
      CALL MODE(10,FLOAT('31313131),9999.,9999.)
      CALL FORM(20,.25,36,.25)
      CALL MODE(10,-1.0,9999.,9999.)
      CALL DRAW(0.,0.,1,9000)
      IPLNUM = IPLNUM + 1
      GO TO 800
C
1000  CONTINUE
C
C ALL DONE
C
      CALL DRAW(0,0.0,9999)
      STOP
      END
      SUBROUTINE GETSTR(ISTR,LEN,IINPT)
      DIMENSION ISTR(30)

      BUFFER IN(IINPT,ISTR,S,30,ISTAT,NWDS)
      CALL STATUS(IINPT)
C
C LIMIT STRING LENGTH TO 60 CHARS

      IF(NWDS.GT.20)NWDS=20
1       CONTINUE
        IF(ISTR(NWDS).NE.0.AND.ISTR(NWDS).NE.'10020040)GO TO 2
        NWDS=NWDS-1
        IF(NWDS.GT.1)GO TO 1
2       CONTINUE
        LEN=NWDS*3
      IDUM=ISTR(NWDS).AND.'377
      IF(IDUM.GT.'40)RETURN
      LEN=LEN-1
      IDUM=ISTR(NWDS).AND.'177400
      IF(IDUM.GT.'20000)RETURN
      LEN=LEN-1
      RETURN
      END
```

```
C
C  FORTRAN PROGRAM 3-D RAY TRACE(TR3D.XXM) FOR MIX RODS
C  BRUCE E. JOHNSON  2-3751  MS AH-35  773-8077
C
C  THIS PROGRAM TRACES RAYS THROUGH A THREE DIMENSIONAL WAVEGUIDE
C  STRUCTURE, COMPUTES LOSS AND DISTRIBUTION AT THE OUTPUT PLANE
C  DIRECTION OF PROPOGATION IS IN THE POSITIVE Y DIRECTION
C
C*****************************************************************
C            DEFINE WAVEGUIDE SURFACES
C*****************************************************************
      COMMON/SUB3/RAYAMP(2000),ALPHA(2000),BETA(2000),GAMMA(2000)
      COMMON/COUNT/RIN(10,10),ROUT(60,60),NS
      COMMON/COUN1/ZMX,XMX,ZMN,XMN
      COMMON/SUB1/A(6),B(6),C(6),D(6),X(8),Y(8),Z(8),G1(6),G2(6),G3(6)
      COMMON/RAY/A1,B1,C1,XO,YO,ZO
      DIMENSION POSA(30),POSB(30),SUM(30),ZRP(20),XRP(20)
      COMMON/ENCODE/E1X(5),E1Z(5),E2X(5),E2Z(5),E3X(5),E3Z(5),E4X(5),
     1E4Z(5)
      REAL N1,N2,HTA,M1,M2,LOSS,NAFIB,NACORE
C
C
C          Z                        GENERAL FORM OF SURFACES:
C                                   A*X+B*Y+C*Z+D=0
C          *   COORDINATE AXES
C          *
C          *                        SURFACES:
C          *                            S1=FRONT     A1*X+B1*Y+D1=0
C          ********** Y                 S2=BACK      A2*X+B2*Y+D2=0
C         *                            S3=TOP       Z=CONSTANT
C        *                             S4=BOTTOM    Z=0
C       *                              S5=OUTPUT    Y=CONSTANT
C      *                               S6=INPUT     Y=0
C
C     X                          Y IS DIRECTION OF PROPOGATION
C
C INPUT WAVEGUIDE PARAMETERS FROM SCREEN
C
      WRITE(1,5)
      WRITE(6,5)
5     FORMAT(20X,21H3-D RAY TRACE VER 2.0,//,5X,21HWAVEGUIDE PARAMETERS:
     1/,5X,37HDATA FORMATS: F10.5(REAL) I4(INTEGER),//)
10    FORMAT(F10.5)
      WRITE(1,15)
      WRITE(6,15)
15    FORMAT(10X,25HWAVEGUIDE LENGTH(INCHES)?)
      READ(1,10)YMAX
      WRITE(1,10)YMAX
      WRITE(6,10)YMAX
      WRITE(1,20)
      WRITE(6,20)
20    FORMAT(10X,25HWAVEGUIDE HEIGHT(INCHES)?)
      READ(1,10)ZMAX
      WRITE(1,10)ZMAX
      WRITE(6,10)ZMAX
      WRITE(1,25)
      WRITE(6,25)
25    FORMAT(10X,24HWAVEGUIDE WIDTH(INCHES)?)
      READ(1,10)WX
      WRITE(1,10)WX
      WRITE(6,10)WX
      WRITE(1,30)
      WRITE(6,30)
30    FORMAT(10X,26HHORN TAPER ANGLE(RADIANS)?)
      READ(1,10)HTA
```

```
      WRITE(1,10)HTA
      WRITE(6,10)HTA
      WRITE(1,35)
      WRITE(6,35)
35    FORMAT(10X,27HBEVEL TAPER ANGLE(RADIANS)?)
      READ(1,10)BTA
      WRITE(1,10)BTA
      WRITE(6,10)BTA
      WRITE(1,40)
      WRITE(6,40)
40    FORMAT(15X,25HCORE INDEX OF REFRACTION?)
      READ(1,10)N1
      WRITE(1,10)N1
      WRITE(6,10)N1
      WRITE(1,45)
      WRITE(6,45)
45    FORMAT(15X,15HCLADDING INDEX?)
      READ(1,10)N2
      WRITE(1,10)N2
      WRITE(6,10)N2
C
C CALCULATE SURFACES S1-S6
C
      WRITE(1,44)
      WRITE(6,44)
44    FORMAT(07X,15HSURFACE NORMALS,/)
      CALL SURFAC(YMAX,ZMAX,WX,HTA,BTA)
      DO 49 JJ=1,6
      WRITE(1,48)G1(JJ),G2(JJ),G3(JJ),A(JJ),B(JJ),C(JJ),D(JJ)
      WRITE(6,48)G1(JJ),G2(JJ),G3(JJ),A(JJ),B(JJ),C(JJ),D(JJ)
48    FORMAT(7F10.5)
49    CONTINUE
C CALCULATE MAX,MIN VALUES FOR PLOTTING
C
      XMX=-999.
      XMN=999.
      ZMN=999.
      ZMX=-999.
      DO 51 J=5,8
      IF(X(J).GT.XMX)XMX=X(J)
      IF(X(J).LT.XMN)XMN=X(J)
      IF(Z(J).GT.ZMX)ZMX=Z(J)
      IF(Z(J).LT.ZMN)ZMN=Z(J)
51    CONTINUE
C CALCULATE NA OF WAVEGUIDE
C
      WGNA=N1**2-N2**2
      WGNA=SQRT(WGNA)
      WRITE(1,46)WGNA
46    FORMAT(/,15X,26HTHE NA OF THE WAVEGUIDE = ,F8.4,/)
C
C INTIALIZE RAY PARAMETERS
C
      WRITE(1,50)
      WRITE(6,50)
50    FORMAT(20X,17HFIBER NA(IN AIR)?)
      READ(1,10)NAFIB
      WRITE(1,10)NAFIB
      WRITE(6,10)NAFIB
      NAFIB=NAFIB/N1
      WRITE(1,55)
      WRITE(6,55)
55    FORMAT(20X,26HTHE NUMBER OF RAYS/SOURCE?)
      READ(1,60)NRAYS
60    FORMAT(I4)
      WRITE(1,60)NRAYS
```

```
      WRITE(6,60)NRAYS
      CALL RAYSET(NRAYS,NAFIB,NR)
      XP=0.0
      YP=0.0
      ZP=ZMAX/2.0
      WRITE(1,66)
      WRITE(6,66)
C FORM FIBER INPUT ARRAY
      DEX=.02244
      DEZ=.02244
      XRP(1)=XP-DEX
      XRP(2)=XP
      XRP(3)=XP+DEX
      XRP(4)=XP-DEX
      XRP(5)=XP
      XRP(6)=XP+DEX
      XRP(7)=XP-DEX
      XRP(8)=XP
      XRP(9)=XP+DEX
      ZRP(1)=ZP+DEZ
      ZRP(2)=ZP+DEZ
      ZRP(3)=ZP+DEZ
      ZRP(4)=ZP
      ZRP(5)=ZP
      ZRP(6)=ZP
      ZRP(7)=ZP-DEZ
      ZRP(8)=ZP-DEZ
      ZRP(9)=ZP-DEZ
66    FORMAT(20X,30HGRID SIZE(NXN SAMPLING ARRAY)?)
      READ(1,60)NS
      WRITE(1,60)NS
      WRITE(6,60)NS
C ********************* MAIN PROGRAM ********** **********************
      NPOS=09
      DO 200 K=1,NPOS
C     POS=FLOAT(K-1)*.6
C     CALL TRANS(POS)
      XP=XRP(K)
      ZP=ZRP(K)
      DO 65 I=1,NR
      WRITE(1,70)I
      RA=RAYAMP(I)
C PROPOGATE RAY DOWN SOURCE MIX ROD
      CALL INTSCT(XP,YP,ZP,ALPHA(I),BETA(I),GAMMA(I),LOSS,N1,N2,RA,IFLG)
      IF(IFLG.EQ.0)GO TO 65
C GLASS-AIR INTERFACE
      CALL REFRAC(N1,1.0)
C 5 MIL AIR SPACE
      CALL PROP(.005)
C SEE IF RAY HITS FIRST TRACK
      CALL COUNT(RA,XO,ZO)
C     ITRACK=0
C     WRITE(1,203)XO,YO,ZO
C     WRITE(6,203)XO,YO,ZO
203   FORMAT(5X,15HPOSITIONS X Y Z,3F10.5)
C     CALL ENCDR(XO,YO,ZO,E1X,E1Z,IFLAG1)
C     IF(IFLAG1.EQ.1)ITRACK=1
C SEE IF RAY HITS SECOND TRACK
C     CALL ENCDR(XO,YO,ZO,E2X,E2Z,IFLAG1)
C     IF(IFLAG1.EQ.1)ITRACK=2
C     IF(ITRACK.EQ.0)LOSS1=LOSS1+RA
C     IF(ITRACK.EQ.0)GO TO 65
C PROPOGATE RAY THROUGH ENCODING PLATE
C  AIR-GLASS INTERFACE
C     CALL REFRAC(1.0,N1)
C     CALL PROP(.060)
C GLASS-AIR INTERFACE
C     CALL REFRAC(N1,1.0)
C 5 MIL AIR SPACE
```

```
C     CALL PROP(.005)
C SEE IF RAYS ACCEPTED BY SMALL MIX RODS
C     IF(ITRACK.EQ.1)CALL ENCDR(XO,YO,ZO,E3X,E3Z,IFLAG1)
C     IF(ITRACK.EQ.2)CALL ENCDR(XO,YO,ZO,E4X,E4Z,IFLAG1)
C     IF(IFLAG1.EQ.0)LOSS2=LOSS2+RA
C     IF(IFLAG1.EQ.0)GO TO 65
C     IF(ITRACK.EQ.1)POSA(K)=POSA(K)+RA
C     IF(ITRACK.EQ.2)POSB(K)=POSB(K)+RA
C     SUM(K)=SUM(K)+RA
65    CONTINUE
C     WRITE(1,205)POSA(K),POSB(K),SUM(K),POS
C     WRITE(6,205)POSA(K),POSB(K),SUM(K),POS
205   FORMAT(10X,3F12.5,10X,F10.5)
200   CONTINUE
C ********** END OF MAIN **********
      WRITE(6,75)LOSS
      WRITE(1,75)LOSS
75    FORMAT(10X,05HLOSS=,F10.5)
70    FORMAT(5X,06HRAY #=,I4)
      DO 90 J=1,6
      WRITE(6,80)A(J),B(J),C(J),D(J)
80    FORMAT(4F10.5)
90    CONTINUE
C WRITE PLOT PARAMETERS TO DISC
C
      WRITE(8,119)NS,NS
119   FORMAT(2I4)
      DO 100 J=1,NS
      DO 110 K=1,NS
      WRITE(8,10)ROUT(J,K)
      WRITE(1,120)J,K,ROUT(J,K)
120   FORMAT(2I10,F10.5)
110   CONTINUE
100   CONTINUE
      TOP
      END
C
C**********************************************************************
C  SUBROUTINE SURFACE- CALCULATES SURFACE PARAMETERS:
C                          UNIT NORMAL VECTORS
C                          SURFACE EQUATION COEFFICENTS
C    SURFACE EQUATION OF THE FORM A*X+B*Y+C*Z+D=0
C    USE THREE POINTS ON THE SURFACE TO CALCULATE COEFFICENTS
C
      SUBROUTINE SURFAC(YMAX,ZMAX,WX,HTA,BTA)
      COMMON/SUB1/A(6),B(6),C(6),D(6),X(8),Y(8),Z(8),G1(6),G2(6),G3(6)
      REAL M1,M2
C
C DEFINE VERTICES OF SURFACE INTERSECTIONS
C
      X(1)=WX/2.0
      Y(1)=0.
      Z(1)=0.
      X(4)=-X(1)
      Y(4)=Y(1)
      Z(4)=Z(1)
      M1=-TAN(BTA)
      X(2)=M1*ZMAX+WX/2.0
      Y(2)=Y(1)
      Z(2)=ZMAX
      X(3)=-X(2)
      Y(3)=Y(1)
      Z(3)=ZMAX
      M2=TAN(HTA)
      X(8)=WX/2.0+(YMAX*M2)
      Y(8)=YMAX
      Z(8)=Z(1)
```

```
      X(5)=-X(8)
      Y(5)=YMAX
      Z(5)=Z(1)
      X(7)=-(X(1)-X(2))+X(8)
      Y(7)=YMAX
      Z(7)=ZMAX
      X(6)=-X(7)
      Y(6)=YMAX
      Z(6)=ZMAX
      WRITE(1,7)
      WRITE(6,7)
7     FORMAT(7X,14HVERTICES X Y Z,/)
      DO 20 J=1,8
      WRITE(6,10)X(J),Y(J),Z(J)
      WRITE(1,10)X(J),Y(J),Z(J)
10    FORMAT(10X,3F10.5)
20    CONTINUE
C
C CALL SNORM TO CALCULATE COEFFICENTS
      CALL SNORM(1,1,2,7)
      CALL SNORM(2,5,6,3)
      CALL SNORM(3,2,3,6)
      CALL SNORM(4,4,1,5)
      CALL SNORM(5,8,7,5)
      CALL SNORM(6,1,2,3)
      RETURN
      END
C*************************************************************
C*************************************************************
C   SUBROUTINE SNORM- CALCULATES NORMALS AND SURFACE COEFF
C
      SUBROUTINE SNORM(N,J,K,L)
      COMMON/SUB1/A(6),B(6),C(6),D(6),X(8),Y(8),Z(8),G1(6),G2(6),G3(6)
C
C COMPUTE COEFFICENTS FOR PLANES
      A(N)=((Y(K)-Y(J))*(Z(L)-Z(J)))-((Y(L)-Y(J))*(Z(K)-Z(J)))
      B(N)=((Z(K)-Z(J))*(X(L)-X(J)))-((X(K)-X(J))*(Z(L)-Z(J)))
      C(N)=((X(K)-X(J))*(Y(L)-Y(J)))-((X(L)-X(J))*(Y(K)-Y(J)))
      D(N)=-(X(J)*A(N)+Y(J)*B(N)+Z(J)*C(N))
C
C NORMALIZE SURFACE VECTORS
      XX=A(N)**2+B(N)**2+C(N)**2
      FCTR=SQRT(XX)
      G1(N)=A(N)/FCTR
      G2(N)=B(N)/FCTR
      G3(N)=C(N)/FCTR
      RETURN
      END
C*************************************
C  SUBROUTINE RAYSET- INTIALIZES DIRECTION COSINES FOR RAY TRACE
C
      SUBROUTINE RAYSET(NRAYS,NACORE,NR)
      COMMON/SUB3/RAYAMP(2000),ALPHA(2000),BETA(2000),GAMMA(2000)
      REAL NACORE
C
C USE RECTANGULAR GRID OF RAYS INSIDE OF A CIRCLE
C DEFINE DIRECTION COSINES RELATIVE TO PLANE Y-1
C
C FORM RAY BOUNDARIES
      THETA=ASIN(NACORE)
      XMAX=TAN(THETA)
      ZMAX=XMAX
      XMIN=-XMAX
      ZMIN=XMIN
C
C CALCULATE RAY SPACING
      YY=1.0/.7854*FLOAT(NRAYS)
      NN=IFIX(YY)
      NRGRID=NN
```

```
5     FORMAT(5X,25HTHE NUMBER OF GRID LINES=,I4)
      YZ=FLOAT(NRGRID)
      GRID=SQRT(YZ)
      NGRID=IFIX(GRID)
      WRITE(1,5)NGRID
      DX=2.0*XMAX/(NGRID-1)
      DZ=DX
C
C FORM DIRECTION COSINE AND RAY AMPLITUDE ARRAYS
      M=0
      POWER1=0.0
      DO 10 J=1,NGRID
      DO 20 K=1,NGRID
      X=XMIN+FLOAT(J-1)*DX

      Z=ZMIN+FLOAT(K-1)*DZ
      RR=X**2+Z**2
      R=SQRT(RR)
      IF(R.GT.XMAX)GO TO 20
      M=M+1
C CALCULATE DIRECTION COS RELATIVE TO ORGIN
      ALPHA(M)=X
      BETA(M)=1.0
      GAMMA(M)=Z
C
C NORMALIZE DIRECTION COS
      XX=ALPHA(M)**2+BETA(M)**2+GAMMA(M)**2
      FAC=1.0
      ALPHA(M)=ALPHA(M)/FAC
      BETA(M)=BETA(M)/FAC
      GAMMA(M)=GAMMA(M)/FAC
C
C CALCULATE RAY AMPLITUDE
C LET RAY AMPLITUDE=.1 AT NA
      SFCOS=ACOS(.1)/NACORE
      TH3=ATAN(R)
      YYY=TH3*SFCOS
      RAYAMP(M)=COS(YYY)
      POWER1=POWER1+RAYAMP(M)
20    CONTINUE
10    CONTINUE
      PP=ATAN(DX)
      PP=PP*57.295779
      WRITE(1,30)M,PP,POWER1
      WRITE(6,30)M,PP,POWER1
30    FORMAT(20X,15HNUMBER OF RAYS=,I5,/,20X,16HTHE RAY SPACING=,F10.6,
     107HDEGREES,20X,/,12HTOTAL POWER=,F14.4,/)
      NR=M
      DO 35 J=1,NR
      WRITE(6,40)J,ALPHA(J),BETA(J),GAMMA(J)
      WRITE(1,40)J,ALPHA(J),BETA(J),GAMMA(J)
40    FORMAT(I6,3F10.5)
35    CONTINUE
      RETURN
      END
C*************************************************************************
C*************************************************************************
C
C SUBROUTINE INTERSECT- CALCULATES INTERSECTION POINTS,PERFORMS
C PROPOGATION AND COMPUTES LOSS
C
      SUBROUTINE INTSCT(X0,Y0,Z0,A0,B0,C0,LOSS,N1,N2,RAYAMP,IFLG)
      COMMON/SUB1/A(6),B(6),C(6),D(6),X(8),Y(8),Z(8),G1(6),G2(6),G3(6)
      COMMON/PAY/A1,B1,C1,X0,Y0,Z0
      REAL LOSS,N1,N2
```

```
C SEE IF RAY STRIKES BOUNDARY ON THE SIX SURFACES
C
      IFLG=1
      A1=A0
      B1=B0
      C1=C0
      X0=X0
      Y0=Y0
      Z0=Z0
C SET SURFACE COMPARE PARAMETER NNN
      NNN=0
5     DMIN=999.0
      DO 10 I=1,5
      ZZ1=-(A(I)*X0+B(I)*Y0+C(I)*Z0+D(I))
      ZZ2=A(I)*A1+B(I)*B1+C(I)*C1
      IF(ZZ2.EQ.0.0)GO TO 10
C     IF(ZZ1.EQ.0.0)GO TO 10
C  T IS PARAMETRIC COEFFICENT FOR LINE EQUATION
      T=ZZ1/ZZ2
      IF(T.EQ.0.0)GO TO 10
      XI=X0+A1*T
      YI=Y0+B1*T
      ZI=Z0+C1*T
C THE VALUE OF Y MUST INCREASE EACH REFLECTION
      IF(YI.LE.Y0)GO TO 10
      W1=XI-X0
      W2=YI-Y0
      W3=ZI-Z0
      YY=W1**2+W2**2+W3**2
      DP=SQRT(YY)
      R=DP-DMIN
C CHECK TO SEE IF SAME SURFACE HIT LAST TIME
      IF((R.LT.0.0).AND.(I.EQ.NNN))GO TO 10
      IF(R.LT.0.0)DMIN=DP
      IF(R.LT.0.0)NN=I
      IF(R.LT.0.0)X1=XI
      IF(R.LT.0.0)Y1=YI
      IF(R.LT.0.0)Z1=ZI
10    CONTINUE
C     WRITE(1,15)NN,X1,Y1,Z1
15    FORMAT(10X,08HSURFACE=,I4,3F10.5)
C     IF(NN.EQ.5)CALL COUNT(RAYAMP,X1,Z1)
      IF(NN.EQ.5)Y0=Y1
      IF(NN.EQ.5)Z0=Z1
      IF(NN.EQ.5)X0=X1
      IF(NN.EQ.5)RETURN
C
C SEE IF RAY REFLECTED OR LOST
C NORMALIZE RAY VECTOR
      SS=A1**2+B1**2+C1**2
      FAC=SQRT(SS)
      AA=A1/FAC
      BB=B1/FAC
      CC=C1/FAC
      AA0=(AA*G1(NN)+BB*G2(NN)+CC*G3(NN))
      TAU=(AA0*N1)**2+N2**2-N1**2
      IF(TAU.GE.0.0)LOSS=LOSS+RAYAMP
      IF(TAU.GE.0.0)WRITE(1,20)
      IF(TAU.GE.0.0)WRITE(6,20)
20    FORMAT(10X,08HRAY LOST)
      IF(TAU.GE.0.0)IFLG=0
      IF(TAU.GE.0.0)RETURN
C IF RAY IS NOT LOST THEN REFLECT
C UNNORMALIZE VECTOR
      A1=A1
      B1=B1
```

```
      C1=C1
      AA1=(A1*G1(NN)+B1*G2(NN)+C1*G3(NN))
      A2=A1-2.0*AA1*G1(NN)
      B2=B1-2.0*AA1*G2(NN)
      C2=C1-2.0*AA1*G3(NN)
C
      XO=X1
      YO=Y1
      ZO=Z1
      A1=A2
      B1=B2
      C1=C2
      NNN=NN
      GO TO 5
      RETURN
      END
C*************************************************************
C*************************************************************
C
C SUBROUTINE COUNT COMPUTES RAY DENSITY AT OUTPUT OF WAVEGUIDE
C
      SUBROUTINE COUNT(RAYAMP,X1,Z1)
      COMMON/COUNT/RIN(10,10),ROUT(60,60),NS
      COMMON/COUN1/ZMX,XMX,ZMN,XMN
C
C COMPUTE DELTAX,DELTAZ
C INSERT BORDERS AROUND PLOT
      XMAX=.30
      XMIN=-.30
      ZMAX=.16
      ZMIN=-.1
      IF(XMAX.GT.ZMAX)ZMAX=XMAX
      IF(XMAX.GT.ZMAX)ZMIN=XMIN
      DELTAX=(XMAX-XMIN)/FLOAT(NS)
      DELTAZ=(ZMAX-ZMIN)/FLOAT(NS)
      DO 10 J=1,NS
      DO 20 K=1,NS
      ZM1=ZMAX-(FLOAT(J-1)*DELTAZ)
      ZM2=ZM1-DELTAZ
      XM1=XMAX-(FLOAT(K-1)*DELTAX)
      XM2=XM1-DELTAX
      IF((X1.LT.XM1).AND.(X1.GE.XM2).AND.(Z1.LT.ZM1).AND.(Z1.GE.ZM2))GO
     1TO 15
      GO TO 20
15    ROUT(J,K)=ROUT(J,K)+RAYAMP
      RETURN
20    CONTINUE
10    CONTINUE
      RETURN
      END
C*************************************************************
C*************************************************************
C
C SUBROUTINE REFRACT(ALPHA,BETA,GAMMA,N1,N2)
C   ALPHA,BETA,GAMMA   RAY DIRECTION COSINES
C   REFRACT RAY FROM N1 TO N2 INDEX OF REFRACTION
C
      SUBROUTINE REFRAC(N1,N2)
      COMMON/RAY/ALPHA,BETA,GAMMA
      REAL N1,N2
C NORMALIZE RAY VECTORS
      SS=ALPHA**2+BETA**2+GAMMA**2
      FAC=SQRT(SS)
      AA=ALPHA/FAC
      BB=BETA/FAC
      CC=GAMMA/FAC
C CALCULATE REFRACTION PARAMETER TAU
C   SURFACE NORMALS G1,G2,G3
      G1=0.0
      G2=-1.0
      G3=0.0
```

```
      AA0=(AA*G1+BB*G2+CC*G3)
      T1=(AA0*N1)**2+N2**2-N1**2
      IF(T1.LT.0.0)WRITE(1,20)
      IF(T1.LT.0.0)RETURN
20    FORMAT(10X,27HRAY IS INTERNALLY REFLECTED)
      T1=SQRT(T1)
      TAU=(AA0*N1)+T1
      AAA=N1/N2*AA-TAU/N2*G1
      BBB=N1/N2*BB-TAU/N2*G2
      CCC=N1/N2*CC-TAU/N2*G3
C     WRITE(1,30)AA,BB,CC,AAA,BBB,CCC
C     WRITE(6,30)AA,BB,CC,AAA,BBB,CCC
30    FORMAT(5X,07HREFRACT,/,5X,3F10.5,/,5X,3F10.5)
C UNNORMALIZE RAY VECTORS
      ALPHA=AAA*FAC
      BETA=BBB*FAC
      GAMMA=CCC*FAC
      RETURN
      END
C*************************************************************************
C*************************************************************************
C
C SUBROUTINE PROP(D)- PROPGATES A RAY A DISTANCE D ALONG THE Y AXIS
C
      SUBROUTINE PROP(D)
      COMMON/RAY/A1,B1,C1,XO,YO,ZO
C CALCULATE INTERSECTION WITH A PLANE D UNITS FROM PRESENT POSITION
      YI=YO+D
C PARAMETRIC QUANITITY T
      T=(YI-YO)/B1
      ZI=ZO+C1*T
      XI=XO+A1*T
      XO=XI
      YO=YI
      ZO=ZI
      RETURN
      END
C*************************************************************************
C*************************************************************************
C
C SUBROUTINE ENCODER(XO,YO,ZO,E1X,E1Z,IFLAG1) - THIS ROUTINE CHECKS
C TO SEE IF A RAY IS PASSED OR BLOCKED BY AN APERATURE IN THE XZ PLANE
C         IF IFLAG1 = 1 THEN PASSED
      SUBROUTINE ENCDR(XO,YO,ZO,EXX,EXZ,IFLAG1)
      DIMENSION EXX(5),EXZ(5)
C USE SUM OF ANGLES TEST TO SEE IF POINT INSIDE OF 4 VERTICES
      CF=57.29577951
      TOT1=0.0
       DO 10 J=1,4
C  TAKE DOT PRODUCT OF VECTORS
      DX1=EXX(J)-XO
      DX2=EXX(J+1)-XO
      DZ1=EXZ(J)-ZO
      DZ2=EXZ(J+1)-ZO
      R1=DX1**2+DZ1**2
      R1=SQRT(R1)
      R2=DX2**2+DZ2**2
      R2=SQRT(R2)
      IF((R1.EQ.0).OR.(R2.EQ.0))IFLAG1=0
      IF((R1.EQ.0).OR.(R2.EQ.0))RETURN
C COMPUTE DOT PRODUCT
      DOTP=DX1*DX2+DZ1*DZ2
      C=DOTP/(R1*R2)
      IF((C.GT.1.0).OR.(C.LT.-1.0))IFLAG1=0
      IF((C.GT.1.0).OR.(C.LT.-1.0))RETURN
      A3=ACOS(C)*CF
C     WRITE(6,40)A3
      WRITE(1,40)A3
40    FORMAT(5X,06HANGLE=,F10.5)
      TOT1=TOT1+A3
10    CONTINUE
```

```
      WRITE(1,30)TOT1
C     WRITE(6,30)TOT1
      IF(TOT1.GT.358.0)GO TO 20
30    FORMAT(5X,14HSUM OF ANGLES=,F10.5)
C  RAY LOST
      IFLAG1=0
      RETURN
20    IFLAG1=1
C  RAY ACCEPTED BY APERATURE
      RETURN
      END
C*************************************************************************
C*************************************************************************
C
C SUBROUTINE TRANS(POSITION)- THIS SUBROUTINE MOVES THE ENCODING PLATE
C TO A POSITION FROM 0 INCHES TO 6 INCHES
C
      SUBROUTINE TRANS(POS)
      REAL L
      COMMON/ENCODE/E1X(5),E1Z(5),E2X(5),E2Z(5),E3X(5),E3Z(5),E4X(5),
     1E4Z(5)
C
C SET ENCODING PLATE AND SMALL MIX ROD PARAMETERS
      WMAX=.1008
      WMIN=.0001
      L=6.3
      XOFF=.09165
      RMAX=.17183821
      RMIN=.12816178
C X AXIS
      E1X(1)=-XOFF-WMAX/2.0
      E1X(2)=-XOFF+WMAX/2.0
      E1X(3)=-XOFF+WMIN/2.0
      E1X(4)=-XOFF-WMIN/2.0
      E1X(5)=E1X(1)
      E2X(1)=XOFF-WMIN/2.0
      E2X(2)=XOFF+WMIN/2.0
      E2X(3)=XOFF+WMAX/2.0
      E2X(4)=XOFF-WMAX/2.0
      E2X(5)=E2X(1)
      E3X(1)=-XOFF-RMIN/2.0
      E3X(2)=-XOFF+RMIN/2.0
      E3X(3)=-XOFF+RMAX/2.0
      E3X(4)=-XOFF-RMAX/2.0
      E3X(5)=E3X(1)
      E4X(1)=XOFF-RMIN/2.0
      E4X(2)=XOFF+RMIN/2.0
      E4X(3)=XOFF+RMAX/2.0
      E4X(4)=XOFF-RMAX/2.0
      E4X(5)= E4X(1)
C Z AXIS
      E1Z(1)=POS+.03+.120
      E1Z(2)=E1Z(1)
      E1Z(3)=E1Z(1)-L
      E1Z(4)=E1Z(3)
      E1Z(5)=E1Z(1)
      E2Z(1)=E1Z(1)
      E2Z(2)=E1Z(2)
      E2Z(3)=E1Z(3)
      E2Z(4)=E1Z(4)
      E2Z(5)=E2Z(1)
      E3Z(1)=.06
      E3Z(2)=E3Z(1)
      E3Z(3)=0.0
      E3Z(4)=E3Z(3)
      E3Z(5)=E3Z(1)
      E4Z(1)=E3Z(1)
      E4Z(2)=E3Z(2)
      E4Z(3)=E3Z(3)
      E4Z(4)=E3Z(4)
      E4Z(5)=E4Z(1)
      RETURN
      END
```

APPENDIX E
SAMPLE VIBRATION AND SHOCK CURVES

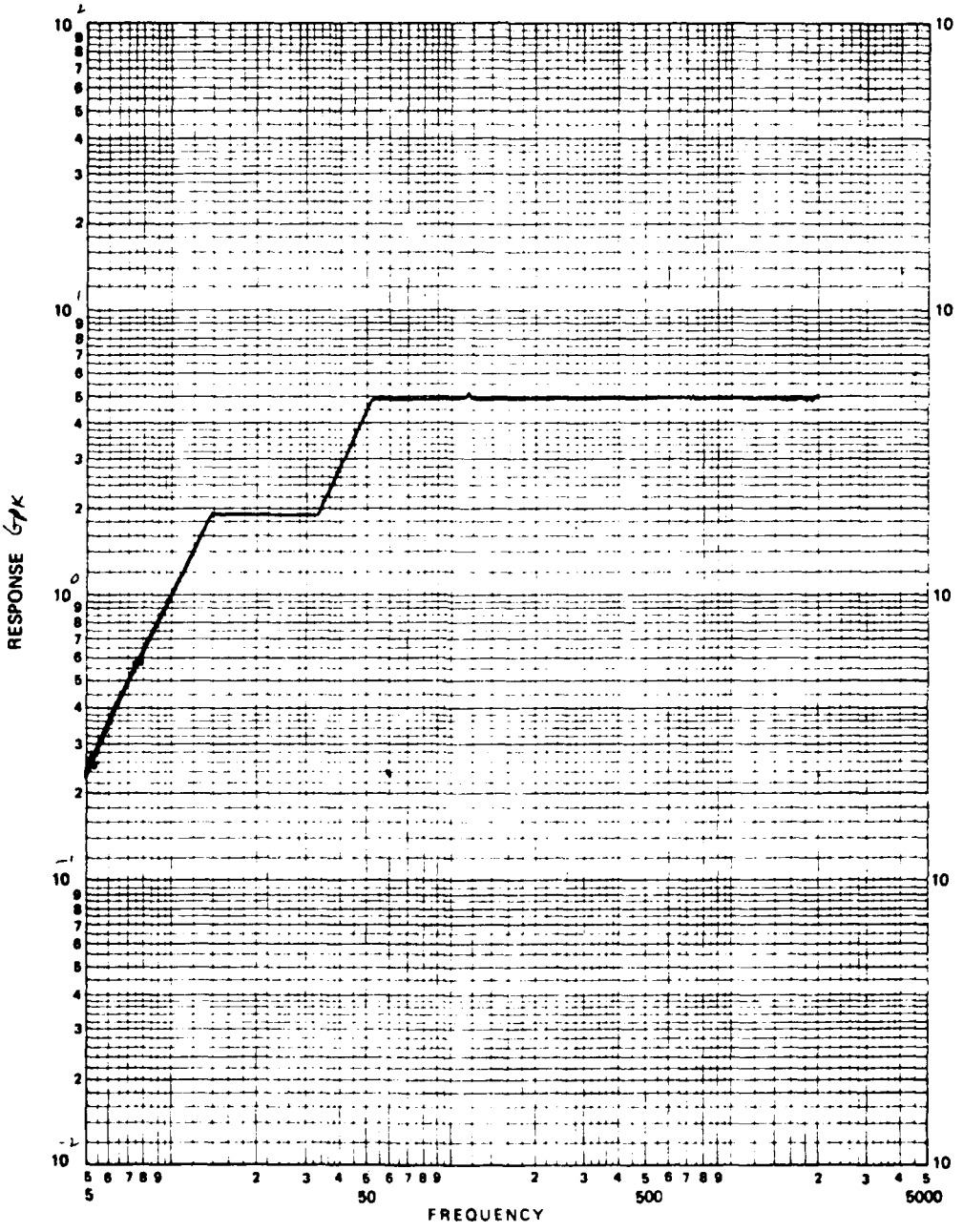

Figure E-1. Y-Axis MIL-STD-810C vibration curve.

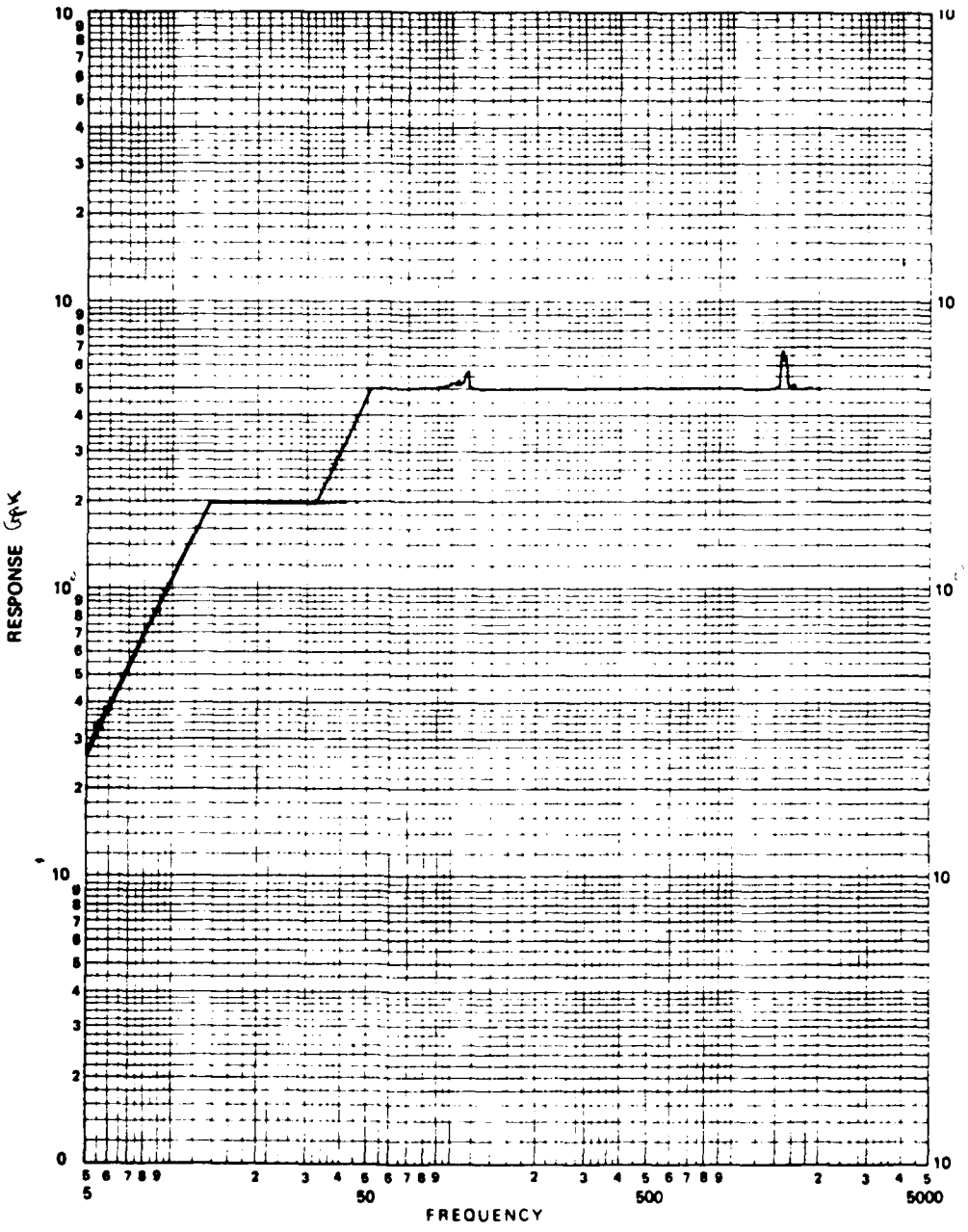

Figure E-2. Z-Axis MIL-STD-810C vibration curve.

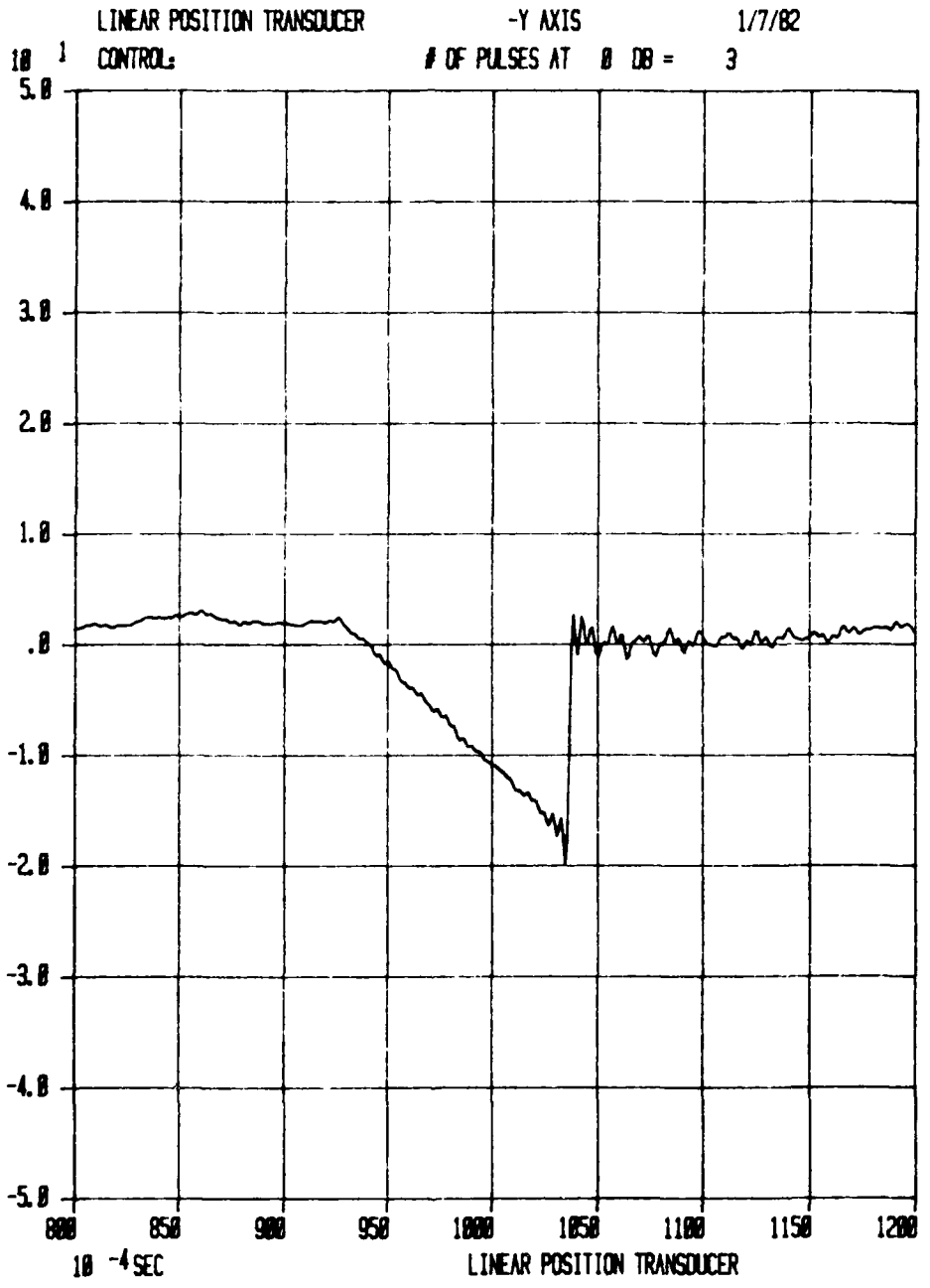

Figure E-3. Y-Axis MIL-STD-810C negative shock pulse.

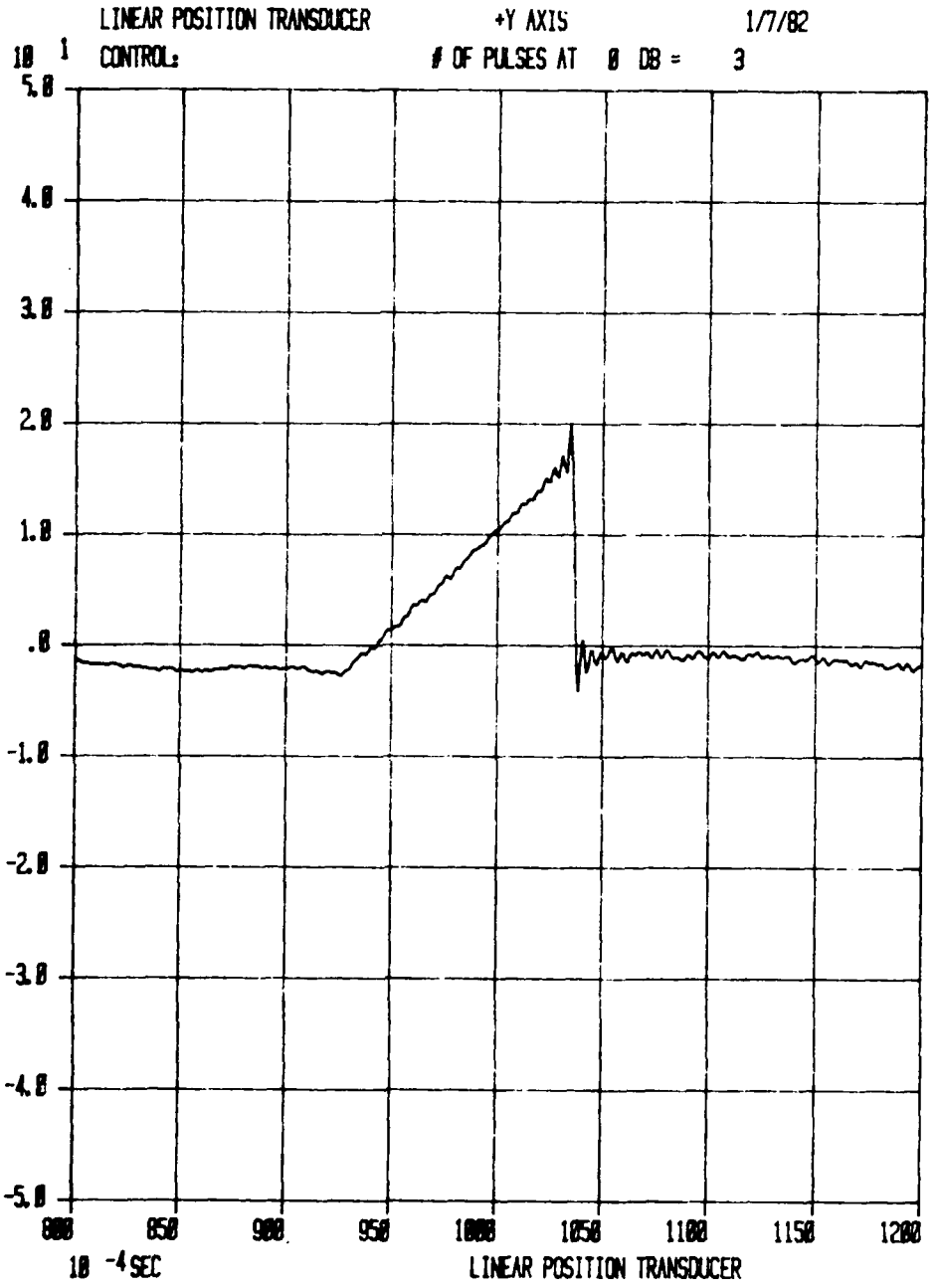

Figure E-4. Y-Axis MIL-STD-810C positive shock pulse.

APPENDIX F

MECHANICAL DESIGN DETAILS

The contractual work statement stipulated a number of design requirements and specified several goals which strongly influenced the mechanical design of the transducer:

1. The stroke shall be 6.00 ± 0.010 inches with 0.10 inch overtravel on each end.

2. Size shall be minimized and possibility of incorporation within a hydraulic actuator shall be considered. Mounting in the test fixture shall be by rod end bearing on the movable end and a clevis or conventional bearing mounting on the housing end. The rod end bearing shall be provided with an adjustment range of 0.20 inch in order to accommodate multiple sensor installation alignment.

3. Optical connectors shall be mounted on the transducer.

4. Since eventual incorporation of the transducer concept into a hydraulic actuator is planned, the transducer shall be designed to function properly in a temperature environment of -65°F to +275°F (-50°C to +135°C).

5. The transducer shall have an MTBF goal of 30,000 hours.

6. Life cycle testing shall be conducted in accordance with paragraph 4.7.8.2.1 of MIL-C-5503C.

7. Environmental testing shall consist of (as a minimum) temperature, altitude, humidity, dust, salt fog, and vibration and shock using methods based upon MIL-STD-810 except the maximum temperature shall be plus 135°C.

The overall length of the transducer package was determined largely by the required 6-inch stroke, but also by other considerations relating to mounting provisions and physical strength necessary to survive the vibration and shock environment. The length of the transducer between mounting centers, when fully compressed, was approximately 19 inches. Assuming a rigid one-piece encoder with a full-scale stroke of 6 inches, and assuming that the encoder must remain within the body even when fully extended, then 12 inches is the absolute minimum length of the body. The additional 7 inches of length were required to meet the mounting and environmental requirements. The various contributions to the length were as follows:

Accommodation of 6-inch stroke	12.0 inches
Rod-end bearing, locknut and wrench flats	1.7

Accommodation of 0.2-inch overtravel	0.5
Rod seal	0.3
Mounting of fiber optic connectors	0.0
Mounting of housing end bearing	1.0
Rod bearing length to provide rigidity at full extensions	3.5
	19.0 inches

The largest single contribution to the excess length is that required to provide the rigidity necessary to withstand the vibration and shock environment when fully extended. This is the length of rod which is still contained within the body when the transducer is fully extended. In many applications, for example when installed on or within a hydraulic actuator, it would be possible to minimize this contribution by designing the package to have mounting provisions at both ends of the body -- thereby greatly reducing the bending moment to which the rod would be subjected under vibration and shock conditions.

Motion Assembly Design

The complete motion assembly, shown in Figure F-1, consists of the encoder, isolator, shaft, shaft bearings and seal, and the bearing/seal housing. Aside from the bearings, seals, and lubrication, which are treated separately, the principal problem in the design of the motion assembly was that of guiding the encoder with sufficient accuracy while also isolating it from all possible sources of stress which might cause fracture.

Under vibration, the encoder is subjected to impact with the guideways in which it slides. To prevent the impact from fracturing the encoder or chipping its edges, the encoder bearing surfaces were made sufficiently large compared with the clearances so that the encoder was essentially protected by an air cushion. No encoder breakage or chipping occurred during the vibration tests, so it appears that this technique was successful.

Under vibration, or with other forms of lateral loading, a fraction of the stress applied to the shaft could be transferred to the encoder. This transfer of stress was prevented by including an isolator between the shaft and the encoder as shown in Figure F-2. The isolator is free to slide in the isolator guideway but, because of the very small clearances, very little relative motion is possible. As a second precaution, the isolator is necked down to form a flexure section at its midpoint so that lateral loading applied to the shaft end of the isolator is poorly transferred to the encoder end. As a third precaution, silicone resin is used to provide a compliant but backlash-free connection between the isolator and the encoder. The silicone is reinforced with nichrome wire which passes through holes in the encoder so that an actual adhesive bond is not relied upon.

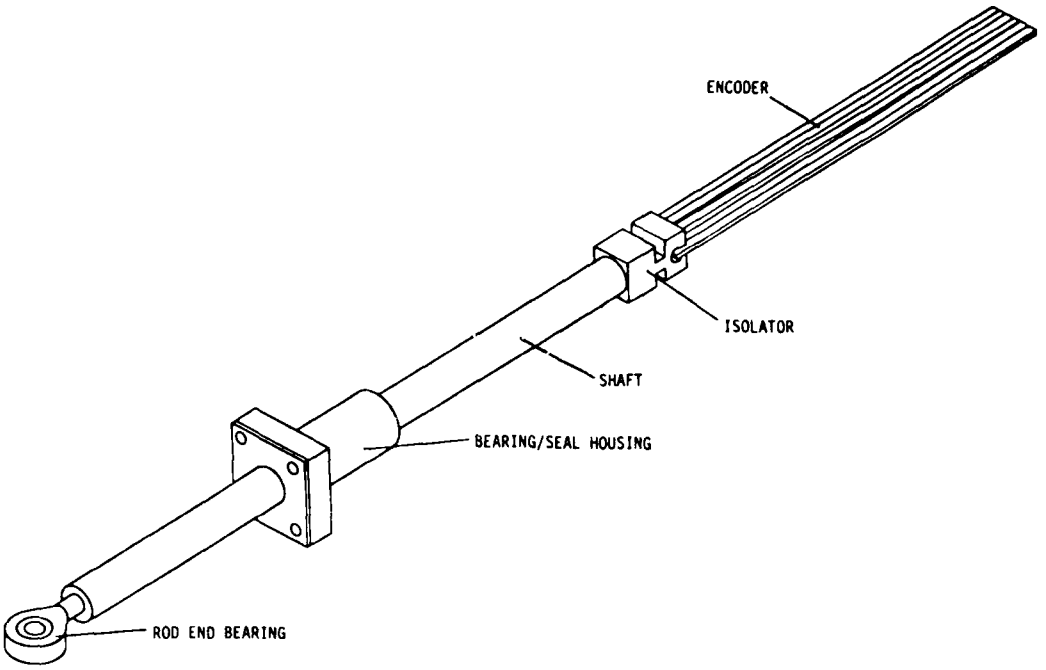

Figure F-1. Complete motion assembly.

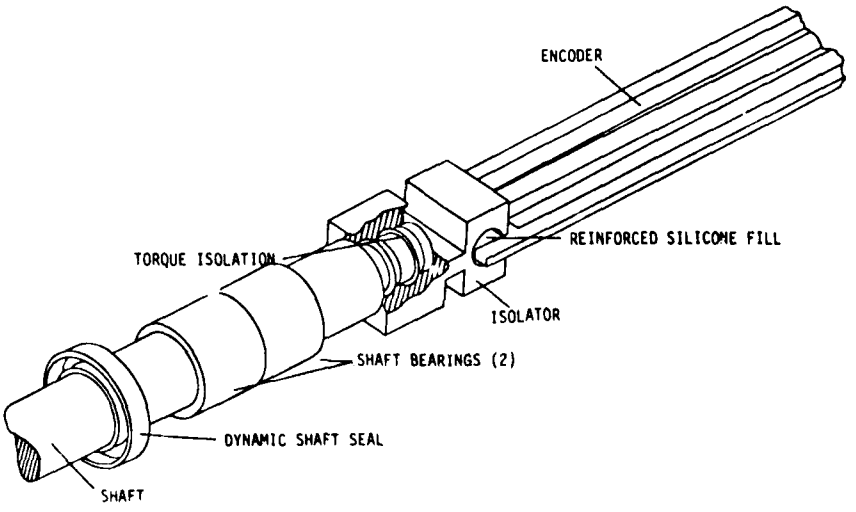

Figure F-2. Motion assembly details.

Torque applied to the shaft, as a result of either normal operation or adjustment of the rod end bearing, could be transferred to the encoder and cause fracture. To prevent this, the isolator is formed around a series of annular rings on the reduced end of the shaft as shown in the cutaway section of Figure F-2. This torque isolation permits relatively free rotation of the shaft, and because the isolator is rectangular and is confined within a rectangular guideway, the small torque which is present is transferred directly to the transducer body rather than through the encoder.

The isolator also serves as a secondary shaft bearing which increases the stiffness of the transducer and improves its ability to accommodate lateral loads.

Lower Body Assembly Design

The lower body assembly, shown in Figure F-3, comprises the lower body, two output mixing rod/prisms, two output fiber optic connectors, and one-half of the encoder guideway and isolator guideway.

The mixing rod/prisms are located approximately 0.005 inch below the plane of the encoder, and are fitted into tapered 70-degree dovetail slots having the same cross sections as the prisms. The prisms are retained in the dovetail slots with semi-rigid silicone resin which has a refractive index sufficiently lower than that of the prisms so that it serves also as an effective optical cladding material. The resin is also sufficiently flexible to cushion the prisms against shock and to reduce stress due to bending and differential expansion of the body and the prisms.

The fiber optic connector receptacles consist of threaded bushings which are compatible with Amphenol 905-series plugs. They are threaded into the body and are adjusted in depth to provide a clearance of approximately 0.005 inch between the plugs and the faces of the mating prisms. After adjustment, the receptacles are locked in place with locknuts and setscrews and the threads are sealed with a high-temperature epoxy to prevent the entry of moisture and to permit the mating plugs to be tightened to the recommended torque without disturbing the adjustment.

The lower body is machined and ground from 6061-T6 aluminum. This alloy was selected because it can be readily machined to close tolerances, has good dimensional stability, has good resistance to salt corrosion, and because preliminary investigation showed that it has good wear characteristics as a bearing material in combination with both Rulon J and glass.

Upper Body Assembly

The upper body assembly, shown in Figure F-4, comprises the upper body, the input mixing rod/prism, the input fiber optic connector, and the other half of the encoder guideway and isolator guideway. In all other respects, it is similar to the lower body assembly.

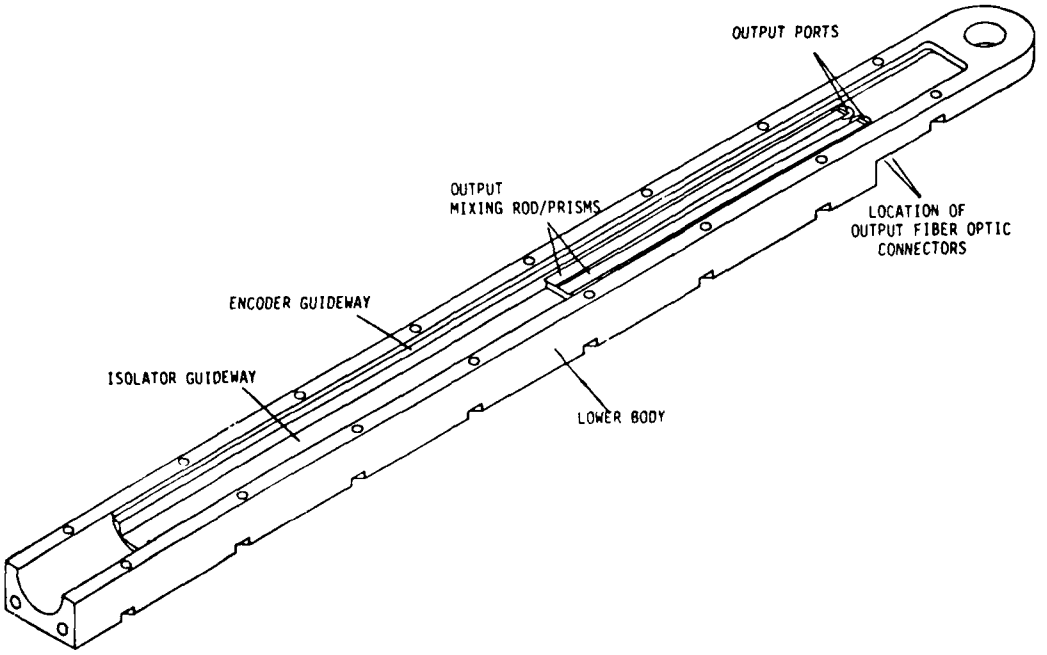

Figure F-3. Lower body details.

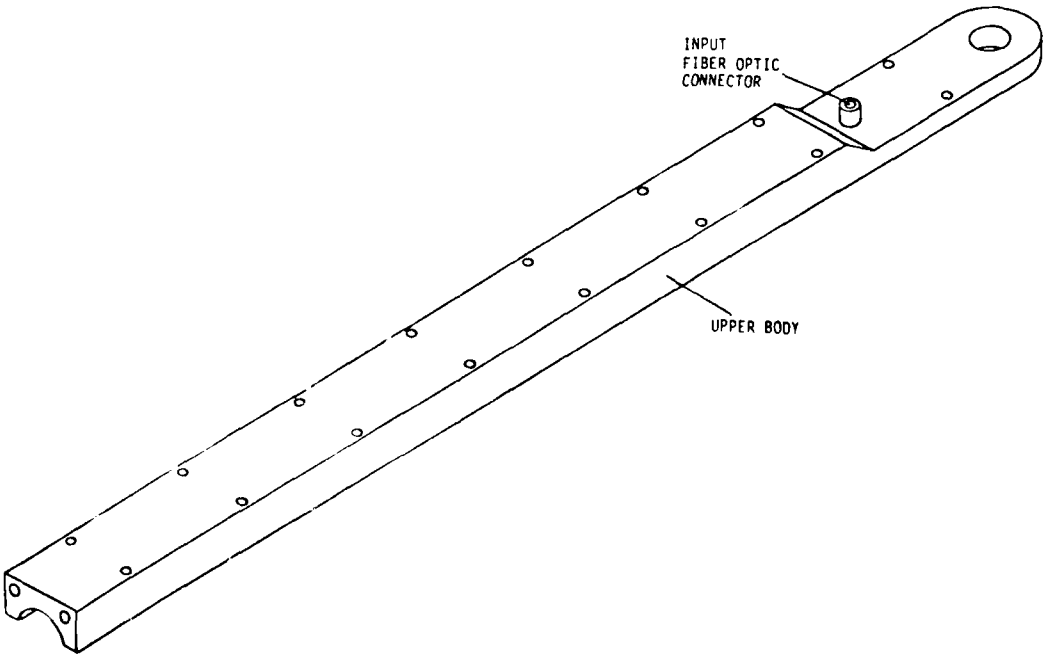

Figure F-4. Upper body assembly.

AD-A117 918 BOEING AEROSPACE CO SEATTLE WA ENGINEERING TECHNOLOGY DIV F/G 20/6
DEVELOPMENT AND TEST OF A DIGITAL/OPTICAL LINEAR POSITION TRANS--ETC(U)
JUN 82 G E MILLER, T A LINDSAY, B E JOHNSON DAAK51-80-C-0028
UNCLASSIFIED USAAVRADCOM-TR-82-D-6 NL

Bearings, Seals and Lubrication

Because of the 30,000-hour MTBF design goal, and because the transducer was required to withstand MIL-STD ranges of temperature, altitude, humidity, dust, salt fog, vibration and shock, the success of the design was critically dependent upon the selection of proper techniques and materials for bearings, for lubrication, and for static and dynamic seals.

Physically, the shaft and its supporting bearing surfaces must be sufficiently rigid to handle the bending moments due to lateral loading, vibration and shock. Also, because of the reliability requirement, all of the sliding surfaces require some form of lubrication -- either wet or dry. If wet lubricants such as oils or greases were used, an elaborate system of seals would be required to prevent contamination of the encoder and other optical components. On the other hand, if the transducer were filled with a fluid which would serve both as a lubricant and as an optical transmission medium, then excellent seals would be required to prevent the escape of fluid. Also, turbulence in the fluid within the optical path might present a problem, as might the selection of a fluid which would retain desirable lubricant and optical properties over the entire temperature range. Another constraint implied for all wearing parts and their lubrication is that the quantity, size and mobility of wear particles be minimized. Measures must also be taken, to the extent possible, to prevent the unavoidable wear particles from being deposited upon critical optical surfaces. These precautions are believed to be highly desirable even though this transducer, with its analog encoding, is considerably more tolerant of contamination of the optics than a transducer with equal resolution using direct digital encoding. This is true because the error is a direct function of what fraction of the total illuminated encoding area is obscured by a contamination particle. With a true digital multi-track transducer, a contamination particle as small as the smallest resolution element could conceivably obscure any one of the encoder tracks; if it happened to obscure the most-significant bit track, it could cause a 50% measurement error. With the analog transducer, the same contamination particle could obscure only a very small fraction of the total illuminated encoding area and could therefore cause only a very small measurement error.

To simplify the seal problem and to eliminate some of the unique problems associated with liquid lubricants, it was decided that the prototype design would use only dry film lubricants and self-lubricating solids. There are many solid films which could have been used to lubricate the bearing surfaces. These include soft metals such as lead, silver, gold, tin, zinc and cadmium; inorganic compounds with layer-latticed structures such as molybdenum disulphide and tungsten disulphide; and polymers such as polytetrafluoroethylene (PTFE), nylon and polyimide. The lubricating films are commonly applied by three different processes: burnishing, resin bonding, and sputtering. Of these, sputtering provides by far the best lubricating coating. Sputtered molybdenum disulphide film has a continuous and structureless appearance with no evidence of grain or grain boundaries, can be applied with a uniform thickness even on irregular surfaces, has superior adhesion and does not spall or flake off the surface, and has a long useful life. The coefficient of friction of the film against stainless steel is about 0.06, which is comparable to that obtained with oils and greases.

Self-lubricating solids include plastic-based materials, metal matrix materials, and carbon-graphite-based materials. Factors which must be considered in the selection of self-lubricating solids include: strength, friction properties, wear resistance, selection of mating materials, preparation of mating surfaces, clearances needed to accommodate differential thermal expansion and dimensional stability as affected by heat and humidity. In general, the self-lubricating solids offer better wear resistance than do the solid film lubricants and are therefore preferred in this application.

Figure F-5 shows the basic motion assembly of the prototype transducer and the various bearing surfaces which support the motion assembly within the transducer body. The encoder bearing surfaces, which are highly polished uncoated optical glass, slide directly against 6061-T6 aluminum alloy which forms the transducer body. Although this glass/aluminum bearing combination is unconventional, preliminary tests showed that this combination has excellent wear properties even when unlubricated.

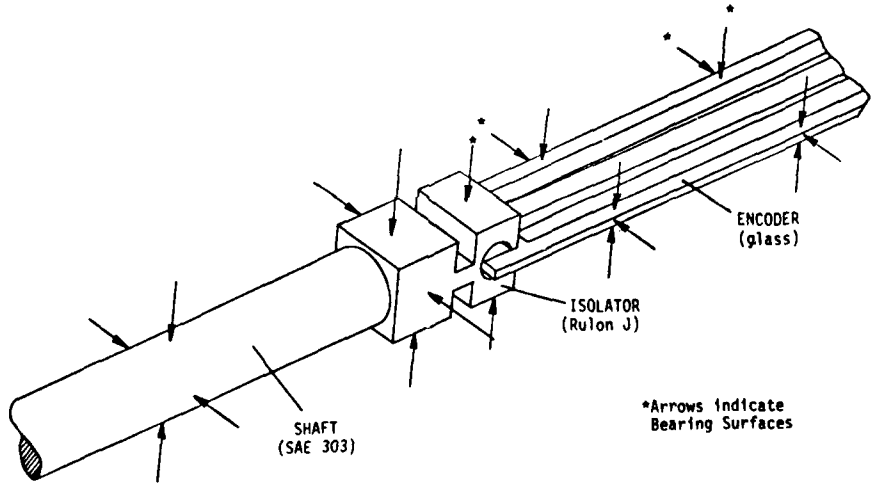

Figure F-5. Motion assembly bearing surfaces.

The suitability of this combination was further confirmed during the life-cycle test where, after two million cycles of operation, the only detectable wear was in the form of a few isolated spots on the encoder bearing areas which appeared to be slightly frosted. The encoder is attached to an isolator which has bearing areas on four sides. The isolator, which was fabricated from Rulon J material, also slides unlubricated against the 6061-T6 aluminum alloy of the transducer body. Rulon J is a fluorocarbon formulation of the Dixon Corporation which is intended specifically to run unlubricated against soft mating surfaces such as

brass and aluminum. It is an all-polymeric reinforced TFE which contains no abrasive or hard inorganic fillers such as glass fibers, ceramics or graphite which can abrade and scratch soft mating surfaces. It is useful as a self-lubricating bearing material over the temperature range of -400 to +500°F (-240 to +228°C), has zero water absorption, and can handle loading to 20,000 psi-fpm and surface velocity up to 400 fpm without lubrication. After two million cycles of operation in the life-cycle test, neither the isolator nor the mating aluminum surfaces showed any detectable wear. The shaft was fabricated from centerless-ground SAE 303 stainless and was polished longitudinally to a 5-microinch finish to minimize wear of the shaft bearings and the shaft seal.

Figure F-2 shows the shaft bearings and the shaft dynamic seal. The shaft bearings have a powdered bronze surface which is sintered onto a steel backing. The bearings are lubricated by a mixture of PTFE and lead which impregnates the porous bronze surface to serve as a lubricant reservoir. As the initial film lubricant is depleted, the relative motion of the mating parts continues to draw lubricant from the porous bronze. Because of the high thermal expansion coefficient of PTFE, additional lubricant is forced to the surface as the bearing temperature rises due to either friction or ambient conditions. This bearing is rated for continuous loading of 50,000 psi-fpm, surface velocity to 1,000 fpm without lubrication, and temperatures from -328 to +536°F (-200 to +280°C). The life-cycle test resulted in no perceptible wear on this self-lubricating bearing.

The shaft seal shown in Figure F-2 has a U-shaped cross section, an outer covering of TFE loaded with 15% graphite, and an inner spring which maintains the seal pressure nearly independently of temperature and wear. This seal is designed to function over the temperature range of -100 to +500°F.

APPENDIX G

DEVELOPMENT OF MICROPROCESSOR TEST FIXTURE

A microprocessor-based test system was developed for the transducer group 2 static accuracy, resolution, linearity, and monotonicity tests decribed in Section 5 of the Hardware Test Plan (Appendix A). The test system is depicted in Figure G-1 and consists of five main parts:

1. Transducer translation fixture
2. Scanning microcomputer translation fixture controller (Intel 86/12A)
3. Intel microcomputer development system (Intel 220)
4. Computation computer (Harris/800)
5. Plotting computer (Harris/100)

Transducer Translation Fixture

The transducer translation fixture consists of a 200-step-per-turn stepper motor (a "SLO-SYN" Type 025) driving a precision lead screw which has 32 threads per inch. The lead screw rotates on precision bearings and drives a nut plate which slides on a pair of parallel guide rods. Each step of the stepper motor causes the nut plate to translate 1/(200 steps per turn X 32 threads per inch) = 0.00015625 inch per step. The transducer under test was mounted in the translation fixture with one end attached to the sliding nut plate and the other end attached to the stationary frame of the fixture. Prior to being mounted in the translation fixture, each transducer was calibrated on the calibration test fixture which permitted the transducer to be positioned quickly to the 0, 3-inch and 6-inch positions with an accuracy of ±0.0002 inch.

The calibration of the translation fixture was checked by calibrating one transducer on the Sixis precision instrument mill and then scanning the transducer over the full 6-inch travel with the translation fixture. The Sixis mill was calibrated with Johansson gage blocks.

Translation Fixture Controller

An Intel 86/12A microprocessor-based single-board microcomputer was used as a scanning translation fixture controller. The microcomputer drove the stepper motor via a "SLO SYN" TTL-compatible stepper motor driver. The microcomputer was connected to the EIU via a 12-bit parallel interface and could update the EIU A/D converter with a TTL update pulse. In normal operation, the controller searched for an end point (0 inch to 6 inches), went

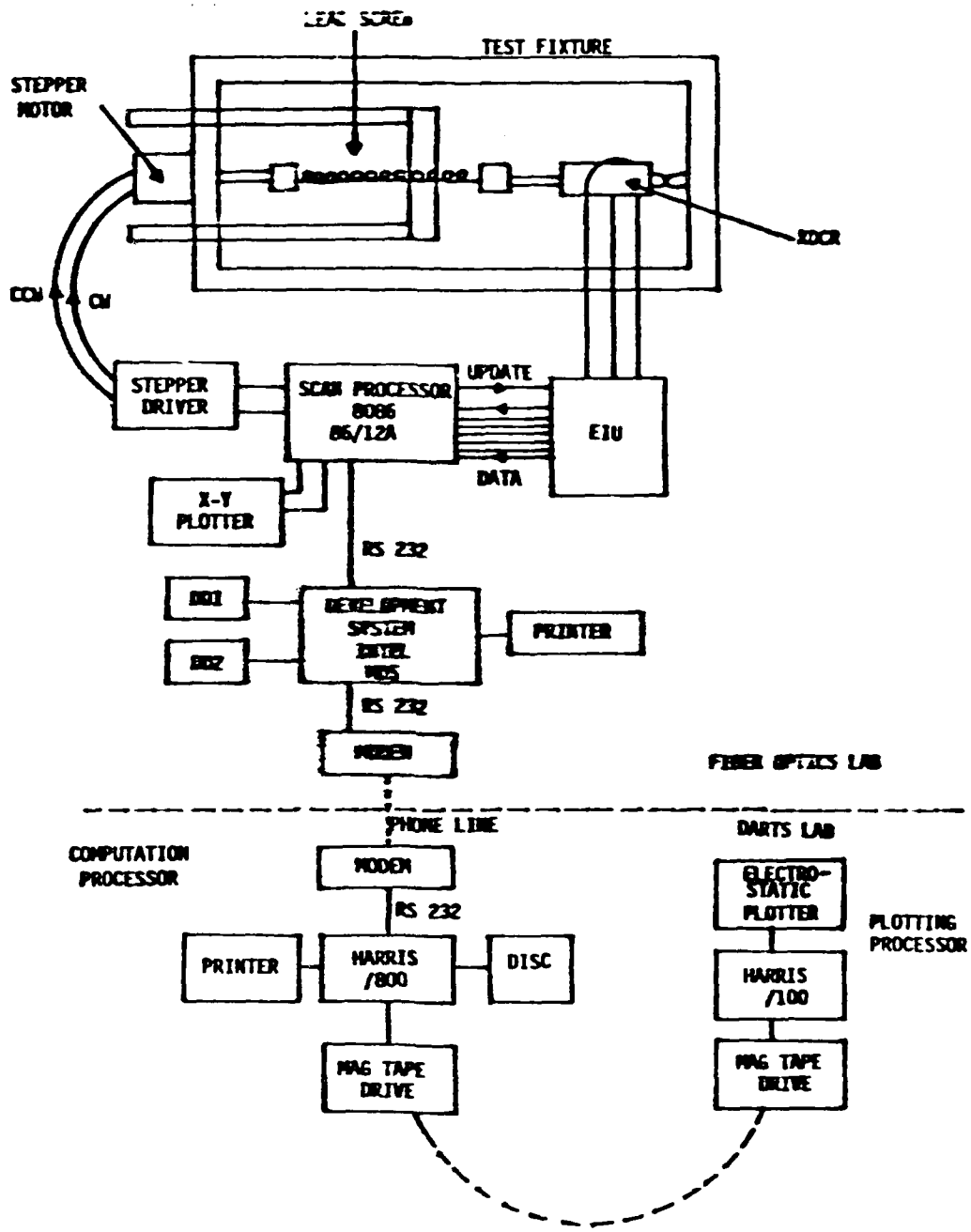

Figure G-1. Microprocessor based test system block diagram.

twenty steps past the end point to take the backlash out of the lead screw, and then scanned from the endpoint for 6 inches of travel, storing the EIU values in RAM at regular intervals. Samples were taken every eight steps (0.00125 inch) for a total of 4801 points in 6 inches. After a scan was completed, the EIU reading versus stepper value was plotted on an X-Y plotter to check the data for integrity and gross error. The powerful read only memory (ROM) monitor on the 86/12A board allowed it to use the disc drives on the microcomputer development system. These routines were utilized to store scan files on floppy discs. All software for the 86/12A microcomputer is contained in Appendix D.

Microcomputer Development System

An Intel 220 microcomputer development system was used during the development and operation of the microcomputer test fixture and served five main functions:

1. Software development and checkout for the 86/12A 8086-based translation fixture controller
2. Download programs into the 86/12A RAM via 9600-baud RS232
3. Communication to 86/12A board for program execution via 9600-baud RS232
4. Disc drives held scan files of all transducer tests
5. Communication and upload of transducer scans from disc files to Harris computer in Boeing DARTS lab facility over 1200-baud modem and phone line

Software for MDS-Harris/800 communication is contained in Appendix D. The communication procedure consisted of:

1. MDS sends ASCII character to Harris
2. Harris sends back ASCII character to MDS when received
3. If proper character, then send next character
4. If wrong character, then MDS send out ASCII "B" (rereceive last character)

Harris/800 Computer

The Harris/800 computer was utilized to perform computations on the transducer scans to determine the group 2 performance tests:

1. Linearity
2. Accuracy

3. Resolution

4. Monotonicity

The Harris/800 received transducer up and down scans over a 1200-baud dial-up modem. Scans of EIU reading vs. actual position were sent in two parts: up scan and down scan. Upon receipt of both an up scan and a down scan for a particular transducer, processing was initiated and an error summary was printed out. Error in bits and inches was tabulated at thirteen different positions and monotonicity was checked. A printout of this data was made on the line printer. Next, a program was run that wrote a plot file to magnetic tape containing the following information:

1. Up-scan EIU reading (inches) vs. actual position (inches)

2. Up-scan error (inches) vs. actual position (inches)

3. Down-scan EIU reading (inches) vs. actual position (inches)

4. Down-scan EIU reading (inches) vs. actual position (inches)

Harris/100 Computer

The Harris/100 computer was used to plot test data. A FORTRAN program read the plot files generated by the Harris/800 computer on magnetic tape and plotted the results on a Versetec model 1100 electrostatic plotter. Unfortunately, the Harris/100 computer did not have a modem and the Harris/800 did not have a graphics capability; otherwise, one computer could have been used to serve both functions.


DATE
ILME
8